THE PULTRUSION OF THERMOPLASTIC MATRIX COMPOSITES.

This thesis is submitted in accordance with the requirements of the University of Liverpool for the degree of Doctor of Philosophy
by Brendan James Devlin.

Department of Materials Science and Engineering
April 1992.

Abstract.

Until recently the pultrusion process has been confined to thermosetting polymer matrices but there is now considerable interest in the possibilities offered by thermoplastic polymers.

Thermoplastic pultrusion is attractive for two main reasons: first, there is no chemical reaction involved, so the achievable line speed is limited only by the rate at which heat can be transferred into the product prior to the shaping process and out of it afterwards. Secondly, the process opens up the field of continuous fibre composites to a wide range of attractive thermoplastic matrices, which were hitherto excluded because of processing difficulties, especially the impregnation stage.

Significant developments are taking place at both ends of the applications spectrum. There is interest from aerospace in the possibilities offered by continuous sectional products in carbon fibre with high performance PEEK, PEI and PPS matrices. However, the economic potential for the use of pultruded glassfibre composites, based on the commodity engineering thermoplastics such as the polyamides and polypropylene may be even greater. The ability to achieve high line speeds is more important in the latter case than in products for the aerospace industry, but close control of processing parameters is equally important for both application areas.

A full scale thermoplastic pultrusion line was developed to produce flat strip sections using preimpregnated precursors. The principal process parameters were identified as line speed, oven temperature and forming pressure and the effect of changing these were examined under instrumented conditions. Sections were produced using either constant pressure, cold forming rollers or constant pressure heated dies.

In roll forming, it was found that the interlaminar shear strength and the flexural strength of the pultruded sections decreased with increasing line speed as a result of reduced forming times in the rolls. It was found that the cold roll surfaces caused rapid cooling of the surface layers of the partially consolidated sections. These solidified layers prevented complete consolidation and cause air to become entrapped in the composite section. Void contents of between 1.5 to 11% were measured for roll formed sections, depending on the line speed. Increasing the roll pressure was found to cause an overall reduction in the mechanical properties of the

Acknowledgements.

I would like to thank the University of Liverpool, the Department of Education for Northern Ireland who provided financial support for the work described here.

The advice and assistance given by members of the Composites Research Group at the University of Liverpool and at The University of Newcastle; D.W. Lamb, S.P. Corscadden, C. Worrall, A. Pickles and A. Longmuir is gratefully acknowledged. Similarily, I would like to thank M. Williams and H. Snaith at Fibreforce Composites Ltd. for their assistance both technically and in the supply of materials. I would like to thank our technician, Mr Ron Jenson for his hard work and dedication.

I would also like to thank my supervisor, Professor A.G. Gibson, for his support, enthusiasm and patience throughout the project.

I would like to thank my Mother and Father (Does it melt or does it burn) and my friends for all their support and encouragement.

Finally, I would like to dedicate this thesis to my wife Alisa, who still probably cannot believe that it is finally finished.

TABLE OF CONTENTS.

Chapter 7. Conclusions

Chapter 1. Introduction

"let us try to imagine a dweller in the "Plastic Age" that is already upon us. This creature of our imagination, this "Plastic Man" will come into a world of colour and bright shining surfaces, where childish hands find nothing to break, no sharp edges or corners to cut or graze, no crevices to harbour dirt or germs..... As for the aeroplane the engine alone will provide an outlet for metal, for here the astonishing lightness of plastics will revolutionize construction. The wings, struts, fuselage, cabin, petrol tanks, and all interior fittings will be mass produced from reinforced plastic."

Yarsley and Couzens (1941)[1].

1.1 General introduction

A composite material is a synergistic combination of two or more different materials. The result of the combination of the constituent materials is to produce an effect greater than the sum of their individual effects. The principle applies to all kinds of properties; physical, chemical and mechanical although the most commonly sought after improvement is in the mechanical properties. The properties of naturally occurring composite materials have been recognised and used for centuries in a wide range of applications. Perhaps the most commonly used natural composite is wood, the structure of which can be seen in Figure 1.1, Gordon (1968)[2], and which comprises of fibrous cells of cellulose supported by a lignin matrix.

In the last fifty years, the most widespread technological advances in the composites field have occurred in polymer composites, which use either a thermoset or a thermoplastic polymer matrix to support, protect and transfer external loads to reinforcing fibers or particles. Although the entirely composite airplane has not yet become a commercial reality, the fanciful predictions of Yarsley and Couzens (1941)[1], made not long after the discovery of nylon, have in a few special cases become reality.

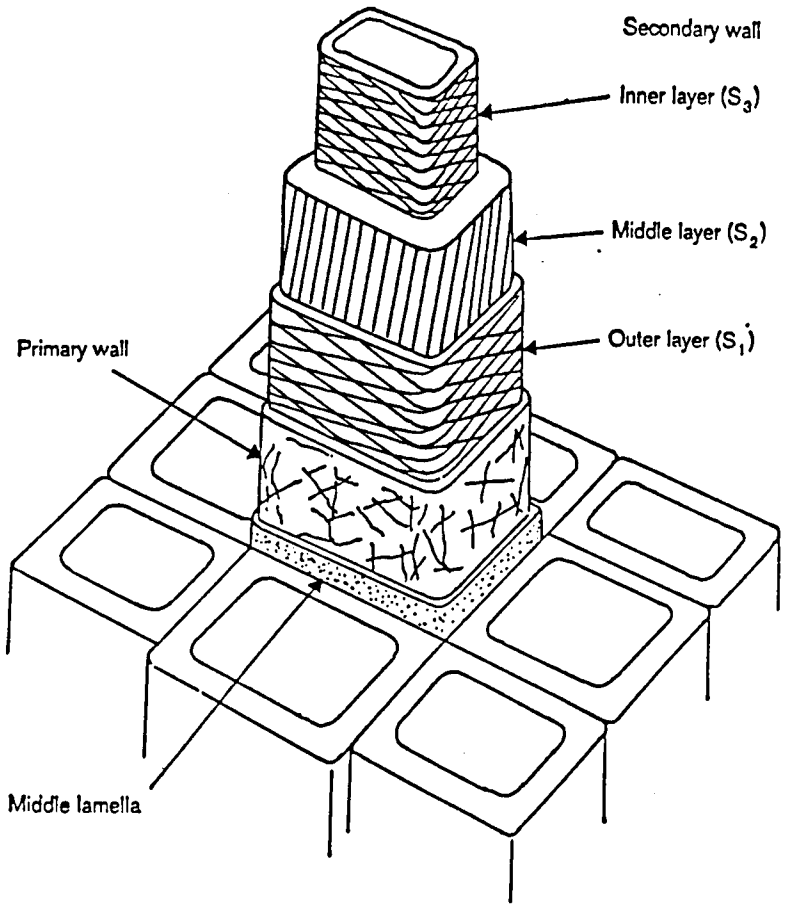

Figure 1.1. The cell structure of wood showing its composite nature, after Gordon (1968).

1.2 Polymer composites

Traditionally, thermoset polymer matrices have been the most widely used in high performance composite applications and there are a number of reasons for this predominance. In the initial stages of processing, before the onset of the curing cycle, thermoset polymers have a low molecular weight which results in a low viscosity. This enables dense bundles of reinforcing fibres, placed in any orientation, to be impregnated with a liquid resin system. It is also relatively easy to achieve a high degree of fibre wet-out and a low volume of entrapped air in the uncured composite using either continuous roving or random mat reinforcements. Only once the impregnation phase of processing has taken place does the viscosity rise rapidly as the cross-linking reaction progresses. Eventually, the composite solidifies as a high-molecular-weight polymer network in an irreversible reaction. This ease of impregnation has allowed the development of a wide range of processing options for thermoset composites, which range from hand lay-up operations to continuous, highly automated processes such as tape laying, filament winding and pultrusion.

Thermoplastic polymers, unlike thermosets, are not cross-linked. They are solid at room temperature and consist of very long, high-molecular-weight polymer chains. Thermoplastic polymers may be classified as either amorphous, having a random structure, or crystalline, having an ordered structure. Amorphous thermoplastics are brittle and glass-like in tension and are susceptible to certain solvents which can cause environmental stress cracking to occur. Some of the earliest developed thermoplastics such as PVC and polystyrene belong to this class. Crystalline and semi-crystalline thermoplastics are tougher and more ductile than amorphous polymers and are much more resistant to solvent attack. They can be effectively reinforced, have greater creep resistance and better elevated temperature properties when compared to amorphous thermoplastics. Commonly used semi-crystalline thermoplastics include nylon and polypropylene, which are typically reinforced with glass or carbon fibres for use in engineering applications. For high temperature, advanced composite applications, poly-ether-ether-ketone (PEEK) and polyphenylene-sulfide (PPS) matrices, typically reinforced with carbon or aramid fibres, have found more widespread use in aerospace applications.

1.3 Thermoplastic composites

Some of the advantages and problems encountered with thermoplastic composite materials are summarised in Table 1.1.

Table 1.1. Advantages and problems encountered with thermoplastic materials.

	Advantages	*Problems*
Storage and handling	Indefinite shelf life. No special storage conditions required.	Pre-preg stiff and boardy with no tack. (Pseudo-thermoplastics may have some tack and drape.)
Properties	High toughness. Good environmental resistance (semi- and liquid-crystalline matrix polymers only).	Limited evaluations of long-term properties (creep, fatigue) and environmental resistance.
Processing/ fabrication	No chemistry during fabrication (true thermoplastics only). Potential for rapid, low cost fabrication. Potential to re-process (true thermoplastics only). Scrap recovery. Potential for easy quality control.	Fabrication processes still being developed. High temperature processing. Tooling, bagging materials, sealants expensive. May need capital investment for new equipment.

When compared to thermoset resin systems such as polyesters and epoxies, thermoplastic composites generally offer high toughness, improved transverse and interlaminar shear properties, chemical resistance, low smoke evolution, low toxicity, low flammability and the potential for recycling. Of these, low smoke evolution, low flammability and recycling potential are major considerations in the increasing use of thermoplastic composites in transport applications. In addition, there are no shelf life restrictions or special storage requirements and the possibility exists for rapid fabrication. Multiple heating cycles are possible, leading to advantages in manufacturing complex shapes, in joining welding and in composite damage repair.

Although the properties of thermoplastics appear to be very attractive, there has been a major restriction to the production of composite materials using thermoplastic matrices. Traditionally this has been the difficulty in impregnating dense bundles of either unidirectional fibres or mat reinforcements with highly viscous thermoplastics. The melt viscosity of thermoplastics is typically about one thousand times greater than liquid thermoset systems. It is possible to reduce the viscosity by either processing at elevated temperatures; by using powdered thermoplastics; or by using solvents or plasticisers to reduce the viscosity. Although using solvents presents the additional problem of removing residual solvents from the final impregnated composite material.

A number of impregnation technologies have been developed for thermoplastics and will be discussed in Chapter 2. Traditionally, the impregnation step in the manufacture of reinforced thermoplastics has involved the extrusion compounding of chopped fibres into a thermoplastic melt. In this process it is impossible to avoid fibre breakage and only discontinuous, random orientated, short fibre reinforced thermoplastic materials can be produced. The most common processing route for these materials is extrusion or injection moulding. The inability to retain long or continuous fibres either in the preimpregnated precursor material or in the finished composite moulding has been a limiting factor in the widespread use of thermoplastics in advanced composite applications.

1.4 The effect of fibre length on composite properties

A number of models have been developed to calculate the tensile stress build-up in aligned, discontinuous fibre composites and the stress at the fibre/matrix interface, Cox (1952)[3], Kelly and Tyson (1966)[4]. As the aspect ratio of the fibres decreases, the effects of the fibre ends become progressively more significant and the stress and strain fields in the composite become modified by the discontinuity at the fibre ends. The deformation around a fibre embedded in a matrix and subjected to a tensile load parallel to the fibre axis is shown in Figure 1.2, Crawford (1987)[5]. If the fibre is well bonded to the matrix, an applied external stress will be transferred to the fibre by shear at the interface between the fibre and matrix. In the region of the fibre ends, the strain in the fibre will be less than in the matrix and the fibres will restrain the deformation of the matrix.

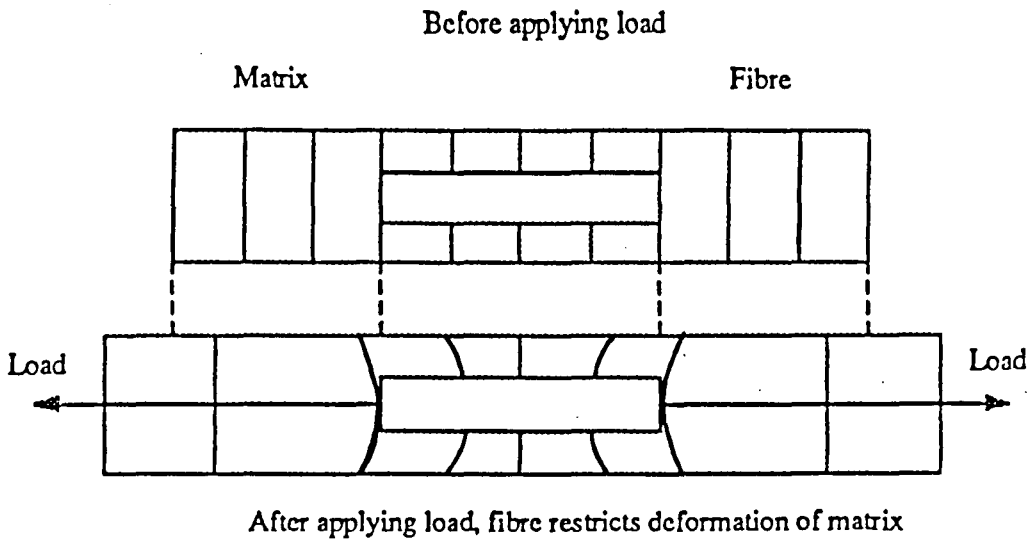

Figure 1.2. Schematic representation of deformation around a discontinuous fibre embedded in a resin matrix and subjected to a tensile load parallel to the fibres, after Crawford (1987).

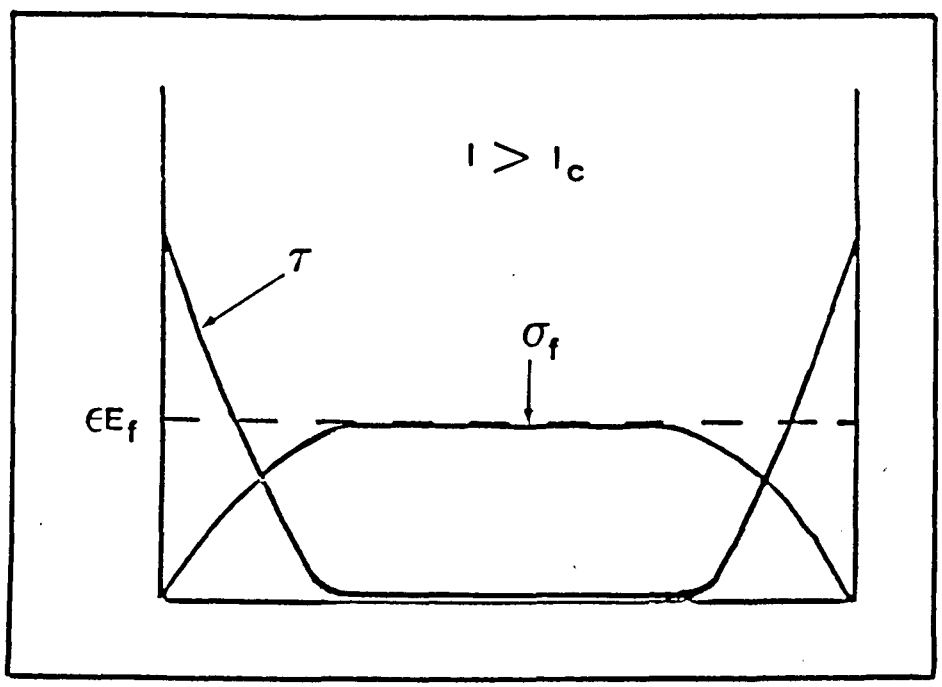

Figure 1.3. Fibre tensile and matrix shear stress distributions for an aligned discontinuous fibre, according to Cox (1952).

In a short fibre composite, the tensile stress distribution in the fibre and the form of the shear stress distribution at the interface is shown in Figure 1.3, Cox (1952)[3]. The tensile stress can be seen to increase from zero at the ends to a value σ_f max in the centre of the fibre. This is the value which it would have had if the fibre was continuous. The shear stress, τ, can be seen to decrease from a maximum at the fibre ends to a very low value at the centre of the fibre. This shows that there are regions at the ends of the fibre that do not carry the full load so that the average stress in a fibre of length, l, is less than in a continuous fibre subjected to the same loading. As the fibre length decreases, a greater proportion of the total fibre length is not fully loaded and the reinforcement efficiency will decrease. From Figure 1.3 it becomes clear that there is a minimum fibre length which will permit the fibre to achieve its full load.

Figure 1.4 shows the distribution of fibre tensile stress for three different fibre lengths, according to Kelly and Tyson (1966)[4]. The calculation of this distribution takes into consideration plastic deformation in the matrix at the fibre ends. Because the matrix was allowed to yield, the maximum shear stress at the fibre/matrix interface was limited to the shear yield strength of the matrix. The stress in a fibre was allowed to increase at a constant rate until the maximum fibre stress, $\sigma_f=\varepsilon E_f$, was reached. To achieve this stress the length of the fibre must be greater than a critical value l_c. Kelly and Tyson have shown that the critical fibre length may be related to the matrix shear strength, τ_m, and the tensile strength of the fibre, σ_f, according to the relationship:

$$l_c = \frac{\sigma_f d}{2\tau_m}$$

where d is the fibre diameter.

In Figure 1.4, if the fibres are shorter than l_c then the stress in the fibre does not reach the fibre fracture stress and the fibre pulls out of the polymer matrix. This can result in increased toughness due to energy dissipation during fibre/matrix debonding. At fibre lengths considerably longer than l_c the strength of the discontinuous composite is significantly improved, since fibre fracture rather than shear failure of the matrix takes place.

One of the main requirements of the impregnation stage, in enabling the maximum potential composite properties to be achieved, can therefore be seen to be the

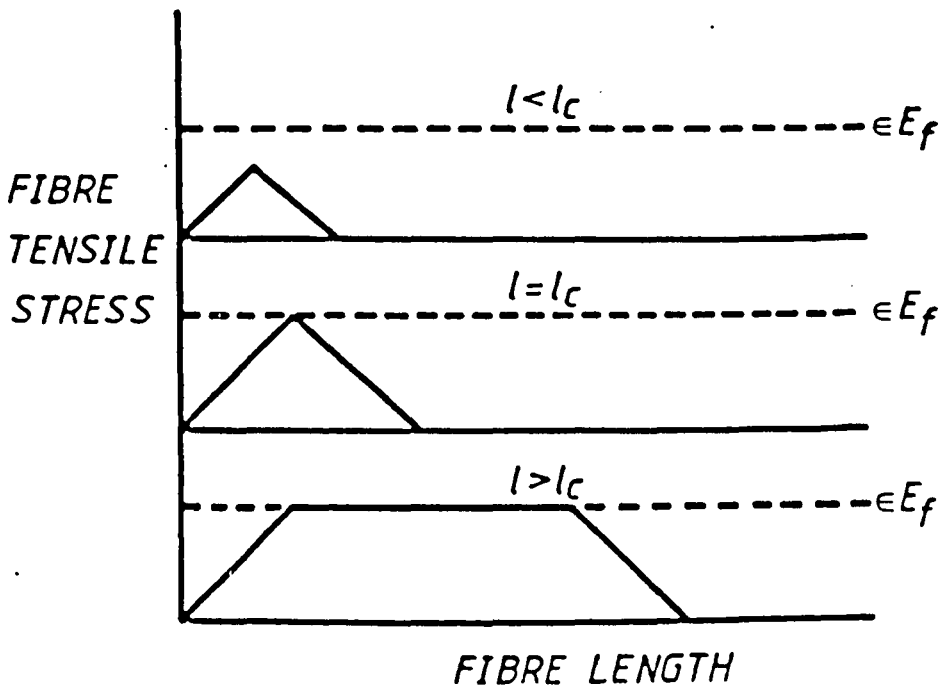

Figure 1.4. Distribution of fibre tensile stress along fibre according to Kelly and Tyson (1966).

retention of a fibre length preferably much greater than l_c. In addition, for efficient load transfer in the composite, a strong interfacial bond is necessary to prevent shear debonding at the interface, cohesive failure of the matrix or fibres and shear yielding of the matrix. However, it is difficult to make conventional extrusion compounding efficient enough to produce a fully wetted out compound with a fibre length distribution in which the majority of fibres are longer than l_c and which have anything other than a random orientation. Therefore, there was a considerable incentive to combine thermoplastic matrices with long or continuous fibres, either as long fibre injection moulding compounds or as continuous precursor materials and significant advances have been made in this field in the last 10 years.

Although full impregnation and the retention of as long a fibre length as possible is very important, the production of a fully wetted out and impregnated precursor is only the first step. The second stage is the conversion of the precursor into a composite moulding or sectional shape, in such a way as to achieve the required properties with consistency and using an economical processing method. In parallel to the development of continuous precursors, processing technologies have developed from thermoset technology: for example, filament winding and pultrusion; from conventional thermoplastic technology: for example, stamping and compression moulding; and from metal forming. In addition, some new processes have been specifically developed. The development and characterisation of one of these processes, thermoplastic pultrusion, has been the subject of the work carried out for this thesis.

1.5 The pultrusion process

The thermoplastic pultrusion process will be discussed in detail in a later section. Although the process shares its name with its thermoset counterpart few similarities actually exist, apart from perhaps the materials dispensing stage and the haul-off mechanism. The thermoset pultrusion process is illustrated in Figure 1.5. In the simplest form of the thermoset process, reinforcement is pulled through a resin bath where it is fully impregnated with a liquid thermoset resin, it is then pulled through a sequence of forming and wipe off dies which preshape the material and feed it into a heated die, usually 70-150 cm in length. This die is heated to the cure temperature of the matrix resin. A fully cured section is produced by the die exit and this is pulled continuously through the process using a haul off mechanism. The process is suitable for almost all thermoset resin matrices although polyesters

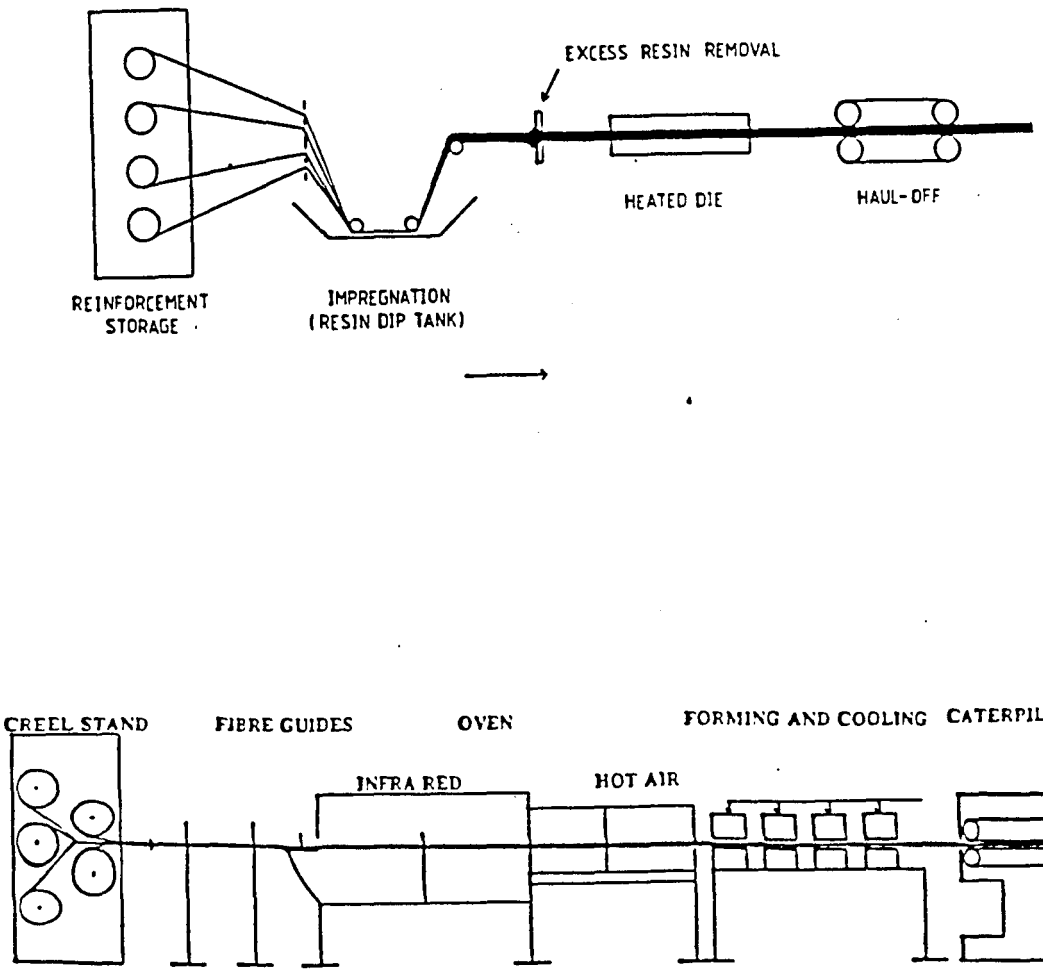

Figure 1.5. Schematic illustration of the thermoset and thermoplastic pultrusion processes, showing the common features and the differences between the two.

and epoxies are most commonly used. Glass and carbon are the most common reinforcement types and sections containing fibre volume fractions of up to 0.6 can be produced, depending on the application.

The development of continuous reinforced thermoplastic precursors has generated interest in the process of thermoplastic pultrusion. The property advantages of thermoplastics over thermosets have been reviewed previously. In addition to these, thermoplastic pultrusion offers productivity advantages over the conventional thermoset process, which is severely limited in its operating speed by the rate at which the cure reaction can be induced to take place within the forming die. Typical line speeds are of the order of 2 m/min, depending on the section thickness. Even if faster resin systems could be developed, along with the pre-heating systems needed to bring them rapidly into their cure temperature range, the die length required for faster operation would increase to such an extent that pull force would become the limiting factor in the process. Because line speed in the thermoplastic pultrusion process is, in principle, limited only by the rate at which the impregnated fibre tow can be heated to a temperature above its melting point, and by the rate at which the formed section can be cooled to form a solid shape, thermoplastic pultrusion offers potential increases in speed up to values comparable to those encountered in thermoplastics extrusion, 20m/min. Some potential end uses of unidirectional reinforced, thermoplastic pultruded profiles are summarised in Table 1.2.

Table 1.2. Potential end uses for thermoplastic pultruded sections.

THERMOPLASTIC PULTRUDED PROFILE

UNIDIRECTIONAL REINFORCEMENT

GENERAL PURPOSE	TENSION MEMBERS	PRECURSOR PRODUCTION
STIFFENERS	LOAD CARRIERS	THIN TAPES/SHEETS
EDGING STRIPS	CABLE PROTECTORS	(LONG LENGTHS)
POLES AND RODS	(VERY LONG LENGTHS & CONSISTENT QUALITY	

TYPICAL APPLICATIONS

MECHANICAL EQUIPMENT	OPTICAL CABLES	THERMOPLASTIC FILAMENT WINDING
AUTOMOTIVE	SUSPENDED STRUCTURES	TAPE LAYING
TRANSPORT	STAYS	THERMOFORMING
MILITARY		

1.6 Objectives

The principal objectives of this work were:

(i) To develop a thermoplastic pultrusion process to produce a flat strip section using continuous, preimpregnated precursor materials under instrumented and controlled processing conditions.

(ii) To investigate and characterise the process of thermoplastic pultrusion.

(iii) To determine the effects of each of the principal process variables and to examine the effects of changing process parameters on the mechanical properties and void content of pultruded sections. The principal mechanical tests were short beam shear and three point bend.

(iv) To measure temperature distributions during processing and to develop a numerical, finite difference heat transfer model for the heating, forming and cooling stages of the process.

(v) To modify the pultrusion process in response to the results of the product evaluation and the modelling results, with the aim of improving product quality and processing speed.

The principal material systems studied were nylon 12/glass, polypropylene/glass and PEEK/carbon. All the precursors were unidirectional reinforced, preimpregnated tapes.

Chapter 2. Literature Review

2.1 Thermoplastic matrix composites

2.1.1 Thermoplastic impregnation

To produce an efficient composite material, regardless of the type of polymer matrix, it is important that the composite microstructure is uniformly wetted out and has a strong fibre/resin interface, Leach (1989)[6].

Thermoset polymers have generally low viscosities, ~ 0.1 Pa.s, during the initial stages of processing before cure reactions have progressed. Therefore, high loadings of reinforcement fibres of any orientation can be readily impregnated using either hand or automated techniques with little difficulty. Thermoset pultrusion, where reinforcement tows are simply immersed in a liquid resin bath, or resin injection techniques where liquid resin is injected under pressure into a reinforcement preform are two examples which demonstrate the ease with which impregnation can be achieved with low viscosity resin systems.

This is not the case with thermoplastic polymers and the impregnation stage has traditionally been one of the major limitations to the widespread use of long or continuous fibre reinforcement in thermoplastic composites, Cattanach et al. (1986)[7].

2.1.2 Discontinuous fibre impregnation

The most common processing route to produce a well wetted out thermoplastic composite moulding material is extrusion compounding, which is shown schematically in Figure 2.1.1. In this process solid polymer granules and chopped fibres, in the form of 3-4 mm strands, are fed into the barrel of either a single or twin screw extruder. The mixture of fibres and granulated thermoplastic is subjected to a high degree of shear as the polymer melts in the barrel and this disperses and distributes the fibres throughout the melt. It is also possible to add the fibres downstream of the resin feed, directly into a polymer melt. This results

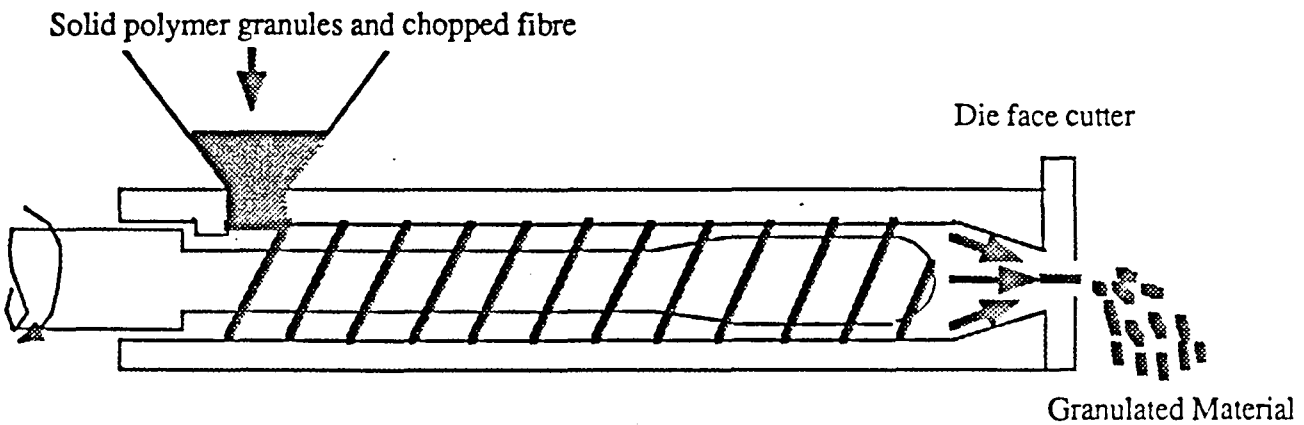

Figure 2.1.1 Extrusion compounding route to produce short fibre, thermoplastic moulding compounds.

in a composite moulding material with a maximum fibre volume fraction of 30% and with mean fibre lengths usually less than 1mm.

The fibre volume fraction which can be achieved in the composite is limited to the range of 10-30% because of two factors. The fibre length distribution and fibre alignment in the composite material produced by extrusion compounding is random and this causes a reduction in the packing efficiency. The maximum fibre volume fraction for a hexagonally packed, unidirectional composite has been calculated as 0.907 and this reduces to 0.785 for fibres arranged in a square array. However, it is difficult to achieve regular packing during processing due to fibre misalignment, fibre bunching and the formation of resin rich areas. Thus the fibre volume fraction is practically limited to a maximum of 0.7 for aligned composites.

The second reason for the limitation to the fibre volume fraction is the practical difficulty in feeding, compounding and moulding compounds containing high fibre volume fractions. Bader and Bowyer (1974)[8] have investigated various extrusion compounding routes and have reported difficulty in producing moulding compounds containing fibre volume fractions in excess of 10 to 15%. This was due mainly to problems in feeding high fibre loadings into the extruder.

In the process of extrusion compounding, the amount of work done to the material during processing can be regulated by controlling the barrel temperature, screw speed and die head pressure, but the achievement of a well wetted out composite microstructure cannot be accomplished without some fibre damage. The fibre length reduction can be minimised by careful design of the screw feed section, where most of the fibre breakage has been found to occur, Von Turkovich et al.(1983)[9], Franzen et al.(1989)[10], by operating at the minimum work input economically viable, Lunt and Shortall (1979)[11], or by reducing fibre attrition through controlling the applied shear and by feeding fibres directly into the barrel of an extruder containing a thermoplastic melt rather than as a dry mix with solid polymer granules. On completion of the mixing and impregnation stage the composite extrudate is most often granulated for use as an injection moulding compound. The process can be used with almost any thermoplastic matrix and any type of fibre.

2.1.3 The production of long and continuous fibre reinforced thermoplastic precursors

The development of thermoplastic impregnation technologies which retain either long or continuous fibres, together with a high degree of fibre orientation have provided a mechanism by which the potential properties of thermoplastic matrices can be utilised in high performance composites. These materials are used most extensively in long fibre injection moulding. However, because the impregnation technology can also be adapted to produce continuous reinforced composite precursors, the development of processing techniques specifically tailored to the continuous processing of thermoplastic composites has also occurred. Both the impregnation and processing developments will be reviewed in the following sections.

2.1.3.1 Powder impregnation

Powder impregnation aims to distribute polymer particles, usually having diameters in the range of 25-150μm, evenly throughout the fibre bundle prior to any subsequent processing stage.

The basic process of powder impregnation of fibre tows has been detailed, Price (1973)[12], Chabrier (1986)[13], and is illustrated schematically in Figure 2.1.2. It consists of pulling continuous fibre tows, at speeds up to 30m/min, under a controlled tension through a bed containing a powdered thermoplastic resin. Ideally, the powder particle diameter should be close to the diameter of the individual fibres to be impregnated, although it has been suggested that the inclusion of a quantity of powder particles outside the average size range, and with irregular and jagged surfaces will further encourage the penetration of the finer particles into the fibre bundle, Price (1973)[12]. Alternatively, it has also been suggested that very fine spherical particles, all of the same diameter give the most effective impregnation.

The powder in the bed may be stationary, it may be fluidised by means of an inert gas or it may be suspended as a liquid dispersion. The reinforcement tows are pulled through the powder bed and pass around rollers, rods or bars which act to spread and open out the fibre tows to allow full powder penetration, and also provide a mechanically forced impregnation of powder particles trapped between

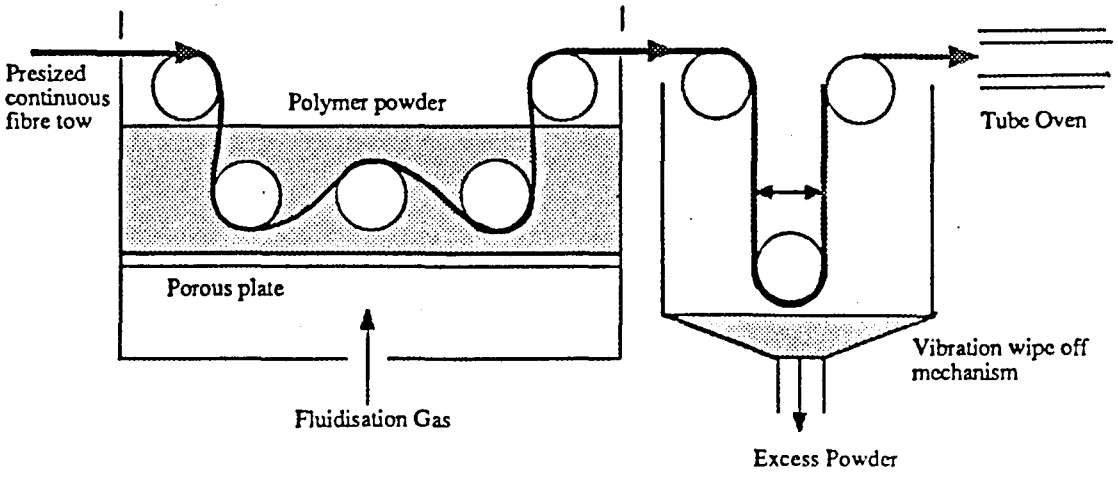

Figure 2.1.2. The powder impregnation process for continuous fibre reinforced thermoplastics.

the roller and the tow into the tow centre. The impregnated tows are pulled out of the fluidised bed and into a process stage where the required volume fraction can be obtained by any one or combinations of a number of methods. The loose powder-filled tow can be pulled through either contact rollers or flexible scrapers to provide a metered volume fraction, although this removes polymer predominately from the tow surfaces. Alternatively, the tow can be mechanically vibrated at predetermined frequencies to shake out excess powder. The entire fibre tow is then pulled through an oven where the individual polymer particles melt and flow. Once molten the tow is pulled through a heated sizing die which wipes off excess resin and determines the volume fraction of the resulting precursor. This method of controlling the volume fraction aids the impregnation process by causing a pressure induced polymer flow through the fibre tow in the die entry region. A drawback is that the excess resin from the wipe off die must be lost or recycled. It is also possible to control the volume fraction of polymer within the bed by varying either the tow tension or the fluidisation flow rate and so regulating the initial degree of polymer pick up, although this assumes no additional powder pick up or shake off will occur during the remainder of the process. After achieving the correct fibre volume fraction in the impregnated tow, the most common route to producing a usable precursor is to heat the impregnated tows to above the resin melting temperature and to form the tows into either tape or rod. The product can be coiled continuously or can be granulated directly on cooling to produce an injection moulding compound.

Another approach involves passing the tow containing unmelted powder particles through a cross-head extruder in which a sheath of the same polymer, approximately 10μm thick is applied to the outside surface. This variation of the process produces a drapeable precursor, in a flexible form which can be wound, braided or woven and which has the trade name "FIT". Processing problems unique to this type of precursor include a tendency for the powder to redistribute itself during handling and the difficulty in preventing the sheath material forming resin rich boundary layers during forming and consolidation, Leach (1989)[6]. As with any continuous impregnation process, it is possible to combine a number of tows to produce a variety of sectional shapes using either dies or rollers directly following the impregnation and heating stage.

A large number of thermoplastic polymers are suitable for use in powder impregnation techniques. The basic requirement is only that the polymer can be produced as or ground to a uniform fine powder. A review of a number of suitable

thermoplastic resins, Hartness (1988)[14], includes semi-crystalline poly-ether-ether-ketone (PEEK), amorphous polyethersulfone (PES) and amorphous polyetherimide (PEI). In addition to these predominately high performance, aerospace orientated matrix materials, the powder impregnation process is suitable for the commodity thermoplastics such as polypropylene and the nylons. The process has been demonstrated to be capable of producing good impregnation of both glass and carbon fibre reinforced thermoplastics.

2.1.3.2 Evaluation of powder impregnated precursors

A number of studies have been carried out on the mechanical properties of laminates produced from powder impregnated prepregs, Hartness (1988)[14], Freidrich et al. (1988)[15].

Hartness (1988)[14] reported on the mechanical properties and void contents of three carbon fibre/PEEK composites, compression moulded using powder impregnated precursors. These are summarised in Table 2.1.1.

Table 2.1.1. Mechanical properties of press moulded laminates, produced using three different grades of unidirectional, powder impregnated Peek/Carbon precursors, after Hartness (1988).

Material system	Flexural strength MPa Four point bend	Flexural modulus GPa Four point bend	Void content %	90° Tensile Strength MPa	90° Tensile Modulus GPa
150 PEEK/Carbon	2261	138	1.3-2.7.	64.4	9.8
380 PEEK/Carbon	2380	136	1.9-2.4		
450 PEEK/Carbon	2310	146	1.7-5.7	70.7	10

Using a nylon 12/carbon "FIT" precursor tow in which unfused nylon powder was surrounded by a nylon sheath, Freidrich et al. (1988)[15] carried out a range of mechanical tests including fracture toughness, interlaminar fracture toughness and flexural tests, and examined the fracture surfaces of various compression moulded laminates. These were produced in a two-step process, which involved firstly producing unidirectional, 0.3-0.4mm thick, prepreg sheets from individual fibre tows, then pressing 3mm thick laminates using different lay-ups of the preformed prepreg sheets.

Unidirectional laminates were produced for which flexural strengths of 627-669MPa and flexural moduli of 104-108GPa, tested using a span to depth ratio of 15, were recorded. These flexural strengths were lower than values obtained by other workers for comparable unidirectional materials systems, Carlsson (1987)[16]. This was attributed in part to the presence of misorientation angles of up to 20° in the unidirectional laminates produced using the "FIT" precursor. In addition, fracture surface studies of failed laminates indicated inadequate wetting and poor fibre/matrix bonding. This resulted in a high degree of fibre pull-out from the fracture surfaces. Although this is generally undesirable in composites, it does contribute to a high value of interlaminar fracture toughness due to extensive matrix deformation. It also contributes to a high through thickness fracture toughness due to the poor interfacial bonding.

It has been shown by Hartness (1988)[14] and Friedrich et al. (1988)[15], that it is possible to uniformly impregnate reinforcements with a range of powdered thermoplastic matrices to produce flexible, drapeable prepregs which give an excellent translation of composite properties after processing. There are, however, a number of disadvantages to the powder impregnation method, especially methods in which the polymer remains unfused, Leach (1989)[6]. In prepregs containing unfused powder, segregation of unfused polymer particles from within the fibre bundle during handling can lead to a non uniform polymer distribution along the prepreg length. Also, wet-out of the fibre bundle must occur during the forming and consolidation stage of processing and will depend on the times, temperatures and pressures used. These processing parameters will also be dependent on the size and distribution of the polymer powder particles.

2.1.3.3 Impregnation using thermoplastic melts

Traditionally, the impregnation of reinforcement fibres with a thermoplastic matrix has involved a processing stage in which the viscosity of the thermoplastic is lowered by heating the polymer above its melting point. As mentioned previously, this melt impregnation step can be achieved in a compounding extruder to produce an extrudate containing a random distribution of short fibre reinforcement of between 1-3mm with a low aspect ratio. This, however, gives rise to an unavoidable reduction in the overall composite properties because of fibre breakage. It is possible to reduce the melt viscosity of thermoplastic resins at elevated temperatures: However, it is virtually impossible to achieve a sufficient reduction

in the melt viscosity to enable total fibre wet-out to occur readily, as happens during impregnation with liquid thermosets. Usually, an additional high work input is needed to force the polymer melt into the fibre bundle, as happens in extrusion compounding. Where the aim is to produce a thermoplastic composite material containing long or continuous fibre reinforcement, a mechanism by which viscous polymer melt can penetrate the entire fibre bundle without resorting to high shear rates is needed.

2.1.3.4 Cross-Head extrusion

One of the first commercial melt impregnation processes was the cross-head extrusion process, Bradt (1951)[17], which was used as early as 1951 to produce the first long fibre reinforced injection moulding compounds. This basic process is illustrated in Figure 2.1.3, Bader and Bowyer (1973)[18], and consists of passing a continuous fibre roving through a specially designed extruder cross-head die in which the tows are coated and partially impregnated with molten thermoplastic. The extrudate is cooled and chopped to produce injection moulding pellets containing parallel unbroken fibres. The volume fraction of polymer can be metered by using sizing and wipe-off dies. Although the process can operate rapidly, it does not produce a composite microstructure which is 100% impregnated. The microstructure usually consists of a solidified polymer sheath, surrounding bundles of dry fibres in the centre of the tow. This becomes most apparent during pelletisation, which can cause a large degree of fibre pull-out to occur. In the cross-head die, impregnation is achieved by the application of pressure from the extruded resin on the outside of the fibre tow. However, the action of this hydrostatic pressure forces the fibres together, so creating a further barrier to full wet-out of the individual fibres by closing up the interstices between them, McMahon (1984)[19]. The basic cross-head extrusion process for producing long fibre injection moulding compounds has been investigated and modified by a number of workers.

Bader and Bowyer (1973)[18] have discussed the factors affecting the strength and stiffness of glass and carbon reinforced nylon and have identified that for the optimum composite properties, the fibre length in the moulded composite should be greater than 5 l_c, where l_c is the critical fibre length. This is shown in Figure 2.1.4 which shows the relationship between the reinforcement efficiency and the relative

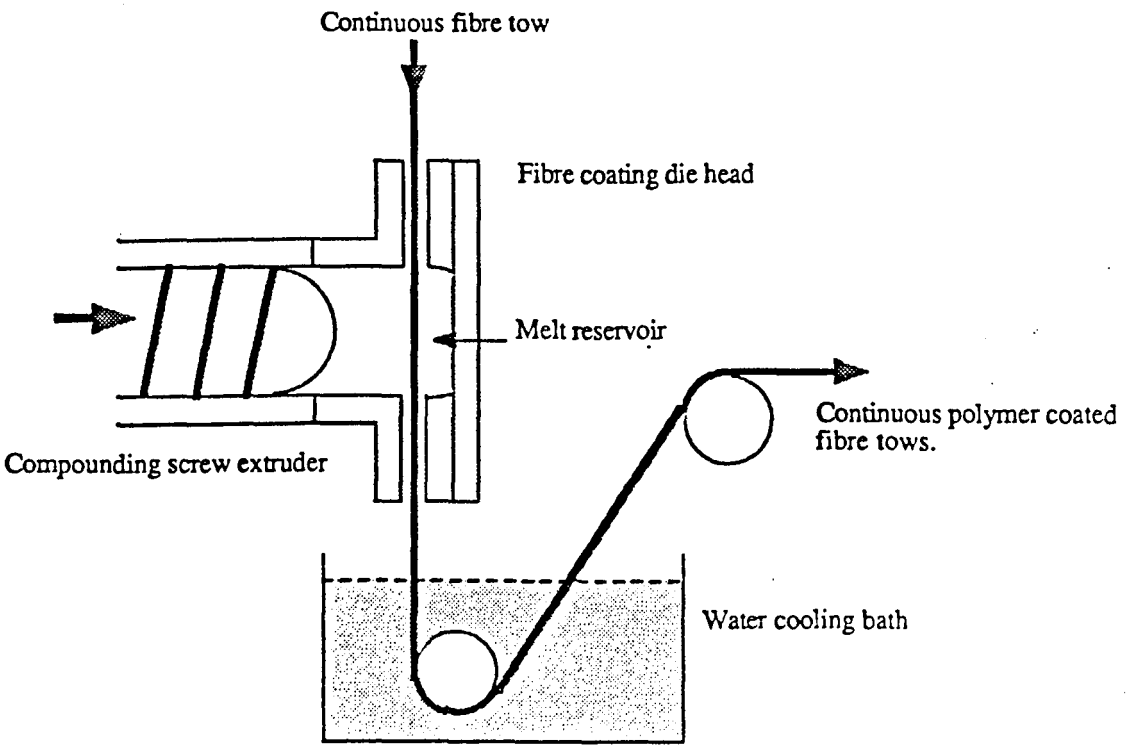

Figure 2.1.3. Continuous impregnation using a cross head extrusion technique, after Bader and Bowyer (1973).

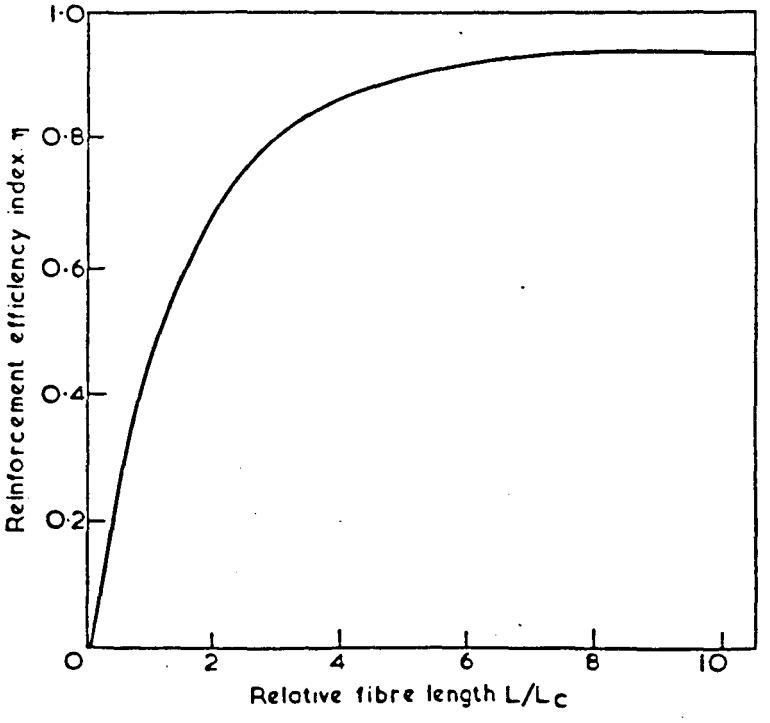

Figure 2.1.4. The relationship between relative fibre length and reinforcement efficiency. For an ideal continuous, unidirectionally reinforced composite, $\eta=1$, Bader and Bowyer (1973).

fibre length. As can be seen, the efficiency only approaches the value of 1, corresponding to continuous aligned fibres, at relative fibre lengths greater than 5. In addition to the fibre length criterion, to obtain maximum strength the volume fraction of reinforcement should be as high as possible.

In attempting to produce long fibre compounds using extrusion compounding, Bader and Bowyer[18] investigated a number of different processing routes which are summarised in Figure 2.1.5. However, with all the routes examined the problem of only achieving low fibre volume fractions, 0.1-0.15, and of not reducing fibre breakage occurred. This resulted in the development of an alternative impregnation procedure which was capable of impregnating continuous fibres. The procedure has been shown schematically in Figure 2.1.3. Using this process, moulding pellets containing 6mm long fibres and having fibre volume fractions in excess of 0.4 for glass and 0.3 for carbon were produced. On subsequent injection moulding, it was possible to produce mouldings containing a significant number of fibres longer than 2 mm.

In later work, Folkes and Kells (1985)[20] also used a cross-head die to produce long fibre carbon reinforced nylon compounds. However, problems still arose from incomplete wetting of the fibres and poor penetration of nylon into the fibre tow. This necessitated the development of a process in which a fluidised bed was used. It was found that passing the fibre tows through a fluidised bed containing powdered nylon and then pulling the bundle through an tube oven at 300°C to melt the powder resulted in improved levels of impregnation although some fibre pull-out still occurred during granulation. This hot tube process is shown schematically in Figure 2.1.6 and similarities can be seen to the powder impregnation process described earlier.

A further proposed modification of the cross-head extrusion process is illustrated in Figure 2.1.7. To improve fibre dispersion it was proposed to use rollers to spread the fibre tows prior to entry into the cross-head die. Using a similar approach, Moyer (1976)[21] has also demonstrated the idea of using impregnation pins as an integral feature of a high pressure extrusion cross head die in a patented process for the production of continuous length composite sections, rovings and tapes. In this case, the bars act to flatten and separate individual fibre tows as an aid to impregnation. Line speeds of up to 30m/min have been reported for this process.

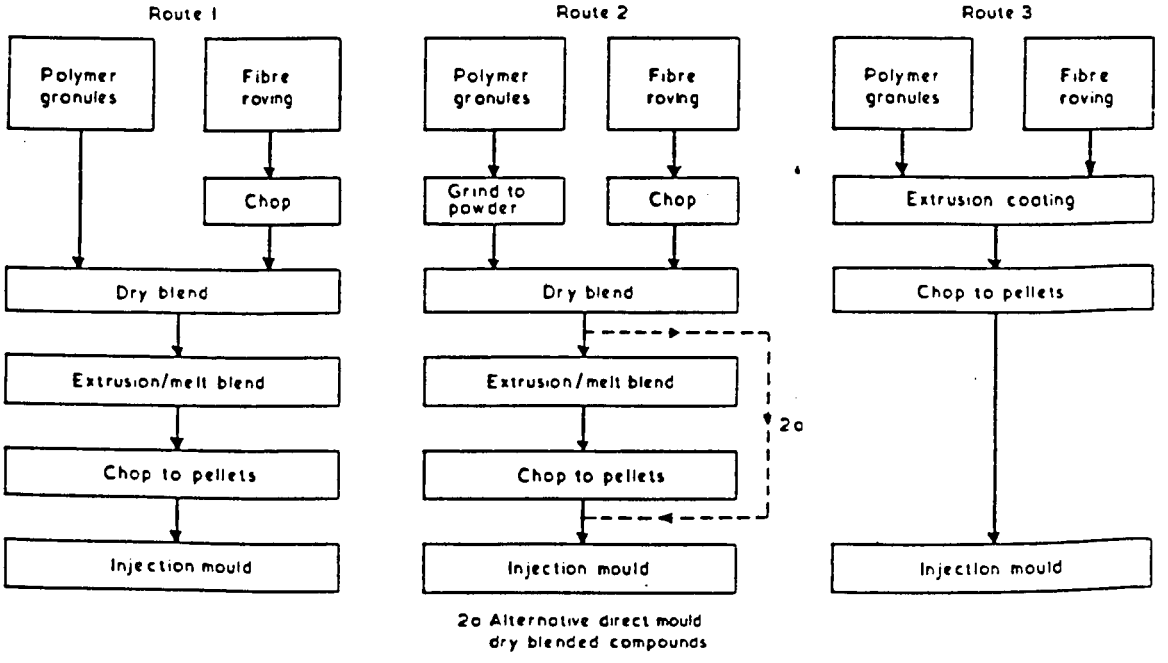

Figure 2.1.5. Alternative routes for compounding and moulding fibre reinforced thermoplastics materials, Bader and Bowyer (1973).

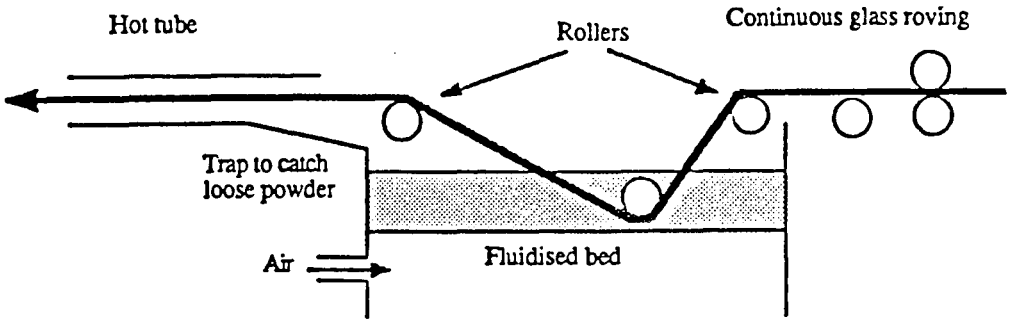

Figure 2.1.6. Schematic diagram of hot-tube process, after Folkes and Kells (1985).

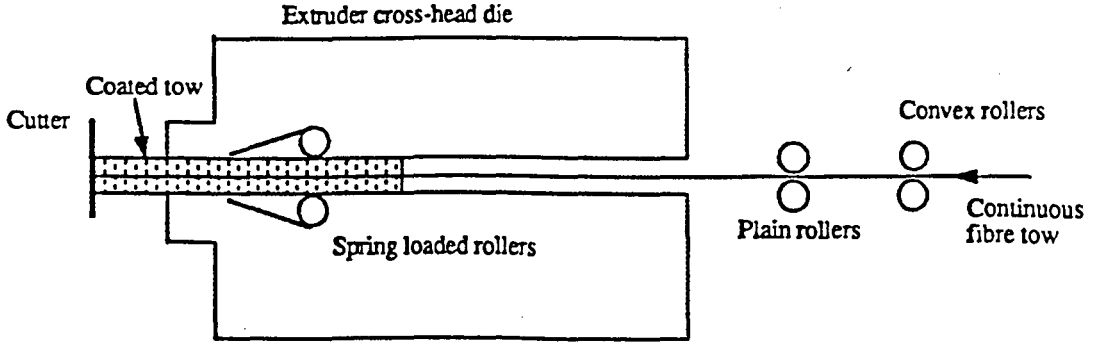

Figure 2.1.7. Redesign of cross head die for thermoplastic impregnation, after Folkes and Kells (1985).

2.1.3.5 Direct melt impregnation

In what has been described as the "impregnation by pultrusion" process, the reinforcement fibres are pulled under tension around a number of cylindrical bars immersed in a melt bath which is fed continuously by an extruder as shown in Figure 2.1.8. The bars perform two important functions and are key features of the process. Firstly, they spread the reinforcement tow, as shown in Figure 2.1.9, and so reduce the penetration depth from the surface to the centre of the tow filament bundle. Secondly, the bars create a pressure gradient as polymer melt is wedged under the tow and between the fibres and the impregnation bar. This pressure build-up encourages flow perpendicular to the fibres comprising the tow bundle and leads to impregnation of the tow bundle. Figure 2.1.10 shows the variation in the film thickness and the associated tension build-up as a fibre tow is pulled around an impregnation bar as described by Chandler et al.(1992)[22]. The action of the fibres passing around the bar is in some ways similar to the mechanism of oil entrainment in a journal bearing.

On leaving the impregnation bath, the fibres are pulled through a tapered, heated wipe-off and sizing die which removes excess polymer melt and performs a final consolidation stage to produce a continuous precursor tow containing a constant volume fraction of polymer matrix. This precursor tow can either be chopped for use as an injection moulding compound, typically into 10mm long pellets, or can be coiled as a continuous precursor. The process may also be used as a direct manufacturing method by using an appropriate number of fibre rovings and a shaping die positioned after the wipe off die, Moyer (1976)[21], Measuria (1986)[23].

Thermoplastic melt impregnation is now an established commercial process which is capable of operating at speeds in excess of 20m/min. However, the mechanisms by which impregnation occurs and the factors which control the levels of impregnation and determine the generation of tension in the fibres within the melt bath are only partly understood, and little published literature exists on the subject.

Bijsterbosch et al. (1990)[24] have investigated the influence of a number of processing parameters on the impregnation of a single glass fibre tow with a nylon 6 melt. Different numbers of spreader bars and different diameter wipe-off dies were investigated at three polymer melt viscosities. Impregnation was carried out at

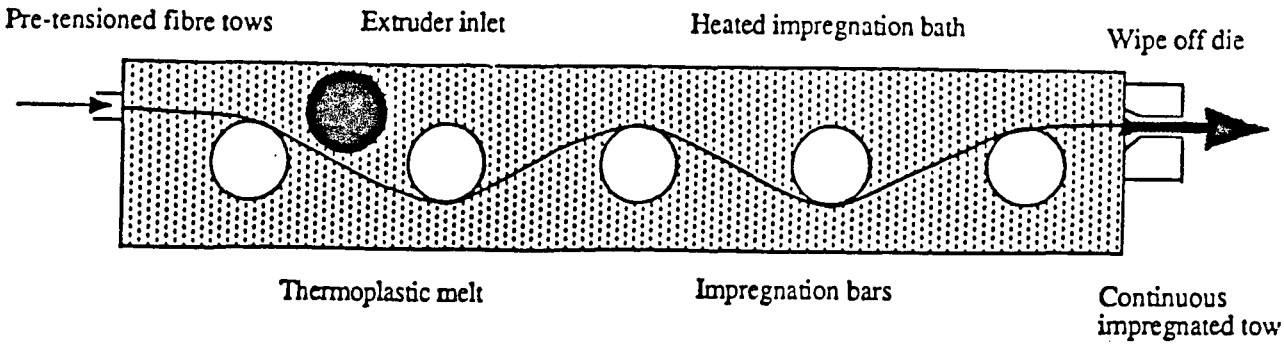

Figure 2.1.8. Thermoplastic melt impregnation bath. This is continuously filled with polymer melt from a cross-head extruder. As the dry fibre tows pass around the fixed bars they become impregnated. A wipe off die removes excess polymer and performs a final impregnation step.

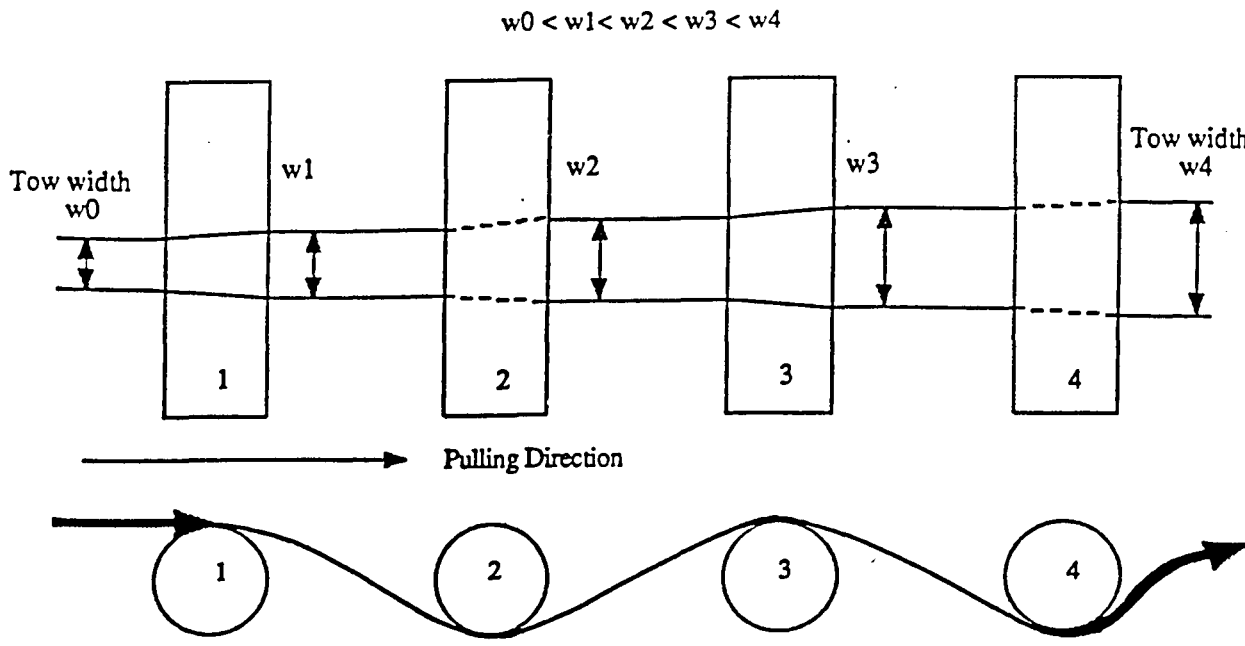

Figure 2.1.9. An illustration of the progressive spreading of a fibre tow as it passes over and under four cylindrical bars. The amount of fibre spreading can be controlled by changing the wrap angle and the radius of the bars.

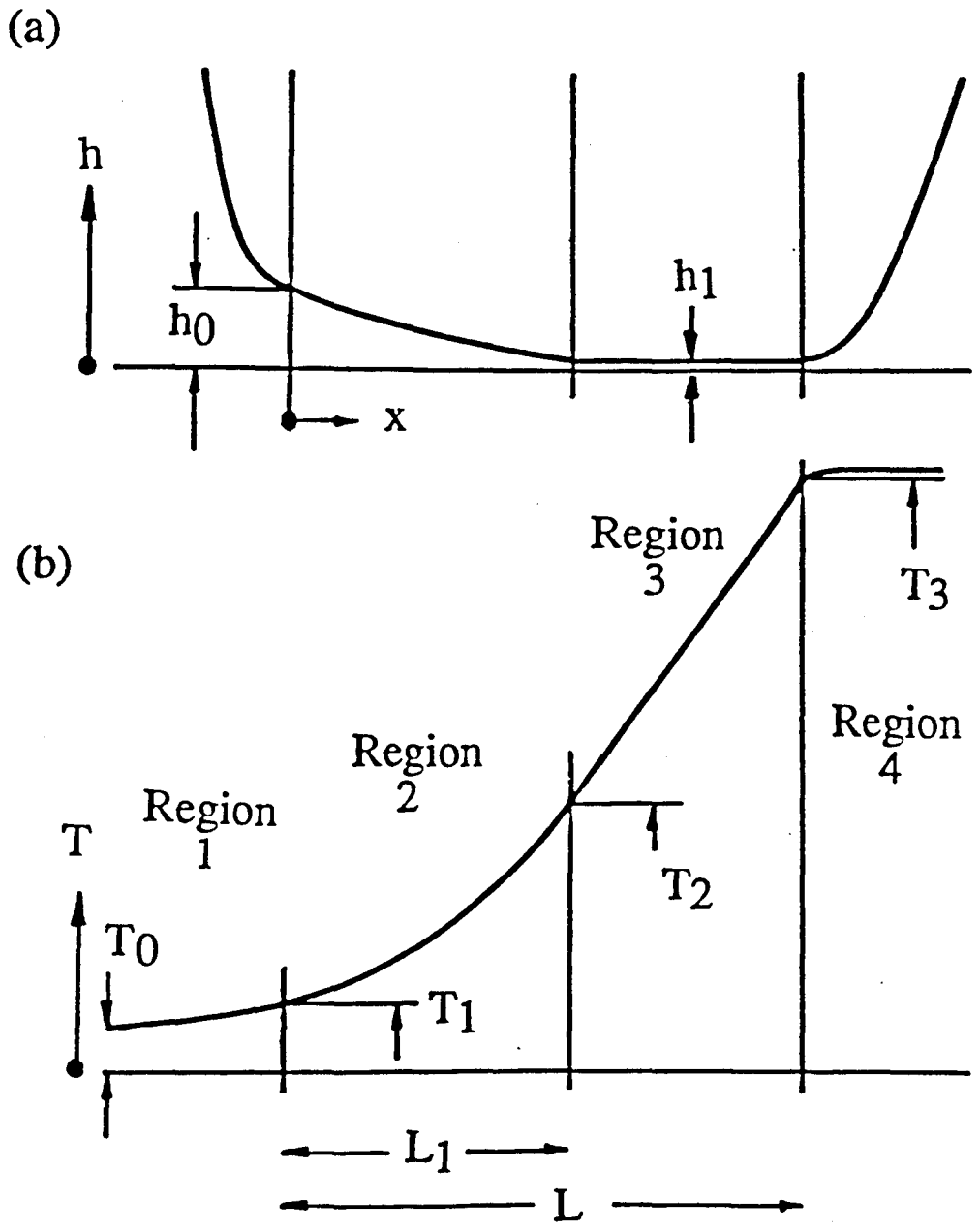

Figure 2.1.10. Schematic of (a) film thickness and (b) tension build-up versus wrap length coordinate in impregnation using cylindrical bars.

line speeds up to 2.5m/min and two types of fibre tow were used, one consisting of 10μm diameter filaments, the other consisting of 20μm filaments. The degree of impregnation was determined by counting the ratio of impregnated to un-impregnated fibres in cross sections taken from the fibre tows. The results of this work are shown graphically in Figures 2.1.11 to 2.1.14.

It was found that the degree of impregnation was very strongly influenced by the use of spreader bars, and that the greatest levels of impregnation were achieved using four bars. Only with four bars was the degree of impregnation independent of line speed for speeds up to 2.5m/min. In addition, it was found that smaller diameter wipe off dies gave greater levels of impregnation. The degree of impregnation was found to decrease with increasing line speed, an effect which was observed for each melt viscosity and for the different filament diameters studied. An increase in the melt viscosity was found to lower the degree of impregnation and the use of larger diameter filaments was found to result in a higher level of impregnation. The effect of wrap angle on impregnation or tension generation in the fibre tow during the process was not investigated.

2.1.3.6 Evaluation of melt impregnated precursors containing continuous fibre reinforcement

The mechanical properties of thermoplastic melt impregnated tapes and rovings, and the effect of different fibre finishes have been investigated by a number of workers.

Mc Mahon and Maximovich (1980)[25] produced a melt impregnated carbon fibre/nylon 6,6 precursor using a two stage impregnation process. This involved cross-head extrusion coating of continuous rovings with a nylon 6,6 melt under a nitrogen atmosphere. This was found to prevent oxidation and moisture absorbtion by the nylon melt. The impregnated fibres were wound onto a drum and the second process stage involved hot rolling to produce an impregnated precursor sheet containing a polymer weight fraction of 0.55. The impregnation process was operated at a line speed of 1.5m/min. The pre-impregnated sheets were then compression moulded, with consolidation times in excess of 10 minutes, in different ply orientations to produce samples for mechanical testing. These tests showed good room temperature tensile and flexural strengths. Unidirectional samples were reported to have an average flexural strength of 1230 MPa and an average interlaminar shear strength of 94.4 MPa.

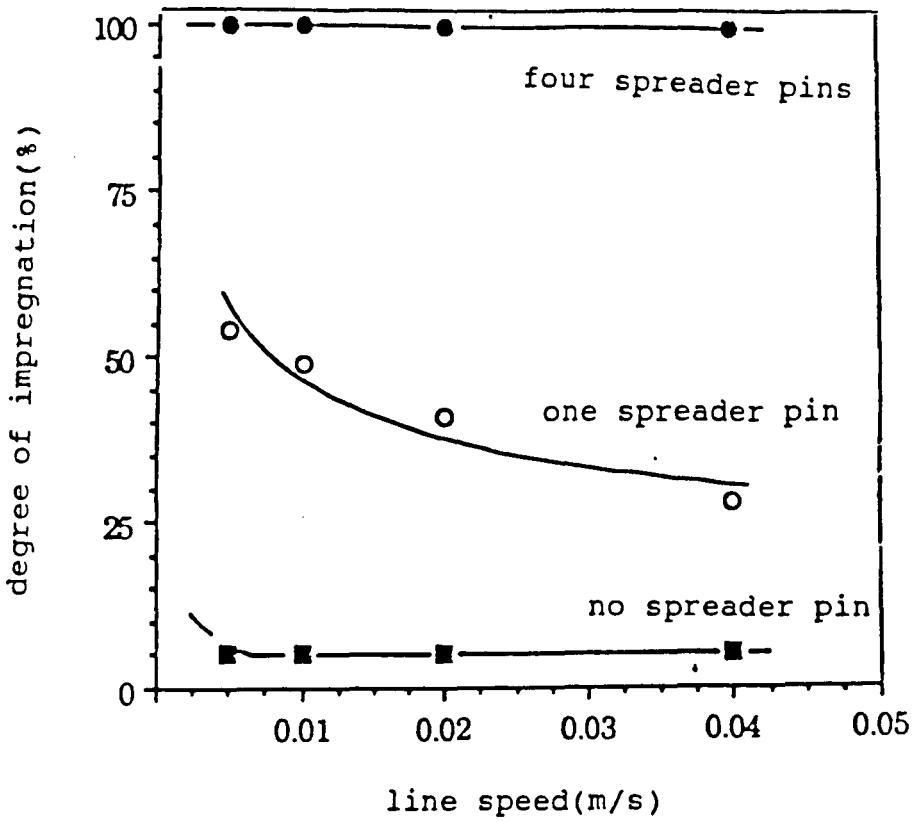

Figure 2.1.11. Degree of impregnation as a function of line speed for different numbers of spreader pins (170Pa.s; 30Vol%; 10μm filaments), after Bijsterbosh et al. (1990).

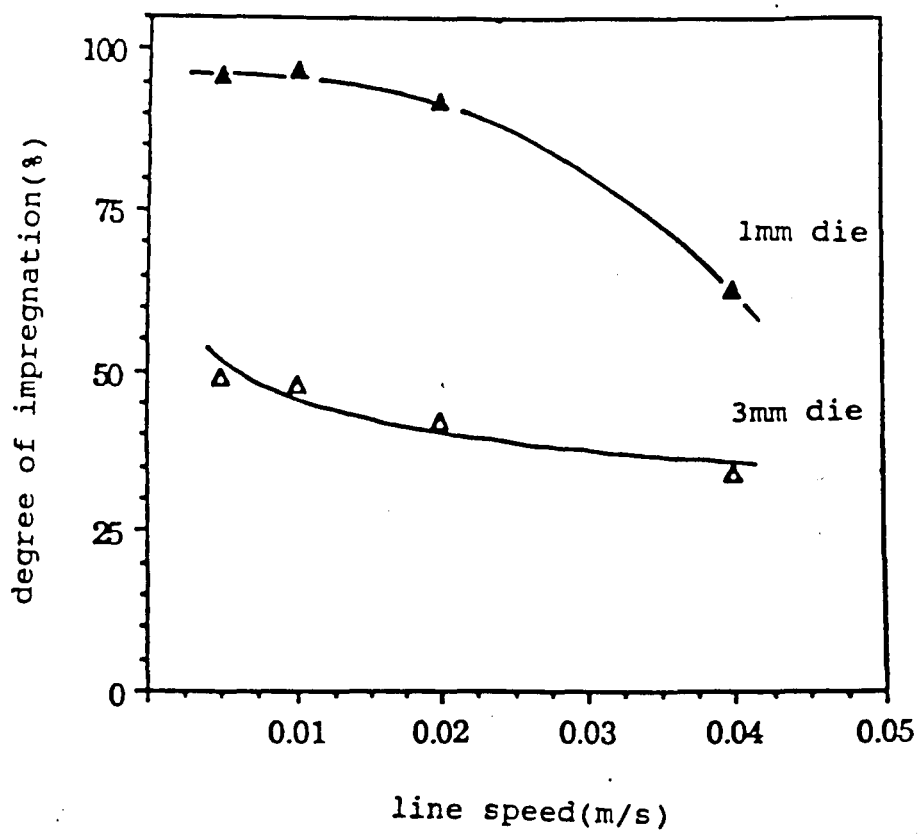

Figure 2.1.12. Degree of impregnation as a function of line speed for different die diameters (3 spreader pins; 170Pa.s; 10μm filaments), after Bijsterbosh et al. (1990).

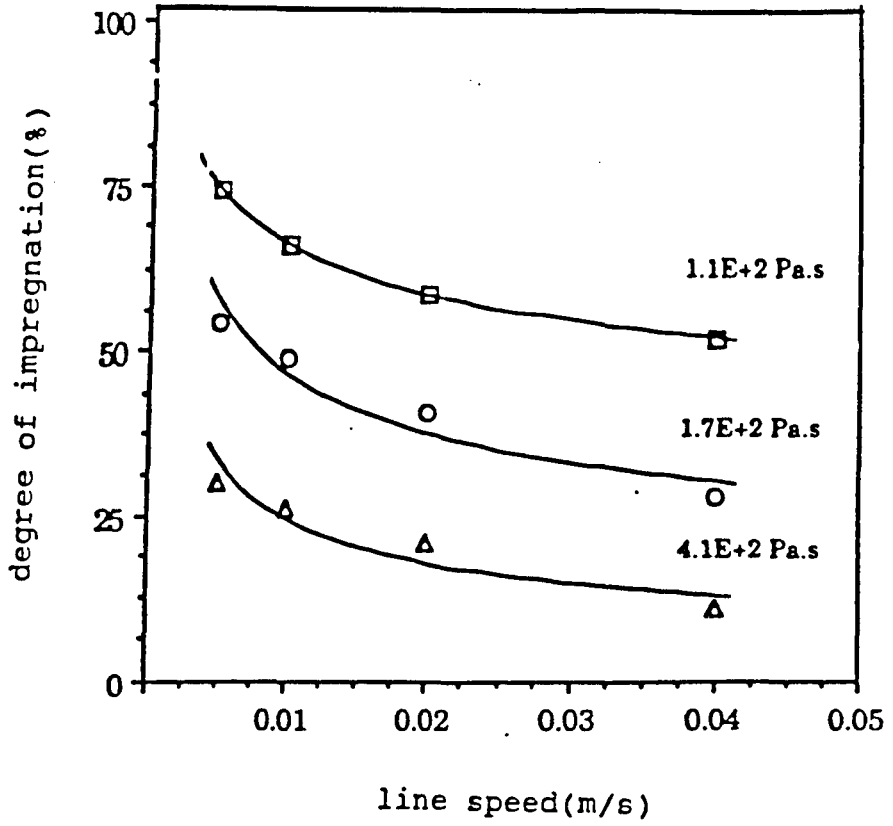

Figure 2.1.13. Degree of impregnation as a function of line speed for different melt viscosities (one spreader pin; 30Vol%; 10μm filaments), after Bijsterbosh et al. (1990).

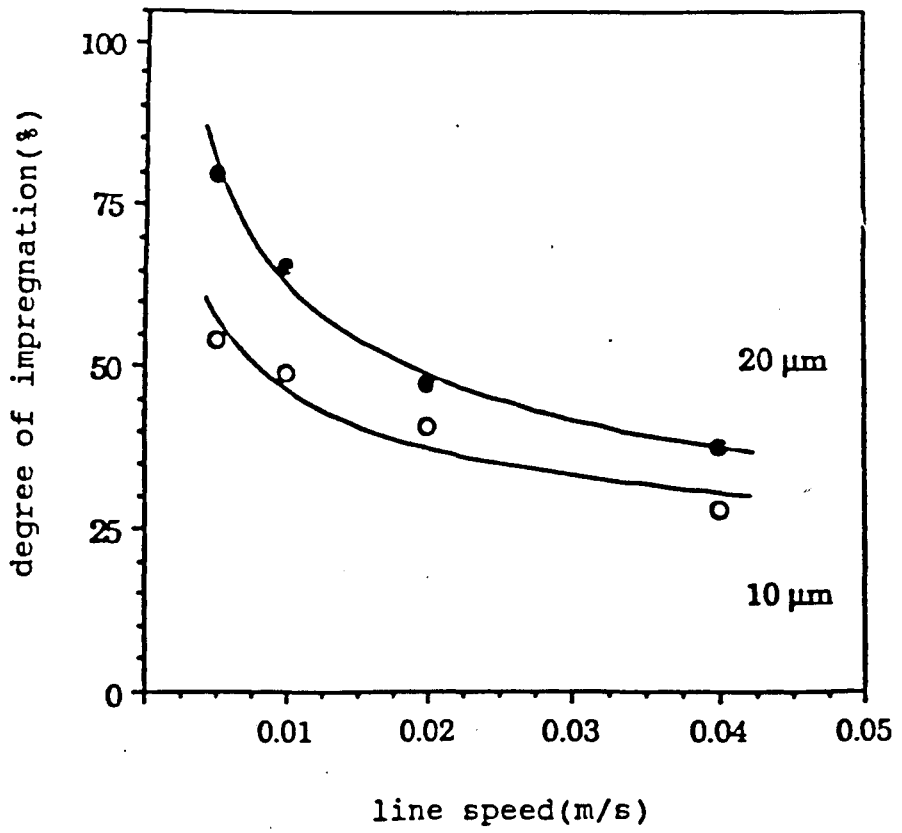

Figure 2.1.14. Degree of impregnation as a function of line speed for different filament diameters (one spreader pin; 170Pa.s; 30Vol%), after Bijsterbosh et al. (1990).

Custer (1988)[26] evaluated melt impregnated glass/polyarylene sulfide (PAS) precursors, produced with a glass volume fraction of 0.55, using a proprietary pultrusion process. Short beam shear tests carried out on compression moulded, unidirectional laminates showed an average interlaminar shear strength of 66.8 MPa. An average flexural strength of 1646 MPa and flexural modulus of 51 GPa was also measured for laminates produced from this material.

Mc Mahon (1984)[19] reports an average flexural strength of 1670 MPa, a flexural modulus of 120 GPa and an interlaminar shear strength of 105 MPa for a unidirectional carbon fibre/PEEK laminate, compression moulded using ICI's APC-1, which has now been superseded by APC-2. An improved flexural strength of 1880 MPa and interlaminar shear strength of 105 MPa have been reported for APC2 [19].

Selected properties which can be achieved from compression moulded laminates, produced from a number of different melt impregnated precursors are summarised in Table 2.1.2.

Selected properties which can be achieved from compression moulded laminates, produced from a number of different melt impregnated precursors are summarised in Table 2.1.2.

Material	Tradename	V_f Reinf.	W_f.Reinf.	Axial flexural strength MPa	Flexural Modulus GPa	Reference
Glass/PP	Plytron	0.35	0.6	436	21	Plytron product literature 82
Glass/Nylon 6,6	Plytron	0.3	---	732	21	Plytron product literature
Glass/Nylon 6,6	Plytron	0.42	---	915	29	Plytron product literature
Glass/Polyurethane	Plytron	0.5	---	105	6	Plytron product literature
Carbon/Nylon 6,6	Plytron	0.39	---	847	58	Plytron product literature
Carbon/PP	Plytron	0.21	---	283	27.4	Plytron product literature
Carbon/PP	Plytron	0.37	---	358	50.6	Plytron product literature
Carbon/PP	Plytron	0.41	---	416	57.8	Plytron product literature

Material	Tradename	V_f Reinf.	W_f.Reinf.	Axial flexural strength MPa	ILSS MPa	Flexural Modulus GPa	Reference
Glass/Nylon		0.5	---	620	41.3	22.7	Youngs et al.(1985, 83
Glass/PP		0.65	---	220	25.5	17.9	"
Carbon/PPS		0.63	---	1364	68.9	124	"
Carbon/PEEK	APC1	0.54	---	1667	103.4	119.8	"
Carbon/Nylon 6		0.2	---	496	42	24.8	"
Glass/PAS	Hexcel	0.52	---	1647	66.8	51	Custer (1988) 26
Carbon/PBT		0.5	0.5	1260	58.6	127	Mc Mahon and Maximovich (1980, 25
Carbon/Nylon		0.6	0.55	1230	94.4	142	"
Carbon/PEEK	APC2	0.61	---	1880	121	105	Leach (1989) 6
Carbon/PPS	Ryton	0.6	---	1897	117	69	"

A number of other impregnation technologies have been developed for the impregnation of long and continuous fibre reinforced materials.

2.1.3.7 Solvent impregnation

It is possible to reduce the melt viscosity of thermoplastic resins by the use of solvent diluents or plasticizers. Solvent impregnation can therefore offer an alternative approach to achieve the uniform coating of each fibre within a fibre bundle. For those polymers for which a suitable solvent systems exist, it is possible to reduce the viscosity of the thermoplastic matrix polymer prior to impregnation. The resulting thermoplastic solution enables impregnation of both unidirectional and woven reinforcement forms to be carried out using similar techniques to those used in conventional thermoset processing. Unfortunately, if the matrix resin is readily soluble it will be liable to attack from certain solvents and will thus have a restricted service performance. It can also prove difficult to fully remove all the residual solvent from the final product, resulting in void formation.

Goodman and Loos (1989)[27] used a solution dip to impregnate continuous graphite fibres with a polyethersulphone (PES) matrix. The impregnation process consisted of mixing a solution of PES and 1-Methyl-2-Pyrrolidinone (NMP) in a nitrogen atmosphere. For solutions containing less than 30 wt% of resin, this mixing could be carried out at room temperature. However at higher resin contents, the high viscosities involved made mixing at temperatures up to 150°C necessary. The carbon fibre tows were heated to 120°C prior to impregnation and pulled through the polymer solution. In order to remove the solvent from the prepreg, it was necessary to heat the prepreg under a vacuum for 2 hours at 275°C. This was followed by a further four hours in a convection oven at 275°C. On examination of the pre-impregnated precursors produced, the importance of fully removing all the residual solvent was highlighted. Voids in the prepreg were attributed to incomplete solvent removal and solvent retention at the fibre/matrix interface, and resin rich areas in the prepreg were attributed to incomplete impregnation.

A range of thermoplastics such as polysulphone, polyethersulphone, polyphenolsulphone, poltetherimide (PEI) and polycarbonate are all suitable polymers for impregnation by the solvent process and, with the exception of polycarbonate, demonstrate an exceptionally good range of mechanical properties. However, it is essential that they possess good solvent resistance, especially

towards aircraft hydraulic fluids.

Van Loo (1988)[28] has discussed the highly successful solvent impregnation of PEI/glass prepregs which can be processed by moulding, deep-drawing or roll-forming. They can also be used to produce Nomex or aluminium sandwich panels. Although the susceptibility of solvent impregnated PEI prepregs to certain solvents has restricted their use in certain environments, they are suitable for interior aerospace applications, where they possess excellent fire, smoke and toxicity properties. Filter housings for the Fokker F-100 aircraft are produced from this material using a deep-drawing technique.

2.1.3.8 Fibre hybridisation and co-mingled fibre yarns

Co-mingled yarn precursors consist of an intimate mixture of continuous, finely spun thermoplastic filaments and reinforcement fibres. The form of the precursor produced is shown in Figure 2.1.15, the diameter of the thermoplastic matrix fibre usually being in the order of 25μm. These yarns are produced using methods adapted largely from textile technology.

Two distinct processes are used to produce co-mingled yarns. One is termed stretch breaking and converts continuous reinforcement filaments into a yarn with a distribution of long and short fibre lengths with a mean fibre length in the order of 7.5 to 10cm. These fibres are then spun along with matrix fibres to produce a yarn. The stretch breaking process is claimed to remove weak points in the fibres and improve their spinnability. A retention of over 80% of the tensile strength and 95% of the tensile modulus has been reported for Courtaulds 'Heltra' material [29]. Another commercially available stretch broken yarn is produced by Schappe [30]. The other production process involves spinning continuous reinforcement and continuous matrix fibres into a yarn with no broken fibres.

These types of yarns offer a distinct advantage over other thermoplastic prepregs in. that they can be produced as a soft fabric form and are highly drapeable. Because of this they can be made into various prepreg forms ranging from unidirectional to woven, braided and knitted structures. A range of thermoplastics can be spun from the melt and these include nylon, polypropylene, polyethylene terephthalate (PET), PEEK and polyphenol sulphone (PPS). These can be combined with any of the

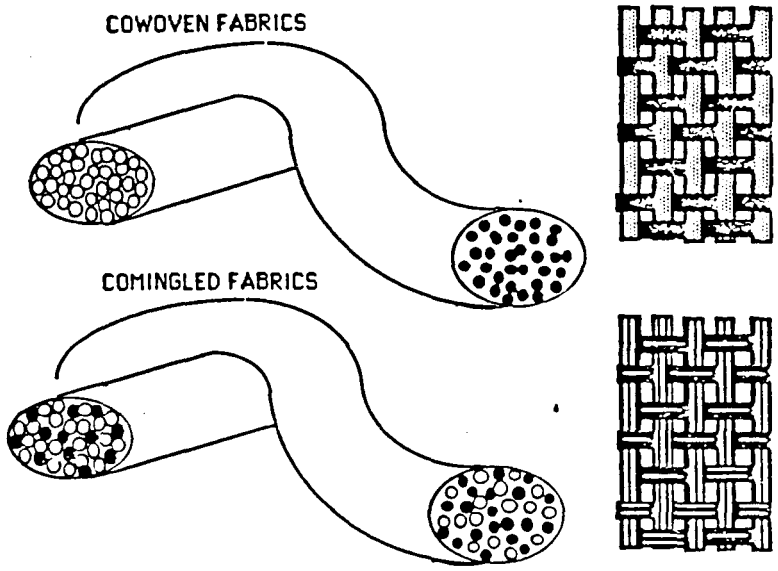

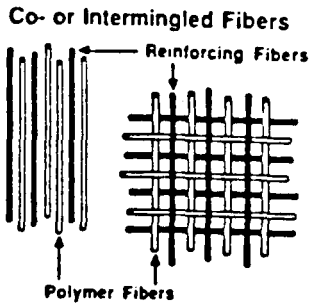

Figure 2.1.15. Co-mingled yarn precursor.

common reinforcement fibres, glass, carbon or aramid, to produce continuous hybrid yarns. The main drawback to these types of materials is that in order to achieve wetting it is necessary to maintain them under temperature and pressure for a considerable length of time. This may preclude their use in continuous processes such as pultrusion or rapid stamping applications.

2.1.3.9 Sheet impregnation processes

Another area of thermoplastics processing where impregnation of continuous fibres is essential is in the production of thermoplastic sheet materials for stamping applications.

The Azdel lamination process is illustrated in Figure 2.1.16, Van Damme (1988) [31]. In this process, continuous strands of unidirectional or random glass mat are combined with a thermoplastic matrix in a continuous process comprising of two stages. Firstly, the reinforcement is deposited at random on a moving conveyer to produce a two dimensional mat and is then processed to provide a third dimension which holds the glass mat together. The mat is then fed together with a resin film and molten resin from a sheet extruder into a belt press with heating and cooling zones and an impregnated sheet is formed under pressure from the belt press. The precursor produced is in the form of a stiff, flat sheet which is incompletely wetted out and which typically contains a high void content.

The Radlite process [31] is similar in some respects to the process of paper making. It involves combining long discontinuous fibres with powdered thermoplastic in an aqueous slurry. This mixture is then drained, dried, heated and consolidated to form an impregnated sheet, as shown in Figure 2.1.17. The form of the precursor is again a stiff, flat sheet, from between 0.4 to 4 mm thick, which can be supplied as a continuous roll.

2.1.4 The processing of pre-impregnated thermoplastic precursors

The production of a fully wetted out and impregnated precursor is only the first step towards producing a composite part which will fully optimise the properties of the constituent components. The second critical stage is the conversion of the precursor into a composite moulding or sectional shape, in such a way as to achieve

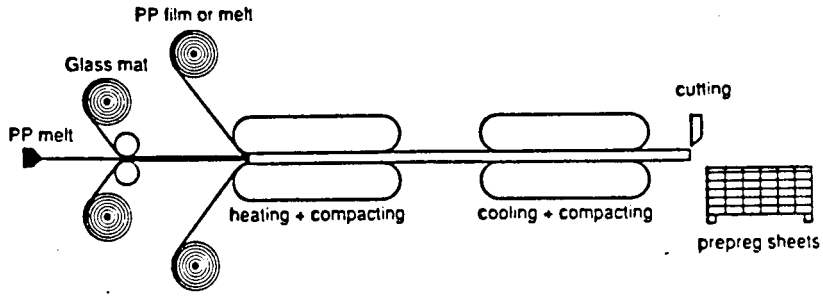

Figure 2.1.16. The AZDEL laminating process for thermoplastic sheet materials. The process combines thermoplastic resin matrices with continuous strands of random or uni-directional orientated, glass fibre mat. After Van Damme (1988).

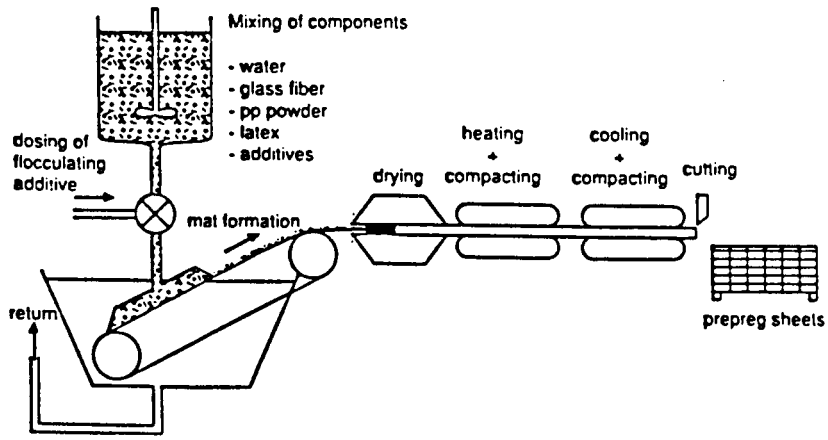

Figure 2.1.17. The RADLITE process for thermoplastic sheet materials, after Van Damme (1988).

the required properties with consistency and using an economical processing method. In parallel to the development of continuous precursors, processing technologies have developed from thermoset technology, from conventional thermoplastic technology and from metal forming. In addition, some new processes have been specifically developed.

2.1.4.1 Discontinuous long-fibre processing

Before the commercial availability of long fibre reinforced injection moulding compounds, the standard process route for reinforced thermoplastic composites was the injection moulding of extrusion compounded precursors. This had the disadvantage that only short fibre lengths remained in the moulded article. However, with the development of well-impregnated, parallel strand reinforced pellets, substantial improvements in the properties of injection moulded components as a direct result of reduced fibre breakage has been demonstrated. Cuff (1984)[32] has measured a weight average fibre length in excess of 5 mm in glass/nylon 6,6 mouldings, containing a fibre volume fraction of 30%. Henshaw and Wilkins (1990)[33] have also demonstrated the significantly increased mechanical performance of a component produced from long fibre carbon/PPS moulding pellets over an identical component moulded using a traditional short fibre injection moulding material.

The development of long fibre moulding compounds was important for composite applications in which a random orientation of long fibre reinforcement provided the required properties. However, many high performance applications of thermoplastic composites require continuous reinforcing fibres in very specific orientations to achieve the specified properties. This has stimulated the development of alternative processing routes which maintain the continuous fibre lengths and the desired fibre orientations in the final moulded product.

2.1.4.2 The processing science of continuous thermoplastic precursors

Before discussing the processing methods applicable, it is important to have an appreciation of the mechanisms by which the fibres and resin flow and deform to produce the required shape. The four principal mechanisms have been identified

and are illustrated in Figure 2.1.18, Cogswell (1987)[34]. These are: resin percolation through and along the fibres; transverse flow (squeezing flow); interply slip between layers of fibres; intraply slip along the fibre direction. Although the fibres are virtually inextensible, individual plies are capable of spreading transversely and in shear, and some or all the deformation mechanisms must occur in order to completely form any particular part. The ability of the thermoplastic precursor to form the part must be considered in the design of both the part and the mould, and this is especially relevant for parts containing regions of curvature. Two undesirable features can occur even in simple bends. Resin can either be squeezed to the outside of the bend or buckling can occur on the inner surface. In high performance applications especially, the effects of fibre misorientation and surface quality can have a great effect on the overall mechanical properties of the composite part.

2.1.4.3 Compression moulding

An attractive process for forming relatively simple shapes is to heat a number of pre-impregnated plies to a temperature above the melting point of the matrix in a matched die mould, press them into shape and then cool the consolidated shape under pressure to below the glass transition temperature of the matrix resin. The solid part can then be removed from the mould. Due to the fact that the precursors are already in a highly impregnated state, the heating, forming and consolidation times can be short. A typical process cycle for a simple laminate produced using carbon/PEEK (APC2) precursor is shown in Figure 2.1.19.

It is possible to reduce cycle times still further by the use of a fast closing press to stamp pre-heated material blanks into shape. In this process the male plunger may be made from a deformable rubber material which allows fibre reorganisation and consolidation to occur in the metal cavity with little fibre wrinkling and buckling. The stamping process has been investigated using 20% carbon fibre/polypropylene precursors to produce a 90° bend Freidrich et al. (1991)[35]. An initial moulding step was carried out to form a pre-consolidated flat laminate by compression moulding pre-heated plies under a pressure of 1.2 MPa for 11 minutes. The pre-heat time was 15 minutes. These laminates were then re-heated and stamped using a cold matched metal tool. The cycle time for the stamping operation was reported to be only 2 minutes. It was found that the success of the stamping operation depended on a number of factors. The temperature of the precursor material had to

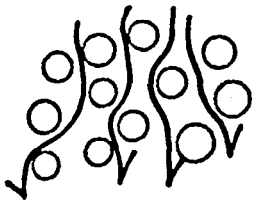

1. Resin percolation through and along the fibres

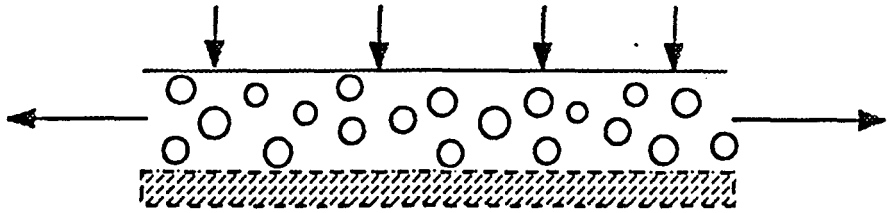

2. Transverse fibre flow (Squeezing flow)

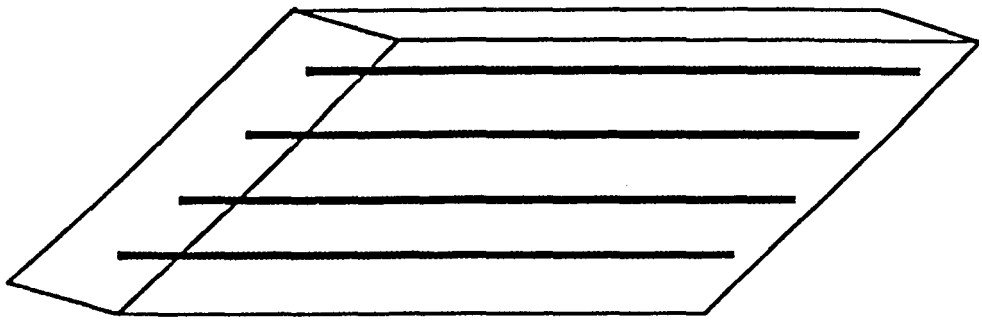

3. Intraply shearing of individual fibres along the fibre direction.

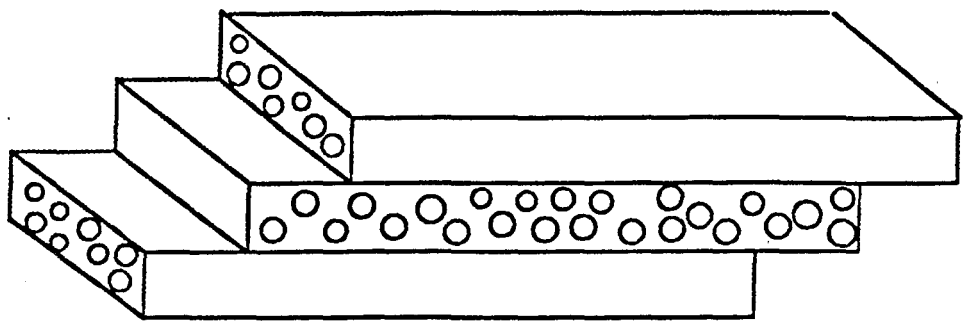

4. Interply slip - cooperative flow in which layers may be of different orientations.

Figure 2.1.18. The four flow mechanisms which occur during the processing of thermoplastic composites, after Cogswell (1987).

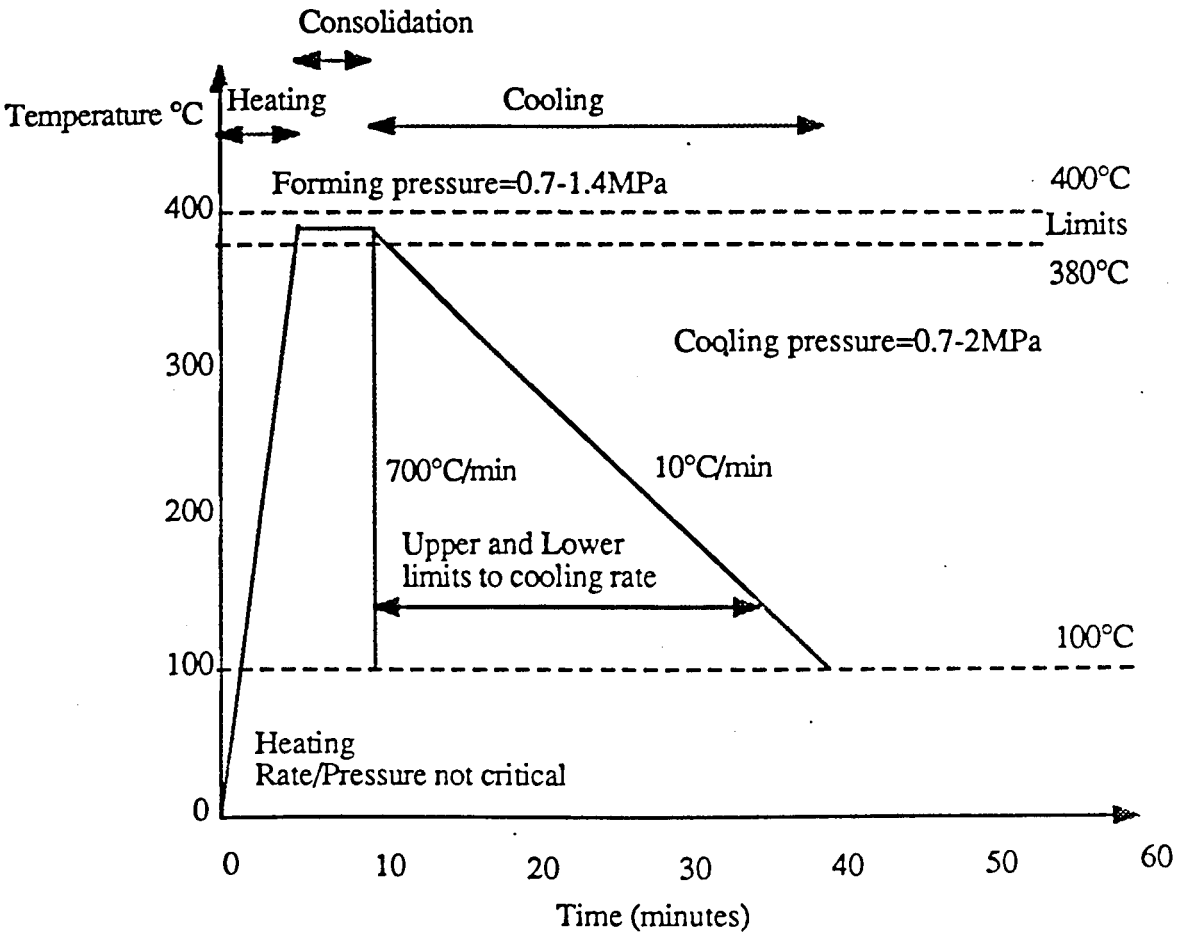

Figure 2.1.19. A typical processing cycle for the compression moulding of an APC2 (carbon/PEEK) laminate, Data from Leach (1989).

remain within a few degrees above the melting temperature of the matrix. This was found to reduce fibre buckling and breakage. Stamping times above 15 seconds were found to produce good mouldings. It was also found that the stamping pressure exerted the greatest influence on the properties of the final part.

2.1.4.4 Diaphragm forming

A key element of the diaphragm forming process is the use of hydrostatic pressure to stretch heated, pre-impregnated materials elastically over the desired shape using a diaphragm to move, mould and consolidate the laminate. In the diaphragm forming process, an unconsolidated composite lay up is produced from individual plies of a well wetted out pre-impregnated precursor. These can be placed in any required orientation. This lay up is then sandwiched between two thin, plastically deformable sheets of material. These sheets are termed the diaphragms and may be metallic, polymeric or of a composite construction. The diaphragms are then clamped and heated in an autoclave to the composite processing temperature. Once at this temperature, the diaphragm/pre-preg sandwich is forced to stretch elastically under over the shape to be produced under an applied hydrostatic pressure. The diaphragm forming of a 90° bend is illustrated in Figure 2.1.20, as described by O'Bradaigh and Mallon (1988)[36]. In this case, the forming takes place by exerting a greater pressure, P+, in the pressure vessel than in the mould cavity, P-. It is necessary for the diaphragm sandwich to be maintained under vacuum to remove any air trapped in the system and to remove any gases which may be given off during the melting of the matrix. During the pressurisation and forming stage, the diaphragm acts to maintain the composite part in biaxial tension and restricts laminate wrinkling, splitting and thin spots Monaghan and Mallon (1990)[37]. The composite deforms by mechanisms such as inter-ply slip and fibre reorganisation. Commonly used diaphragm materials are thin, high temperature polyimide films, Kapton, which possess good elongational properties at elevated temperatures. A typical process cycle for the diaphragm forming of an APC2 (carbon/PEEK) component is shown in Figure 2.1.21. Providing that the autoclave is preheated then cycle times of about 60 minutes are possible. Process temperatures of 360-390°C, at a pressure of 0.42 MPa, during forming and consolidation have been found to produce the optimum properties for parts formed using APC2 precursors, O'Bradaigh and Mallon (1988)[36]. A disadvantage of this process is the long cycle time for each part, the high pressure autoclave required and the complex nature of

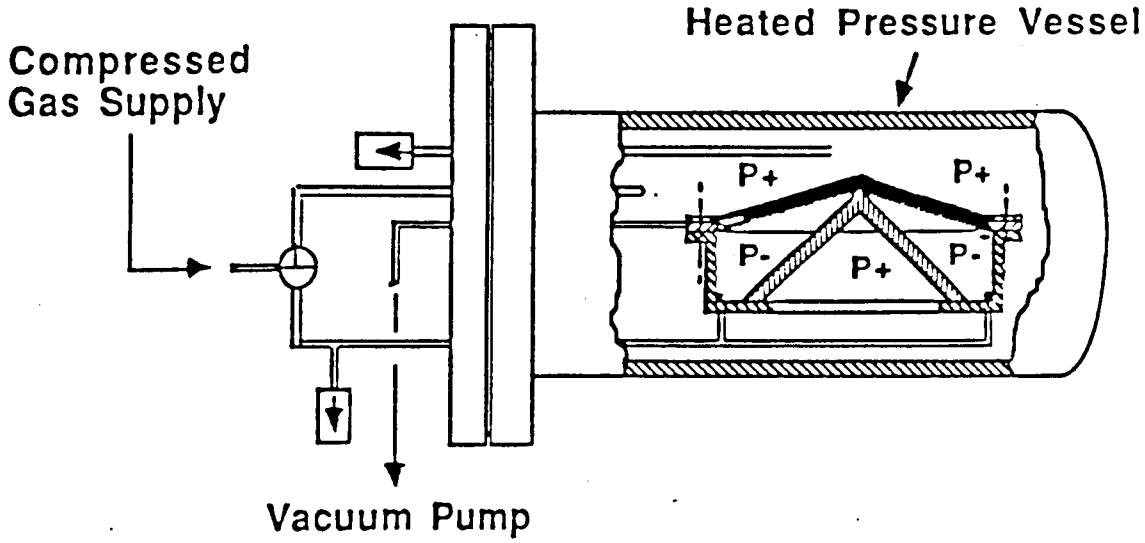

Figure 2.1.20. Polymeric Diaphragm forming process, for a 90° bend, inside an autoclave, after O'Bradaigh and Mallon (1988).

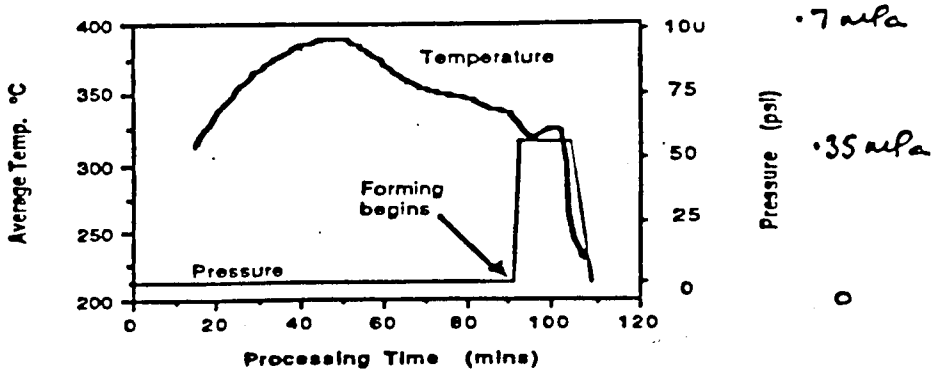

Figure 2.1.21. Process cycle for APC2 90° part, heated to 385°C, cooled to, and formed at 335°C, after Monaghon and Mallon (1989).

the process.

2.1.4.5 Thermoplastic filament winding

The reduction of cycle times in the production of thermoplastic composite components requires an automated processing method which is capable of laying up the required ply orientation and of applying sufficiently high temperatures and pressures to fuse and consolidate the structure.

In the process of thermoset filament winding, continuous rovings or fibre strands are pulled under tension through an impregnation bath and then wound with a high degree of accuracy onto a mandrel in pre-determined angles. After curing, hollow components can be produced which can be either cylindrical or spherical in shape for applications which include rocket motor cases, pressure vessels, driveshafts, storage tanks and pipes.

The availability of pre-impregnated precursors in thin tape form has allowed the extension of the filament winding process to thermoplastic composites. As in any manufacturing process using thermoplastic precursors, three stages must occur. The matrix polymer must be heated to above its melting point, the shape must be formed and consolidated under pressure and the new shape must be cooled with a minimum of distortion.

The thermoplastic filament winding process is shown schematically in Figure 2.1.22. The prepreg tape must be heated and allowed to remain molten as it is laid down onto the surface of the mandrel or laminate. To facilitate this it is possible to attach a hot air oven to the traverse carriage of the filament winding machine. This ensures that the distance between the oven exit and the mandrel remains constant and ensures that the precursor arrives at the mandrel at a constant temperature. In thermoplastic filament winding it is necessary for the average temperature between incoming tow and the previous layer to be above the melting temperature of the matrix polymer. As the precursor comes into contact with either the mandrel or the previously laid down substrate layer, a hot air gun or an infra red source can be used to provide a localised melt zone in which consolidation pressure can be applied. In many cases this pressure can be generated by regulating the tension applied to the incoming tape, although an additional nip point roller can be used to apply a mechanical pressure.

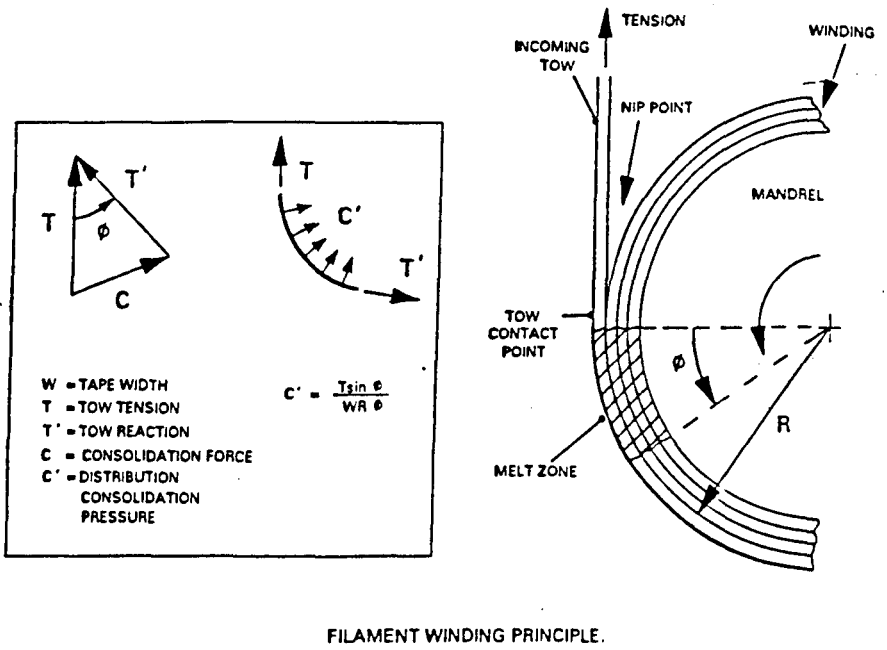

Figure 2.1.22. Filament winding process whereby tension is used to apply consolidation force to localised melt zone, after Whiting (1991).

Thermoplastic filament winding has been demonstrated to produce good quality hoop wound polypropylene/glass and nylon/glass pipes of various wall thicknesses. An alternative approach to heating the thermoplastic tape is to use only localised heating to provide a carefully controlled melt zone, Whiting (1988)[38]. This zone must extend far enough into the substrate to allow full consolidation but not too far to cause tape slippage between the incoming tow and the substrate which will alter the winding angle. In addition the heat source must be of sufficient intensity to achieve sufficiently high heat transfer rates to allow a high winding speed. Whiting (1988)[38] has demonstrated the production of a number of components including a 200 mm diameter filament wound tube for use as an underwater weapon systems structure. This was wound using APC2 precursor and incorporated fibres wound at 0°,± 45° and 90°. The resulting composite structure was found to contain void contents of less than 2% which is an essential requirement in obtaining the optimum composite properties.

Work has also been carried out on winding the precursor using high speeds at a temperature just sufficient to tack the plies together. This stage is then followed by post consolidation under vacuum in an autoclave after removal from the winding machine, Anderson (1991)[39]. This has been found to produce reasonably good hoop wound tubes although the technique is limited to thin walled structures if surface wrinkles are to be avoided.

2.1.4.6 Roll forming of thermoplastic composites

Using an adaptation of a standard cold-roll, sheet metal forming technique, flat thermoplastic pre-impregnated materials can be rolled to form long structural sections. In this process the thickness of the laminate formed did not change appreciably during rolling. The feasibility of this process has been demonstrated, Cattanach and Harvey (1984)[40], using a number of stands of driven rolls and carbon/PEEK (APC2) precursors. Top hat and channel sections were successfully produced at speeds of between 7.6-15.2 m/min. The effectiveness of this process was found to depend on the adequate pre-heating of the flat material blank using an infra red heat source prior to rolling and in preventing premature freezing of the material blank before forming was completed.

2.1.5 The pultrusion of composite sections

The word pultrusion is often used to describe both the process and the resulting product, which is a solid shape or profile, having a constant cross section and continuous length. The thermoset pultrusion process was developed in 1948, Martin (1984)[41], to produce continuous, unidirectional reinforced solid rods which were used for fishing rod blanks. A typical form of the thermoset pultrusion process is illustrated in Figure 2.1.23. In the 1960's, the introduction of continuous strand glass mat into the process allowed the production of structural profiles having more isotropic properties. It is now possible to produce a wide range of standard shapes including rod, tube, bar and channel sections which can combine unidirectional, bi-directional and random in-plane orientations of fibre reinforcements.

Both thermoset and thermoplastic pultrusion are illustrated in Figure 2.1.23, which highlights the main differences between the two. In the simplest form of the thermoset process, reinforcement is pulled through a resin bath where it is fully impregnated with a liquid thermoset resin, it is then pulled through a sequence of forming and wipe off dies which preshape the material and feed it into a heated die, usually 70-150 cm in length. This die is heated to the cure temperature of the matrix resin. A fully cured section is produced by the die exit and this is pulled continuously through the process using a haul off mechanism. The process is suitable for almost all thermoset resin matrices although polyesters and epoxies are most commonly used. Glass and carbon are the most common reinforcement types and sections containing fibre volume fractions of up to 0.6 can be produced, depending on application.

The thermoplastic pultrusion process consists basically of a material dispensing stage, a heating stage to melt the thermoplastic resin, a forming and consolidation stage and a cooling stage. It is possible to produce impregnated thermoplastic precursors on-line as an integral part of the process. In all the work carried out in this thesis various preimpregnated precursors were used and no on-line impregnation was undertaken.

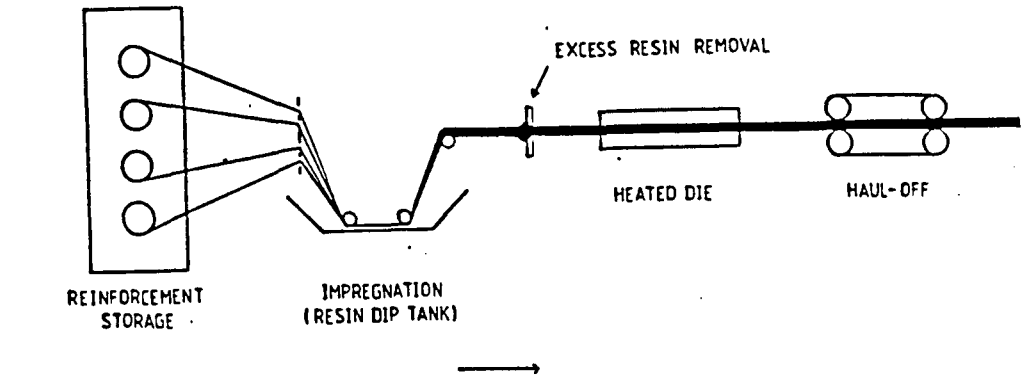

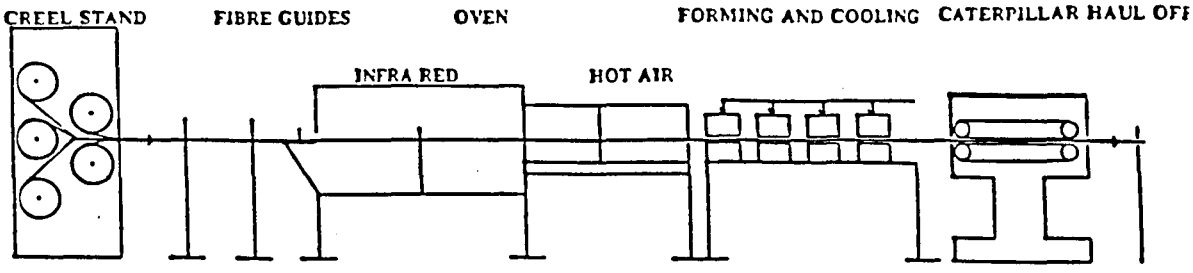

Figure 2.1.23. Schematic illustration of the thermoset and thermoplastic pultrusion processes, showing the common features and the differences between the two.

2.1.5.1 Thermoplastic pultrusion

The thermoplastic pultrusion process can be thought of as direct development from the continuous impregnation methods reviewed earlier, although the specific purpose is to produce a continuous composite sectional shape or profile. A generalised thermoplastic pultrusion production line is illustrated in Figure 2.1.24 as a flow chart which summarises the various options available for each stage. The process can either combine a fully integrated on-line impregnation stage with the forming and consolidation stage, or can use continuous precursors as a feedstock which then must pass through a heating stage to remelt the matrix before forming can take place. There is not yet a standard accepted form for the various stages which make up the thermoplastic pultrusion line and a number of workers have attempted several different approaches which will be reviewed. It is important that each individual stage performs its particular functions as a fully integrated on-line manufacturing process.

Precursors produced either on-line or off-line can be used in the thermoplastic pultrusion process without causing major changes in the design of the forming, consolidation and cooling stage. However, some pre-impregnated precursor forms have been found to be more suitable than others for pultrusion. In cases where on-line impregnation is necessary, it is important that an impregnation method is chosen which is suitable for the matrix polymer and which can be carried out at operating line speeds compatible with the operation of the forming stage. The current impregnation technology has been reviewed earlier and all of the reported techniques for continuous fibre impregnation can be made suitable for on-line impregnation. However, this requires that the control of the fibre volume fraction also occurs on-line and that impregnation speeds are sufficiently high to make the process commercially viable. A disadvantage in using on-line impregnation may arise from any limits imposed on the line speed so as to remain within limits of efficient impregnation, or conversely, to allow sufficient consolidation time in the forming stage. It may also be difficult to simultaneously impregnate the number of fibre tows necessary to produce large sectional shapes.

Once an impregnated precursor has been produced it is necessary for either the polymer to be heated to above its melting point before it is collimated and fed into the forming stage of the process. A number of heating methods can be used to fulfill the heating stage of the process and the most important consideration is that all the product cross section is heated uniformly.

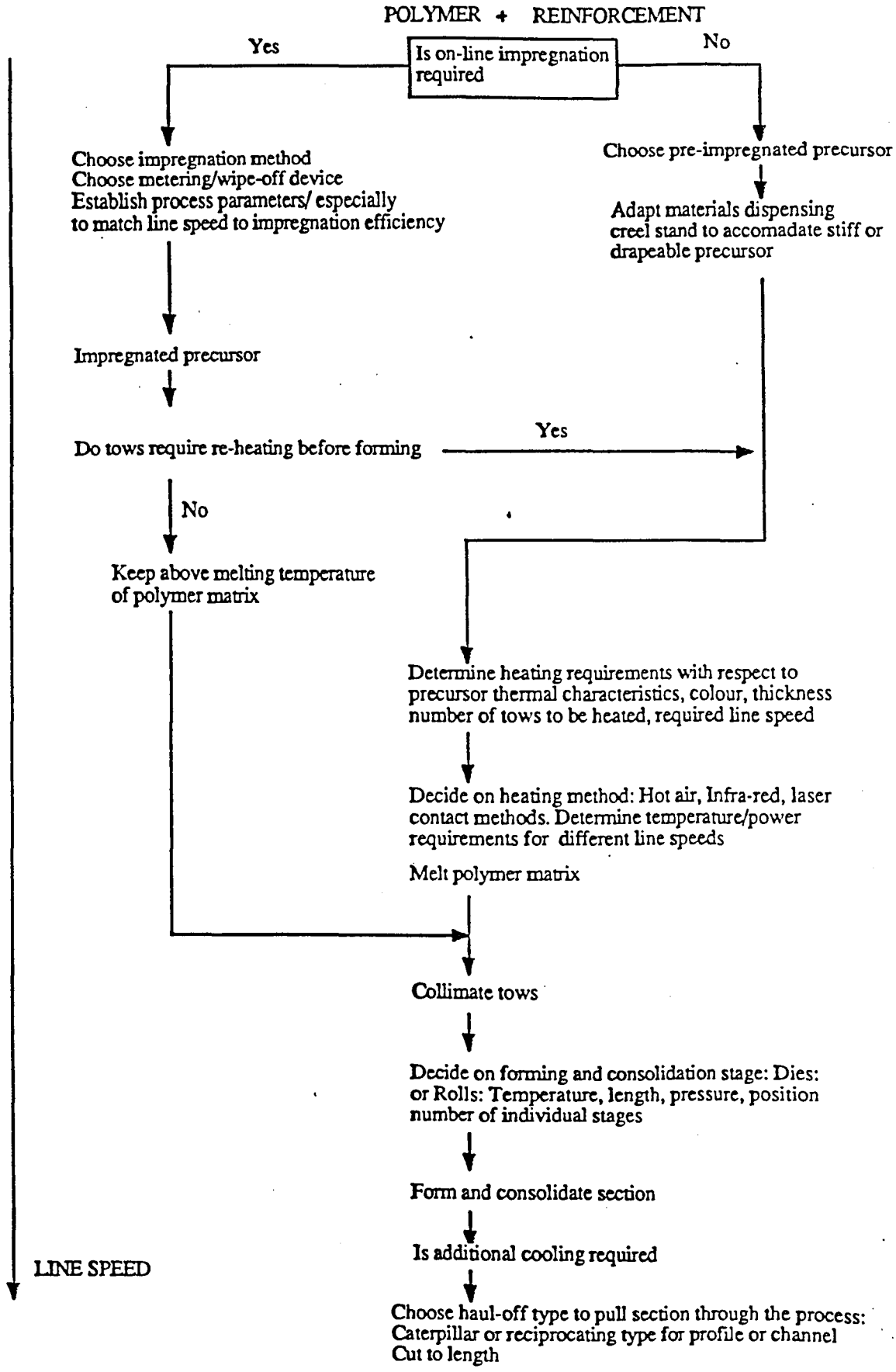

Figure 2.1.24. Flow diagram illustrating the various process options possible for thermoplastic pultrusion.

The most simple non-contact heating method is to use a hot air oven which combines conductive and convective heating to melt the precursor material. An inert gas atmosphere can be used to prevent oxidation and degradation of the polymer matrix. A disadvantage of this heating method is that precise control of the air temperature is difficult and heating involves only surface absorbtion of heat. All the through-thickness heating must therefore occur by conduction. In addition, excessively high temperatures are required to achieve the high heat transfer rates necessary to run at high line speeds.

It is possible to greatly increase the temperature gradients to which the precursor material is subjected to by using a high intensity heat flux such as an infra-red heat source, and a choice of wavelengths is available to suit particular thermoplastic polymers. The choice of infra-red wavelength is influenced by a number of factors which include the physical characteristics of the polymer matrix and the colour of the precursor material. Although short wave emitters can facilitate the greatest degree of temperature control due to their fast response time in both heating and shut down, they are only effective on tinted precursors. On the other hand, long and medium wave infra-red emitters are capable of efficiently heating both clear or tinted sheet precursor materials, produced in a range of thermoplastic matrices, Committee for Electroheat (1990)[42]. For sheet materials over 2mm thick, medium or short wave will provide the most efficient penetration and cause less surface overheating. The infra-red transmission spectrum for a 1mm thick, unpigmented nylon 6 thermoplastic is shown in Figure 2.1.25 [42]. This shows that short wave radiation is mainly transmitted while medium and long wavelengths are strongly absorbed.

A comparison of the temperatures at the base of a 2mm thick laminate, heated by different heat sources is shown in Figure 2.1.26, Grove (1988)[43]. This illustrates the temperature gradients which can be achieved with different convection heat transfer coefficients and with heat fluxes typical of infra-red and laser heating. The convective heating rate depends on the temperature difference between the hot air and the laminate surface, so that the temperature approaches the set temperature asymptotically. As can be seen, increasing the heat flux not only reduces the time taken to reach the desired temperature, but also creates higher temperature gradients, especially near the surface. It is for this reason that laser heating is not very suitable when the aim is to heat individual precursor tows to a uniform temperature through their thickness without surface degradation. Another important consideration is to ensure that the precursors are as thin as possible in order that

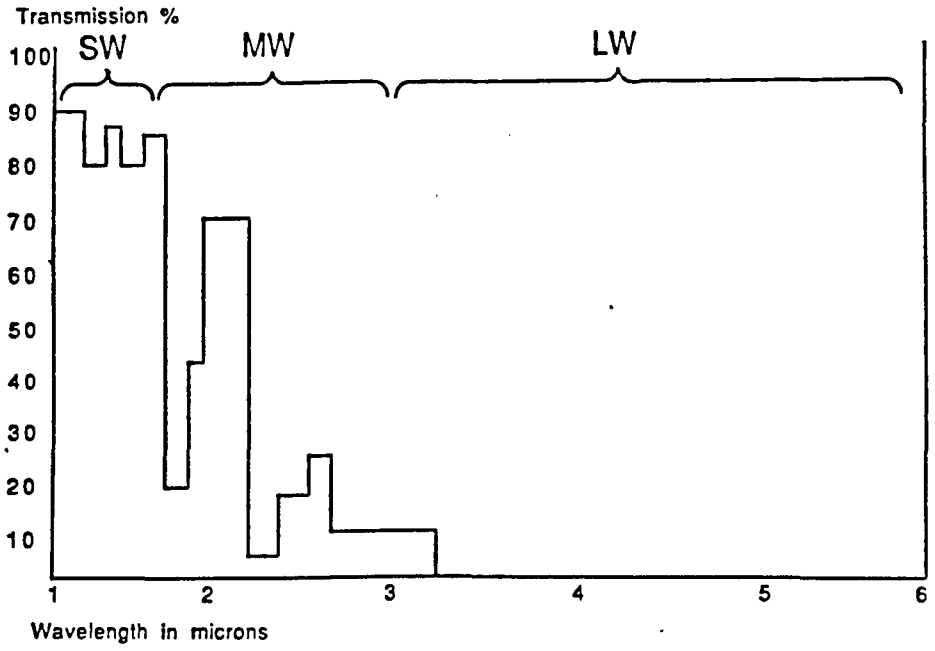

TRANSMISSION SPECTRA OF NYLON 6 : 1mm THICK

Figure 2.1.25. Typical infra-red spectrum for an unpigmented nylon 6 thermoplastic section, 1mm thick.

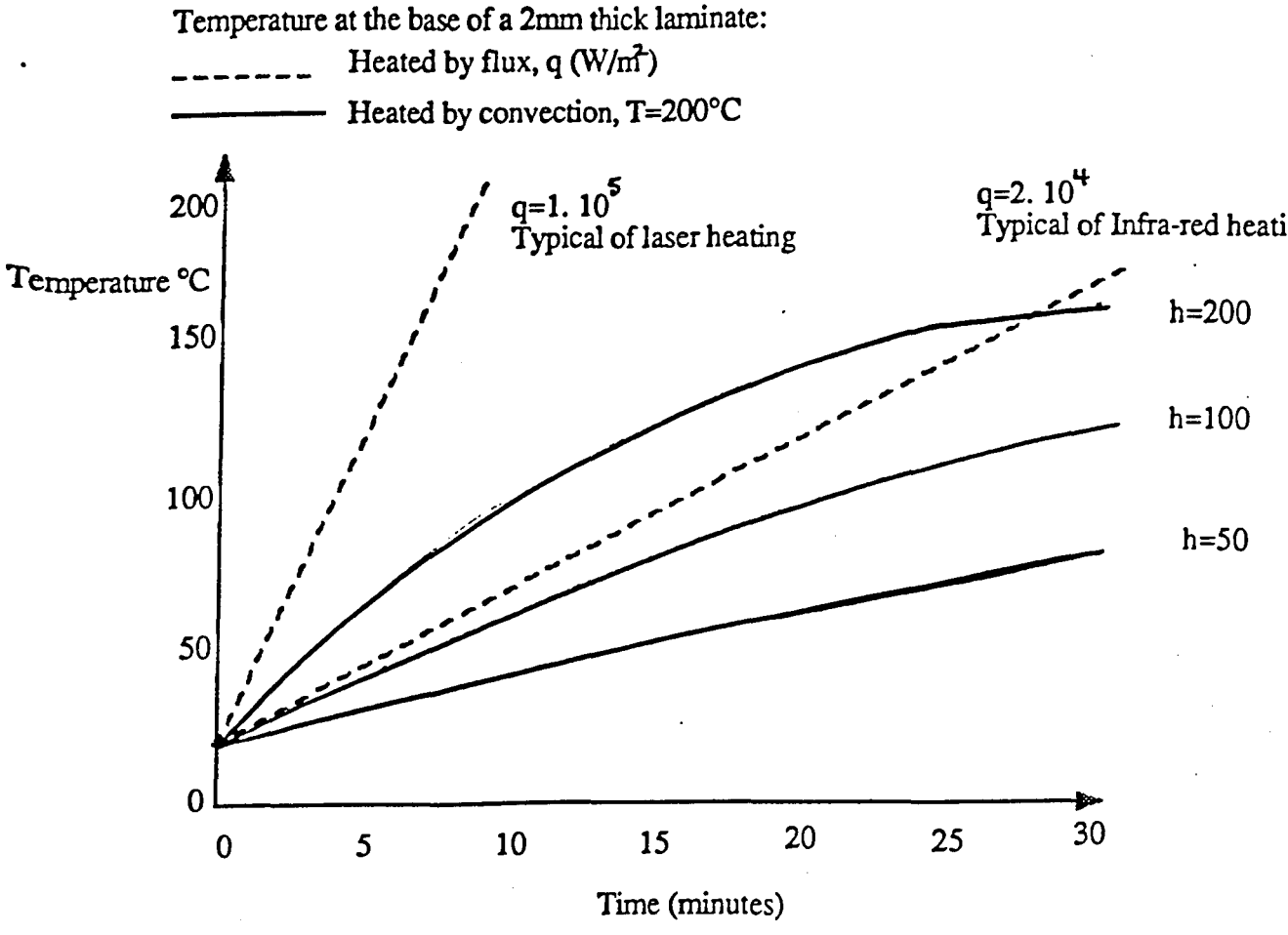

Figure 2.1.26. Comparison of the temperatures at the base of a 2mm thick laminate, heated by different heat sources: laser; infra-red; convection with different surface heat transfer coefficients.

they absorb the majority of the incident radiation. This then reduces the necessity for heat transfer through the material thickness by conduction.

Once the precursor has been heated to its processing temperature, the next process stage is the forming of the individual precursor tows into the desired shape and the consolidation and cooling of these to produce a composite section. As yet no consensus exists as to the most efficient way of achieving this and three methods have received the greatest attention. Three forming options are available; constant geometry, split dies typical of thermoset pultrusion dies, variable geometry split dies and variable geometry rolls. The three options are shown in Figure 2.1.27.

It is possible to use fixed geometry, split dies, as is common in thermoset pultrusion, and to combine a heated, tapered forming die with a parallel sided, cooled consolidation die. This forming method relies on internal pressure build up in the converging material entering the taper and on thermal expansion-induced pressures in the heated die to form the product shape. A disadvantage of this type of fixed geometry die system is that it cannot compensate for dimensional changes which may occur on cooling and which will cause a reduction in the consolidation pressure exerted on the section.

A pulling force will be required to pull the material through the die and the resistance of the die is made up of a combination of factors, Astrom (1991)[44]. A viscous resistance arises from the shearing of the thin polymer-rich layer between the surface of the fibre/matrix bundle and the die wall. The tapered section of the die gives rise to a compaction resistance as the bundle is compacted and this is influenced by both the pressure generated by matrix flow relative to the fibres and by the pressure load carried by the unidirectional fibres. There is also a contribution due to friction resulting from fibre/die wall contact in the heated die and solid composite/die wall contact in the cooling die. There will also be a viscous drag resistance on the fibres. Temperature induced forces arising from changes in matrix viscosity and resin thermal expansion will also affect the magnitude of the pull force required to pull the section being formed for any given line speed.

Little work has been done to address the problem of optimising the die length for thermoplastic pultrusion. The optimum die length will probably depend on a number of factors, not least line speed which will determine the consolidation time in the die and which will influence pressure build up in the die entry.

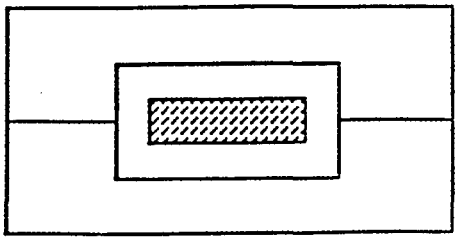

Constant geometry split die

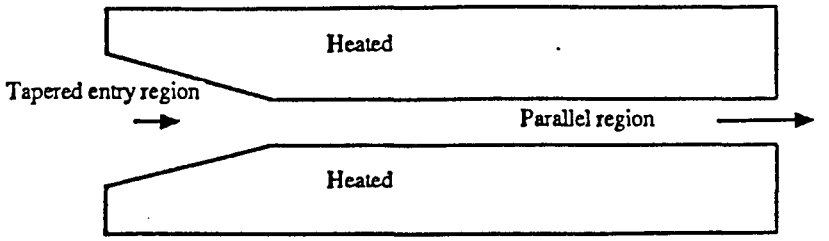

CONSTANT PRESSURE
DYNAMIC DIES

CONSTANT PRESSURE
ROLLERS

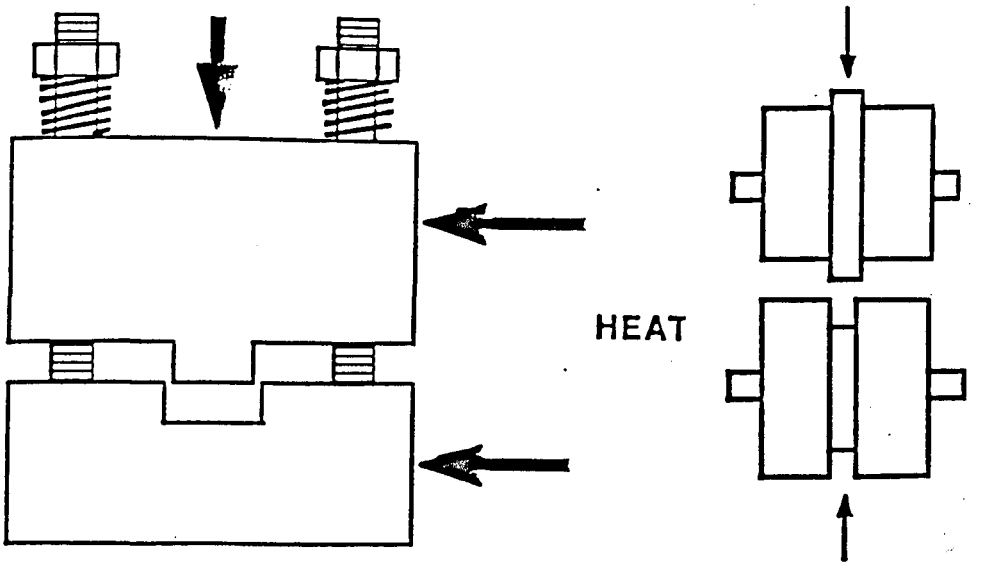

Figure 2.1.27. Forming options available for use in the thermoplastic pultrusion process.

The second approach to the problem of forming and consolidation, to produce flat or channel sections is to use variable geometry split dies, through which a constant pressure can be applied to the material being formed. This has an advantage in that changes in material dimensions are compensated for by movement of the dies, allowing a constant pressure to be applied to the material being formed. The forming pressure can be applied by a number of methods, the two most common being through mechanical pressure generated by compressed springs, or by a pneumatic pressure. A limitation to this forming technique is the difficulty in fully consolidating circular sections under a constant pressure, especially if shrinkage occurs on cooling. The dies can be heated or cooled if necessary.

As an alternative to dies and using an adaptation of the metal roll forming technique, it is possible to use profiled rolls as the mechanism by which a section is formed. The rolls need not necessarily be driven as has been reported, Cattanach and Harvey (1984)[40], and can be operated directly via the haul-off through movement of material through the rolls. The use of rolls should reduce the build up of pulling forces as line speed increases and therefore facilitate running at higher line speeds than may be possible with dies. Pressure can be applied to the rolls in a similar way as that used to load the constant pressure dies discussed previously. A disadvantage in using sets of rolls is that the contact length in the roll gap will in most cases be much shorter than that typically found with dies. Thus the effect of increasing line speed will have a much more pronounced effect on the consolidation times. As discussed for the constant pressure dies, it is not possible to produce circular sections under a constant pressure using profiled rolls.

2.1.5.2 Studies of the thermoplastic pultrusion process

The process of thermoplastic pultrusion has been investigated by a number of authors using a variety of precursor types and methods of producing continuous pultruded sections.

Madenjian et al. (1985)[45] have acknowledged the necessity of developing new, high speed processing techniques for thermoplastic structural composites in order for them to gain widespread use. They have examined the effect of processing variables on the properties of a pultruded 60% glass/Surlyn AD 5001 flat strip section produced using an experimental pultrusion line. A factorial experimental

technique was used to determine the product response to processing changes.

The experimental pultrusion line consisted of five sections: a material dispensing stage, a fluidised bed, a heated die, a cooled die and a haul off. The glass reinforcement was wound onto 90mm diameter spools and placed on a creel stand. The glass was pulled through a metal grommet to align the fibres and was fed into a compressed air fluidised bed. The fibres were fed into the fluidised bed at a temperature below the resin melting point to prevent polymer fusing onto the outside of the tows.

The heating and forming stage of the process consisted of a constant pressure die which was found to reduce the pull force exerted on the fibre bundle. The normal force exerted by the top half of the die on the pultruded section was limited by allowing the die to change its cross sectional area. The die was 30cm long and consisted of a compaction zone with a 13° taper for the first 20cm. The remainder of the die was parallel-sided. A flat strip section 12.7mm wide and up to 12.7mm thick was produced. The forming pressure was applied by the use of a controllable hydraulic ram acting on the top half of the die. A water cooled die, 15cm long, was placed directly after the heated die. This die was also designed so as to exert a constant pressure on the pultruded section and the pressure was applied using a hydraulic ram as before. The haul off mechanism used was a reciprocating hydraulic type.

Four significant process variables were identified for study. These were line speed, degree of fluidisation, heating and cooling die pressure and heating die temperature. The effect of these on the physical properties of the pultruded sections produced were then determined using a full factorial experimental design. Two levels were examined for each variable, die pressures 1.2 and 2.8 MPa, fluidisation gas off and full on, die temperatures 150° and 220°C and line speeds of 0.15 and 0.9m/min. The flexural and tensile modulus of the sections produced at each level were measured to determine the product response to process changes. The experimental results are shown graphically in Figures 2.1.28 to 2.1.35 and show a number of significant features.

It was found that as the die temperature was increased the tensile modulus increased (2.1.28). This was attributed to the lower matrix viscosity at higher temperatures leading to good fibre alignment, good wet out and good consolidation in the composite section. It was also found that increasing line speed caused a reduction

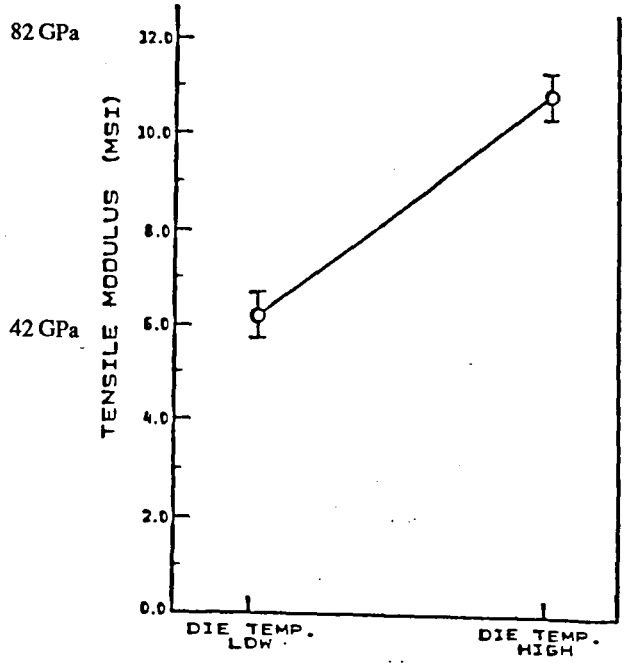

Figure 2.1.28.

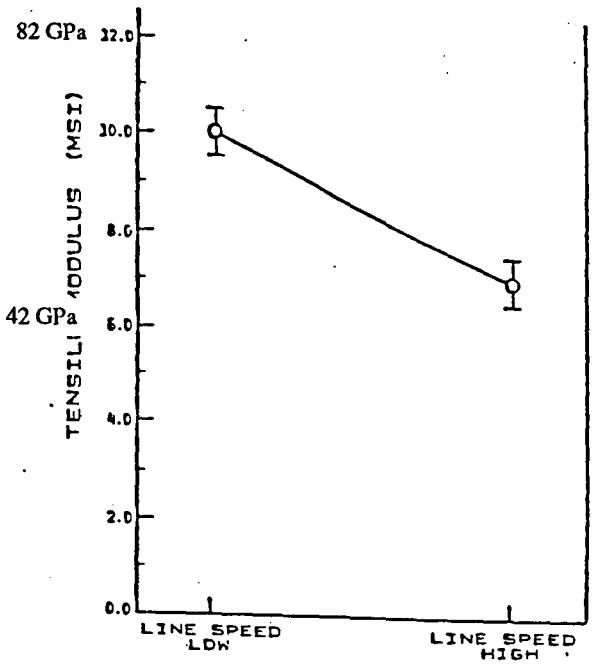

Figure 2.1.29.

Figure 2.1.28. Tensile modulus as a function of die temperature, after Madenjian et al. (1985).

Figure 2.1.29. Tensile modulus as a function of line speed, after Madenjian et al. (1985).

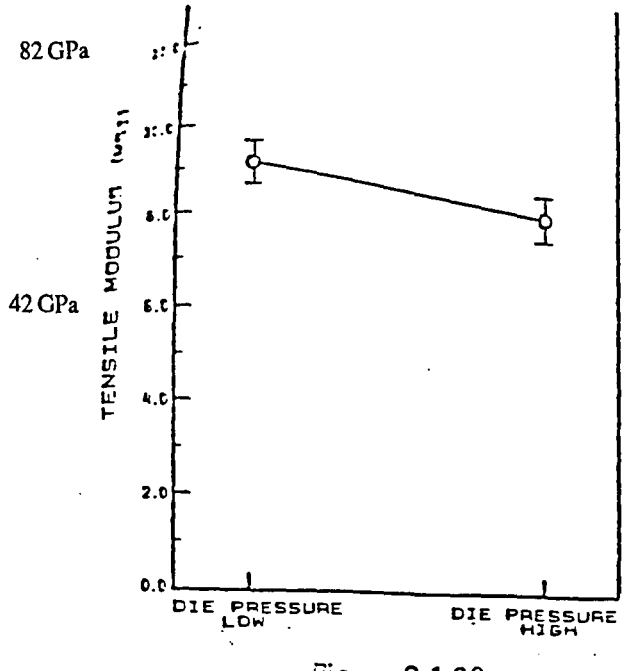

Figure 2.1.30.

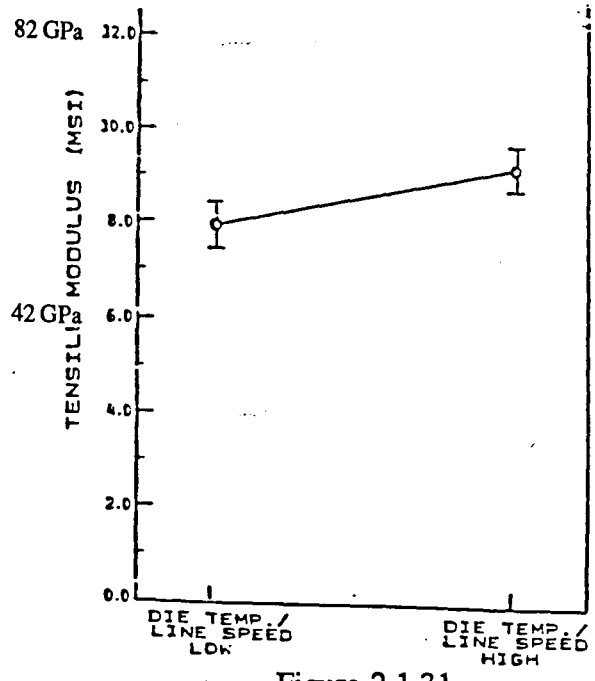

Figure 2.1.31.

Figure 2.1.30. Tensile modulus as a function of die pressure, after Madenjian et al. (1985).

Figure 2.1.31. Tensile modulus as a function of die temperature and line speed, after Madenjian et al. (1985).

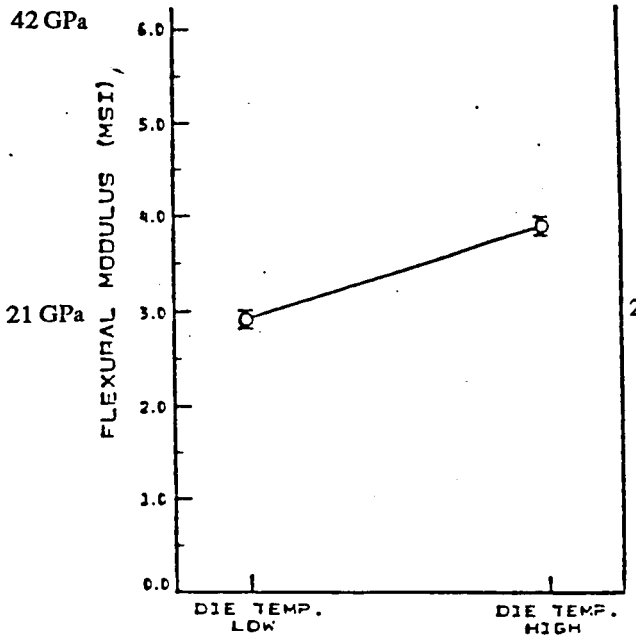

Figure 2.1.32.

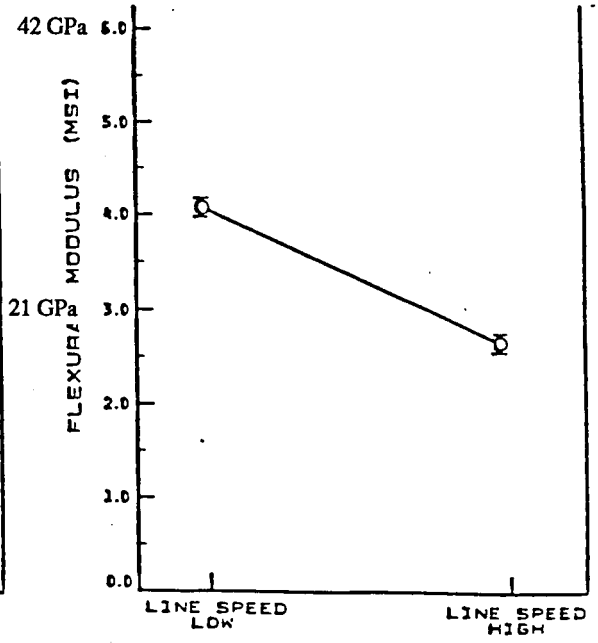

Figure 2.1.33.

Figure 2.1.32. Flexural modulus as a function of die temperature, after Madenjian et al. (1985).

Figure 2.1.33. Flexural modulus as a function of line speed, after Madenjian et al. (1985).

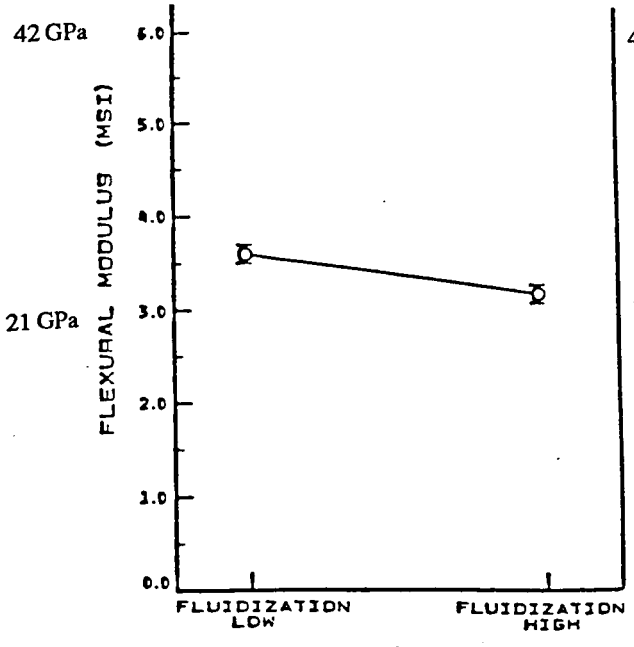

Figure 2.1.34.

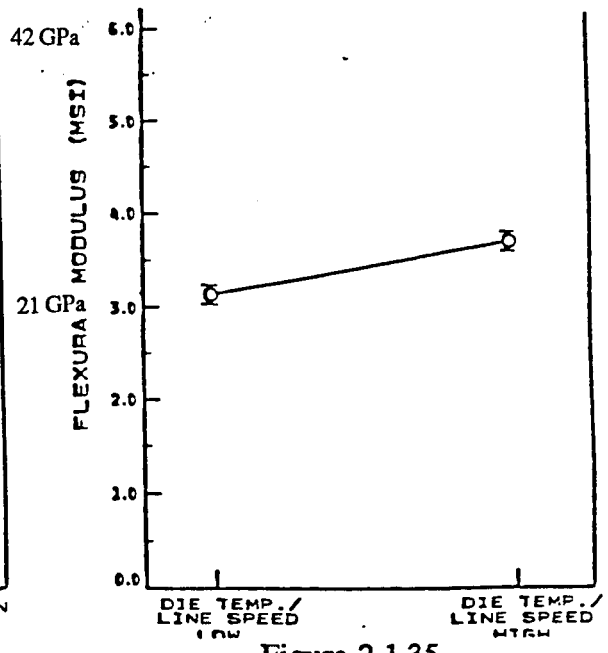

Figure 2.1.35.

Figure 2.1.34. Flexural modulus as a function of fluidization, after Madenjian et al. (1985).

Figure 2.1.35. Flexural modulus as a function of die temperature and line speed, after Madenjian et al. (1985).

in tensile modulus due to the decreased residence time in the forming die at higher line speeds (2.1.29). Also, the effect of increasing die pressure was found to cause a decrease in the tensile modulus and this was considered to be caused by increased fibre misalignment and fibre damage at higher pressures (2.1.30). It was found that increasing the die temperature and line speed resulted in a higher tensile and flexural modulus (2.1.31, 2.1.35). As was found for tensile modulus, the most significant effects on the composite flexural modulus were caused by changes in the die temperature and the line speed (2.1.32, 2.1.33). It was found that decreasing the melt viscosity by an increased die temperature resulted in a higher flexural modulus. The effect of fluidisation was found to reduce the flexural modulus as a result of poor resin pick up and wet out of the fibre bundles (2.1.34). It was concluded that for optimum tensile and flexural modulus properties, the predominant process variables were die temperature and line speed.

Cowen, Measuria and Turner (1986)[23] have investigated the feasibility of thermoplastic pultrusion using a combination of carbon, glass and aramid fibres with matrices such as nylon 6,6, polypropylene, PET and PEEK.

Using a modification of the impregnation technology used to produce continuous precursors consisting of glass/nylon 6,6 (Verton) and carbon/PEEK (APC2), a number of unidirectional reinforced sectional shapes, including strip, rod, tube and channel were produced. The forming and cooling stage of the pultrusion process consisted of a series of water cooled dies which operated under a constant pressure and which rapidly formed and cooled the molten precursor tows. Sections were produced at line speeds up to 2m/min and the effect of line speed on the product properties was determined by measuring the flexural strength and modulus of the sections produced. In addition, the effect of glass type and finish on the properties of the pultruded section were investigated for a nylon 6,6 matrix pultrusion. The elevated temperature performance of the pultruded sections was also investigated.

As can be seen in Figure 2.1.36, both the flexural strength and modulus were found to decrease as the line speed increased. This was attributed to increased void contents and less efficient consolidation and cooling at the higher end of the speed range.

A number of pultrusions were produced at a line speed of 0.5m/min using different glass fibre reinforcements to investigate the effect of the reinforcement type on the final composite properties. The flexural properties of the pultruded sections are

detailed in Figure 2.1.37. It was found that the use of a direct roving, Vetrotex RO99 in which all the filaments are drawn together from the same bushing and are therefore equi-tensioned, resulted in the best overall composite properties even when compared directly to polyamide compatible sized glass rovings.

For nylon 6,6 pultrusions reinforced with glass and carbon fibres, a high degree of modulus retention at elevated temperatures was reported. This is shown in figure 2.1.38. As can be seen the carbon/nylon 6,6 pultrusion retained 70% of its modulus at 200°C and the glass/nylon 6,6 retained about 50% at 100°C.

Larock, Evans and Hahn (1989)[46] have investigated the pultrusion process using graphite/PPS hybrid yarns, in which the relative diameters of the reinforcement and matrix fibres were 7 and 25μm respectively. An experimental pultrusion line was used which incorporated a pre-heating stage before the entrance to different heated rod and strip dies, between 30mm and 900mm long. The die temperatures used were a pre-heating die temperature of 185°C and a forming die temperature of 275°C. The line was operated at a constant line speed of 0.1m/min. The pultruded sections were cooled in air, without the presence of additional cooling dies. It has been reported that most of the sections pultruded showed a lack of adequate flow and compaction and this has been attributed to difficulties in feeding the tows through the die and generating a sufficiently high consolidation pressure as the material passed through the die.

It is possible to combine the impregnation stage as a fully integrated on-line feature of the process. Wilson et al. (1989)[47] have demonstrated the pultrusion of graphite/PEI sections using on-line impregnation. Impregnation was carried out in a conventional pultrusion resin bath after dissolving the PEI matrix in a methylene chloride solvent. As has been described earlier for a number of impregnation processes, spreader bars in the resin bath were used to separate and open out the graphite tows. After impregnation, the solvent was flashed off in hot air before the collimated tows entered a series of heated consolidation dies. These were designed so that any residual solvent vapours could be removed as the material passed through the different heated zones of the dies. Consolidation occurred by a gradual reduction in die size. A final cooling die was used to cool the pultruded section to below 66°C. A rectangular section 7.8mm x 25.5mm was produced at a line speed of 0.2m/min and a pull force of 2.2 KN was quoted for this particular line speed. The flexural and interlaminar shear properties of the pultruded sections were

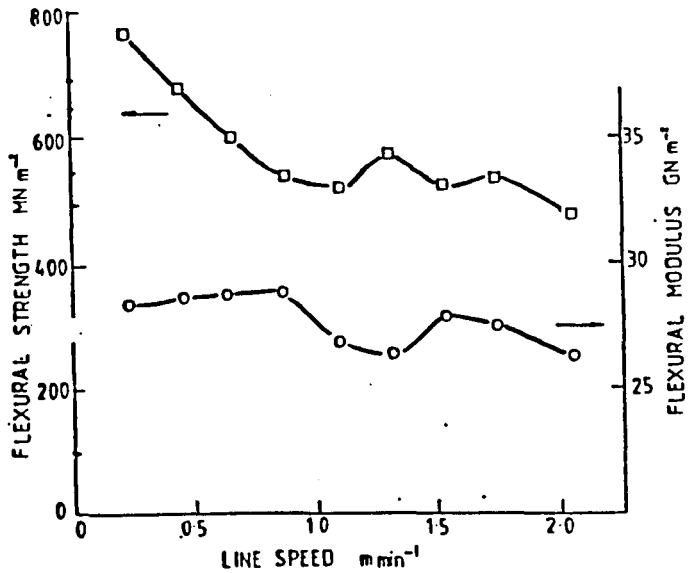

Figure 2.1.36. Effect of line speed on the flexural strength and modulus of nylon 6,6/ glass pultruded sections, after Measuria et al. (1988).

Effect of glass type and finish in nylon 6-6

	FLEXURAL MODULUS GN/m^2	% THEORETICAL MODULUS	FLEXURAL STRENGTH MN/m^2
OCF 429 XY	31.0	97	664
Fibreglass FGRE 5/2	26.9	90	836
Vetrotex P388	27.0	84	820
Vetrotex K099/P103	31.2	97	865

Figure 2.1.37. Effect of glass type and finish on the flexural strength and modulus of nylon 6,6/ glass pultruded sections, after Measuria et al. (1988).

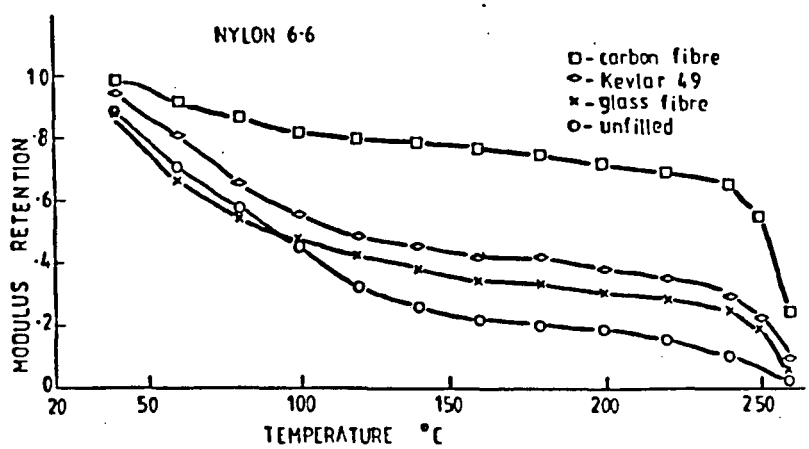

Figure 2.1.38. Modulus retention with temperature for polypropylene pultrusions, after Measuria et al. (1988).

measured and these values were compared to those obtained for compression moulded samples of the same volume fraction. These are detailed in Table 2.1.3.

Table 2.1.3. Property comparison between moulded and pultruded unidirectional graphite/PEI samples, after Wilson et al. (1989).

Property	Pressed Prepreg 1	Pressed Prepreg 2	Post-Pressed Pultrusion 3	Pultrusion 4
Fibre volume fraction %	64.8	61	61.8	60.9
Void content %	2	1.2	1.4	1.9
Density g/cm^3	1.59	1.56	1.56	1.55
Flexural strength MPa	1624	1421	1421	1169
Flexural modulus GPa	115	106	107	107
ILSS MPa	91	87	81	66

It can be seen that the pultruded samples demonstrate 72% of the interlaminar shear strength of the pressed sample. Similarily, the pultruded section achieves 72% of the flexural strength and 93% of the modulus. It is interesting to note that the flexural and interlaminar shear strengths of the pultrusion can be increased to 90% of those measured for the pressed samples and the void contents reduced, by post moulding pultruded sections at a temperature of 260°C under a pressure of 2.1 MPa. These improvements were reported to be the result of additional consolidation and give an indication that improvements to the efficiency of the consolidation stage are necessary.

Ma et al. (1989)[48] have studied the pultrusion of glass, carbon and aramid fibres in nylon 6, thermoplastic polyurethane (TPU) and polymethyl methacryalate (PMMA) matrices. Sections were produced using a proprietary process which incorporated on-line impregnation and a heated die as the forming and consolidation stage. A rectangular section 12.7mm x 2.1mm was produced at line speeds between 0.1 to 0.9m/min. For a nylon 6/aramid pultruded section, the effect of line speed on the heat distortion temperature and the flexural strength was examined and is shown in Figure 2.1.39. It was found that both properties showed a decrease as the line speed increased and a deterioration in the product surface finish was also reported at the higher line speeds. This reduction in properties was attributed to incomplete wet-out and impregnation of the fibres as the residence time in the resin bath decreased with increasing line speed.

While the majority of material published on the thermoplastic pultrusion process has been concerned with experimental processing, the mechanical properties of pultruded composites and studies on the feasibility of the process, some work has

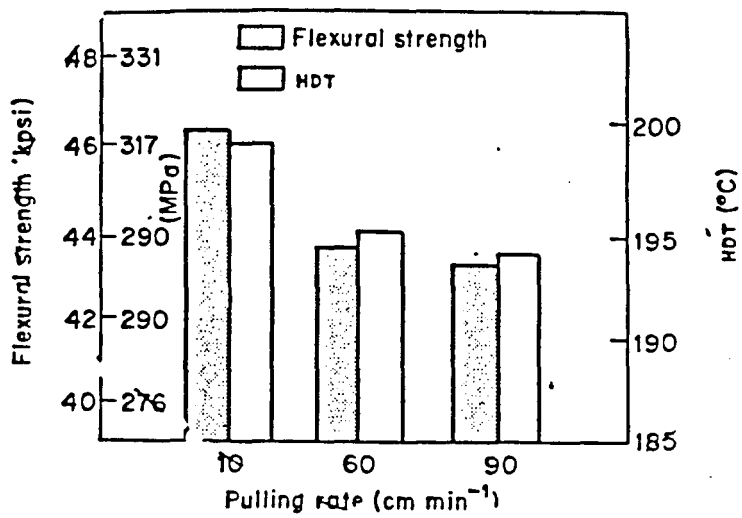

Figure 2.1.39. Flexural strength and heat distortion temperature of pultruded Kevlar fibre reinforced nylon 6 composites vs. pulling rate, after Ma et al. (1990).

also been carried out on modelling the process.

In an attempt to develop an understanding of the effects of processing parameters and die geometry on the thermoplastic pultrusion process, a mathematical model has been developed, Astrom and Pipes (1991)[49]. Temperature and pressure have been identified as two of the most important parameters to understand and control in the thermoplastic pultrusion process because of their influence on the heat transfer during processing, the levels of consolidation and the generation of pull forces.

Three models were developed, detailed descriptions of which can be found in Astrom and Pipes (1991)[49]. The temperature in the pultruded section was modelled analytically as steady state heat transfer in a one dimensional flat slab. The pressure build up in the molten tows entering and passing through the forming die was modelled to predict the matrix pressure generated in the composite as it passed through the die taper and the pressure load carried by the fibres as they passed through the remainder of the heated die. In addition, a model was developed to predict the pull force necessary to pull the composite section through a die, taking into consideration viscous, compaction and friction resistance within the die.

Using an instrumented thermoplastic pultrusion line experiments have been conducted to verify the predictions of the models outlined above, Astrom and Pipes (1991)[50], using glass/polypropylene and carbon/PEEK (APC2) precursors to produce flat strip sections. Temperature, pressure within the composite and pull force were all measured continuously under different processing conditions, at line speeds ranging from 0.03 to 0.6m/min. A favourable correlation was reported for the temperature distributions through the heated and cooled dies, for both material systems and over a range of line speeds. A typical result is seen in Figure 2.1.40, showing both measured and modelled temperature distributions in a glass/polypropylene section, 25.4 x 3.2mm, pultruded at a very slow line speed of 0.006m/min. Difficulties in accurately measuring the pressure profile through the dies was reported. Nevertheless a reasonable comparison was made between the measured and the modelled results as illustrated in Figure 2.1.41, for a glass/polypropylene section produced at 0.03m/min. A sample of the results of the pull force model is shown in Figure 2.1.42, again for a glass/polypropylene section. The graph shows the pulling force dependence on line speed, as measured and as predicted by the model. The solid line and the two dashed lines represent different model conditions which take into account the tendency for the die taper to

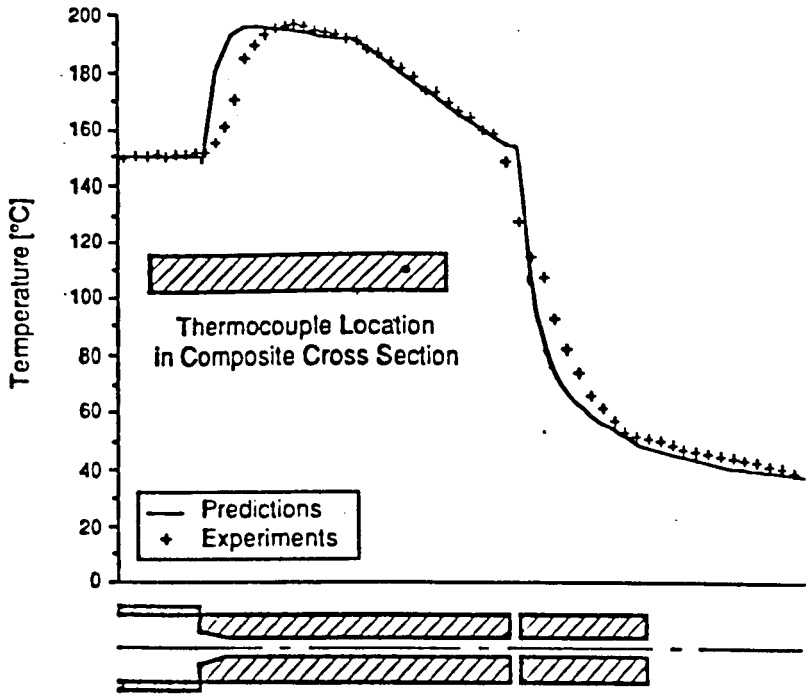

Figure 2.1.40. Experimentally determined temperature distribution within a glass/pp composite together with predictions from temperature model at a pulling speed of 0.981mm/sec, after Astrom and Pipes (1992).

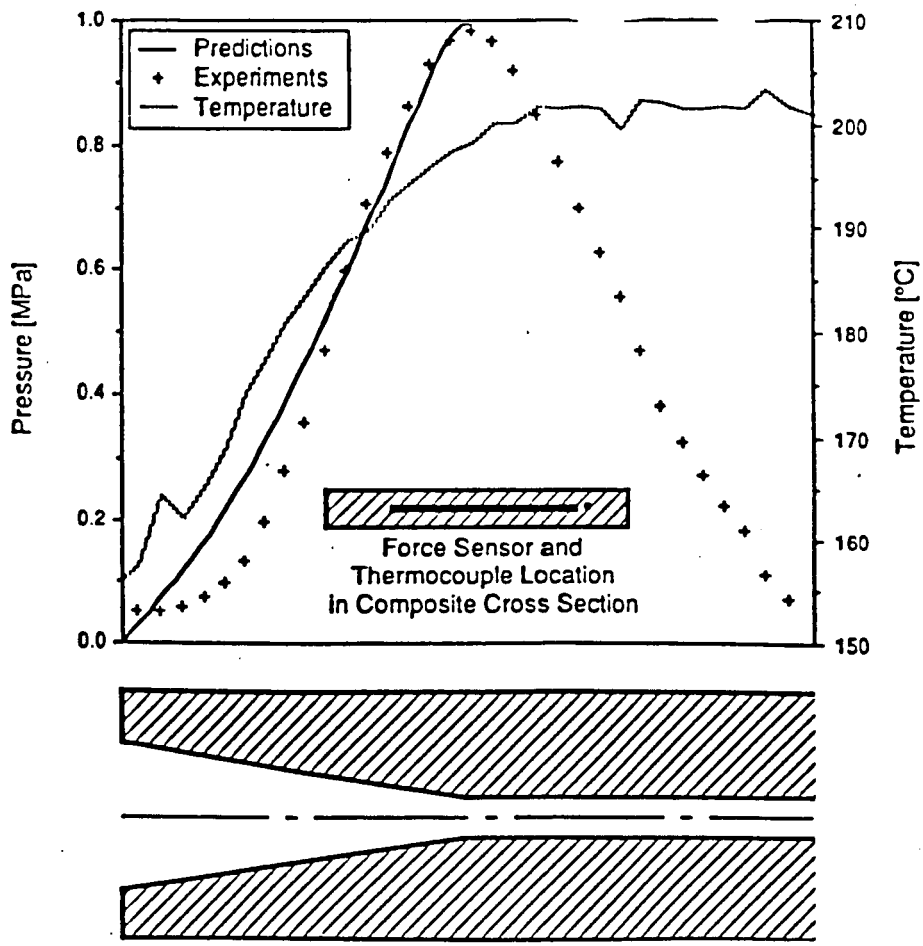

Figure 2.1.41. Experimentally determined temperature and pressure distributions within a glass/pp composite together with predictions from pressure model at a pulling speed of 0.512mm/sec, after Astrom and Pipes (1992).

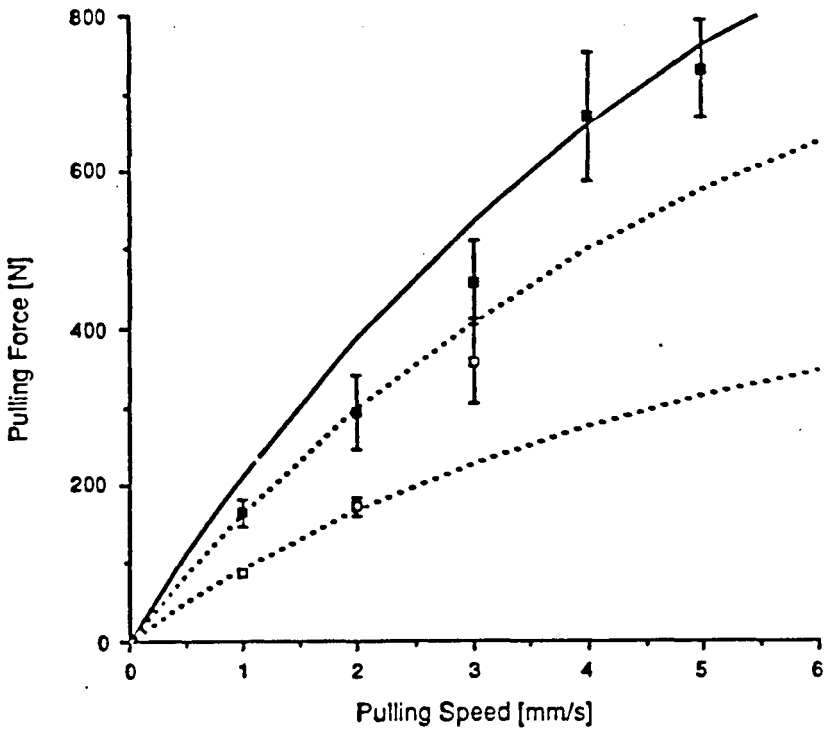

Figure 2.1.42. Experimentally determined pulling force as a fuction of pulling speed for pultrusion of glass/pp composite together with predictions from pulling force model model, after Astrom and Pipes (1992).

fill with polymer during experimental runs. The filled data points were recorded as the taper gradually filled up. The unfilled points were recorded during experiments when the taper was cleaned, although this proved impossible at speeds greater than 3mm/sec and the pull force was seen to rise. In conclusion, Astrom and Pipes[50] felt that even though the models required further development, the governing mechanisms of the process had been included in the set of models reported.

2.2 Studies of the melt impregnation process

A key feature of many impregnation processes which use either a polymer melt or a low viscosity solution has been reported to be the presence of one or more cylindrical bars or pins. The impregnation bars are illustrated in Figure 2.2.1 and are used to spread the fibre tows and to aid the overall impregnation process. In processes such as pultrusion and filament winding, involving low viscosity (0.2-2 Pa.s) thermosetting matrix polymers, impregnation bars are often an integral part of the resin impregnation bath. Because of the low viscosity of the resin, impregnation occurs readily and there has been little need for significant process optimisation. However, this is not the case when impregnating with thermoplastic matrices which have a much higher viscosity (10-100 Pa.s).

The aims of impregnation processes are to achieve a high degree of fibre wetting, with a controlled resin volume in the tow, along with the fastest possible throughput, without undue tension generation in the fibres, which can cause fibre damage and breakage. The tension build-up depends on a number of factors including the number and radius of the impregnation bars, the melt viscosity, the line speed, the wrap angle and the type of wipe-off die used at the bath exit. The wrap angle is defined as shown in Figure 2.2.2. The combined result of all these effects is that the line speed will be limited by the tension build-up in the various stages of the process. Few studies have been published which have investigated the fundamental mechanisms operating during the continuous melt impregnation process, although individual aspects such as flow of resin through fibre beds have been studied. However, analogies can be made with features of lubrication theory and bearing design which can be applied to the understanding and modelling of continuous melt impregnation processes.

2.2.1 Flow of resin through fibre beds

For full impregnation to occur, resin must flow through the fibre bundle and coat each individual fibre making up the fibre tow. In modelling the impregnation process, Darcy's law is commonly used to describe matrix flow of a Newtonian fluid through aligned fibre beds. This law relates the resin flow rate to the pressure gradient in the resin, the resin viscosity and the fibre bed permeability and can be

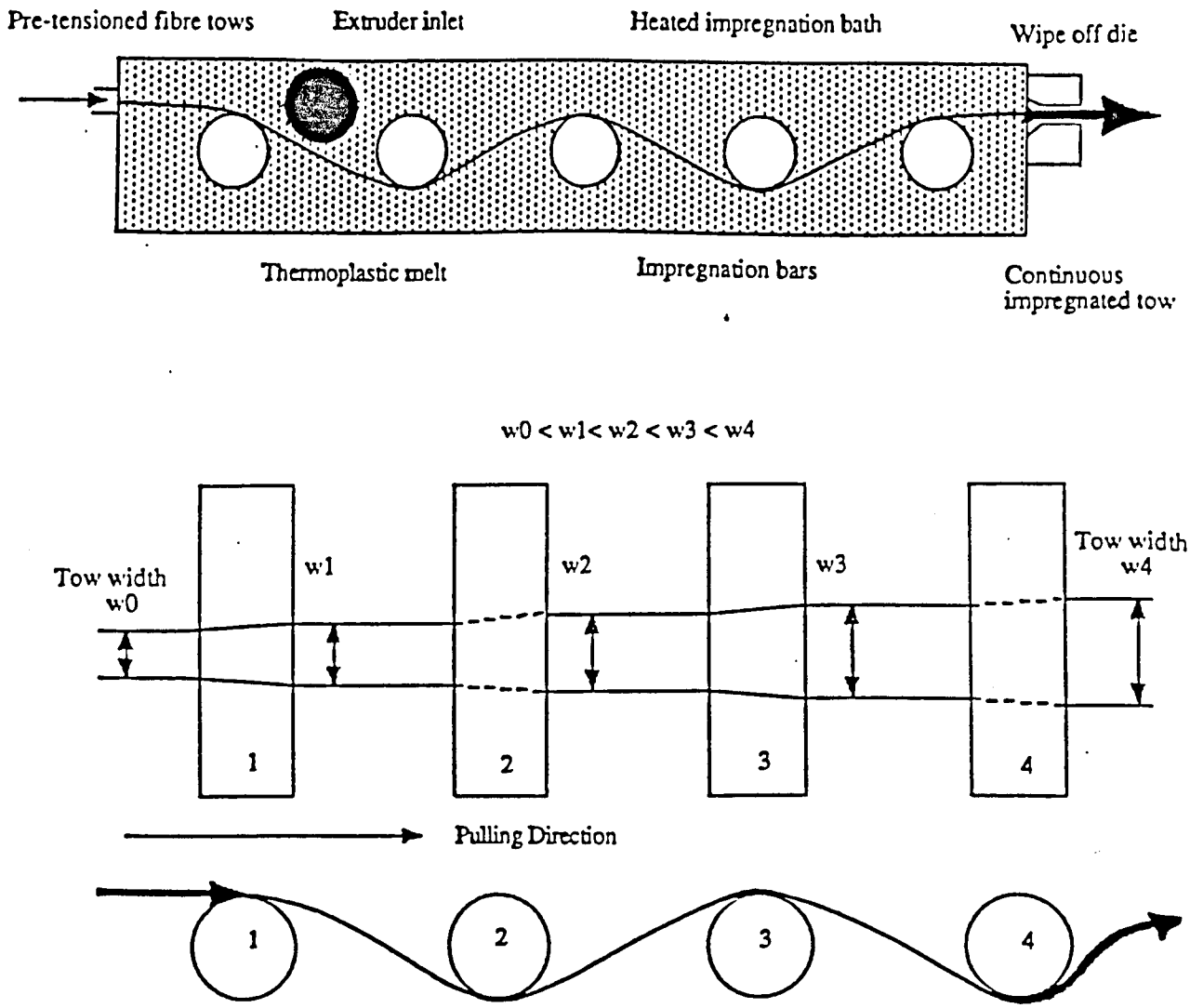

Figure 2.2.1. An illustration of the progressive spreading of a fibre tow as it passes over and under four cylindrical bars. The amount of fibre spreading can be controlled by changing the wrap angle and the radius of the bars.

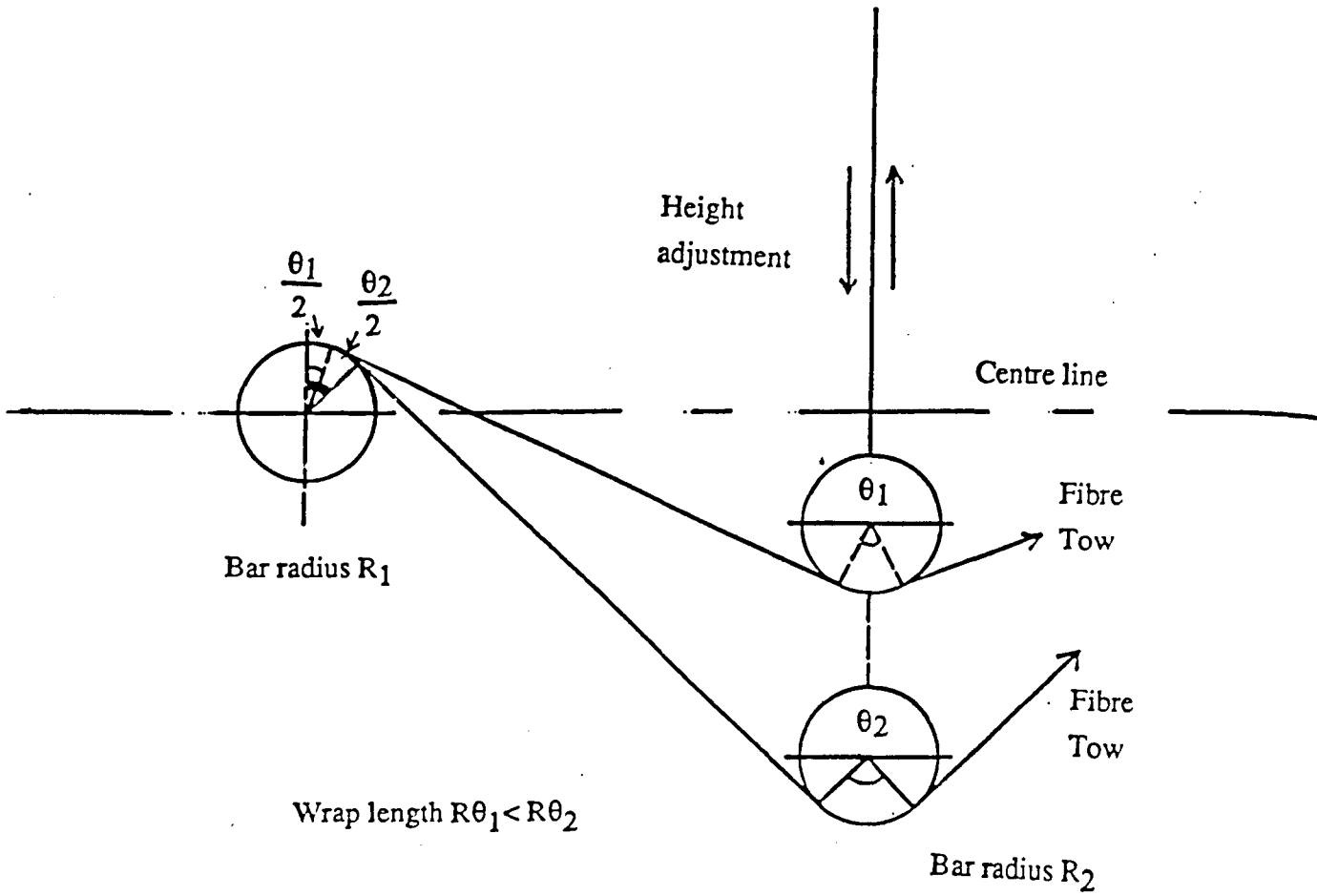

Figure 2.2.2. The effect of changing the vertical distance between centre lines of impregnation bars on the wrap angle, θ.

expressed for the one dimensional case as equation 2.2.1.

$$v = \frac{\phi}{\eta} \frac{\Delta P}{L} \qquad 2.2.1$$

where Δp is the applied pressure difference in the direction of flow, v is the average velocity, L is the bed length, η is the fluid viscosity and ϕ is the permeability of the medium. In the general case, the value of ϕ in any particular direction can be calculated in terms of the principal permeabilities of the medium.

The modelling of flow through fibre beds will not be reviewed in detail here. However, Astrom et al.(1991)[49] have reviewed a number of relationships which have been derived to model the flow of Newtonian fluids through isotropic porous media and aligned fibre beds. Skartsis et al.(1990)[51] have also studied and modelled resin permeation through fibre beds during composite processing and have highlighted some of the difficulties involved in modelling the flow behaviour during polymer processing realistically. A bed comprising of thin and flexible fibres can not be considered to be a random porous medium because the non uniform fibre arrangement will give rise to a distribution in the pore uniformity through the bed. The nature of the fluid permeant can also affect the fibre arrangement, as can the diameter and stiffness of the fibres. The applied pressure gradient may cause fibre deflection and close up pores in the bed and it is very important that the nature and features of the particular process are considered, especially the uniformity of the consolidation stage. The behaviour of the resin can change during processing, especially under high shear rates, to become strongly non-Newtonian and this must also be considered in the formulation of accurate models.

The impregnation of dry fibres with a thermoplastic matrix has been investigated as an integral part of the manufacturing process for thermoplastic composites, Lee and Springer (1987)[52]. The impregnation mechanism is illustrated in Figure 2.2.3. Impregnation was assumed to occur by a combination of axial resin flow along the fibres which are not perfectly straight driven by surface tension, and flow across the fibres. The impregnation was modelled lengthwise as laminar flow in an annular channel and as flow through a porous medium. A model was proposed to determine the time required for complete impregnation to occur. The effect of applying an additional pressure, either by pulling the fibres over bars or by simply squeezing the fibre/matrix bundle together during impregnation was not considered although it is likely to have a major effect on the impregnation stage of the process.

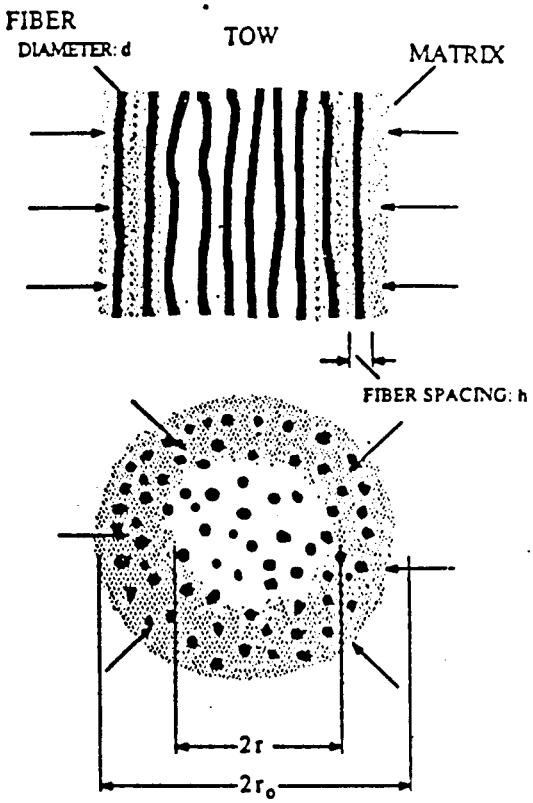

illustration of the impregnation of a fiber tow.

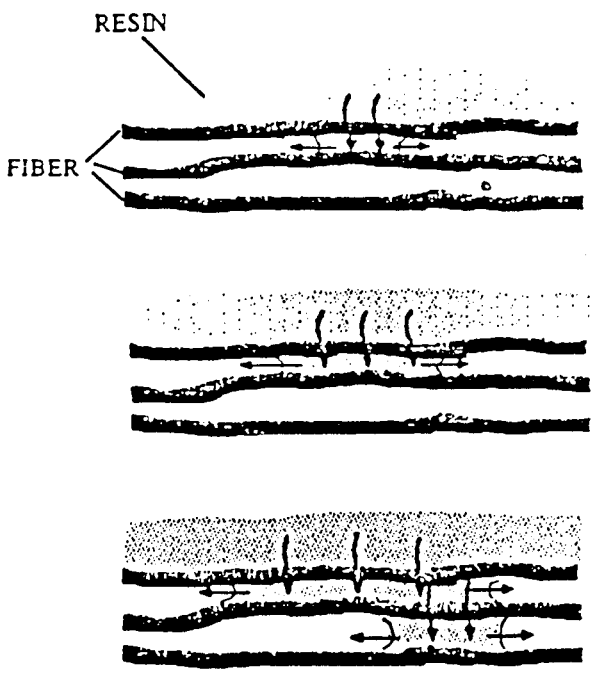

. Illustration of the progressive motion of the matrix between fibers inside a tow.

Figure 2.2.3. Illustration of impregnation mechanism, after Lee and Springer (1987).

It is also likely that the axial flow along the fibres will occur to a much less extent than the flow perpendicular to the fibres. When the surface tension is sufficiently large to drive axial flow it is also likely to result in air entrapment between the fibre surfaces and the liquid resin, Bascom (1965)[53].

Bascom (1965)[53] has studied the wetting behaviour of epoxy resins on glass filaments as part of the filament winding process. Examination of sections taken from impregnated rovings revealed that a significant amount of air becomes entrapped during the impregnation stage of the process. The air entrapment was explained to be the result of the viscous resistance to flow in the capillary spaces between the fibres in the roving, and the capillary resistance to flow due to poor wetting. It was estimated that the maximum possible capillary pressure available for axial flow was orders of magnitude too low to allow the resin to penetrate the fibres. It was therefore concluded that the dominant mechanism of resin penetration was lateral flow of resin, perpendicular to the fibre axis from the sides of the fibre tow. Because this lateral flow will be opposed by a capillary pressure, the entrapment of air in the capillary spaces will occur unless the resin viscosity is low or the surface tension is high enough to offset the viscous resistance.

Increases in the contact angle between the liquid resin and the solid surface as the velocity of the liquid front increases has also been reported to contribute to air entrapment, Elmendorp et al (1988)[54]. When the contact angle tends towards 180°, flow induced instabilities on the liquid surface or irregularities in the solid surface have been found to induce air entrainment between the solid surface and the moving liquid.

It is possible to apply lubrication theory to describe and help understand the process of melt impregnation. The following section aims to briefly review some relevant aspects of lubrication theory that can be adapted to apply to the impregnation situation.

2.2.2 Lubrication theory

Four types of lubrication can be defined to classify any of the lubrication regimes which exist and these are hydrodynamic, boundary, elasto-hydrodynamic and hydrostatic.

Only the first two cases, hydrodynamic and boundary lubrication will be considered further. Hydrodynamic lubrication occurs when moving surfaces are completely separated by an interfacial fluid film. Boundary or mixed lubrication is a combination of hydrodynamic and solid contact between moving surfaces and occurs whenever the fluid film breaks down. Boundary lubrication is unstable and will either result in seizure of the moving surfaces or will regenerate to the full hydrodynamic lubrication state.

When a fluid is dragged into a convergence a pressure film is generated, as illustrated in Figure 2.2.4. It is possible to express this process mathematically, subject to certain assumptions, by the use of Reynold's equation, Cameron (1981)[55]. The assumptions are that body forces are neglected, ie. no extra forces act on the fluid. The pressure is constant through the film and the curvature of the surfaces is large compared to the film thickness. Surface velocities do not vary with direction and there is no slip at the boundaries. Flow components perpendicular to the moving surfaces are also neglected. It is also possible to assume that the fluid is Newtonian, flow is laminar and the viscosity is constant through the film thickness. Reynold's equation can be expressed in one dimension, for an infinitely long bearing as equation 2.2.2.

$$\frac{d}{dx}\left(h^3\frac{dP}{dx}\right) = 6\eta V\frac{dh}{dx} \qquad 2.2.2$$

Where h is the film thickness, V is the velocity in the x direction, η is the viscosity and P is the film pressure.

It is possible to adapt the general Reynold's equation to include a permeability term to describe a porous bearing. Flow is governed by Darcy's law which can be expressed as equation 2.2.3.

$$Q = \frac{\phi}{\eta}\frac{dP}{dz} \qquad 2.2.3$$

Where Q is the volume flow/unit area which equals the velocity of flow across unit area, dp/dz is the pressure gradient in the direction of flow, η is the resin viscosity and ϕ is the permeability of the fibre bed. The modified Reynolds equation for a porous bearing can thus be expressed:

$$\frac{d}{dx}\left(h^3\frac{dP}{dx}\right) = 6\eta V\frac{dh}{dx} + 12\phi\frac{dP}{dz} \qquad 2.2.4$$

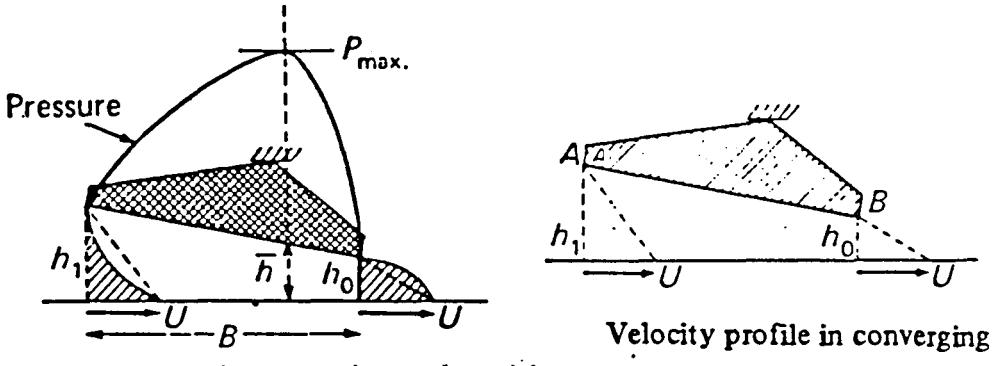

Velocity profile in converging wedge with pressure.

Velocity profile in converging wedge.

Figure 2.2.4. Pressure gradient and velocity profile resulting from fluid flow in a converging wedge.

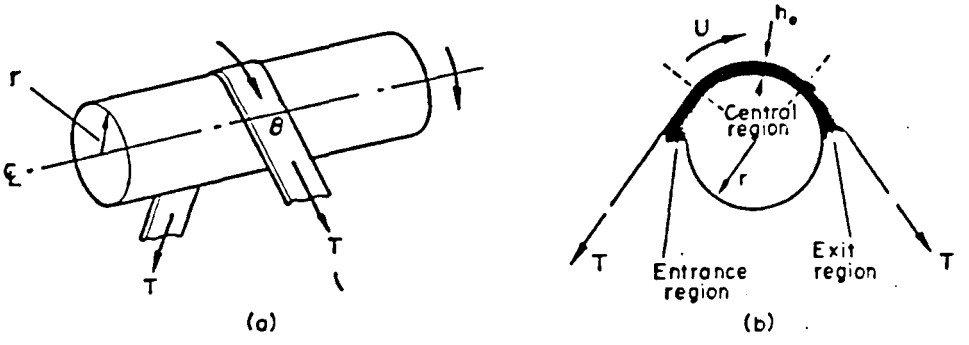

The foil bearing showing (a) general view, and (b) infinitely wide foil.

Figure 2.2.5. Schematic illustration of a foil bearing, after Moore (1975).

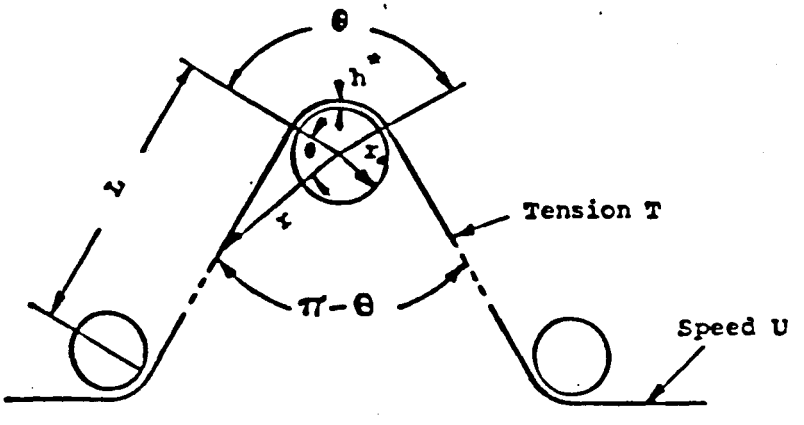

Figure 2.2.6. The passage of a magnetic tape over a spindle, showing the similarities to the case of the foil bearing, after Eshel et al. (1965).

A specific type of bearing, the foil bearing, exhibits a number of similar features to the action of fibre tows passing over a fixed impregnation bar

2.2.3 Lubrication of foil bearings

The general design of the foil bearing and the lubrication regimes around the bearing are shown in Figure 2.2.5, Moore (1975)[56]. The foil bearing consists of a flexible band or foil wrapped partially around a rotating shaft with an interfacial lubricant between the foil and the shaft. In other cases, the shaft can be held stationary while the foil moves or both the shaft and foil can rotate.

The passage of a magnetic tape over a spindle is shown in Figure 2.2.6. Comparing this to Figure 2.2.5 illustrates a number of similarities to the action of a foil bearing in which the interfacial lubricant is air.

A number of numerical and analytical studies have been carried out to investigate the action of pulling magnetic tape at high speeds over guiding spindles and tape heads Eshel et al (1965)[57]. Consider the tape in Figure 2.2.6 which approaches a spindle of radius r at a velocity v. If the guide locations are considered to be at a relatively large distance, L, away from the spindle compared to the fluid film thickness, then the wrap angle will be known. As the tape passes over the spindle it will entrap an air film which will generate a pressure over most of the contact length. This film thickness will be a function of a number of parameters including the position around the spindle, the line speed, the spindle diameter and the tape tension. The formation of this type of film is the operating principle of foil bearings, in which a flexible foil can form a self acting fluid film which is capable of carrying a load.

Ma (1965)[58] has investigated the passage of magnetic recording tape over cylindrical heads and experimentally measured the film thickness using capacitive sensors and conductive foils to formulate empirical expressions for the film thickness h. A number of similar expressions were formulated and all were found to be very similar in form to equation 2.2.5. In several independent numerical and experimental studies, Moore (1975)[56], Eshel et al (1965)[57], the film thickness, h, has been found to be given by:

$$h_o = 0.643R\left(\frac{6\eta V}{T}\right)^{2/3} \qquad 2.2.5$$

In this equation, R is the bar radius, V is the tape velocity, T is the tape tension per unit width and η is the fluid viscosity. This equation has been applied not only to infinitely wide, perfectly flexible foil bearings but has been found to remain essentially the same when the effects of foil stiffness, finite foil width and lubricant compressibility are taken into consideration.

The form of the film thickness and pressure variation with wrap length, for a perfectly flexible foil bearing, is illustrated in Figure 2.2.7, Moore (1975)[56]. Three regions can be seen; an exponential entry region in which the pressure increases as the film thickness decreases, a central region in which the film thickness and pressure remain at a constant level and an exit region where the film thickness exhibits a characteristic ripple which also appears as a peak in the pressure profile.

It is possible to apply the theory of foil bearings to the passage of fibre tows around a cylindrical bar in the presence of a viscous liquid, as is the case in melt impregnation.

2.2.4 The similarities between the behaviour of foil bearings and the behaviour of fibre tows passing over a cylindrical impregnation bar.

An analogy can be made between the foil bearing and the situation which exists as a tow of fibres is pulled around an impregnation bar. In the foil bearing three regions of different behaviour have been identified, the entry, the central and the exit region, as shown in Figure 2.2.7. It is also possible that similar regimes of behaviour may be present when a fibre tow is drawn over a bar in the presence of a liquid resin, according to the thickness variation of the resin film. The different zones which may occur are illustrated schematically in Figure 2.2.8, Chandler et al. (1992)[22]. The variation in film thickness and tow tension with the wrap length is shown in Figure 2.2.9, from which the four zones of behaviour can also be identified.

As the fibre tow approaches the bar at an angle determined by the geometry of the process, an entry zone will be formed in which the gap between the fibre and the

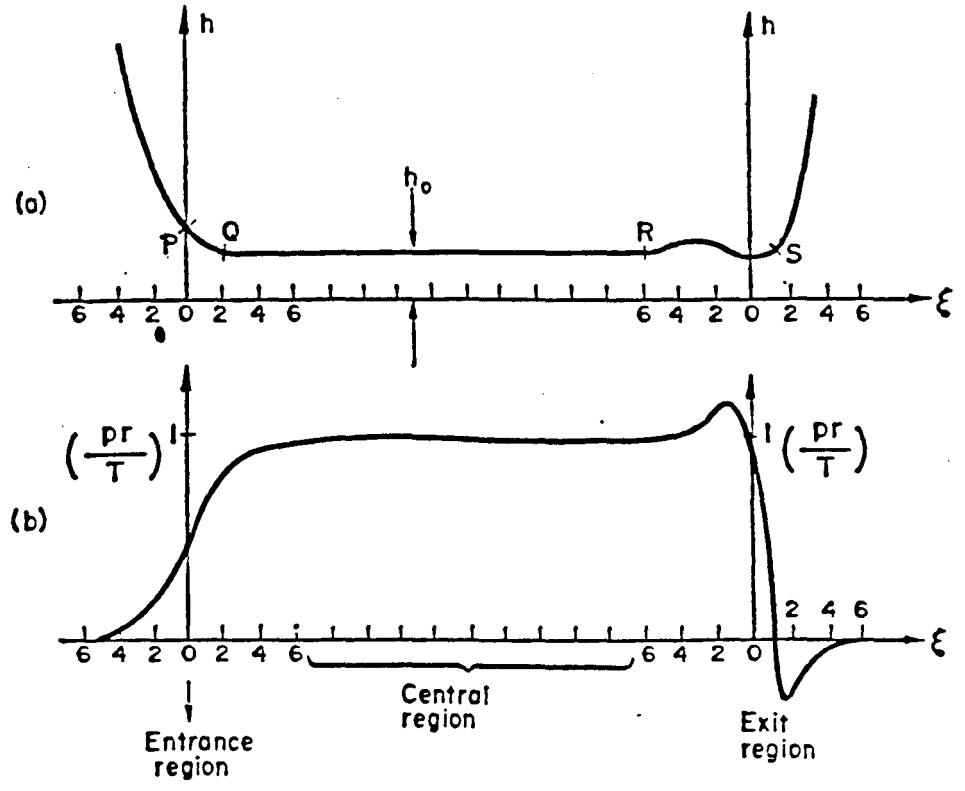

Gap and pressure in perfectly flexible foil bearing.

Figure 2.2.7. Film thickness variation and pressure profile plotted against wrap length around a perfectly flexible foil bearing, after Moore (1975).

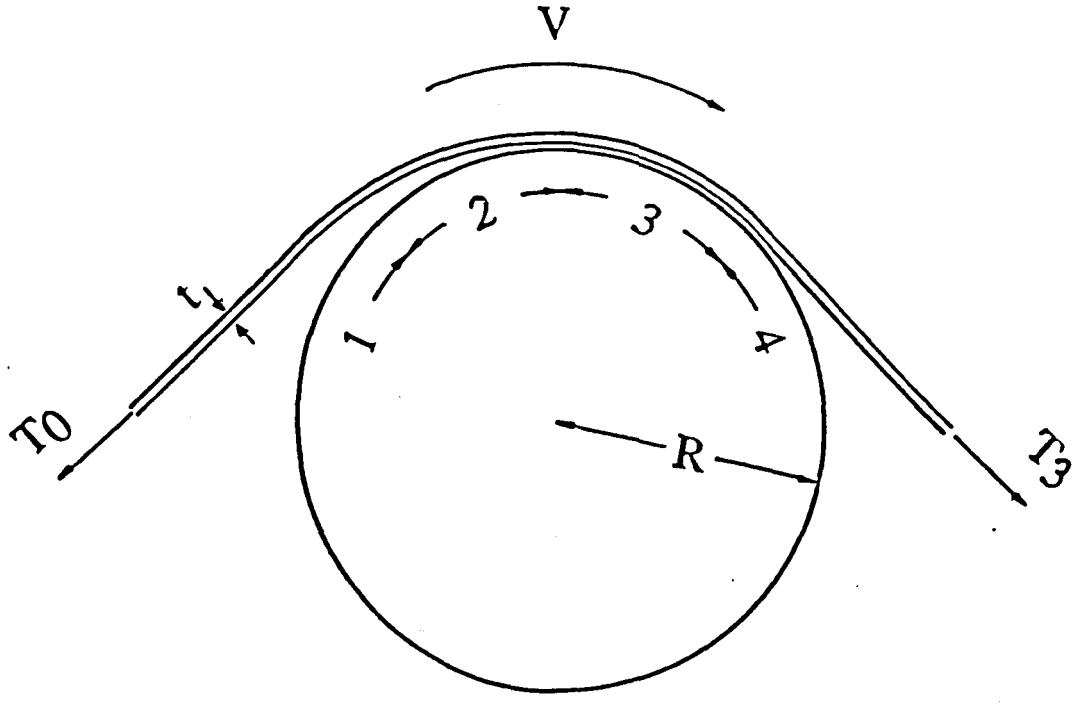

Regions of behaviour in pin impregnation: 1 entry; 2 impregnation; 3 contact; 4 exit.

Figure 2.2.8. Possible impregnation zones when a fibre tow is pulled around a cylindrical bar, after Chandler et al. (1992).

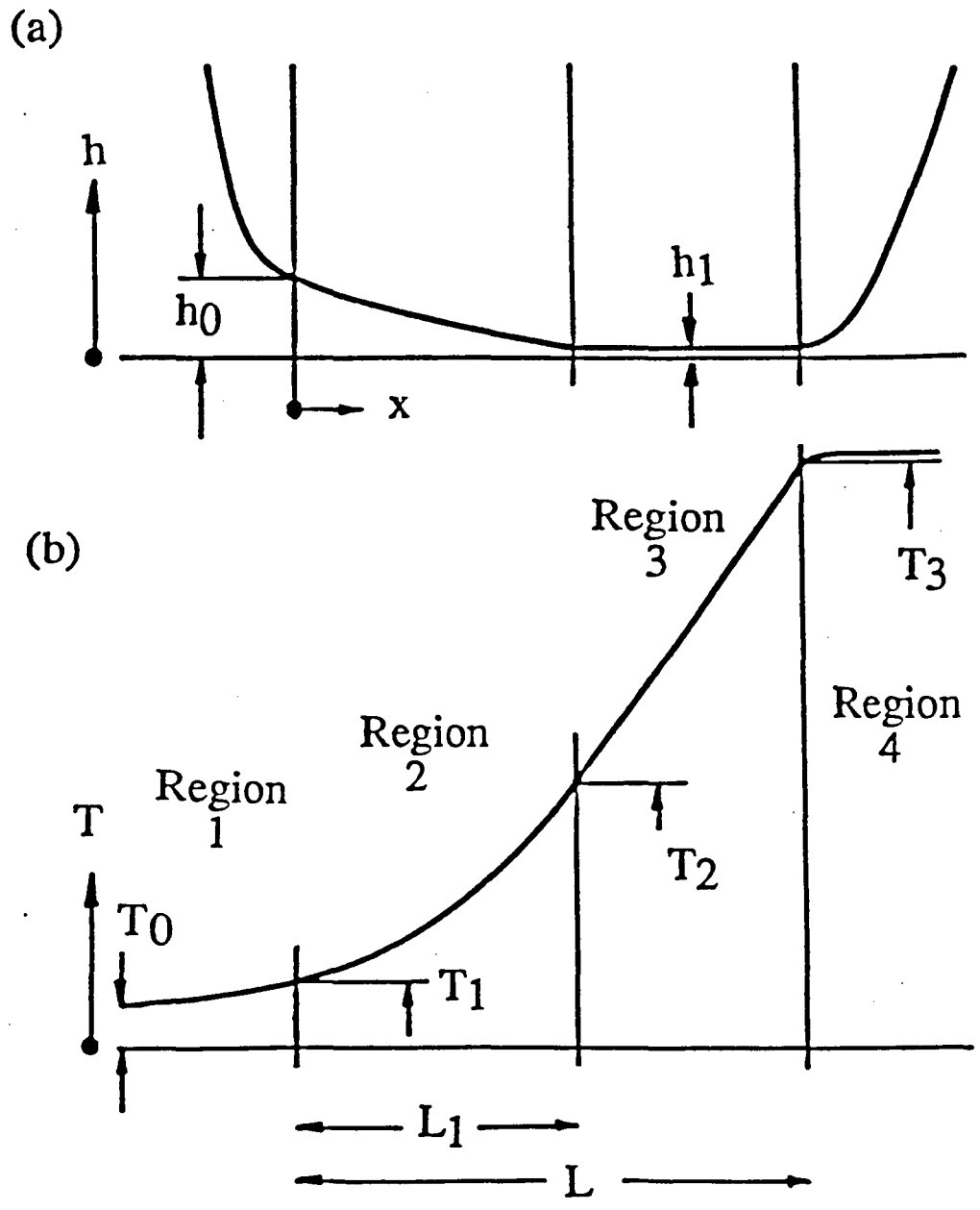

Figure 2.2.9. Schematic illustration of (a) film thickness and (b) tension build-up versus wrap length coordinate in impregnation of a fibre tow using cylindrical bars, after Chandler et al. (1992).

bar decreases as the fibre approaches the bar. A pressure will be generated in the resin film separating the pin and the fibre tow, in a manner analogous to the entrainment of oil in a journal bearing. The second zone is a region in which the pressure generated in the resin film causes resin to be pumped through the thickness of the porous fibre tow. This zone will be referred to as the impregnation zone. The third zone will be termed the contact zone and will begin when sufficient resin has been pumped through the fibre tow to allow contact between the fibres and the impregnation bar. The combination of Coulomb friction and viscous drag in the residual resin film results in a high rate of build-up of tension in the fibre tow in this region. The final zone is the exit zone where the fibre leaves the pin, again at an angle determined by the geometry of the process.

Often it is convenient to plot the film thickness against the circumferential distance, or wrap length, around the impregnation bar to effectively flatten out the surface of the bar.

2.3 Mechanical testing of unidirectional composites

The efficiency of any manufacturing process can be determined by whether or not the products produced exhibit the required mechanical properties, the dimensional tolerances and the finish quality required to satisfy the design of the part. In the case of composite materials, the properties of the moulding or laminate will depend strongly on the manufacturing process and the interaction effects of processing conditions on the final product properties.

It is important that the manufacturing process does not adversely change important features of the raw material, for instance fibre length distributions in injection moulding compounds. It is therefore equally important that the range of mechanical tests performed on the final product can accurately reflect the overall composite properties and highlight the effects that changing process parameters may have. In the pultrusion process, changing line speed, die temperature or forming pressure can exert a major effect on the properties of the final section, although not all of these changes will necessarily be picked up by conventional tensile and flexural test methods. The same applies to processes such as autoclave moulding where careful control of the temperature and pressure cycle is required to produce a product with the optimum properties. Again, it is vital that the range of mechanical tests performed on the finished part highlight deviations from the optimum processing conditions.

The stress applied to a composite is transferred from the matrix polymer to the fibres via shear stresses at the fibre/resin interface and it is therefore important that the interface is properly formed during processing. Assuming that there is good compatibility between the fibres and the resin, then the interfacial strength can be influenced by a number of factors, which include the degree of impregnation, the fibre distribution and the presence of voids. All of these factors are influenced by the processing cycle.

In thermoplastic pultrusion the most significant contributions to the overall properties of the pultruded section have been found to arise from the quality and level of impregnation, the void content, the uniformity of the fibre distribution and the degree of consolidation. Therefore, to reliably evaluate the effectiveness of the

process in maximising the composite properties, a mechanical test method is required which is sensitive to changes in each of these. It is also important that the mechanical test method is sensitive to changes in the non-fibre dominated properties of the composite. This again directs the choice of test method towards one which evaluates the shear and interfacial properties of the composite.

2.3.1 Methods of characterising the shear properties of fibre composites

In composite materials, the interface between the fibres and the matrix transmits the stresses acting on the composite from the matrix to the fibres. In order to utilise the high strength and stiffness of the fibres, they have to be bonded strongly to the matrix. Figure 2.3.1 represents a hexagonal array of fibres subjected to an externally applied strain, Hull (1981)[59]. The strain distribution within the two phase composite is not uniform and the majority of strain in a slice XX' will be taken up by the matrix since $E_f \gg E_m$. The strain in the slice YY' which passes completely through the matrix will be more uniform and the average strain will be lower than in the resin in slice XX'. The presence of the fibres causes a strain magnification in the resin between the fibres. The dependence of the strain magnification on the fibre volume fraction is shown also in Figure 2.3.1, Hull (1981)[59], and very large strain magnifications can be seen to occur at high fibre volume fractions. Shear forces acting in the regions between fibres can initiate shear failures and a common failure mode in composites, when the composite is loaded in bending, is the interlaminar separation of laminate or fibre layers parallel to the fibre axis which results in delamination in the composite. Intralaminar shear, as opposed to interlaminar shear, occurs through the thickness of the composite, often in individual laminate layers and perpendicular to the fibre direction.

A number of methods are available to measure the shear strength of composite materials. The requirements which must be fulfilled to ensure a good test method have been discussed, Chiao et al (1977)[60]. Shear strength is difficult to measure unambiguously as most of the common test methods also introduce tensile and compressive stresses in addition to pure shear during testing. Ideally, the testing method should produce pure shear, it should give reproducible results and should require no special equipment either for sample preparation or testing. It is also important that the test can be adapted to work for a range of sample sizes and shapes and can accommodate both flat and round samples.

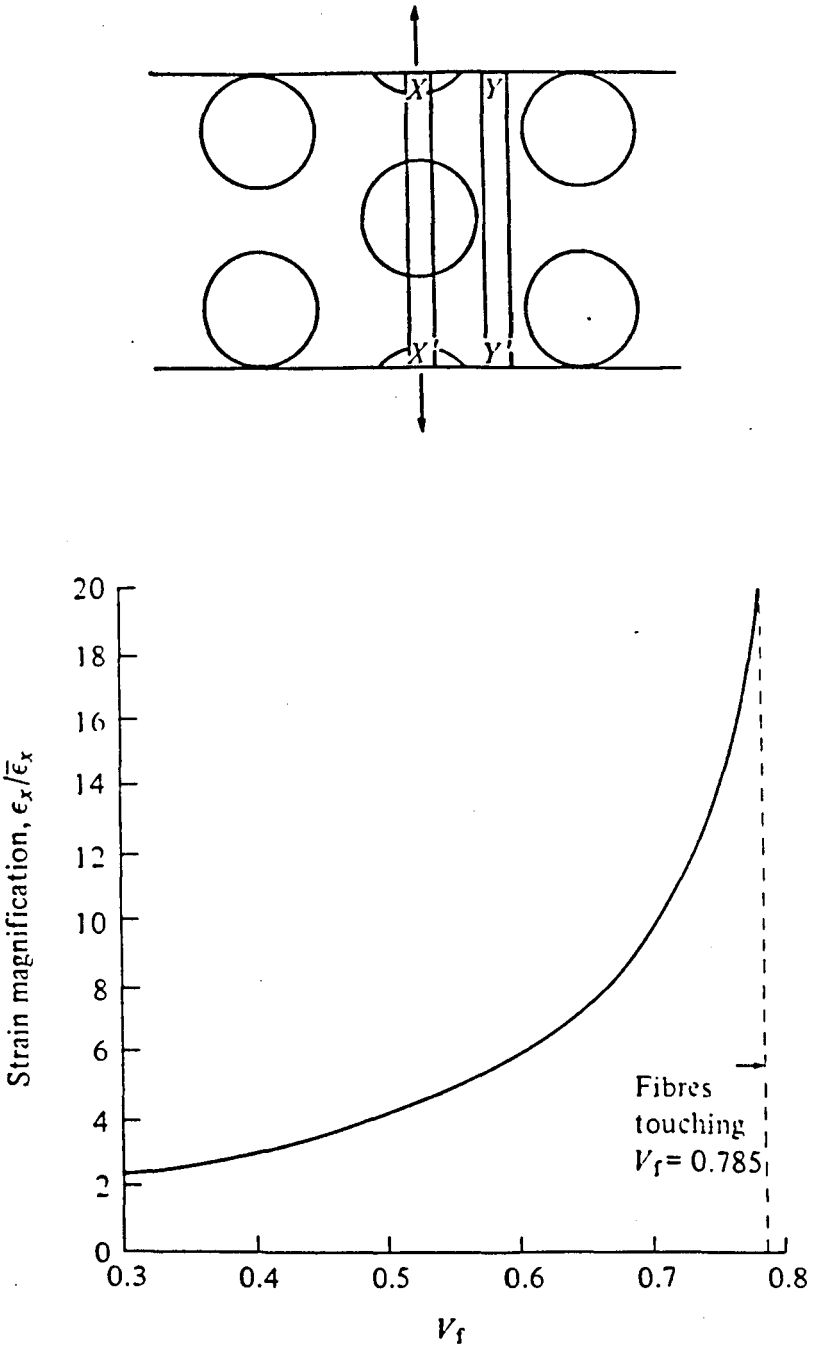

Figure 2.3.1. Schematic representation of strain magnification in a unidirectional lamina subjected to an externally applied strain. Dependence of strain magnification on V_f for a glass fibre-polyester resin, after Hull (1981).

The ideal method for determining the shear response of a composite is from a thin walled tube subjected to torsion, which results in pure shear stress and strain in the tube wall. However, this test has drawbacks in that it is restricted in sample geometry to thin walled tube specimens and buckling of the tube wall is difficult to avoid. The shear stress is not constant and a maximum occurs at the surface of the tube where the presence of small surface flaws may initiate premature failure. The method is also impractical when a large number of tests are required.

Two methods can be considered as suitable for characterising the shear strengths and hence the overall integrity of composite sections produced by thermoplastic pultrusion. These are the short beam shear test and the torsion pendulum test and these will be discussed in the following section.

2.3.1.1 Short beam shear test

The short beam shear test can be used to measure the apparent interlaminar shear strength (ILSS) of reinforced composites. The test uses three point bend loading with a span to depth ratio much less than that used in conventional flexural tests. This increases the level of shear stress relative to the flexural stress experienced by the test pieces, thus inducing an interlaminar failure along the centreline of the specimen rather than a tensile failure at the lower surface, as is common in flexural tests. The test is detailed in BS 2782: pt 3: Method 341A[61] and in ASTM D-2344-72[62].

When a sample, comprising uni-directional fibres parallel to the x axis, is under stress as shown in Figure 2.3.2, three shear stresses can result: τ_{xz}, τ_{yz}, and τ_{xy}. The stresses τ_{xz} and τ_{yz} are the interlaminar shear stresses. The short beam shear test is illustrated in Figure 2.3.3, with support dimensions as described in BS 2782. The shear stress distribution across the specimen thickness is also shown, Chiao and Moore (1975)[63]. This is a parabolic function with a maximum at the neutral axis of the specimen and which decreases to zero at the upper and lower surfaces. The ILSS can be calculated using equation 2.3.1, where P is the load at failure and A is the cross sectional area.

$$ILSS = \frac{3P}{4A} \qquad 2.3.1$$

Interlaminar failure will occur under three point bending when the shear stress at the

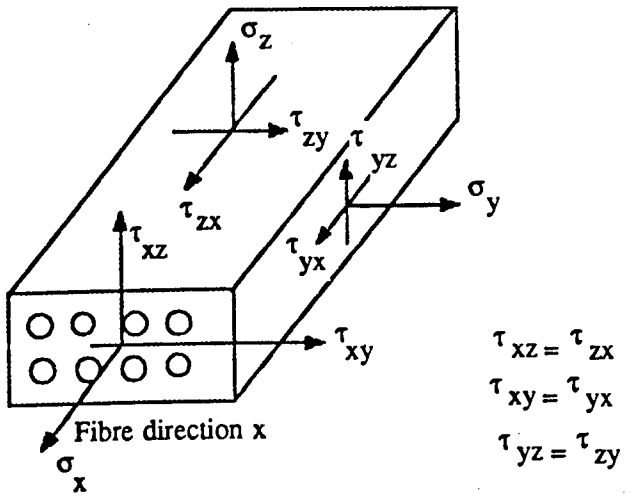

Figure 2.3.2. Stress componants in an unidirectional lamina, after Chiao and Moore (1975).

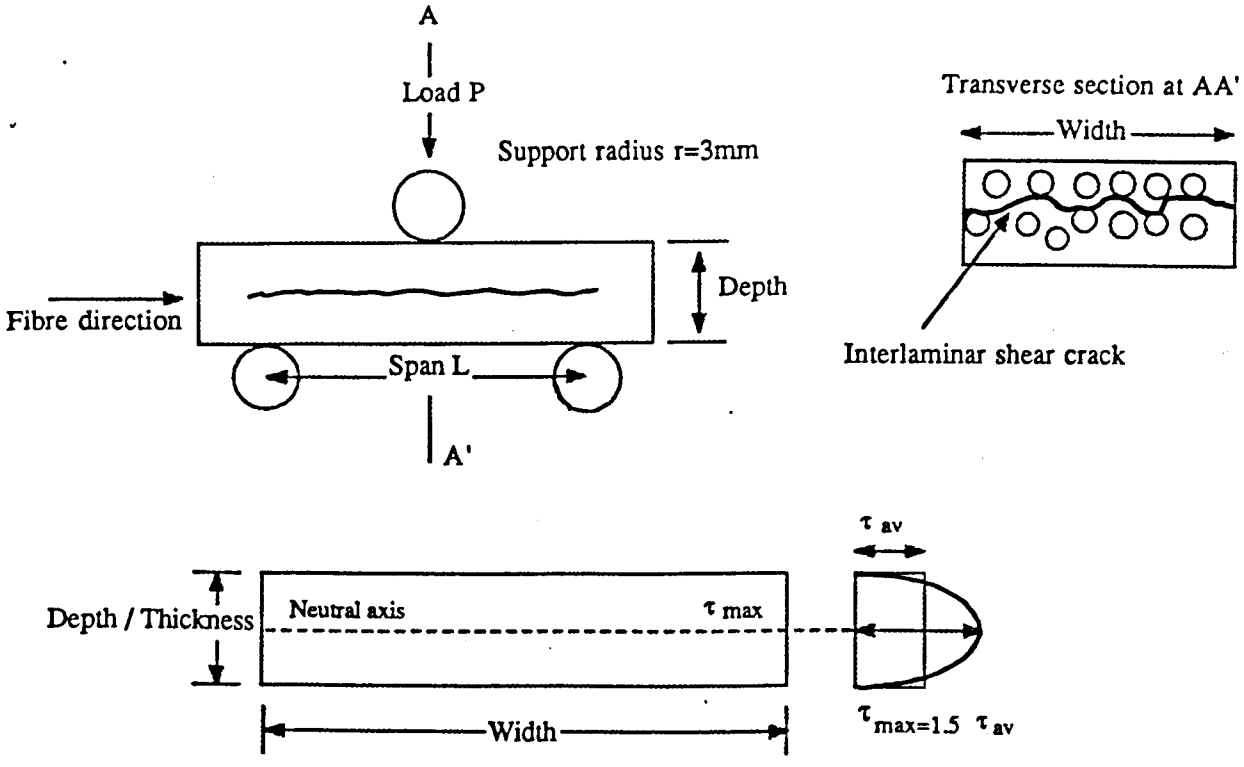

Figure 2.3.3. Schematic diagram of the short beam shear test and stress distribution across specimen thickness, after Chiao and Moore (1975).

neutral axis locally exceeds the shear strength of the composite, before the tensile stress in the fibres at the surface reaches the composite tensile failure stress. If the span-to- depth ratio of the composite beam is L/D then the beam will fail by interlaminar shear if equation 2.3.2 is fulfilled, where σ_c is the composite tensile failure stress, τ_I is the composite shear strength, Harris (1986)[64].

$$\frac{L}{D} > \frac{\sigma_c}{2\tau_I} \qquad 2.3.2$$

The data obtained from the short beam shear test have been found to be highly dependent on a number of factors including span to depth and width to depth ratios, support diameter and specimen preparation, Chiao and Moore (1975)[63].

The effect of the span to depth ratio has been studied, Sattar and Kellogg (1969)[65], who found that failure was limited to either shear mode at the centre of the beam or flexural failure at the outer fibres. It was reported that the possibility of flexural failure could be minimised by choosing a specific span to depth ratio for the composite to be tested. A procedure was proposed for determining this based on the approximate flexural to shear strength ratio of the material to be tested. Figure 2.3.4 can then be used to calculate the maximum span to depth ratio which can be used without causing flexural failure. The method of determining the span to depth ratio, as described in the ASTM standard, is based on the Young's modulus of the reinforcement fibres. For fibres with a Young's modulus less than 10^5 MPa a ratio of 5 is recommended, for other fibres a ratio of 4 is recommended.

Chiao and Moore (1975)[63] have evaluated the short beam shear test on three types of aramid/epoxy composite specimen and have found that the measured ILSS can be dependent on specimen preparation and increases with the diameter of the beam supports. They have also reported poor reproducibility of the test results which was attributed in part to the presence of voids and defects in the specimens.

A modified short beam shear test was proposed by Whitney and Short (1987)[66] in response to the difficulty in interpreting the test data which arises due to the mixed mode failures which are often observed. The range of failures which may occur is illustrated in Figure 2.3.5. In an attempt to produce uniform shear stress in the composite it has been proposed to sandwich the composite between two thin steel plates bonded to each surface to produce a single sandwich beam specimen. In this configuration the composite is confined to the midplane of the sandwich beam where the stress state is one of uniform shear and where failures in the area under

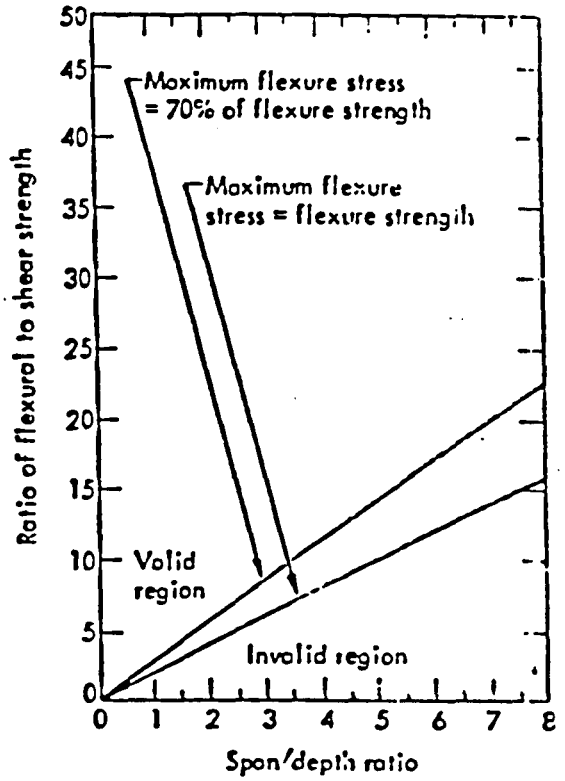

Figure 2.3.4. Ratio of flexural strength to shear strength versus span-to-depth ratio, after Sattar (1969).

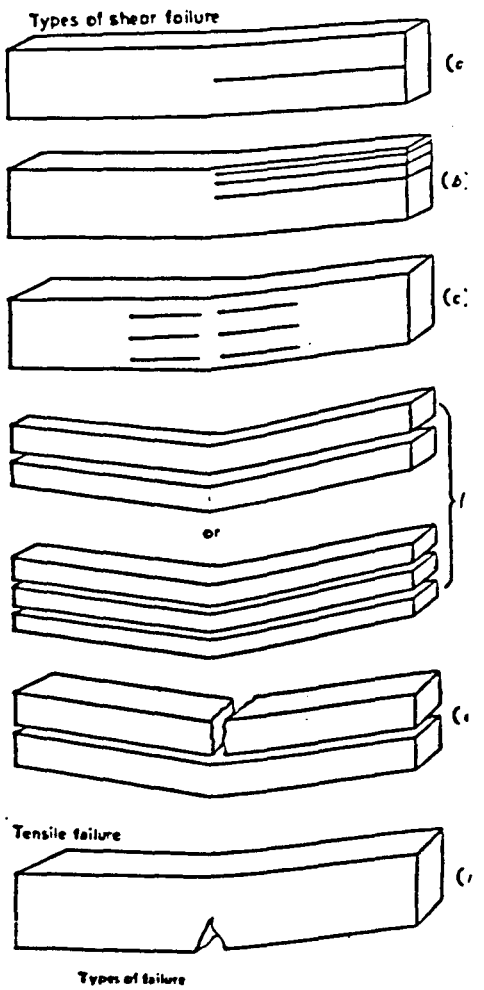

Figure 2.3.5. Types of shear failure possible in short beam shear test. after BS 2782: Part 3: Method 341A: 1977.

the loading nose will be absorbed by the metal plates. However, this is not a practical procedure if a large number of tests are to be performed and a range of failure modes were still observed, including compressive fracture of the plates themselves.

In the light of the reported variations in absolute test results which can arise due to different testing parameters and the presence of mixed failure modes, the test is not suitable for the determination of absolute shear strength values for design specification purposes, as any comparison of results would also have to include a comparison or discussion of testing conditions. However, the short beam shear test is suitable for quality control and research and development applications as a comparative testing method when care is taken to keep testing conditions consistent. A major advantage of this method is that the test samples are easy to prepare, there are no major limitations to specimen geometry and both flat and curved specimens can be tested and the test itself is simple to perform and evaluate.

A number of authors have used this test to characterise different fibre/matrix interfacial characteristics and the effects of void content on the properties of different composite materials.

The interfacial characteristics of carbon/epoxy composites fabricated using sized and unsized carbon fibres has been investigated using the short beam shear test with a span to depth ratio of 10, Banerjee et al.(1988)[67]. The apparent interlaminar shear strengths were found to vary between the two samples and it was reported that the samples failed in combined tension and shear modes. Higher values of ILSS were found for the unsized fibres compared to the sized fibres and this was attributed to the larger degree of misaligned fibres in the unsized samples and this result highlights another parameter which may influence the test results.

The relationship between void content and the ILSS of carbon/epoxy and carbon/polyester composites has been investigated, Yoshida et al.(1986)[68]. In this work a foaming agent was used to produce laminates containing a wide range of void contents. It was found that the ILSS reduced with increasing void content for both types of specimen tested. The decrease was also found to have an almost linear relationship with increasing void content as illustrated in Figure 2.3.6. A similar result has been reported concerning the effect of voids on the ILSS of carbon/epoxy laminates as shown in Figure 2.3.7, Beaumont and Harris (1972)[69]. A typical average shear stress versus displacement graph for a short beam shear test

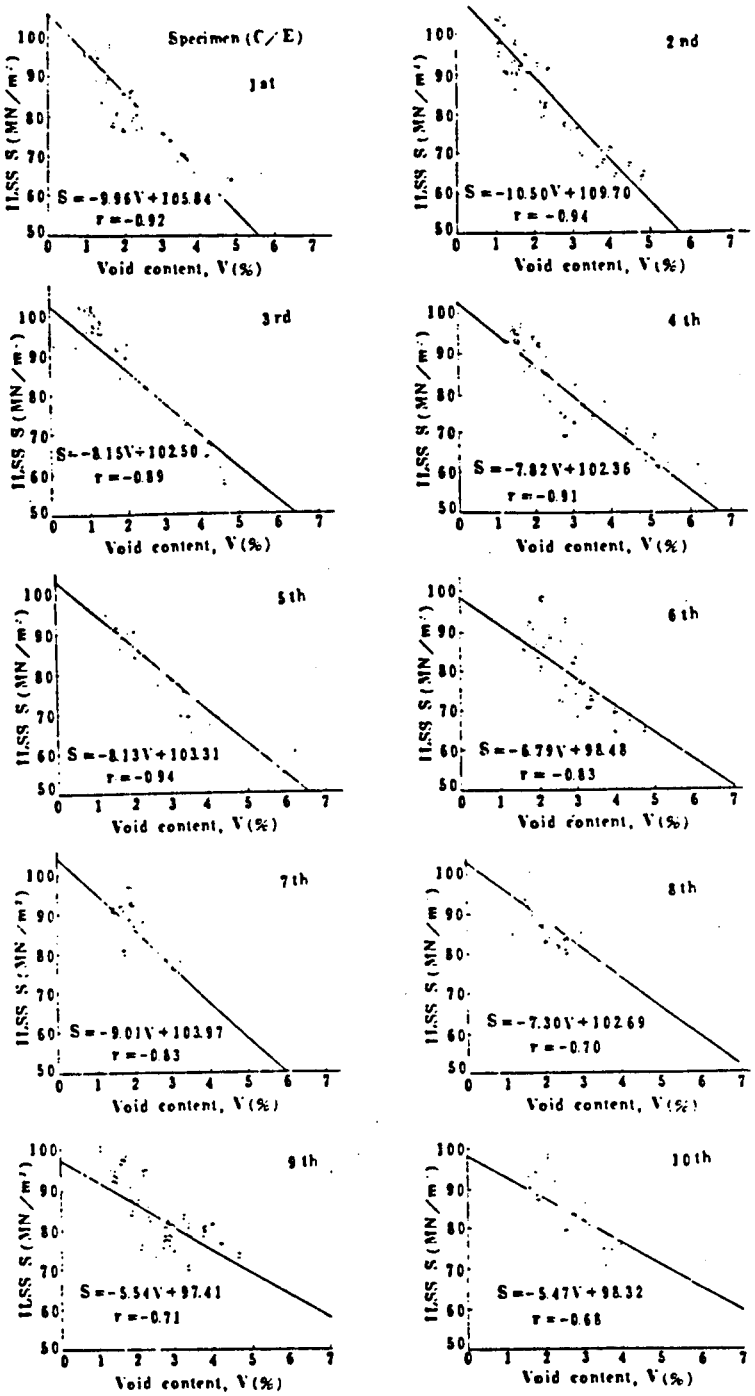

Figure 2.3.6. Reduction in ILSS with increasing void content for carbon-epoxy specimens, after Yoshida (1986).

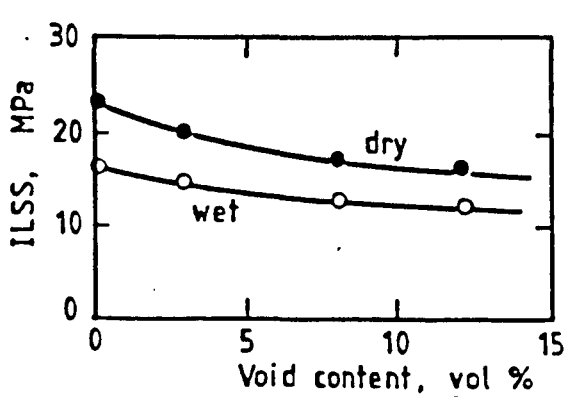

Figure 2.3.7. Effect of voids on the ILSS of carbon-epoxy laminates, after Beaumont and Harris (1972).

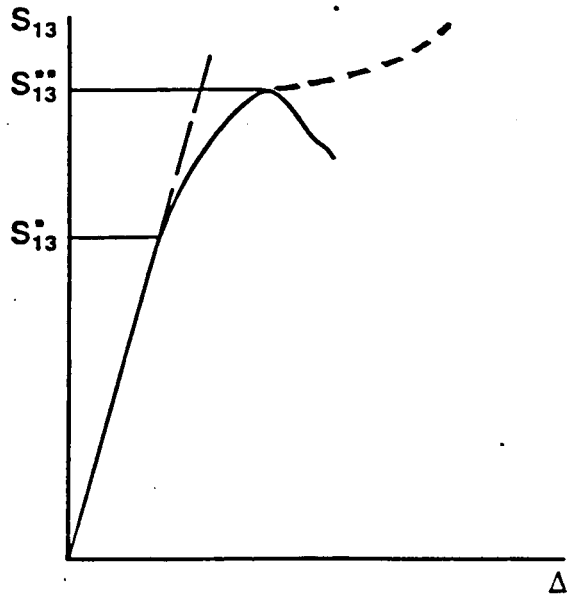

Figure 2.3.8. Shear stress versus load displacement diagram in a three point bend, short beam shear test, after Palley (1985).

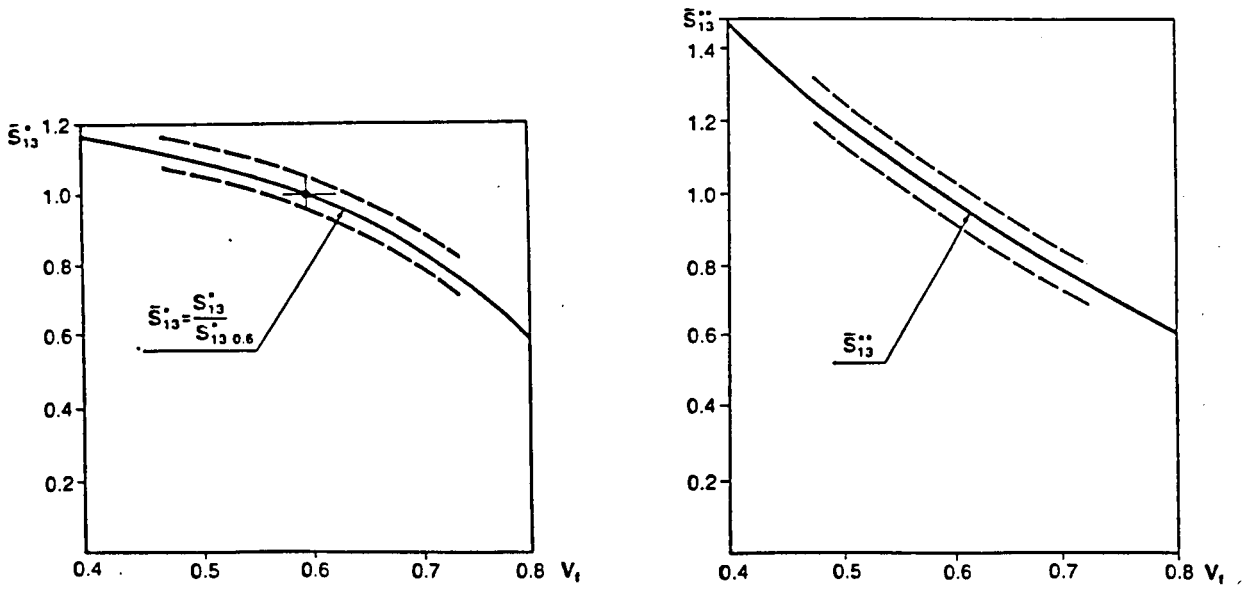

Figure 2.3.9. Graph showing the relative value of shear stress at the moment of crack initiation as a function of fibre volume content and a graph showing the relative value of the ultimate shear stress as a function of fibre volume content, after Palley (1985).

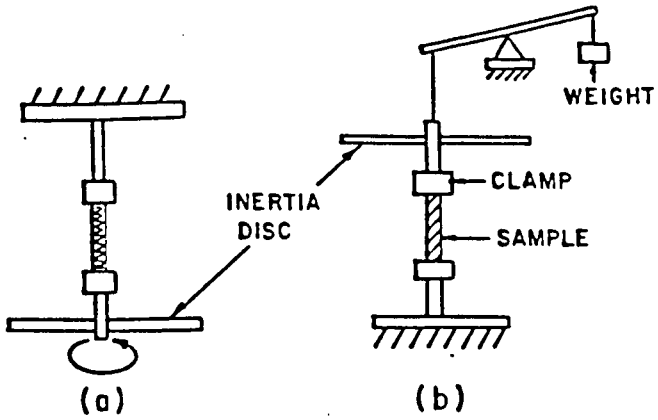

Simple diagram of torsion pendulum.

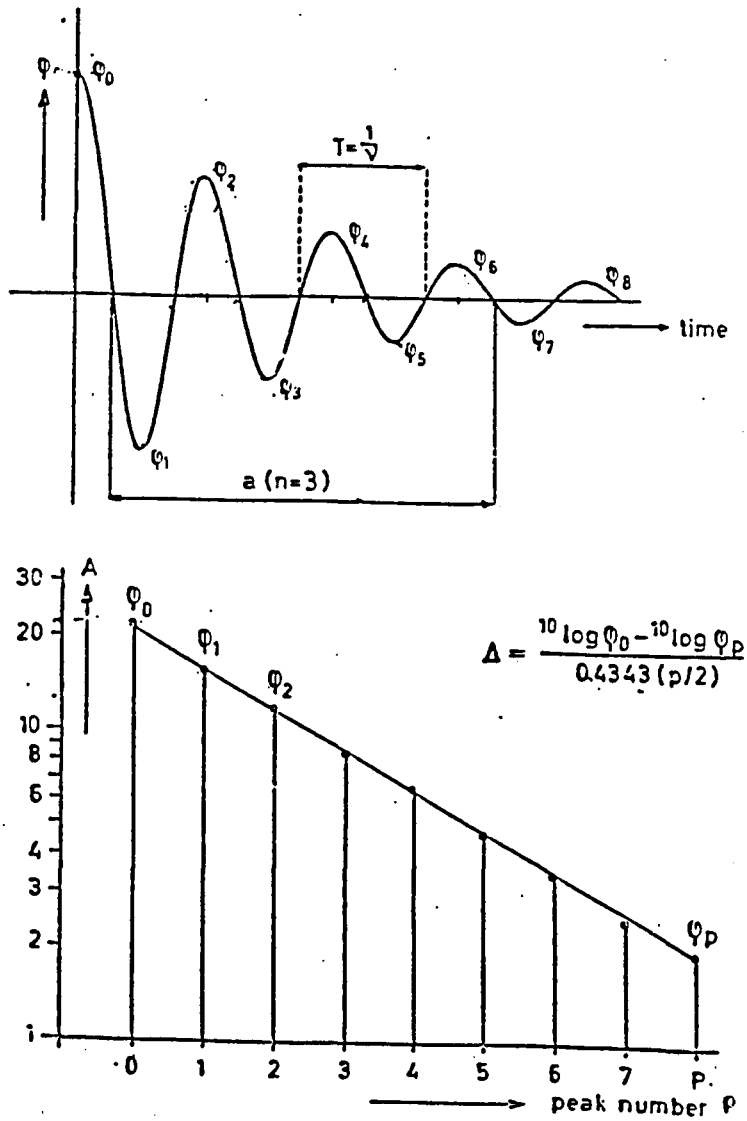

Figure 2.3.10. Schematic illustration of two variations of the torsion pendulum test and showing a typical output trace. This shows the decay in the sample oscillation and a semi-log plot of the peak height against the peak number, p.

is shown in Figure 2.3.8, Palley (1985)[70]. In composites with a brittle matrix the stress level S^* corresponding to the deviation from the linear portion of the curve can be attributed to the initiation of cracking. The maximum value of stress, S^{**} corresponds to the merging of the interfacial cracks. It is sometimes the case that the stress level will begin to rise again after S^{**}, due to compression of the sample between the supports. In this case S^{**} is not clearly defined and requires interpolation. This rise is illustrated by the dashed line in Figure 2.3.8. The dependence of the shear stress on the reinforcement volume fraction has also been investigated, Palley (1985)[70]. This is illustrated in Figure 2.3.9 as the relative value of shear stress at the moment of crack initiation, S_* and the relative value of the ultimate shear stress, S_{**}, versus the fibre volume fraction for an unspecified glass/thermoset system. The value S_*,0.6 is the stress at a volume fraction of 0.6. The graph shows marked decrease in the value of S_* as the volume fraction increased. This decrease was also observed in the relative value of the ultimate stress, S_{**} for increasing fibre volume fractions.

This work demonstrates the value of the short beam shear test as a comparative test between composite materials, especially where void contents and the integrity of interface formation may be a function of changes in process parameters.

2.3.1.2 Torsion pendulum test

Another test which can be used to measure the quality of both the impregnation and the interface produced in the composite is the torsion pendulum test. This test measures the torsional shear modulus and mechanical damping characteristics of samples which can be either cylindrical or rectangular in section, although certain restrictions do apply to rectangular sections. The torsion pendulum is shown schematically in Figure 2.3.10. The sample is allowed to oscillate in torsion under free vibration with one end rigidly clamped. As the oscillations twist and untwist the specimen the decay of the vibration is recorded to produce a torsional displacement-time curve the form of which can also be seen in Figure 2.3.10. From this it is possible to determine the dynamic shear modulus, G', and the logarithmic decrement, Δ. The shear modulus is calculated using equation 2.3.3 for a cylindrical specimen and equation 2.3.4 for a rectangular specimen, Murayama (1978)[71].

$$G' = \left(\frac{8\pi IL}{r^4}\right)\left(\frac{1}{p^2}\right) \qquad 2.3.3$$

$$G' = \left(\frac{64\pi IL}{u6h^3}\right)\left(\frac{1}{p^2}\right) \qquad 2.3.4$$

In these equations, L is the specimen length, I is the moment of inertia, b is the specimen width, h is the specimen thickness, u is a shape factor depending on the ratio of width to thickness, r is the specimen radius and P is the period of oscillation.

The log decrement, Δ, is calculated from the log of the ratio of the amplitude of two successive oscillations. In equation 2.3.5, A_1 is the amplitude of the first oscillation and A_2 is the amplitude of the second.

$$\Delta = \ln\frac{A_1}{A_2} = \ln\frac{A_2}{A_3} = \ln\frac{A_{n-1}}{A_n} \qquad 2.3.5$$

Δ is related to the dissipation factor tan δ and the loss shear modulus, G", by equations 2.3.6 and 2.3.7.

$$\Delta = \tan\delta \qquad 2.3.6$$

$$\frac{G''}{G'} = \tan\delta \qquad 2.3.7$$

The torsion pendulum has been successfully demonstrated, Banerjee et al. (1988)[67], as a characterisation test to differentiate between the effects of fibre sizing in carbon/epoxy composites. The poor interfacial bonding arising from using unsized fibres was illustrated by measuring the loss modulus, G", which was higher for unsized fibres than for sized fibres due to larger viscous dissipation at the poor fibre/matrix interface.

2.4 Heat transfer in the processing of thermoplastic composites

2.4.1 Mechanisms of heat transfer and governing equations

In order to successfully process thermoplastic composites heat must be applied to melt the matrix. This heat must then be removed to solidify the composite in its new form. It is important that this heating and cooling is carried out with control to prevent degradation and oxidation during heating and to control shrinkage in the formed product. An understanding of the mechanisms of heat transfer is vital in establishing the temperature requirements of the processing stage in the production of thermoplastic composites. There is a combination of three heat transfer mechanisms which will operate, conduction, convection and radiation.

Heat transfer through a solid body or fluid occurs by conduction. The steady state heat flow is proportional to the temperature difference and to the area normal to the direction of heat flow and is expressed as Fourier's law, equation 2.4.1, in which Q_x is the rate of heat flow in the x direction, A is the area normal to the x direction, (dT/dx) is the temperature gradient in the x direction and k is the thermal conductivity.

$$Q_x = -kA\left(\frac{dT}{dx}\right) \qquad 2.4.1$$

The second important heat transfer mechanism is convective heat transfer, which occurs by bulk motion of liquids and gases from one place to another at a different temperature. Convection is usually associated with heat transfer between fluids and solid boundaries and can take two forms. Free convection occurs when motion of the fluid is induced by buoyancy forces and the rates of heat transfer are dependent only on the particular properties of the fluid media. On the other hand, if the motion of the fluid is externally induced then forced convection is said to occur.

The velocity and temperature boundary layers resulting from fluid flow past a flat plate are shown in Figure 2.4.1. In heat transfer between a solid wall and a fluid medium, the greatest resistance to heat flow occurs in the comparatively thin boundary layer adjacent to the wall, of thickness Δt in Figure 2.4.1.

It is customary to describe rates of heat transfer between a fluid and a solid wall

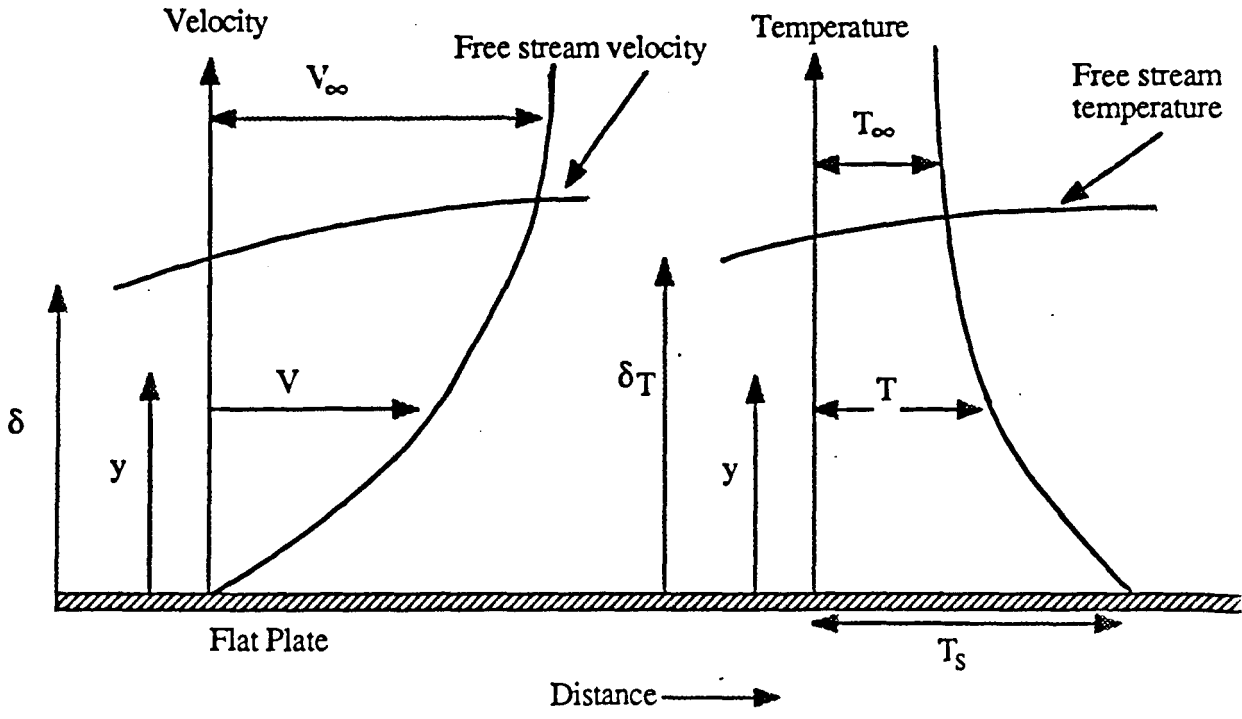

δ = boundary layer thickness

δ_T = thermal boundary layer thickness

Figure 2.4.1. Velocity and thermal boundary layers resulting from fluid flow past a flat plate, after Bayley (1972).

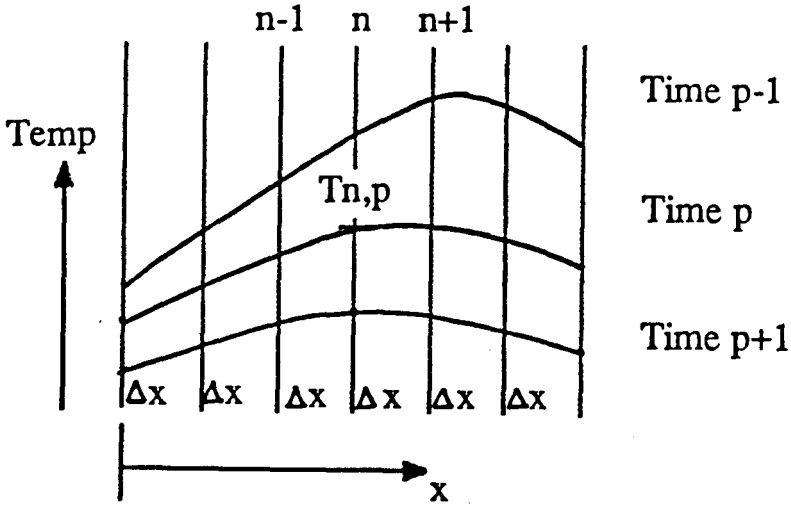

Figure 2.4.2. Unsteady state heat transfer, one-dimensional time and space intervals.

using an equation of the form 2.4.2, in which h is the surface heat transfer coefficient, the value of which depends on the properties of the fluid media and the flow conditions in which heat transfer is operating. T_s and T_f are the surface and fluid temperatures respectively.

$$Q = -hA(T_s - T_F) \qquad 2.4.2$$

It is difficult to measure the heat transfer coefficient directly. However, it is possible to calculate the local heat transfer coefficient at a distance x from the surface of the plate from the relation:

$$\frac{h_x x}{k} = 0.332 Pr^{1/3} Re^{1/2} \qquad 2.4.3$$

Where h_x is the local heat transfer coefficient, x is the distance from the leading edge of the plate and k is the thermal conductivity of the fluid.

In this expression, the dimensionless heat transfer coefficient, $(h_x x)/k$, is termed the Nusselt number, Nu_x. This is an expression for the rate of heat transfer by convection and can be seen to be a function of the Reynold's number which describes the flow and the Prandtl number which is a property of the fluid, Rogers and Mayhew (1967)[72].

There has been little data published concerning convective heat transfer during polymer processing and because of this, a single value for the heat transfer coefficient is often used as an approximation to describe the complete situation at the thermal interface.

The third mechanism of heat transfer is radiation, which does not require a solid or fluid for its propagation and which is transmitted by electromagnetic waves. The amount of energy transmitted by this mode depends on the temperature of the emitting body, the wavelength of the emitted radiation and the nature and area of the surface of the emitter. Radiative heat transfer can be expressed by equation 2.4.4.

$$Q = E\sigma(T_1^4 - T_2^4) \qquad 2.4.4$$

The constant σ is the Stefan Boltzmann constant and has a value of $5.67.10^{-8}$ W/m^2K^4 and E is termed the emissivity and this determines the fraction of blackbody radiation transmitted. E is a strong function of the surface finish and

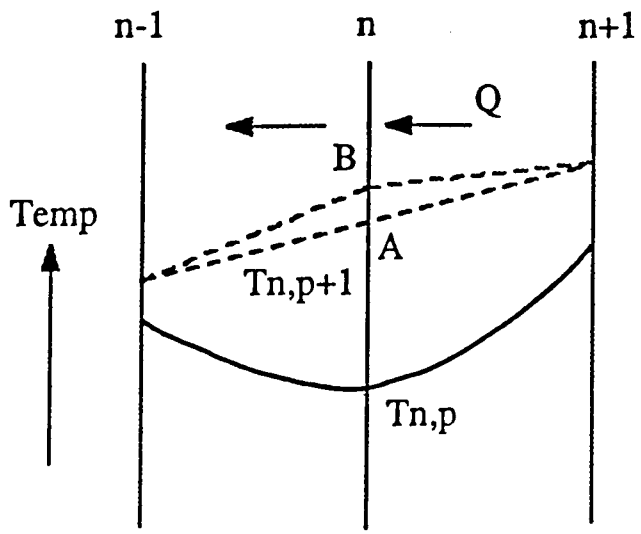

Figure 2.4.3. Illustration of the effect of the Fourier number on the stability of the solution to one-dimensional numerical heat transfer.

tends towards 1 for unpolished matt black finishes. Often radiative and convective heat transfer occur simultaneously and although radiative heat transfer involves the difference in the fourth power of the temperature, it is possible to treat radiation by means of a radiation heat transfer coefficient based on the temperature difference between the radiator and the receiver. This can be expressed:

$$Q = h_{rad} (T_1 - T_2) \qquad 2.4.5$$

Where Q is the radiative heat flow and T_1 and T_2 are the temperatures of the two bodies exchanging heat by radiation. The net heat transfer can be expressed by equation 2.4.4. Thus the radiation heat transfer coefficient can be expressed:

$$h_{rad} = \frac{E\sigma(T_1^4 - T_2^4)}{(T_1 - T_2)} \qquad 2.4.6$$

At the levels of temperature normally associated with radiative heat transfer in engineering applications, substantial variations in the lower temperature, T_2 in equation 2.4.6, have little effect on the rate of heat flow. In the case of heating thermoplastic precursors, the surface temperature of the infra-red emitter far exceeds the temperature of the polymer being heated. Thus, the radiative heat transfer coefficient behaves approximately like a convective heat transfer coefficient in linking heat flow linearly with temperature difference for a fixed upper temperature, T_1.

This coefficient can be added to the convection heat transfer coefficient to describe the total heat transfer in situations where both convection and radiation occur. The radiation heat transfer coefficient is, unlike the convective coefficient, strongly temperature dependent.

2.4.2 Partial differential equation for unsteady state heat transfer

A wide range of different methods are available to model heat transfer and so predict the temperature distributions which will be experienced during processing. The choice of method and the complexity of the solution required depend on the particular problem to be solved. Two methods commonly used are analytical and numerical finite difference techniques. Of these, numerical finite difference techniques tend to be more straightforward and generally applicable when compared

to analytical methods, the solutions of which usually take the form of an infinite series or as complex integrals.

A one dimensional partial differential equation for time dependent, unsteady state conduction can be derived from Fourier's law to give Laplaces's equation:

$$\dot{T} = \alpha \nabla^2 T \qquad 2.4.7$$

The term α (m^2s^{-1}) is the thermal diffusivity, and this term partially quantifies the rate of response of the material to temperature change in a time dependent system. The Laplacian operator in three dimensional Cartesian co-ordinates is:

$$\nabla^2 = \frac{\partial^2}{\partial x^2} + \frac{\partial^2}{\partial y^2} + \frac{\partial^2}{\partial z^2} \qquad 2.4.8$$

Equation 2.4.8 can be reduced for one dimensional conduction to give equation 2.4.9:

$$\frac{dT}{dt} = \frac{k}{\rho C_p}\left(\frac{d^2T}{dx^2}\right) \qquad \alpha = \frac{k}{\rho C_p} \qquad 2.4.9$$

2.4.3 Finite difference equations for unsteady state, one dimensional conduction

The finite difference method requires that the governing partial differential equation, equation 2.4.9, is replaced by a set of algebraic equations. The solution of these gives an approximate solution to equation 2.4.9, although it is possible to achieve a high degree of accuracy.

To solve the equation 2.4.9 for unsteady state heat flow, it is necessary to develop a set of finite difference equations which are used to determine the temperature at a discrete number of sections, x_{n-1}, x_n, x_{n+1}, separated by equal space intervals, Δx. The time and space intervals are shown in Figure 2.4.2, for a slab with its parallel surfaces perpendicular to the x direction. However, since the temperature of these varies with time, it is also necessary to find the values at successive time intervals, t_{p-1}, t_p, t_{p+1}, separated by equal time intervals, Δt.. Each temperature must be represented by two suffixes, n and p, which denote, for instance, $T_{n,p}$ as the temperature of the section x_n at time t_p.

It is possible to express the temperature variation in the x direction as a power series when T varies continuously in the solution field:

$$T = b_o + b_1 x + b_2 x^2 + b_3 x^3 + ... \qquad 2.4.10$$

Using Maclaurin's theorem it is then possible to express a value of T at any distance x in terms of the differential coefficients of T= fn(x) at x=0. Therefore the finite difference equation for the differential coefficient can be written:

$$\frac{d^2T}{dx^2} = \frac{T_1 + T_2 - 2T_o}{\Delta x^2} \qquad 2.4.11$$

Using the same notation as in Figure 2.4.2 this can be rewritten as:

$$\frac{d^2T}{dx^2} = \frac{T_{n+1,p} + T_{n-1,p} - 2T_{n,p}}{\Delta x^2} \qquad 2.4.12$$

The differential coefficient of equation 2.4.9 can also be written as a finite difference equation:

$$\frac{dT}{dt} = \frac{T_1 - T_2}{\Delta t} = \frac{T_{n,p+1} - T_{n,p}}{\Delta t} \qquad 2.4.13$$

Therefore, the partial differential equation expressed in 2.4.9 can be replaced by the finite difference equation, applied at the section x_n at time t_p to give:

$$T_{n,p+1} = \frac{\alpha \Delta t}{\Delta x^2}\left[T_{n+1,p} + T_{n-1,p} + \left(\frac{1}{F_o} - 2\right)T_{n,p}\right] \qquad 2.4.14$$

An equation in the form of 2.4.14 can be written for every mesh point in the temperature field and thus the partial differential equation, which must be satisfied for every point in the solution field, can be replaced by an equation which must only be satisfied at a finite number of points, the accuracy of the solution therefore can be seen to depend on the density of the mesh chosen.

An important function in unsteady state heat transfer arises in equation 2.4.14. The Fourier number, Fo, which can be expressed as equation 2.4.15, is a dimensionless group which represents a dimensionless time scale and gives an

indication of the speed at which a body will respond to a temperature change.

$$F_o = \frac{\alpha \Delta t}{\Delta x^2} = \frac{Rate\ condition\ of\ heat}{Rate\ storage\ of\ heat} \qquad 2.4.15$$

The Fourier number cannot be chosen arbitrarily and is an important parameter in ensuring the stability of the numerical solution achieved using finite difference equations. Although the Fourier number could be given any value by an appropriate choice of Δx and Δt, not all values will result in a stable solution and Δx and Δt cannot be chosen independently. The choice of Fo therefore places a restriction on the choice of values for Δx and Δt. This can be best illustrated by the example given in Figure 2.4.3, Rogers and Mayhew (1967)[72]. At a given instant in time, t_p, the temperature distribution is shown as a solid line in Figure 2.4.3. The higher the value of Fo then the higher will be the temperature rise ($T_{n,p+1}$-$T_{n,p}$) as governed by equation 2.4.14. Assuming that the boundary temperatures do not change during a time interval, Δt, the maximum rise in $T_{n,p+1}$ will be to point A. At this point the flow of heat into and out of section x_n is balanced. This corresponds to a value of Fo=0.5. For a Fourier number, Fo >0.5, a temperature rise to point B will occur and this implies that an increase of temperature is achieved with a heat outflow from section x_n which is greater than the heat input and this is obviously physically impossible. For unsteady state conduction, the stability criterion is that Fo<=0.5, and this ensures that the solution does not diverge from or oscillate about the exact solution.

In order to solve the finite difference equation for unsteady state conduction, it is necessary to specify boundary conditions. The temperature distribution throughout the field of solution must be given for time, t_p=0, and the temperature variation with time of the two boundary planes of the field of solution must also be specified.

In order to calculate the temperature distributions for the various processing conditions, a computer model was developed. All programs were written in Basic.

Chapter 3 Modelling heat transfer during thermoplastic pultrusion

3.1 Description of the physical problem during the heating and cooling stages of the pultrusion process

When the individual precursor tapes are pulled into the heated section of the process they are heated by a combination of three heat transfer mechanisms, medium wavelength infra-red radiation, surface convection from heated air within the oven in both the infra-red heating section and in the hot air oven and conduction through the precursor thickness. As the tapes are heated they are guided so that the flat surfaces of greatest surface area are normal to the incident radiation and are kept separated until they enter the hot air oven. Here, they are gradually collimated so as to leave the oven in a rectangular bundle. Guides at the oven exit are used to squeeze this tape bundle lightly together to remove trapped air and to present a semi-formed material pack to the first forming and consolidation stage. In some experiments a heated die was placed at the oven exit to provide additional consolidation without causing any cooling of the material pack. The precursor tapes used in the experimental stages of this work have ranged in thickness from 0.25mm to 2.25mm, all have been between 10 to 15mm wide and all have been off white in colour except for the carbon/PEEK (APC2) precursor which was black.

The purpose of modelling was to predict the temperature distributions in the composite material as it passed through the process before, during and after consolidation.

3.2 Assumptions

To simplify the physical problem a number of assumptions have been made concerning the geometry of the composite section, the thermal properties of the constituent phases, the overall composite properties, the dominant heat transfer mechanisms operating and the effect of the phase changes in the matrix polymer during processing.

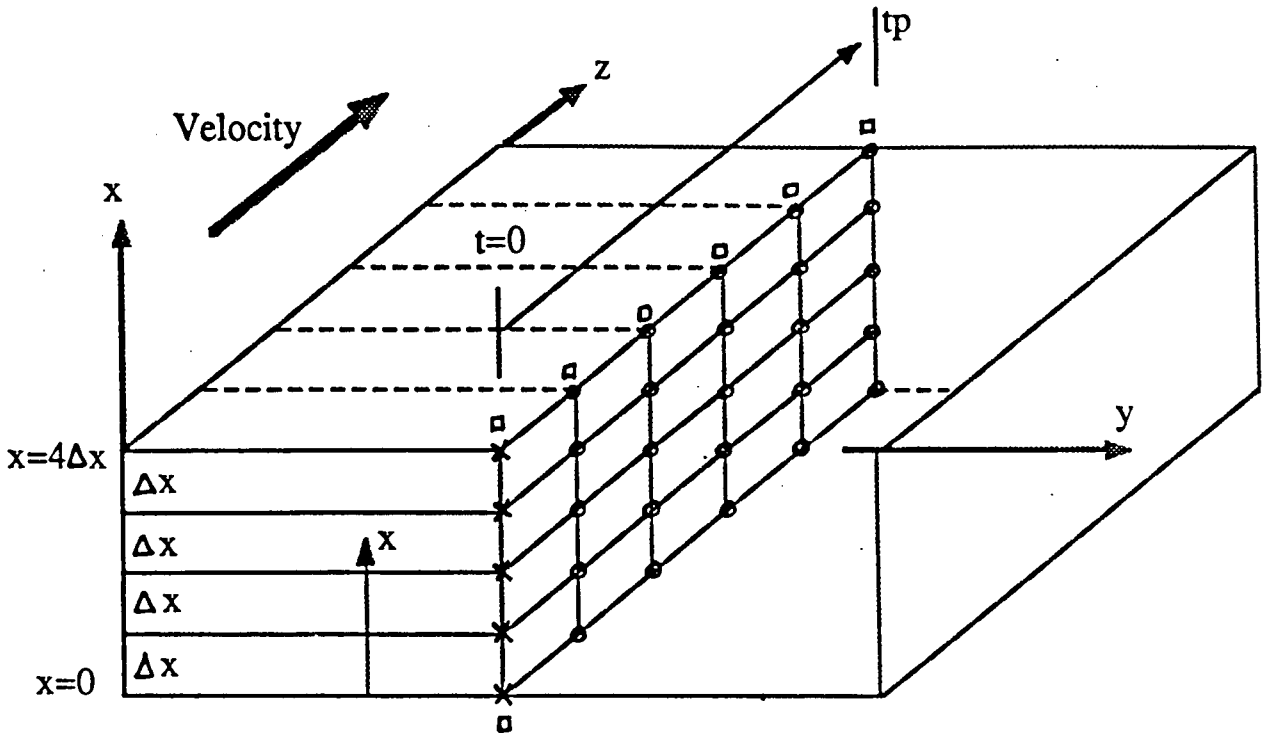

x = Boundary condition specified at t=0

□ = Boundary condition specifying the temperature variation with time of the boundary planes

o = Temperature distribution required at successive time intervals between t=0 and t=tp

Dimension y>>x
Dimension z>>y>>x

Figure 3.1. Heat transfer problem represented as a one dimensional flat slab in cartesian coordinates.

3.2.1 Geometrical Assumptions

In formulating the geometry of the solution, it has been assumed that maximum heat transfer will occur through the parallel surfaces of greatest surface area, and because the section width is greater than its thickness, heat transfer effects at the edges of the section have been neglected. The geometry of the problem together with the cartesian coordinate system used is illustrated in Figure 3.1. There are no internal heat sources or heat sinks. As the composite section cools, the thickness has been assumed to remain constant. The composite section is moving with a velocity v, in the z direction as shown in Figure 3.1, during the thermoplastic pultrusion process. This speed can be considered to be sufficiently high so that the rate of axial heat conduction along the fibres in the direction of movement can be neglected with respect to the rate of heat transfer in the x direction, perpendicular to the fibres. Therefore, axial heat transfer has been neglected and heat transfer has been modelled in one direction, perpendicular to the fibres and the problem can be considered to be equivalent to heating or cooling a stationary sample as a function of time.

The time scale for conduction in a composite can be expressed:

$$t = \frac{L}{\alpha} \qquad 3.1$$

Where t=characteristic time, L=appropriate conduction length and α=thermal diffusivity of the composite, Grove (1988)[43]. Arbritrarily setting l=1mm and $\alpha=2.10^{-7}m^2/s$, a typical value for a nylon/glass composite, the characteristic time for conduction over this length can be calculated as 5 seconds. Assuming that the pultrusion line speed is in the order of 3m/min then the composite section will travel 250mm in this time. Therefore the through-thickness conduction will occur at a much greater rate than the internal conduction of heat in the axial direction, which can thus be neglected.

3.2.2 Thermal properties of constituent phases and calculation of the overall composite thermal properties

One of the most important material properties governing the thermal response of the composite is the thermal conductivity of the constituent phases, the matrix, k_m, and

fibres, k_f. The thermal conductivity of both the matrix and fibres has been assumed to be constant over the processing temperature range. Experimental studies have been carried out, Ott (1981)[73], to measure the temperature dependence of the thermal conductivity for a number of different polymers and composites in the temperature range 25-140°C, and a number of models to calculate the thermal conductivity of composite materials have also been reviewed. The thermal conductivity of nylon 6 and polypropylene in this temperature range can be seen in Figure 3.2.

Glass fibres have almost equal values of thermal conductivity parallel and perpendicular to the fibres and can be assumed to be isotropic, similarily the conductivity of the matrix polymer has been assumed to have little directional dependence. However, although the composite has been assumed to be macroscopically homogeneous, the thermal conductivity of the composite cannot be considered to be isotropic and will obviously be a function of position within the two phase composite microstructure. For the purpose of modelling it is necessary to calculate an overall thermal conductivity, k_t. A number of relationships exist to calculate the composite thermal conductivity and these constitute the upper and lower bounds to k_t, Springer and Tsai (1967)[74]. The Halpin-Tsai equation has been used to calculate the transverse thermal conductivity, assuming the structure to be completely void free.

$$\frac{k_b}{k_m} = \frac{1 + \xi\eta V_F}{1 + \eta V_F} \qquad \eta = \frac{\frac{k_F}{k_m} - 1}{\frac{k_F}{k_m} + \xi} \qquad 3.2$$

Where v_f is the volume fraction of the reinforcing fibres. This equation incorporates a geometrical factor, ξ, which can range in value from 0 to infinity, Halpin and Tsai (1967)[75]. For the transverse properties of a continuous, unidirectional reinforced composite, ξ=2, and the Halpin-Tsai equation results in a value of k_t which lies between the upper and lower bounds as calculated from the rules of mixtures given in equations 3.3 and 3.4, Springer and Tsai (1967)[74].

$$K = k_F V_m + k_m V_m \qquad 3.3$$

$$\frac{1}{K} = \frac{V_F}{K_F} + \frac{V_m}{K_m} \qquad 3.4$$

For a 50% volume fraction nylon/glass composite, the range of transverse thermal

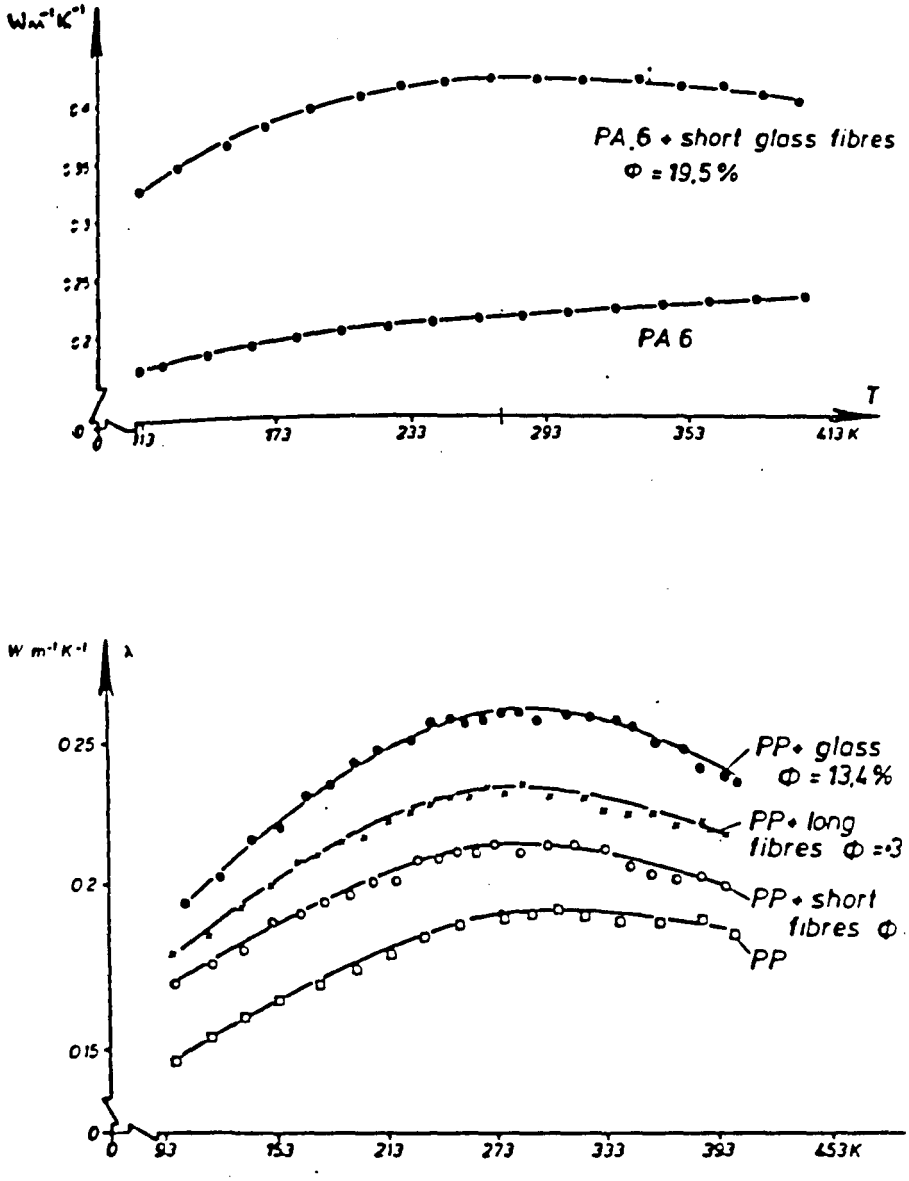

Figure 3.2. Thermal conductivity of nylon and polypropylene as a function of temperature, after Ott (1981).

conductivity can be calculated to be between 0.403 J/smK and 0.645 J/smK, and these values represent the lower and upper bounds. In comparison, the Halpin-Tsai equation results in a transverse conductivity of 0.508 J/smK.

The specific heat capacity at constant pressure, c_p, is another important thermal property of the composite. As the composite material is heated or cooled it undergoes phase changes and latent heat is released over a range of temperature. The enthalpy and heat capacity as a function of temperature for polypropylene cooled from the melt at 20K/min is shown in Figure 3.3a, Richardson (1978)[76], and both properties can be seen to be functions of temperature, the position of the peak also being strongly dependent on the cooling rate. Figure 3.3b shows the variation of enthalpy with respect to temperature for APC2 prepreg tape, Blundell et al (1986)[77] and the variation of enthalpy and heat capacity with temperature is illustrated schematically in Figures 3.3c and 3.3d. As can be seen, the heat capacity is the first derivative of the enthalpy temperature function and this accounts for the peak value of heat capacity recorded at the melting temperature. However, for modelling purposes, the gradient of the enthalpy / temperature curve has been assumed to remain constant throughout the processing temperature range and the heat capacity of both the matrix and the reinforcement has been assumed to be independent of temperature throughout the range of process temperatures.

During processing, the composite material experiences heating and cooling rates, in the order of 100°C/min at 1m/min. As illustrated in Figure 3.4, for semi-crystalline polyethylene heated to above the melt temperature, the higher heating rate causes a decrease in the peak heat capacity occurring at the melt temperature, Richardson (1978)[76]. Higher cooling rates have a similar effect on the heat capacity peak measured during cooling.

In addition, although a significant change in heat capacity can be associated with the glass transition temperature, this has been neglected because the T_g of both polymer matrices used, Tg nylon=60°C, Tg polypropylene=-10°C, are outside the temperature range of interest during processing. It has also been assumed that the latent heat given off by the polymer during crystallisation is much less than the overall heat loss during cooling and can thus be ignored. Figure 3.5 shows the form of the crystallisation and melting curves for polypropylene, heated and cooled at 20 K/min, Richardson (1978)[76]. The heat capacity has been assumed independent of the degree of crystallinity.

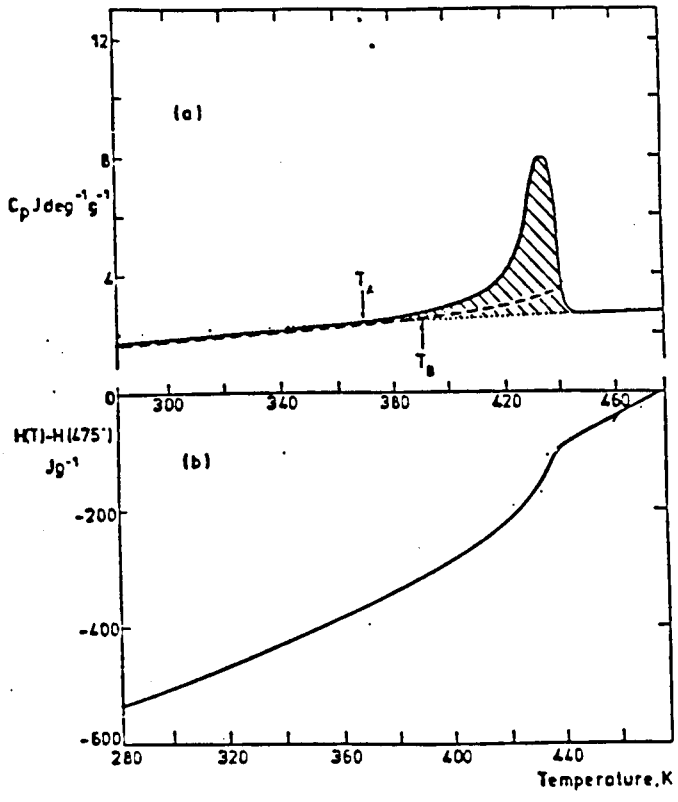

Figure 3.3a. Specific heat and enthalpy of polypropylene cooled from the melt at 20 K/min, after Richardson (1978).

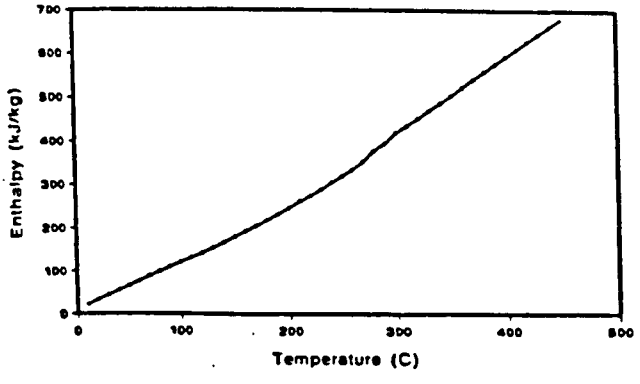

Figure 3.3b. Variation of enthalpy with temperature for APC2 prepreg tape, after Blundell (1986).

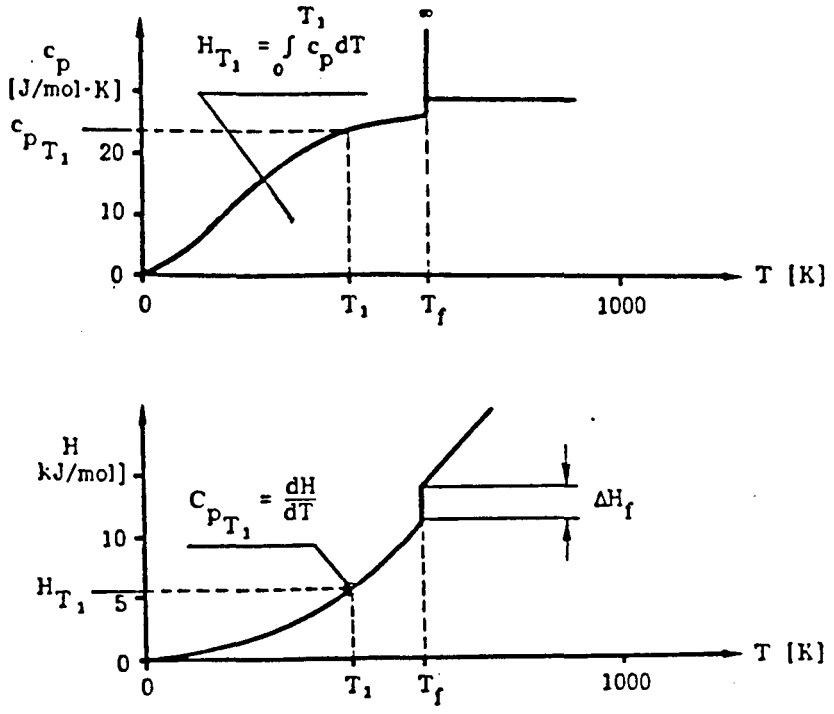

Figure 3.3c. Schematic illustration of the variation of enthalpy and heat capacity with temperature.

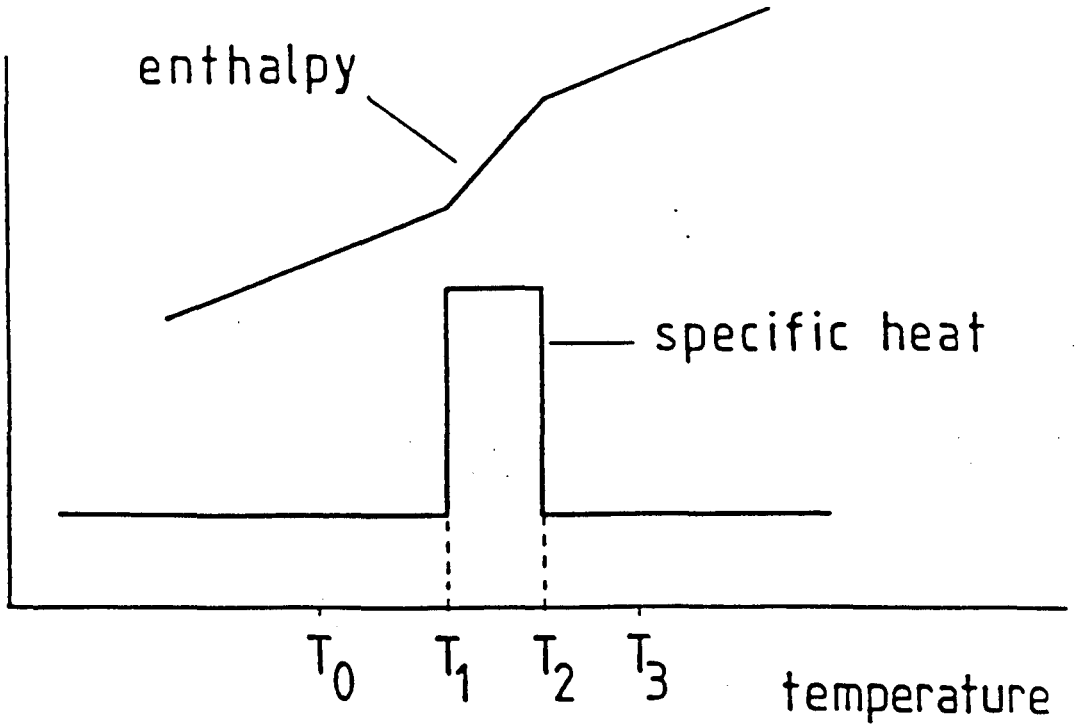

Figure 3.3d. Idealised representation of phase change between temperatures T_1 and T_2 in terms of enthalpy and specific heat, after Grove (1988).

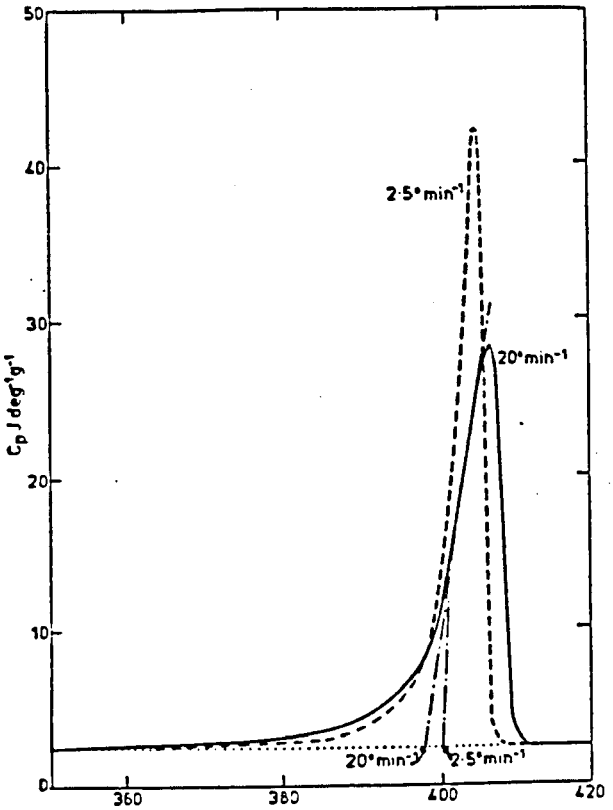

Figure 3.4. Heat capacity variation with temperature for polyethylene melted at 20 K/min and 2.5 K/min, after Richardson (1978).

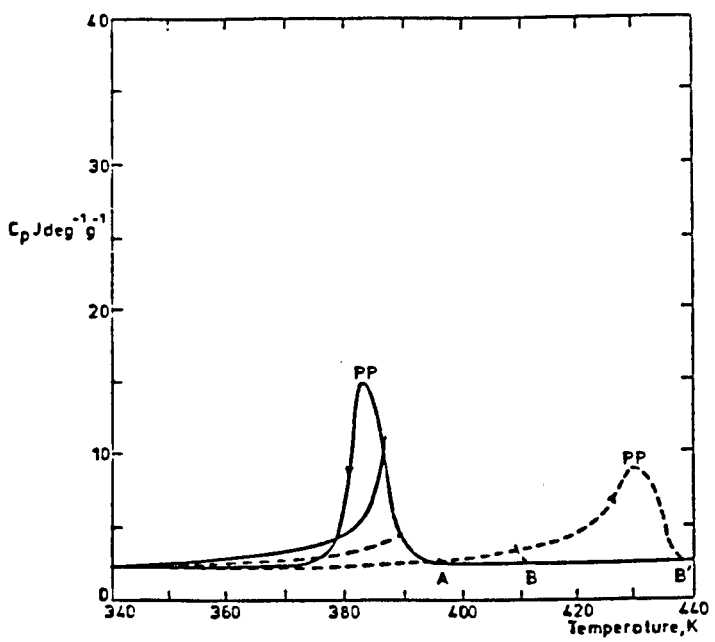

Figure 3.5. Crystallisation and melting curves for polypropylene in the cycle 450-280-450 K. All rates 20 K/min, after Richardson (1978).

It is necessary to combine the heat capacity of the matrix and reinforcement to provide the bulk heat capacity of the composite. A mass average rule of mixtures applies to the composite and is used to calculate an overall bulk heat capacity, c_{pb}, for the composite. This is given in equation 3.5, Velisaris and Seferis (1988)[78].

$$C_{p_b} = W_m C_{p_m} + W_F C_{p_F} \qquad 3.5$$

In this equation, W_m, is the mass fraction of the matrix and W_f is the mass fraction of the fibres.

For the purpose of the model the fibre and matrix density have been assumed constant through the processing temperature range. The matrix density has also been assumed to be independent of the degree of crystallisation. It is necessary to calculate a bulk composite density from the constituent phase densities and assuming that no void phase is present, then the bulk composite density, ρ_b, can be expressed by equation 3.6.

$$\rho_b = V_m \rho_m + V_F \rho_F \qquad 3.6$$

where V_m=matrix volume fraction, V_f=fibre volume fraction, ρ_m=matrix density and ρ_f=fibre density.

From the properties k_t, c_{pb}, and ρ_b, it is possible to calculate the composite thermal diffusivity, α_b, equation 3.7.

$$\alpha_b = \frac{k_t}{\rho_b C_{p_b}} \qquad 3.7$$

In all the calculations used to determine the overall composite properties, the respective volume fractions of the constituent phases have been assumed to remain constant at all points within the composite, the distribution of fibres and matrix has also been assumed to be regular, with no resin rich areas and without fibre clumping occurring.

3.2.3 Heat transfer mechanisms operating during thermoplastic pultrusion

During the heating of the precursor tapes, only convection and conduction have been considered to operate for simplicity. Although the oven consists of an infra-red heating section, the range of line speeds which have been studied have been below the speeds necessary to utilise the infra red oven to its maximum potential. To operate at its maximum efficiency the surface temperature of the emitters should be between 800-1200°C. This will inevitably result in very high air temperatures within the oven and to run continuously at line speeds sufficiently high to prevent surface degradation under such high heating rates would require, in the case of this project, a prohibitively large amount of precursor materials. Therefore, running at lower line speeds requires the infra-red oven to be considered to operate as an efficient hot air oven, heating the precursor tapes through a combination of convection and radiation, with a high surface heat transfer coefficient and conduction through the tape thickness. The precursors used experimentally have generally been white in colour and this further reduces the efficiency of the radiative contribution to heat transfer due to reflection and scattering effects. They may also be considered as too thick for full infra-red penetration to occur. The heating problem has therefore been simplified to one of conduction with high rates of surface convection.

During the cooling regime of the process, as the tapes leave the oven, the heat transfer problem becomes one in which the dominant cooling mechanism is internal conduction coupled with surface convection as the pultruded section moves down the line between the individual forming stands. As the section passes through the forming sections the dominant heat transfer mechanism is conduction between the composite section and the walls of the dies or rollers. The pultruded sections usually ranged in thickness between 2.5 and 3mm and all sections were 15mm wide.

3.3 Finite difference equations; method of solution; boundary conditions and stability considerations

The finite difference equations for one dimensional conduction have been derived previously, Section 2.3.3, and these can be applied directly to all the internal nodes

of the solution. However, to take into consideration the convective heat transfer operating at the surface, a further set of finite difference equations must be derived to calculate the temperature at the surface nodes of the solution.

In cases where the temperature variation of the air adjacent to the surface of the composite section is known, it is possible to calculate the surface temperature by incorporating a surface heat transfer coefficient into the finite difference equation. This case is illustrated in Figure 3.6. At the wall surface, x_w, the condition for continuity of heat flow, for unit area, can be expressed:

$$-k\left(\frac{dT}{dx}\right)_{w,p} = -h(T_{w,p} - T_{s,p}) \qquad 3.8$$

In this expression, $T_{s,p}$ is the bulk fluid temperature at time t_p. This condition can be applied by sub-dividing the wall as shown in Figure 3.6. Section x_1 is a distance $\Delta x/2$ in from the surface and the introduction of an imaginary extension of the wall to plane x_0, also at a distance $\Delta x/2$ from the wall surface, enables equation 3.8 to be satisfied by writing:

$$K\left(\frac{T_{1,p} - T_{o,p}}{\Delta x}\right) = h(T_{w,p} - T_{s,p}) \qquad 3.9$$

The term T_w can be replaced by:

$$T_{w,p} = \frac{T_{1,p} + T_{o,p}}{2} \qquad 3.10$$

Upon substitution of eqn. 3.10 into eqn. 3.9, an expression for $T_{o,p}$ can be written:

$$a.\quad T_{o,p} = \left(\frac{2Bi}{2+Bi}\right)T_{s,p} + \left(\frac{2-Bi}{2+Bi}\right)T_{1,p} \qquad 3.11a$$

$$b.\quad Bi = \frac{h\Delta x}{K} = \frac{Surface\ conductance}{thermal\ conduction\ of\ solid} \qquad 3.11b$$

The Biot number is a dimensionless number which provides a measure of the relative resistance to heat flow of the inside of the solid to that of the adjacent fluid. A low Biot number implies that most of the resistance is in the fluid boundary layer,

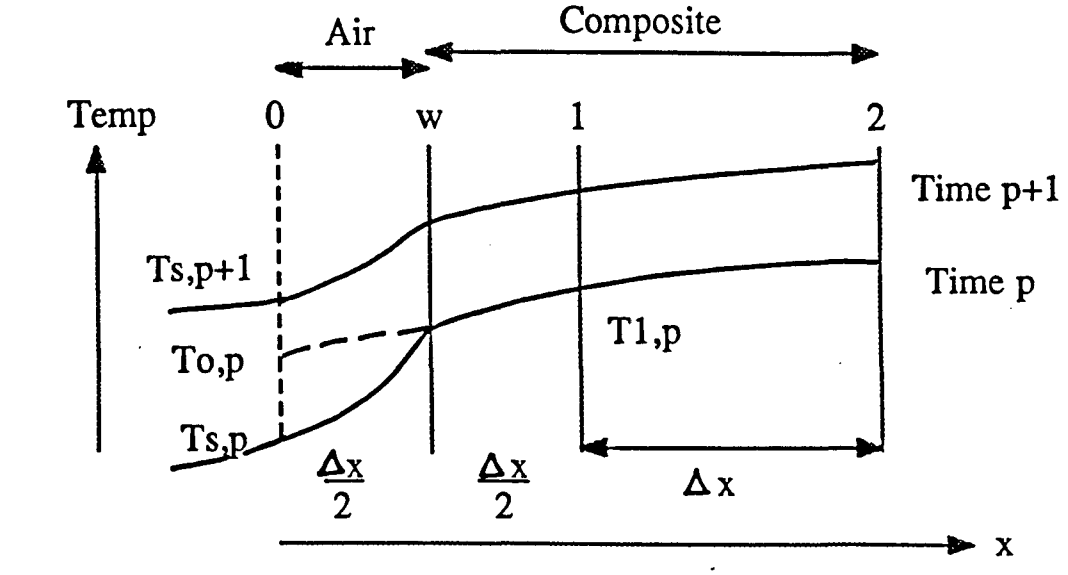

Figure 3.6. Convective boundary, finite difference grid development.

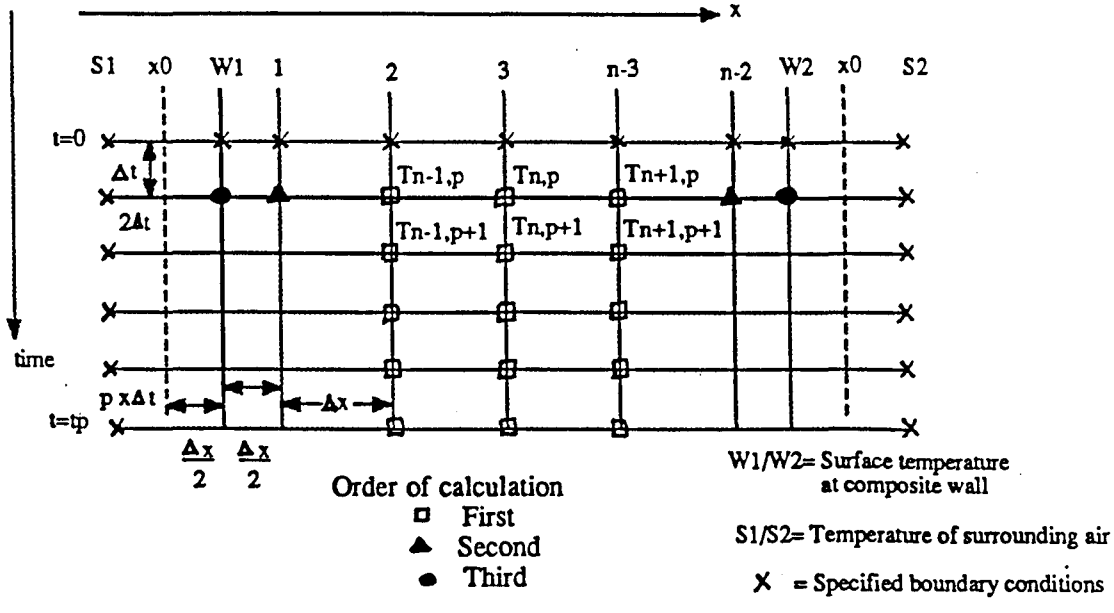

Figure 3.7. One dimensional finite difference grid for conduction coupled with convective boundary conditions, illustrating the sequence of calculation, starting with the internal nodes first and calculating the composite surface temperature last.

conversely, a high number implies that the greatest resistance is in the solid.
Equation 2.3.18 can be applied to sections x_0, x_1 and x_2 to obtain an equation for $T_{1,p+1}$:

$$T_{1,p+1} = Fo\left[T_{2,p} + T_{o,p} + \left(\frac{1}{Fo} - 2\right)T_{1,p}\right] \qquad 3.12$$

On substituting for $T_{o,p}$, the expression for $T_{1,p+1}$ becomes:

$$T_{1,P+1} = Fo\left[T_{2,p} + \frac{2Bi}{2+Bi}T_{s,p} + \left(\frac{1}{Fo} - \frac{2+3Bi}{2+Bi}\right)T_{1,p}\right] \qquad 3.13$$

The values of Tw can be calculated after substituting eqn.3.11 into eqn 3.10 to give:

$$T_{w,p} = \frac{2T_{1,p} + Bi\,T_{s,p}}{2+Bi} \qquad 3.14$$

Three equations, 2.4.18, 3.13 and 3.14, are necessary to calculate the unsteady state temperature distribution through the section, when a surface heat transfer coefficient is included. These must also be applied to the solution in the same order as listed, so that the calculation proceeds from the internal nodes, to the nodes just below the surface and finally to calculate the temperature of the surface nodes themselves. This sequence is illustrated in Figure 3.7.

An explicit solution method has been used in which a known temperature distribution throughout the mesh is used to calculate the distribution after a time interval Δt. Forward difference estimates of the temperature distribution are in terms of the present and subsequent temperatures at a given point. These allow the explicit calculation of the unknown temperature, $T_{n,p+1}$, in terms of known values of $T_{n+1,p}$, $T_{n-1,p}$ and $T_{n,p}$. This procedure is then repeated using these results to calculate the distribution after $2\Delta t$.

This solution method requires that boundary conditions are specified for the initial problem. These are the temperature throughout the solution field at time, $t=t_o$, and the temperature variation with time of the two boundary planes. The boundary temperatures which must be specified are also indicated in Figures 3.1 and 3.7.

There are two further conditions which must be fulfilled so that the solution remains stable. The first of these is that the Fourier number, Fo, must be less or equal to 0.5, Croft and Stone (1977)[79]. This places a constraint on the size of the time and space intervals, Δt and Δx, which cannot be chosen independently when using an explicit method of solution. The second stability condition is given in equation 3.15.

$$Fo \leq \frac{2 + Bi}{2 + 3Bi} \qquad 3.15$$

In the heat transfer model, the heat transfer mechanism at the composite surface has been modelled as convection and the rate of heat transfer at the surface has been assumed to be controlled solely by the surface heat transfer coefficient, h. This is not a physical constant of the fluid and is a very difficult value to measure. Its value is highly dependent on a number of parameters including the flow velocity, fluid viscosity, the condition and surface area of contact and the fluid properties and often only a range of values corresponding to certain conditions are given in the literature. For the case of free convection, h can take values between 1-100 W/m^2K for gases, with the coefficient for air lying between 10-15 W/m^2K, and between 100-1000 W/m^2K for liquids, Rogers and Mayhew (1967)[72]. Very little data has been found which relate heat transfer coefficients directly to conditions experienced during polymer processing operations.

In obtaining solutions to the heat transfer model the surface heat transfer coefficient could be altered so as to give a good degree of fit to experimentally determined temperatures.

3.4 Further assumptions

3.4.1 Roll forming

The forming and consolidation stage of the thermoplastic pultrusion process consisted of either cold rollers or temperature controlled dies.

For a section being roll formed, the contact length in the roll gap has been estimated

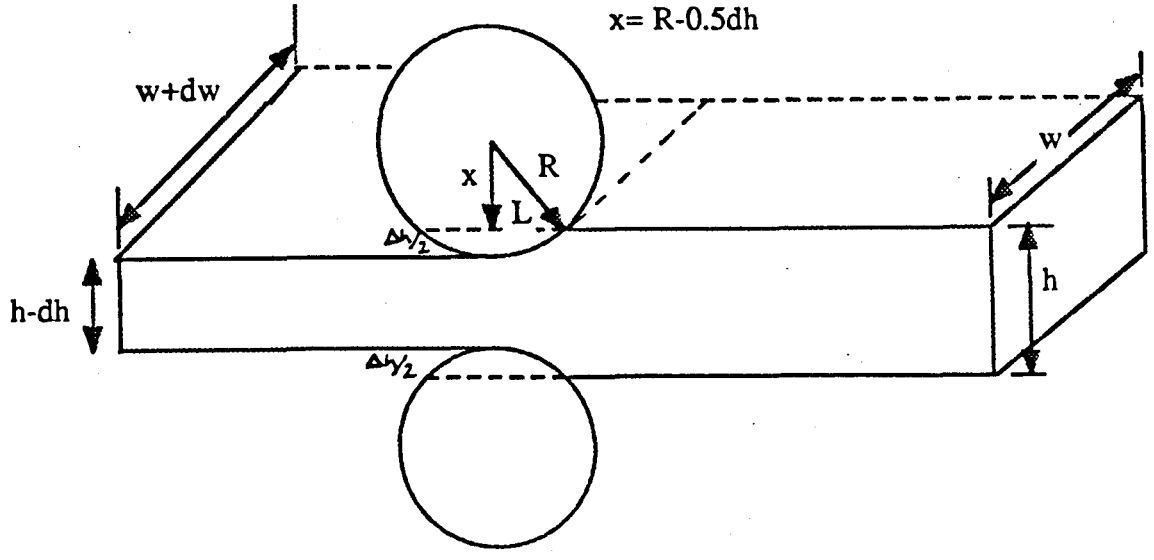

Figure 3.8. Schematic illustration of thickness reduction during roll forming of thermoplastic pultrusions. The contact length can be estimated using the expression $L=\sqrt{R\Delta h}$.

to be 10mm. It was also possible to estimate the contact length from experimentally measured temperature profiles by fitting the experimental and calculated temperature profiles. The reduction in thickness as the material bundle enters the roll gap is shown in Figure 3.8. The length of section in contact with the roll surface can be estimated using Pythagoras' theorem to give an expression for the contact length, L, where R=radius of roller and Δh=reduction of thickness, although this gives only a very approximate value for the contact length.

$$L = \sqrt{\Delta h R} \qquad 3.16$$

For a roll diameter of 140mm and an average thickness reduction measured to be about 1.4mm, the calculated contact length will therefore be 9.9mm. The precursor used to produce the 15mm wide flat sections was usually between 9-10mm wide and spreading had to occur in the roll gap. This spreading was assumed to take place uniformly across the width of the roll profile and the contact was assumed to be perfect. The effect of increasing the forming pressure applied to the rolls on the contact length was neglected. In order to fit the model solutions to the experimentally determined temperature distributions, the contact length in the rolls was varied from the initial calculated contact length until a good fit was achieved.

As the line speed increases, the time in which the composite section is in contact with the roll surface will decrease proportionally and this contact time is invariably short due to the short contact length. The surface temperature of the composite has been measured to decrease almost instantly on contact with the steel rolls by as much as 100°C in some cases. As the surface undergoes this rapid quench, the surface boundary condition was changed to reflect the instant decrease of the surface temperature. The heat transfer model then calculates the effect of roll cooling as simply internal conduction without surface convection using the lower surface temperatures. On leaving the roll gap the model calculation reverts to conduction coupled with surface convection.

The use of water sprays or water baths as the dominant cooling method can be incorporated into the model by altering the value of the heat transfer coefficient, h.

3.4.2 Die forming

Heated dies, maintained at a constant temperature on the die surface and maintained

under a constant pressure, have also been used to produce pultruded sections. The temperature distribution of the pultrudate before the die entry can be modelled using the equations for conduction with surface convection. This provides the initial condition at the die entry. As the composite section enters the die the dominant heat transfer mode becomes conduction between the composite surface and the die wall. This contact region has been assumed to be perfect over the total die length. The thermal conductivity of the die is much greater than that of the composite material and therefore, it can be assumed that the greatest resistance to heat flow will arise in the composite. The problem is illustrated schematically, and the finite difference grid system is shown in Figure 3.9.

It is possible to reduce the transient heat transfer problem in the composite as it moves through the die to a steady state problem, from the point of view of a stationary observer, by use of the material, or convected, derivative. From this point of view, heat conduction in the composite obeys Fouriers' law which can be written as equation 3.17.

$$\rho C_p V \frac{DT}{Dt} = K\left(\frac{d^2T}{dx^2}\right) \qquad 3.17$$

This uses the material derivative which can be written in the form of equation 3.18.

$$\frac{Dt}{Dt} = V\frac{dT}{dy} + \frac{dT}{dt} \qquad 3.18$$

Fouriers' law can now be written

$$\rho C_p\left(V\frac{dT}{dy}\right) = k\,\frac{d^2T}{dx^2} \qquad 3.19$$

The time dependent term can be ignored because conduction within the die has been assumed to be at steady state. This equation has a similar form to equation 2.4.11 and it is possible to derive finite difference equations using the method described previously in Section 2.4.3. The finite difference equation for conduction in the die can therefore be written as:

$$T_{n,p+1} = \frac{K\Delta y}{\rho C_p V \Delta x^2}\left[T_{n+1,p} + T_{n-1,p} + \left(\frac{\rho C_p V \Delta x^2}{K\Delta y} - 2\right)T_{n,p}\right] \qquad 3.20$$

The die is maintained at constant temperature and therefore can be considered to be at a steady state. Assuming that the die length is much greater than the die wall thickness and that the thermal conductivity of the die material is much greater than the conductivity of the composite, Laplaces' equation can be written in one dimension:

$$K\left(\frac{d^2T_{die}}{dx^2}\right) = 0 \qquad 3.21$$

For a die wall thickness, b, the heat flow between the composite wall and the die can be written:

$$q = -h(T_I - T_d) \qquad 3.22$$

where T_I= Interface temperature and T_d= Die temperature. This can be written as equation 3.23 on substituting the term k_d/b for the surface heat transfer coefficient, h.

$$q = \frac{-K_d}{b}(T_I - T_d) \qquad 3.23$$

Therefore, in order to neglect the complicated solution for the interface region between the moving composite and the die wall, a Biot number can be formulated which depends on the thermal conductivity of the die material and the thickness of the die wall. This altered Biot number can be expressed by equation 3.24 in which k_d is the thermal conductivity of the die, b is the die thickness, k_c the composite conductivity and Δx is the segment thickness.

$$Bi' = \frac{K_d \Delta x}{bK_c} \qquad 3.24$$

The finite difference equation for the boundary surface between the composite and die then becomes:

$$T_{n,p+1} = \frac{\alpha \Delta y}{V\Delta x^2}\left[T_{n+1,p} + \left(\frac{2Bi'}{2+Bi'}.T_{s,p}\right) + \left(\frac{V\Delta x^2}{\alpha \Delta y} - \frac{2+3Bi'}{2+Bi'}\right)T_{n,p}\right] \qquad 3.25$$

This can now be solved in the same way as conduction with surface convection subject to initial boundary conditions which specify that the temperature distribution of the material entering the die is equal to that calculated by the model for the end of the cooling section previous to the die, and that the composite surfaces remain at the

die temperature throughout the die length. The calculation then proceeds in the same order as shown in Figure 3.8 until the material exits the die. After that, the calculation than reverts to conduction with surface convection.

3.5 Material properties used in heat transfer modelling

The properties of glass; nylon 6; 6,6; and 12; and polypropylene which were used in the heat transfer modelling are summarised in Table 3.1. The data has been taken from the following sources: 1. Engineering properties of thermoplastics. Ed. R.M Ogorkiewicz, Wiley [80]; 2. Fibres, Films, Plastics and Rubbers. Ed. Roff and Scott [81]; 3. Data supplied with precursor material.

Table 3.1. Material properties used in the modelling of heat transfer in the pultrusion process.

Material	Density Kg/m^3	Heat capacity J/KgK	Thermal conductivity J/secmK	Melting temperature ℃	Comments
Nylon 6,6	1140 [1]	2130 [1] 1670-2300 [2]	0.25 [1] 0.19-0.29 [2]	264 [1]	
Nylon 6	1130 [1]	1670 [1]	0.25 [1]	264 [1]	
Nylon 12		1828 * 1244 ** 934 ***		180 * 183 ** 192 ***	DSC measurements 20/50/100°C/min
Polypropylene	900-910 [1]	1920 [1,2]	0.15-0.21 [1]	165-175 [1,2]	
Polypropylene	905 [3]	1974 * 2089 ** 2007 ***	0.23 [3]	160 * 171 ** 163 ***	DSC measurements 20/50/100°C/min
Nylon 6,6	1390 [1]	1250 [1]	0.23 [1]	264 [1]	0.33 Vf glass
Glass	2540	800	1.04	-----	

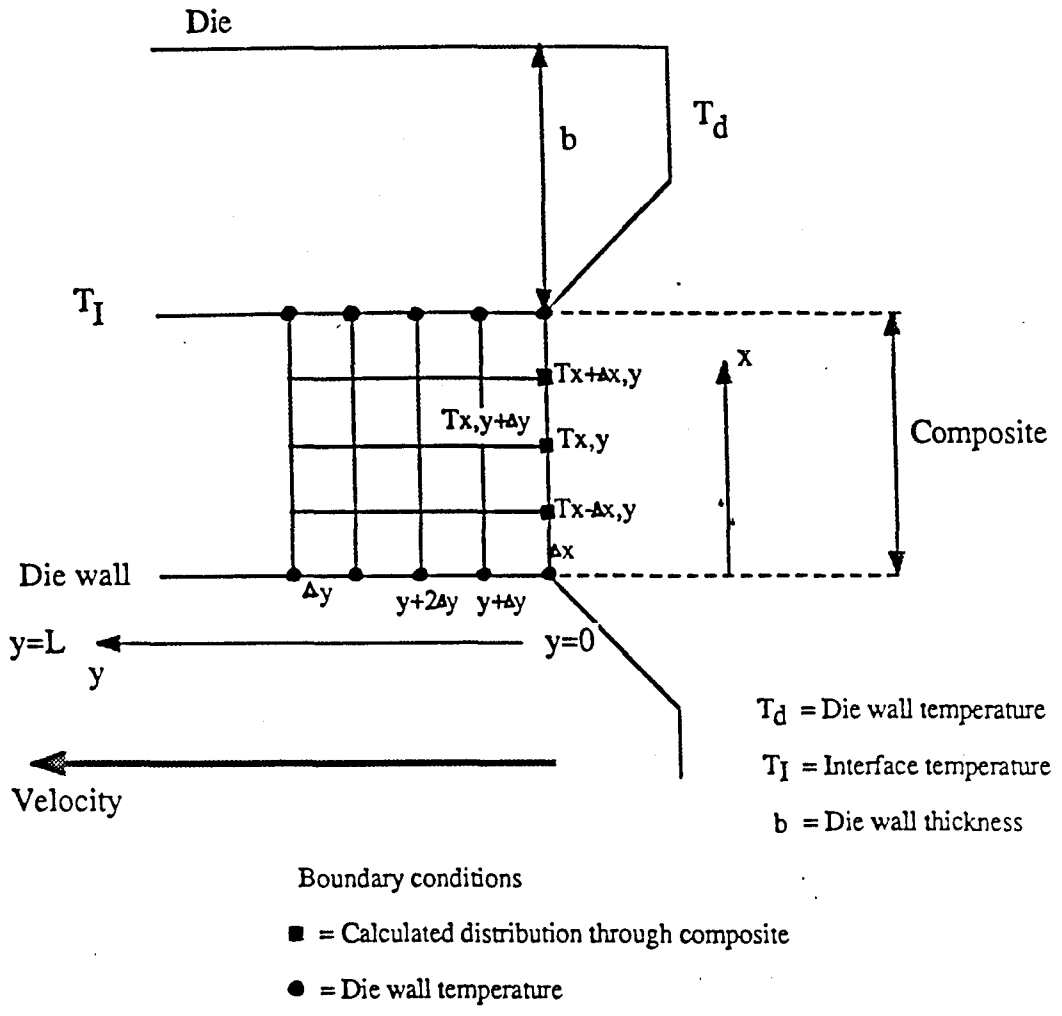

Figure 3.9. One dimensional finite difference grid for the problem of heat transfer during die forming, calculated as a steady state problem by use of the material derivative.

Condition	Surface heat transfer coefficient W/m^2K
Still air	10-15
Air at 5m/sec	50-200
Steel	500
Water at 5°C	1000
Water spray	1500

Thermal conductivity of Steel W/mK	Thermal conductivity of Brass W/mK
45	200

Differential scanning calorimetry was also used to determine the melting temperature and the heat capacity of the precursor materials used in the pultrusion experiments. DSC traces for nylon and polypropylene samples, measured at three heating rates: 20, 50, 100°C/min can be seen in Figures 3.10 and 3.11. Figure 3.12 shows the experimentally determined heat capacity for polypropylene, heated at 100°C/min, between 150 and 220°C. Figure 3.13 shows the experimentally determined heat capacity for nylon 12, heated at 50°C/min, between the temperatures of 100 and 220°C. The baseline shown in Figures 3.12 and 3.13 was determined by the microprocessor system attached to the DSC measuring cell. The melting point of polypropylene at 100°C/min and nylon at 50°C/min can also be determined from the respective graphs.

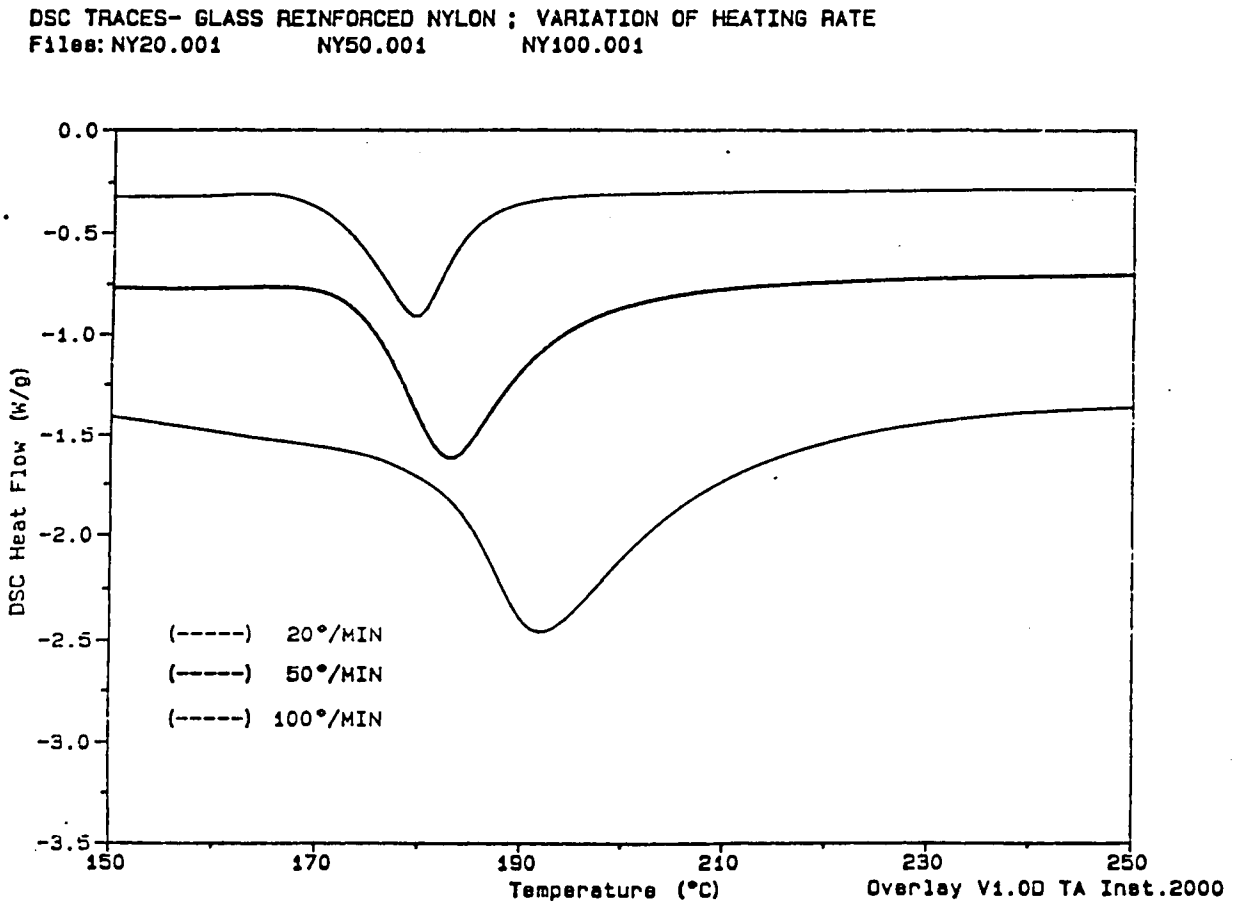

Figure 3.10. DSC traces for nylon heated at three heating rates: 20, 50 and 100°C/min.

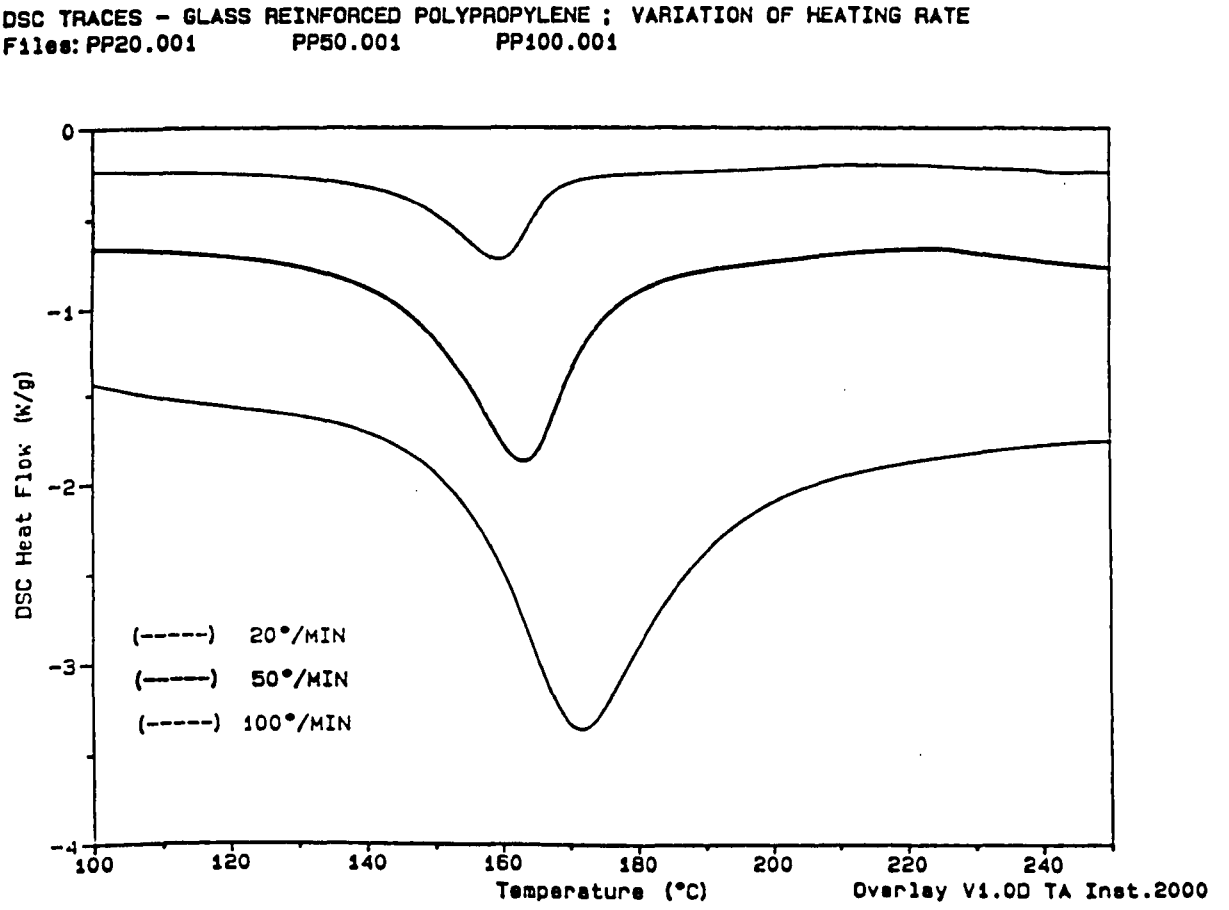

Figure 3.1.11. DSC traces for polypropylene heated at three heating rates: 20, 50 and 100°C/min.

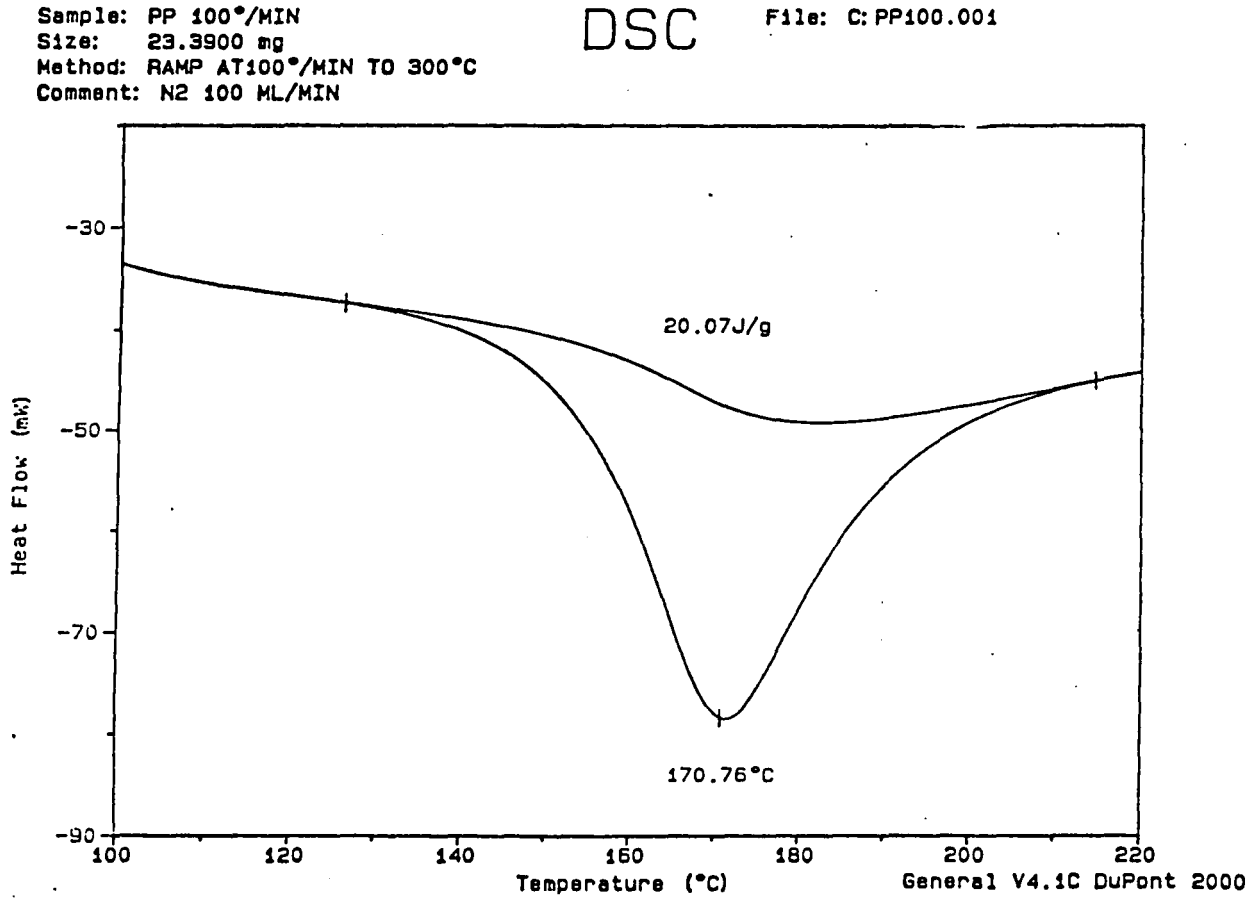

Figure 3.1.12. Experimentally determined heat capacity and melting temperature for polypropylene, heated at 100°C/min.

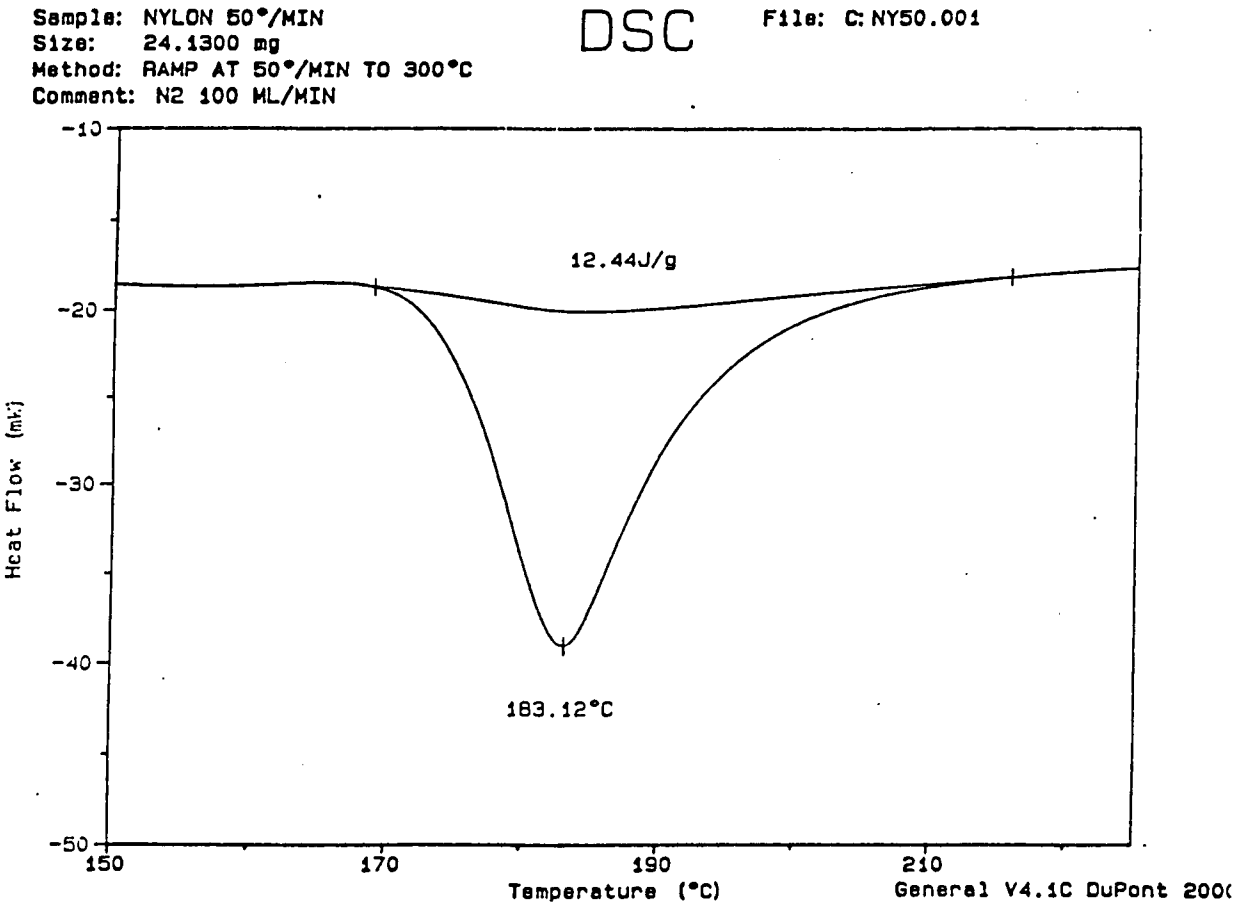

Figure 3.1.13. Experimentally determined heat capacity and melting temperature for nylon, heated at 50°C/min.

Chapter 4.

Modelling the thermoplastic impregnation process

4.1 Background

The action of a fibre tow drawn around an impregnation bar has been described in Section 2.2 and was considered to be similar in some respects to the operation of a lubricated foil bearing. Lubrication theory and Reynolds equation have been used to describe and model problems of this type, Cameron (1981)[55], Moore (1975)[56]. The form of the general Reynolds equation has also been discussed in Section 2.2.

In impregnation processes in which fibre tows are drawn around cylindrical bars, it is important that the highest possible degree of fibre wet out occurs along with the lowest possible tension build-up in the fibres as they pass around the bar. There have been few studies into the basic mechanics of the impregnation process and the purpose of the model was to model tension build-up in the fibre tows to provide an initial basis for understanding the results of tension generation experiments and in optimising the impregnation process.

4.2 General assumptions

Four separate zones of behaviour have been assumed to occur around the impregnation bar, an entry zone, an impregnation zone, a contact zone and an exit zone. The tension build-up in each has been modelled to calculate the overall tension build-up in the fibre tow. The zones and the corresponding film thickness variation around the bar are shown in Figure 4.1.

A number of general assumptions have been made: The resin has been assumed to be Newtonian; Sideways flow parallel to the axis of the bar has been neglected. This is equivalent to assuming either that the tow is very wide or there is some form of side restraint preventing sideways flow of resin out of the gap; The impregnation flow of resin into the fibre tow has been assumed to be constant, despite the fact that the Darcy permeability of the fibre tow will decrease from an initial high value

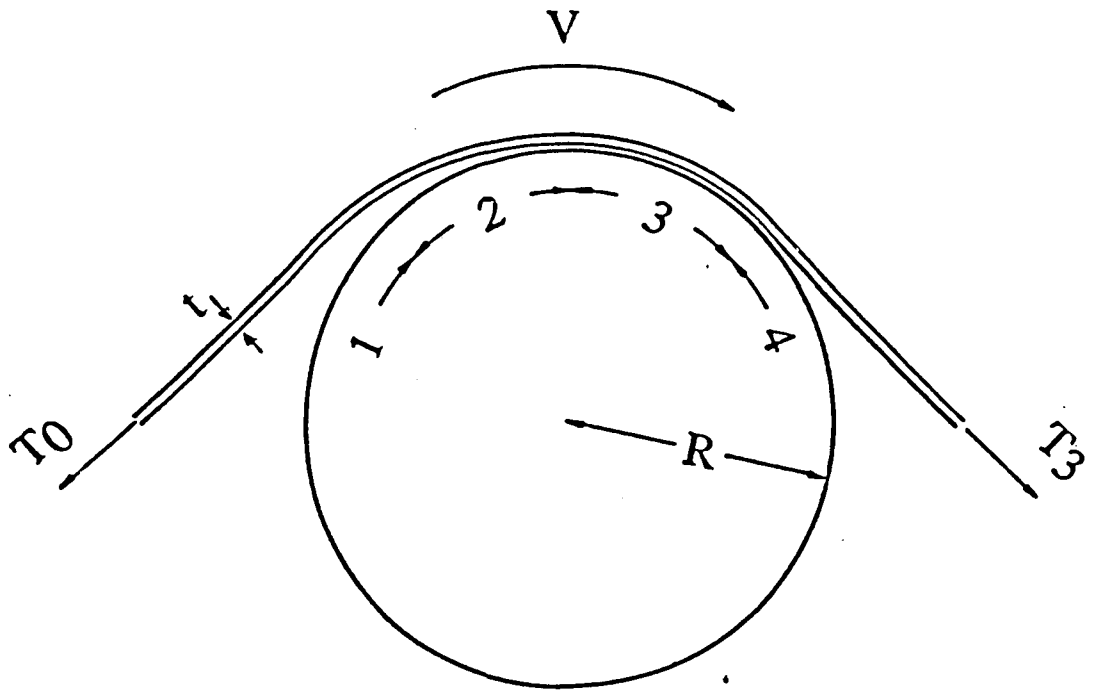

Figure 4.1. Regions of behaviour in impregnation of fibre tows using cylindrical bars.

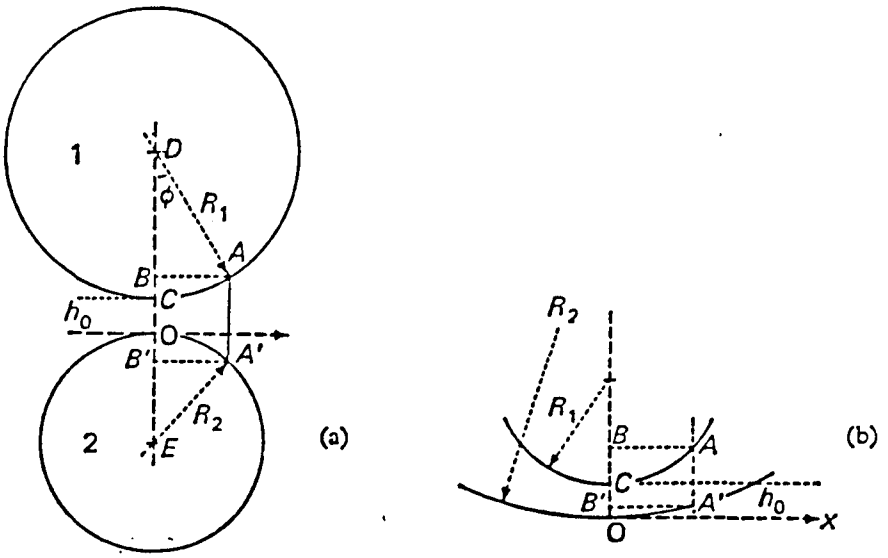

Figure 4.2. Representation of the film thickness between two discs in terms of distance x, after Cameron (1981).

for a dry tow, to a lower steady value as the tow fills with resin.

The Reynolds equation for a porous bearing can be written in the form:

$$\frac{1}{12\eta}\frac{d}{dx}\left(h^3\frac{dp}{dx}\right)=\frac{V}{2}\frac{dh}{dx}+\frac{\phi P}{\eta t} \qquad 4.1$$

In describing the impregnation process, the term on the right will be taken to represent the impregnation flow into and through the fibre.

A number of further simplifying assumptions have been made and these will be described in the regions in which they apply.

4.3 Modelling the impregnation process

Region 1

The basic assumption in this region is that because the pressure build-up in the resin film is relatively small, resin flow through the tow thickness can be neglected. Reynold's equation can therefore be written:

$$\frac{1}{12\eta}\frac{d}{dx}\left(h^3\frac{dp}{dx}\right)=\frac{V}{2}\frac{dh}{dx} \qquad 4.2$$

This can be integrated to give:

$$\frac{h^3}{12\eta}\frac{dP}{dx}=\frac{V}{2}(h-h_o) \qquad 4.3$$

At some point, the pressure will reach a plateau value where dp/dx=0. At this point the pressure induced flow is zero and the velocity profile across the gap between the fibre tow and the bar is linear so that $Q \sim Vh_o/2$, where Q is the flow rate per unit width, V/2 is the mean velocity and h_o is the film thickness at the end of region 1. This point is taken as defining the exit point of region 1, so in this region equation 4.3 can be written:

$$\frac{h^3}{12\eta}\frac{dP}{dx}=\frac{Vh}{2}-Q \qquad 4.4$$

It is possible to express the film thickness between a disc and a plane in terms of a distance, x, from the line of centres. Consider two discs of radius R1 and R2,

shown in Figure 4.2. The minimum oil thickness, h_0, is on the line of centres, DOE.

Consider any point on the surface of disc 1. The distance of point A above the x axis is equal to OB and can be written:

$OB=(OC+CB)= h_0 + (DC-DA \cos \phi)$

Where ϕ is the angle ADB. OB can also be written:

$OB= h_0+R1(1-\cos \phi)$

This is an accurate expression for the film thickness between a disc and a plane. However, in the case of two discs the pressure is localised near the line of centres, ie. ϕ is always small. It is thus possible to expand the cosine term and to neglect the higher terms. If ϕ is very small, it can be written as (x/R1) and all terms higher than ϕ^2, or $(x/R1)^2$, can be neglected. Thus;

$OB= h_0+x^2/2R1$

If A' is the equivalent point on disc 2, an identical treatment results in the expression:

$OB'= x^2/2R2$

Hence the film thickness, h, can be written:

$$h = h_o\left\{1 + \frac{x^2}{2h_o}\left(\frac{1}{R_1} + \frac{1}{R_2}\right)\right\} \qquad 4.5$$

If a reduced radius, R, is defined so that 1/R=1/R1+1/R2, h can then be expressed:

$$h = h_o\left(1 + \frac{x^2}{2h_oR}\right) \qquad 4.6$$

This relation is the expression for a parabola. It is justified providing that the film thickness near the line of centres only is required, ie. providing that ϕ is small.

The fibre tow approaching the bar has been assumed to follow a linear path, giving

a film thickness variation as shown in Figure 4.3. Near the point where the tow approaches the bar the gap profile has been approximated to a parabola, provided R»h the film thickness variation will then be given by equation 4.6.

In order to solve Reynolds equation a substitution must be made. This involves the substitution angle, defined by:

$$\tan\gamma = x/\sqrt{2h_0R}$$

so that in conjunction with equation 4.6 the film thickness, h can be written:

$$h = h_o \sec^2\gamma \qquad 4.7$$

On substitution of $h=h_0 \sec^2\gamma$ and $dx=\sqrt{2Rh_0}.\sec^2\gamma.d\gamma$ in equation 4.4, re-arranging gives:

$$dP = \frac{6\eta V}{h_o^2}\sqrt{2Rh_o}\,(\cos^2\gamma - \cos^4\gamma)d\gamma \qquad 4.8$$

Integrating this expression and observing that at $x=-\infty$ ($\gamma=-\pi/2$) then P=0, results in an expression for the pressure P:

$$dP = \frac{6\eta V}{h_o^2}\sqrt{2Rh_o}\left(\frac{\gamma}{8} - \frac{\sin 4\gamma}{32} + \frac{\pi}{16}\right) \qquad 4.9$$

The pressure P_0 at x=0 ($\gamma=0$) is therefore:

$$P_o = \frac{3\pi\eta V\sqrt{2Rh_o}}{8h_o^2} \qquad 4.10$$

The equilibrium of an elemental length of tow, R.dθ within the angle of wrap shows that the pressure force PR.dθ, exerted on the element by the shaft is matched by the tension component T.dθ, Moore (1975). Thus, for equilibrium when the film thickness is small compared with R:

$$P = \frac{T}{R} \qquad 4.11$$

Where T is the tow tension per unit width. If the change in tow tension is neglected in region 1 then:

$$P_o = \frac{T_o}{R}$$

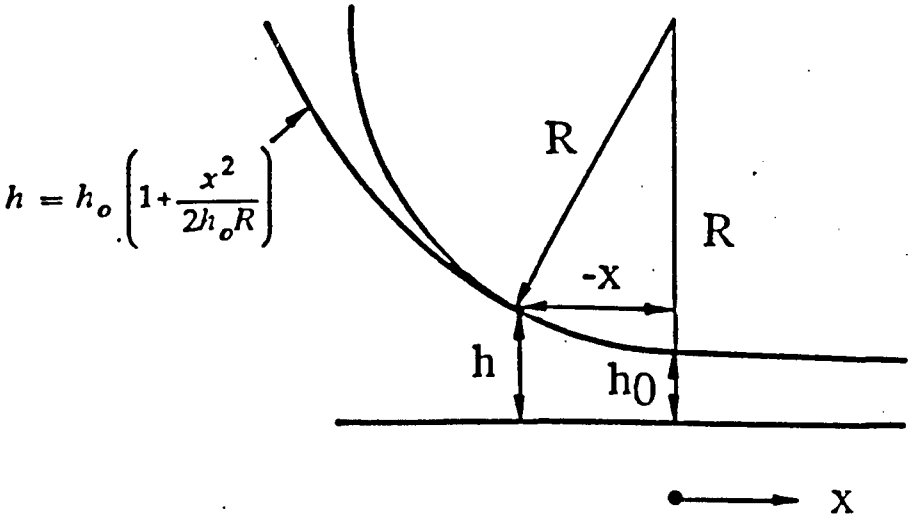

Figure 4.3. Film thickness variation as a fibre tow approaches a cylindrical bar.

4.12

Substitution for P_0 in equation 4.10 and re-arranging results in an expression for h_0:

$$h_o = \left(\frac{\pi^2}{128}\right)^{1/3} R\left(\frac{6\eta V}{T_o}\right)^{2/3} \qquad 4.13$$

This relationship for h_0 can be seen to have the same form as the relationship found previously for the foil bearing, equation 2.2.5.

It is now possible to calculate the tension build-up in the fibre tow in region 1:

$$T_1 - T_o = \frac{5\pi\eta V}{4}\sqrt{\frac{2R}{h_o}} \qquad 4.14$$

Region 2

In region 2 it has been assumed that 1/h varies linearly with x. Therefore:

$$\frac{dT}{dx} = \tau = \frac{\eta V}{h} = \eta V\left[\frac{1}{h_o} + \left(\frac{1}{h_1} - \frac{1}{h_o}\right)\frac{x}{L_1}\right] \qquad 4.15$$

Where T is the shear stress at the resin/tow interface. Integrating this expression and observing that at x=0, $T=T_1$ gives:

$$T - T_1 = \eta V\left[\frac{x}{h_o} + \left(\frac{1}{h_1} - \frac{1}{h_o}\right)\frac{x^2}{2L_1}\right] \qquad 4.16$$

Similarily, at $x=L_1$, $T=T_2$:

$$T_2 - T_1 = \frac{\eta V L_1}{2}\left[\frac{1}{h_o} + \frac{1}{h_1}\right] \qquad 4.17$$

The term L_1 is the length of the impregnation region. To find this it is necessary to use equation 4.1. As the pressure is unlikely to vary greatly through region 2, the first term in equation 4.1 may be neglected so that:

$$\frac{V}{2}\frac{dh}{dx} = -\frac{\phi P}{\eta t} = -\frac{\phi T}{R\eta t} \qquad 4.18$$

In this expression, t is the tow thickness per unit width. T can be substituted from equation 4.18 to give a quadratic expression for L_1, which can be solved to give:

$$L_1 = \frac{-T_1 + \sqrt{T_1^2 - \frac{\eta V R t}{3\phi h_o h_1}(h_1 - h_o)(2h_1 + h_o)}}{\eta V(2h_1 + h_o)/6h_o h_1} \qquad 4.19$$

If the total wrap length is less than the length of the impregnation region, L_1 then there will be no region 3 and the tension build-up in region 2 will be given by equation 4.18 putting x=L. Otherwise, the tension build-up will be given by equation 4.19. If $L \geq L_1$, the exit of region 2 occurs when contact takes place between the tow and the impregnation bar. There will however, still be viscous drag forces present because of the residual resin in the impregnated tow.

Region 3

In this region, an 'effective' value of the film thickness of the shearing resin will be assumed. The value of h_1 has been assumed to lie between the value of the fibre spacing and half the tow thickness.

The value of the effective film thickness, h_1, has been assumed to remain constant in region 3 and, in addition to viscous drag, there may also be coulomb friction acting on the tow. These factors have been assumed to contribute to the tension build-up so that:

$$\frac{dT}{dx} = \frac{\mu T}{R} + \frac{\eta V}{h_1} \qquad 4.20$$

where μ is the coefficient of friction and η is the viscosity.

This equation can be solved for the boundary conditions, $T = T_2$ at $x = L_1$ and $T = T_3$ at $x = L\ (L_1+L_2)$ to give an expression for the tension build-up per unit tow width in region 3:

$$T_3 - T_2 = \left[\exp\left[\frac{\mu L_2}{R}\right] - 1\right]\left[T_2 + \frac{\eta V R}{h_1 \mu}\right] \qquad 4.21$$

It has been assumed that region 4, the exit zone, will not contribute significantly to the tension build-up and will therefore be ignored. It is possible to calculate the tension build-up per unit tow width, in each of the impregnation zones using these equations. Three parameters can be varied: the permeability/tow thickness ratio, Φ/t; the effective film thickness, h_1; and the friction coefficient, μ. Although it is possible to calculate the first two terms, both require an in-depth study of polymer flow through fibre beds which has not been attempted in this case. The results of

the modelling will be discussed in Chapter 6, Section 6.2.

Chapter 5. Experimental

5.1 The pultrusion of thermoplastic composites

The aim of the initial work carried out was to develop a process for the pultrusion of a flat strip section using continuous pre-impregnated thermoplastic precursors.

5.1.1 Pre-impregnated precursor materials

Several precursors, different in both materials combinations and physical form were available for early development work and these are summarised in Table 5.1.1. The processability of each of these as pultrusion precursors, in terms of their ease of handling, their heating characteristics and their formability will be discussed later.

Table 5.1.1. Summary of thermoplastic preimpregnated precursors available for pultrusion experiments

Matrix	Reinforcement	V_f	Melting Temp. °C	Form	Size	Handling	Colour	Trade name
Nylon 6,6	Glass	.35	264	U-D rod	3mm diameter	Very stiff	White	Verton
Nylon 12	Glass	.4	176	U-D tow	3mm diameter	Flexible	White	FIT
(A) Nylon 12	Glass	.5	176	U-D Tape	10x1.5mm	Stiff/springy	White	----
(B) Polypropylene	Glass	.33	176	U-D Tape	10x.5mm	Stiff/springy	White	Plytron
Polypropylene	Glass	.5	179	U-D Tape	10x1.5mm	Stiff/springy	White	----
(C) PEEK	Carbon	.61	343	U-D Tape	12.5x0.25mm	Boardy	Black	APC2
Nylon 6,6	Glass	.5	264	U-D Tape	3x1mm	Springy	Brown	Ircha
PPS	Glass	.5	285	Co-mingled	1mm diameter	Yarn	Yellow	-----

5.1.2 Prototype pultrusion line development

In order to begin development of an experimental thermoplastic pultrusion line, five individual processing stages were identified, each of which were to be integrated into the continuous pultrusion process. This is illustrated schematically in Figure 5.1.1 and Figure 5.1.2 shows a photograph of the current experimental pultrusion line.

The first stage was material storage from which precursor materials were pulled into, and continuously through all the subsequent processing stages. The creel stand required to store and deliver the materials through the process consisted of a frame containing horizontal bars on which the drums or reels of precursor rotated freely. Some pre-tensioning was required to prevent the material springing off individual reels during unwinding and sagging as it passed through the oven, but the total effect of tow tension when using preimpregnated precursors was found to be fairly small.

The second stage was a heating stage in which the moving precursor was heated to a temperature above its melting point within the length of the oven.

Stages three and four consisted of a combined forming and consolidation stage where the individual molten precursor tows were continuously formed and consolidated into shape. Finally, there was a cooling stage where the now consolidated section underwent sufficient cooling to allow a solid shape to be pulled through the haul off machine. Two different caterpillar type haul-off machines were available. A Boston Matthews extrusion haul-off with a speed range of 0.31 to 6.5m/min was used for all the early development work. However, increasing pull forces generated during forming placed a limit to the speeds achievable within the power of this haul-off. A Speedex CT/3 haul-off unit with a speed range 0.1 to 20m/min was used for experiments combining high forming pressures with relatively high line speeds.

Preliminary development trials were undertaken with prototype designs for the five stages outlined above. These trials indicated that the most critical step to successful processing appeared to be the controlled heating of the moving precursor tows to a temperature above the melting point of the matrix resin. This appeared to control the effectiveness of the subsequent forming and consolidation of these tows into a continuous pultruded section.

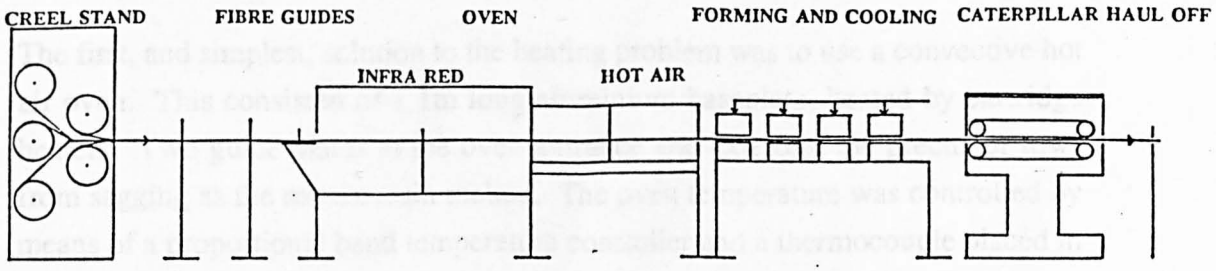

Figure 5.1.1. Schematic illustration of a thermoplastic pultrusion process to use preimpregnated precursor materials. This shows the individual process stages required for the on-line heating, forming, consolidation and cooling of pultruded sections.

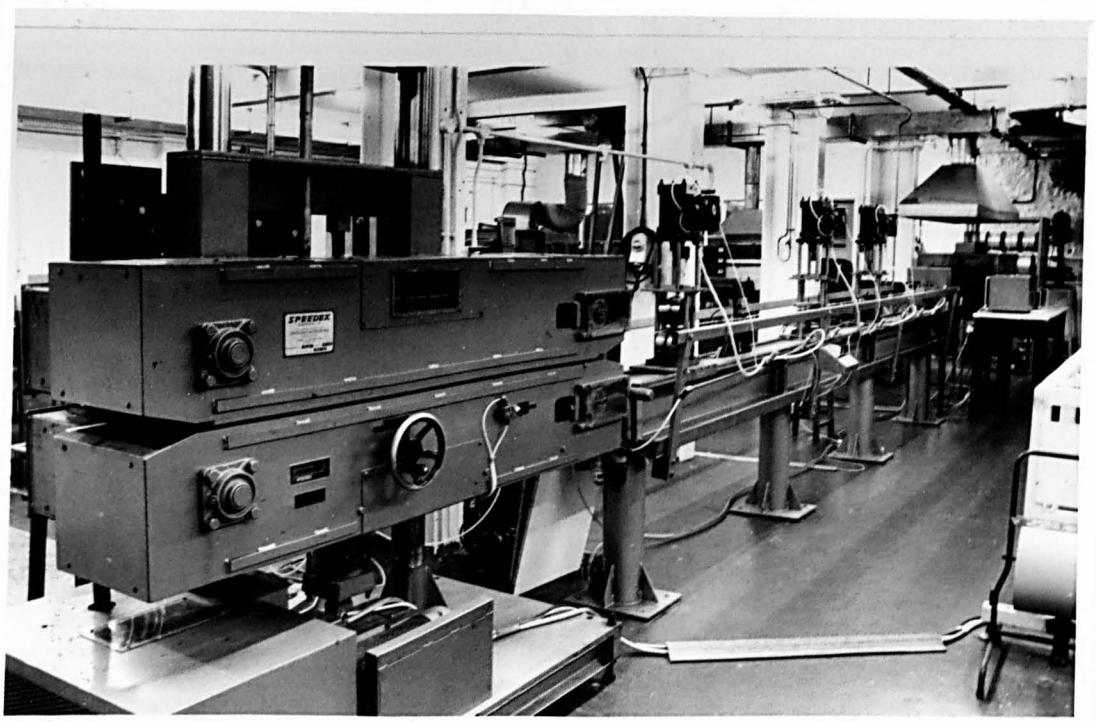

Figure 5.1.2. Experimental thermoplastic pultrusion line, in this case set up with constant pressure rolls as the forming and consolidation stage of the process.

5.1.3 Heating methods for thermoplastic pultrusion

Two heating methods were investigated during the development of the experimental pultrusion line.

The first, and simplest, solution to the heating problem was to use a convective hot air oven. This consisted of a 1m long aluminium baseplate, heated by cartridge heaters. Two guide plates at the oven entrance and exit kept the precursor tows from sagging as the matrix resin melted. The oven temperature was controlled by means of a proportional band temperature controller and a thermocouple placed in the centre of the oven interior, and the cavity was covered by an insulating lid. As line speeds were increased it became necessary to increase the oven temperature progressively above the melting point of the matrix resin in order to achieve complete heating of the precursor tows before the oven exit. A nitrogen gas bleed into the oven was available to minimise surface oxidation and degradation if required.

Trials, heating a range of different precursors using this hot air oven, proved to be reasonably successful and served to highlight some aspects of the heating stage which needed to be improved upon, namely insufficiently high heating rates at line speeds greater than 1m/min, ie. dwell times less than 60 seconds, accurate control of the air temperature within the oven and surface degradation at high processing temperatures.

The second potential solution to the problem of heating the moving tows quickly, without using excessively high air temperatures to provide rapid conductive and convective heating, was to construct a 1m long medium wavelength infra-red oven. This oven consisted of three 1kW infra-red tubes, arranged with the precursor tows passing through the focal point of the heaters. The heaters were again controlled by proportional band controllers coupled to a thermocouple which measured the air temperature alongside the precursor tows. As in the previous oven design, guides at the oven entrance and exit kept the tows spread apart and prevented sagging as they passed under the heaters.

Both the development ovens were capable of heating the moving precursor tows at sufficiently high line speeds, 0.5-1.5m/min, to allow combined forming and consolidation stages to be tested under realistic processing conditions. In order to develop the forming and consolidation stage of the process, two options were

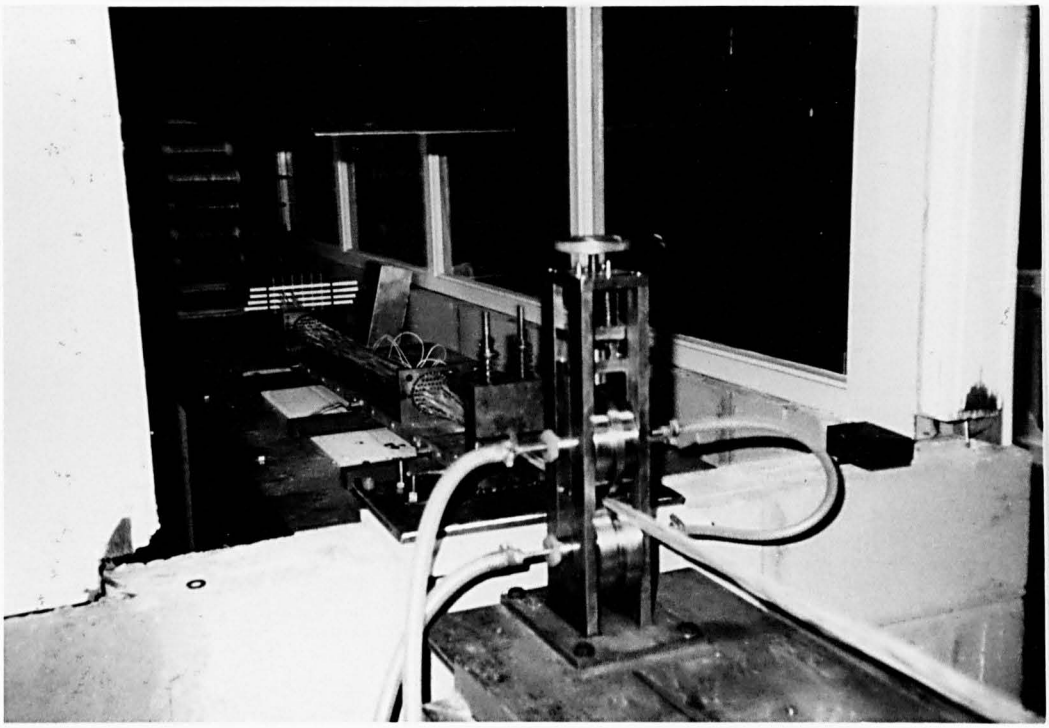

Figure 5.1.3. Development pultrusion line showing hot air oven, heated, constant pressure forming die and water cooled consolidation rolls. The brown precursor material is a nylon 6,6/glass tape, produced by Ircha.

evaluated. These were a set of variable geometry, water cooled profiled rolls and a set of variable geometry dies. Both the dies and rolls allowed a constant force to be applied, using compressed springs, and maintained on the section being formed, thus compensating for any shrinkage of the polymer matrix as the composite section cooled. The development dies and rollers can be seen in Figure 5.1.3 which also shows the prototype hot air oven with its lid removed. The precursor material is a thin nylon 6,6/glass tape manufactured by Ircha.

5.1.4 Precursor assessment trials

The development and evolution of the various stages of the experimental pultrusion line were carried out in tandem with an evaluation of the overall processability of the precursor materials detailed in Table 5.1.1.

The availability of some of the precursors was limited, which restricted the amount of process characterisation which could be carried out during the early program of work. However, sufficient materials were available to identify the principal processing parameters. These were: line speed, which determined the dwell time in the oven, the contact time in the forming and consolidation stage; oven temperature, which determined the overall heating rate to which the moving precursor tows were subjected to; forming pressure, which determined the degree of consolidation.

5.1.5 Current pultrusion line

The experimental pultrusion line was shown schematically in Figure 5.1.1. The pre-impregnated materials were stored as continuous rolls on a creel stand. A minimal degree of tension was applied to the material as it was unwound by passing the tows around fixed bars attached to the creel stand. The tows passed through simple guides which prevented twisting and which ensured that the material entered the heating stage spread out without overlapping occurring.

During preliminary trials with the prototype infra-red and hot air ovens mentioned previously, it became apparent that both heating methods had advantages and disadvantages. The essential requirements of the oven were to provide high heating rates without resorting to excessively high air temperatures and to completely melt

the precursors through their thickness before the oven exit. The precursor thickness ranged between 0.25 and 3mm.

After tests using both hot air and medium wave infra red ovens individually to provide the necessary process heating, a hybrid oven design was adopted. This combined advantages of both types of heating and is shown in Figure 5.1.4.

The oven consisted of a medium wave infra-red section, 1.5m long, with a heated width of 600mm. The infra-red oven contained 16 x 800 watt, medium wavelength gold reflector infra-red elements, placed eight above and eight below the moving precursor. The precursor tows passed through the centre of the oven. The air temperature within the oven was sensed using a thermocouple probe placed at the same height, relative to the infra-red heating elements, as the moving precursor materials. The 600mm heated width allowed several individual tows to be heated flat and side by side so as to avoid shadowing effects. This allowed each tow to be subjected to a more uniform heating rate. As the tows were pulled through the oven they were gradually brought together.

The second heating stage consisted of a hot air oven, 1.3m long. The air was heated by convection from a heated base plate and the air temperature within the oven cavity was controlled using a thermocouple probe, again at the same height as the moving tows. This section of the hybrid oven was designed to act as a temperature soak in which temperature gradients in the tows were allowed to even out, and where the tows were collimated so that they entered the forming stage as an unconsolidated but discrete tow bundle. It also considerably reduced the total cost of the oven.

5.1.5.1 Roll forming of pultruded sections

The combined forming and cooling section of the thermoplastic pultrusion line in this case consisted of three sets of hollow, stainless steel profiled rolls which were allowed to operate at ambient temperature. These are shown in Figure 5.1.5. The diameters and wall thicknesses of both the top and bottom rolls are given below:

	Roll diameter	Wall thickness
Top	140mm	14.5mm
Bottom	140mm	12.5mm

Figure 5.1.4. Photograph of the oven used as the heating stage of the experimental thermoplastic pultrusion line.

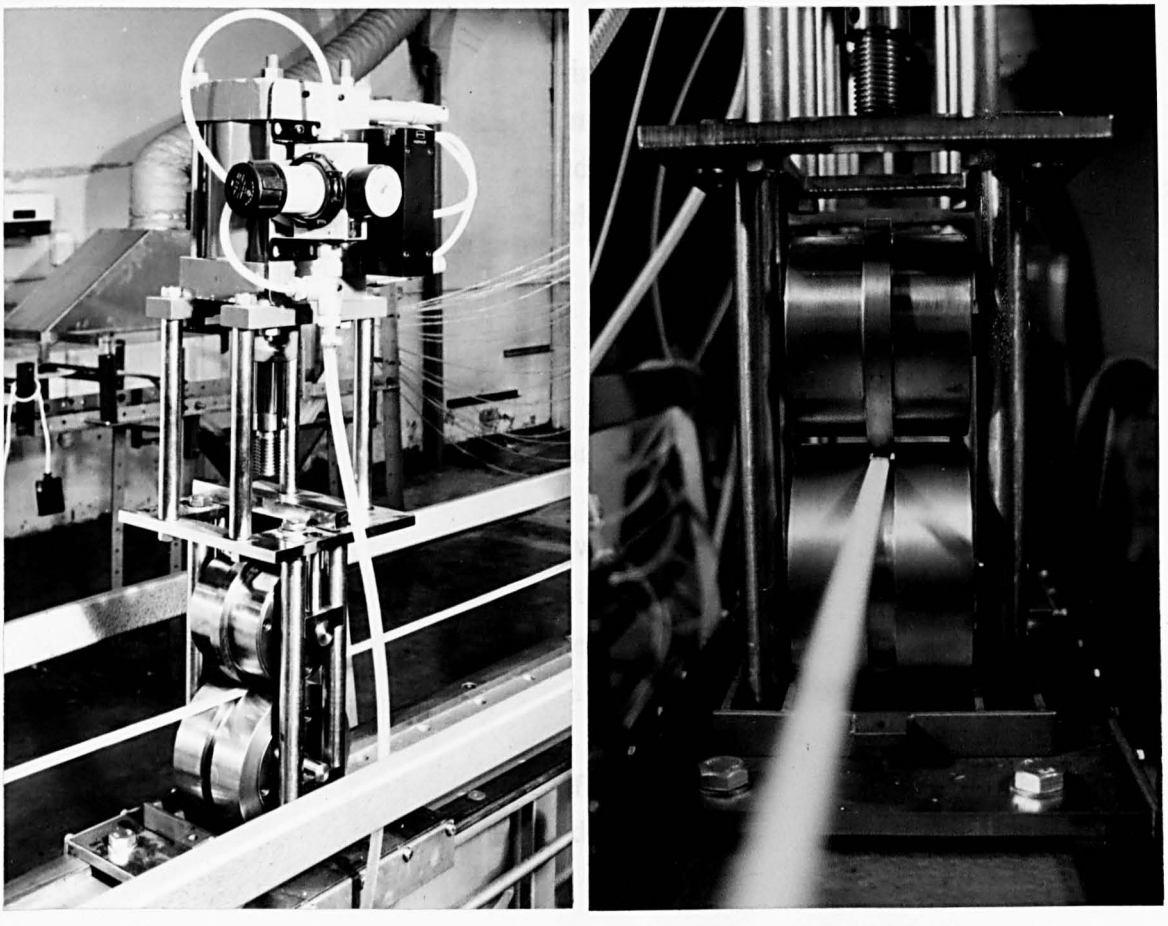

Figure 5.1.5. Unheated, stainless steel profiled rolls used as the forming, consolidation and cooling stage.

The rolls were driven solely by the movement of the pultruded strip through the roll gap.

A constant forming pressure was maintained through the application of a thrust force through a pneumatic piston mounted above the rolls. This force was controlled by a pressure gauge attached to each cylinder and the force was calculated using equation 5.1.1 which relates the gauge pressure reading to the thrust applied by the cylinder.

$$\text{Thrust} = \left(\frac{\pi D^2}{40} \text{ x } P \right) \qquad 5.1.1$$

Where D is the piston diameter (127mm) and P is the gauge pressure in bar.

The forming pressure applied to the rolls was varied from 5 N/mm, corresponding to the top roll weight only with no additional pressure, to a maximum of 345 N/mm. This roll forming pressure is expressed as a force per unit width of section, acting across the width of the pultruded section, because of the uncertainty in measuring the contact length in the rolls. The spacing of the roll stands could be changed for different process conditions if necessary. The pultruded sections were air cooled between roll stands and the product was pulled through the process using a caterpillar haul-off.

The use of a forming mechanism consisting of moving rolls allowed the pultrusion line to run without a significant build-up of viscous drag forces at the roll nip entry and hence without greatly increased pull forces at increasing line speeds. In addition, unwanted removal of matrix polymer, as can happen in the entrance region of tapered dies, did not occur at the roll entry.

5.1.5.2 Die forming of pultruded sections

In addition to roll forming pultruded sections, pultrusion using a set of three temperature controlled brass dies was investigated. The pultrusion die and the experimental set up is shown schematically in Figure 5.1.6. The die dimensions were 270mm x 15mm and the die entry region consisted of a 10mm radius and had a shallow entry angle. The position of the dies could also be altered along the bed of the pultrusion machine. The first die was positioned close to the oven exit and

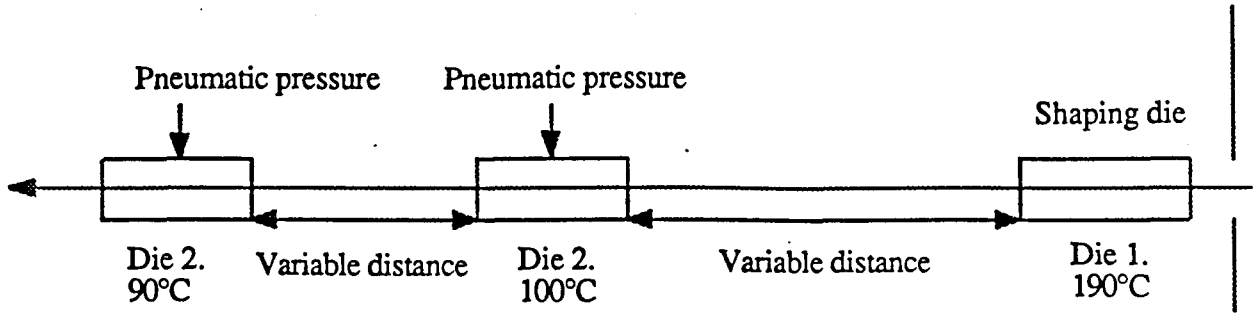

Figure 5.1.6. Experimental pultrusion of thermoplastic sections using three heated forming and consolidation dies positioned after the oven exit. The forming pressure was applied using the pneumatic cylinders used with the roll system.

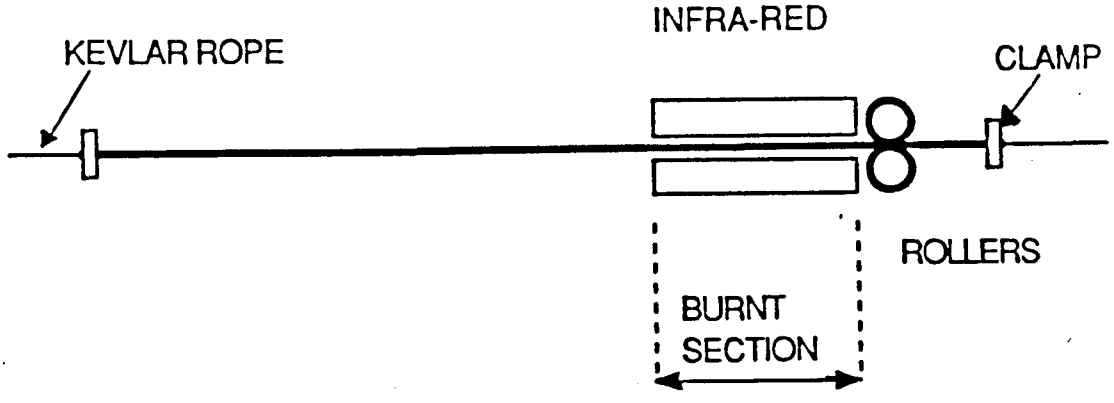

Figure 5.1.7. Discontinuous pultrusion technique used to produce sections using 2m lengths of APC2 precursor material.

was maintained at a constant temperature of 190°C. It was found that without heating, the dies reached an equilibrium temperature which depended on the temperature of die 1, the temperature of the material, the line speed and the relative distances between the dies. The temperature of dies 2 and 3 were maintained at 100°C and 90°C respectively. The relative die positions were determined by the use of experimental temperature measurements coupled with a heat transfer model. It was possible to maintain a constant forming pressure on dies 2 and 3 using the same pneumatic cylinders as used for the rollers.

The forming pressures were varied between 5 KPa and 475 KPa, corresponding to a cylinder pressure of 1.5 bar producing a thrust of 1905 N. The total thrust plus the additional force resulting from the weight of the top half of the die was divided by the area of the die profile to calculate the forming pressure. The main advantage of using a series of long forming dies is that the reduction in residence time with line speed will not affect the consolidation efficiency to such a severe extent as in the forming rolls. At low line speeds it was possible to form sections using forming times substantially greater than with the roll system. In addition, it was relatively easy to control the temperature of the stationary dies compared to heating and controlling the roll surface temperature. A disadvantage is that wipe-off may occur at the die entrance causing viscous drag forces to build-up, resulting in higher pull forces than required for rolls.

5.1.6 Experimental examination of processing parameters

Three types of precursor were eventually made available in sufficient quantity for a detailed study to be undertaken into the effects of changing process parameters.

Precursor A was a nylon 12/glass tape. The tape was 10mm wide, nominally 1mm thick and had a glass volume fraction of 45%, although some variation did occur along the length of the tape. Four ends were required to produce a rectangular section, 15mm wide and between 2.5-3mm thick. The tape was off-white in colour and very springy. This precursor was a non-commercial, development grade and was supplied by Fibreforce Composites Ltd. as continuous rolls, 200m long.

Precursor B was a polypropylene/glass tape. The tape was 10mm wide and 0.25mm thick and had a glass volume fraction of 0.33%. Nine ends were required to produce a rectangular strip, 15mm wide and 2.5mm thick. The precursor was

off-white in colour and was springy. This precursor material was commercially available under the trade name "Plytron" and was supplied by ICI Wilton, as continuous rolls, each containing 400m lengths.

Precursor C was a carbon/PEEK (APC2) tape, supplied by ICI Wilton. The tape was 0.25mm thick and was supplied as a single continuous roll, 25mm wide. In order to pultrude sections using this material seventeen ends were required. Therefore, it was necessary to slit the roll by hand into individual 12.5mm wide tapes in discrete 2m lengths. This caused some minor damage to the edges of the tape. In view of the limited total length of precursor available, it was not possible to run the process continuously using this material. This precursor was black in colour and is a widely used commercial precursor.

The process conditions under which each were pultruded are detailed in Table 5.1.2.

Table 5.1.2 A. Experimental processing conditions for precursor A, nylon 12/glass tape.

PRECURSOR	NUMBER OF TAPES	PROCESSING TEMPERATURE		ROLL PRESSURE N/mm			LINE SPEED M/MIN
		INFRA RED	HOT AIR °C	1	2	3	
Nylon 12/glass	4	180	180	5	5	5	0.3 - 3.0
				90	90	90	0.3 - 3.0
				175	175	175	0.3 - 3.0
				260	260	260	0.3 - 3.0
Nylon 12/glass	4	190	190	5	5	5	0.3 - 3.0
				90	90	90	0.3 - 3.0
				175	175	175	0.3 - 3.0
				260	260	260	0.3 - 3.0
Nylon 12/glass	4	240	240	5	5	5	0.6 - 5.0

Table 5.1.2.B. Experimental processing conditions for precursor B, polypropylene/glass (Plytron) tape.

Precursor	Number of tapes	Processing temperature °C		Die pressure KPa				Die temperature °C			Line speed m/min
		Infra red	Hot air	1	2	3	4	1	2	3	
Plytron PP/glass	9	220	220	---	---	---	---	190	100	90	1.0-3.5
	9	220	220	---	5	5	5	190	100	90	1.0-3.5
	9	220	220	---	162	162	162	190	100	90	1.0-3.5
	9	220	220	---	319	319	319	190	100	90	1.0-3.5
	9	220	220	---	475	475	475	190	100	90	1.0-3.5

Table 5.1.2 C. Experimental processing conditions for precursor C, carbon/PEEK (APC2) tape.

Precursor	Number of tapes	Processing temperature °C		Roll pressure N/mm			Line speed m/min
		Infra red	Hot air	1	2	3	
APC2 PEEK/Carbon	17	380	----	5	5	5	1.0
	17	380	----	90	90	90	1.0
	17	380	----	175	175	175	1.0
	17	380	----	260	260	260	1.0

Table 5.1.3. Die positions used for pultrusion of Plytron precursor at different line speeds.

Line Speed m/min	Distance Die 1 to Die 2 m	Distance Die 2 to Die 3 m
1	0.69	.33
1.5	0.69	.33
2	1.29	.33
3	1.29	.33
3.5	2	.33

5.1.7 Experimental Processing

A flat rectangular strip was chosen as the most suitable shape on which to develop the basic processing procedures, and to identify and study the principle processing parameters. After initial experimental pultrusion runs during the development of the equipment, the principal processing parameters chosen for study were: line speed, oven temperature, and roll forming pressure.

The general procedure for setting up and running the line was basically the same for all precursors investigated and for pultruding using either rolls or dies as the forming and consolidation stage. Precursor tows were placed on the creel stand and were threaded through the guides and into the cold oven. It was important to avoid twisting and cross over between the tows as they passed through the infra-red section as this prevented the tow surfaces sticking together during processing, before they entered the hot air section of the oven. Sticking could result in some fibre misalignment, fibre breakage or birds nest formation around the internal guides and was found to be generally undesirable. As the tows entered and passed through the hot air oven they were gradually brought together and formed roughly to shape using guides before the oven exit. Adjustable guides were used at the exit of the hot air oven to squeeze air out of the tow bundle and to help collimate and feed the material into the first forming stage. The tows were then pulled through the forming stages and into the haul off machine. It was helpful to tack the tow ends together using a high temperature heat gun to ensure that the tows did not twist and were pulled with an equal tension. It was necessary to complete the start-up procedure with the oven cold. When the oven had stabilised at the required processing temperature, the line was run at a slow speed until a solid, consolidated section entered the haul off. The line speed was then increased and pressures applied to the forming stages.

In order to pultrude sections using APC2 precursors, a discontinuous pultrusion technique was developed because of the limited total length available. Individual 2m lengths were cut from the material roll. Seventeen of these were required to produce a section 2.3mm thick. The ends of these were attached to the ends of a co-mingled PPS/aramid 'rope' using clamps. By using this rope it was possible to pull the short APC2 lengths through the oven and the rollers. The experimental set up is illustrated in Figure 5.1.7. The burnt section was the result of setting the line up cold before turning on the heating elements. The PEEK resin is known to act as an excellent high temperature adhesive and to prevent it sticking to the roll surfaces

these were coated with 'Frekote FRP' mould release between each experimental run.

5.1.8 Mechanical testing and process characterisation

In order to assess the quality of the pultruded sections produced, and to compare sections produced under changing process conditions, the short beam shear test (BS 2782 Method 341A) was used as one of two principle mechanical tests. The short beam shear test evaluates the interlaminar shear properties of the composite which are strongly influenced by the interfacial characteristics of the composite microstructure. These are a function of both the degree of impregnation and the effectiveness of the consolidation stage which must remove any air bubbles trapped between the tows and produce a void free microstructure with an uniform fibre distribution. The test has been discussed in the literature review and aims to induce an interlaminar failure along the centreline of a beam subjected to three point loading. A span to depth ratio of 5:1 was used. The test specifies a specimen width of 10mm. The 15mm wide pultruded strip was cut to size using a high speed band saw. This was found to be a quick and efficient way of preparing test samples without inducing damage prior to testing. Five specimens were tested to provide an average apparent interlaminar shear strength for each set of process conditions examined. The standard deviation for each set of interlaminar shear strength results was calculated and a 95% confidence limit will give interlaminar shear strengths of ±4 to 7%. The coefficient of variation was also calculated to lie between 0.1 and 0.03 for the interlaminar shear strength results.

As discussed in the literature review, a range of failure modes were observed, the most common being tensile failure on the lower surface followed by crushing under the loading support. The failure mode depended strongly on the quality of the pultruded sample and usually gave rise to a characteristic load versus deflection trace in which no peak failure load was apparent. In the cases where no obvious peak load was apparent due to the onset of compressive damage and crushing failure, a maximum load was determined as shown in Figure 5.1.8.

The interlaminar shear strength (ILSS) was then calculated using equation 5.1.2.

$$ILSS = \frac{3P}{4A} \qquad 5.1.2$$

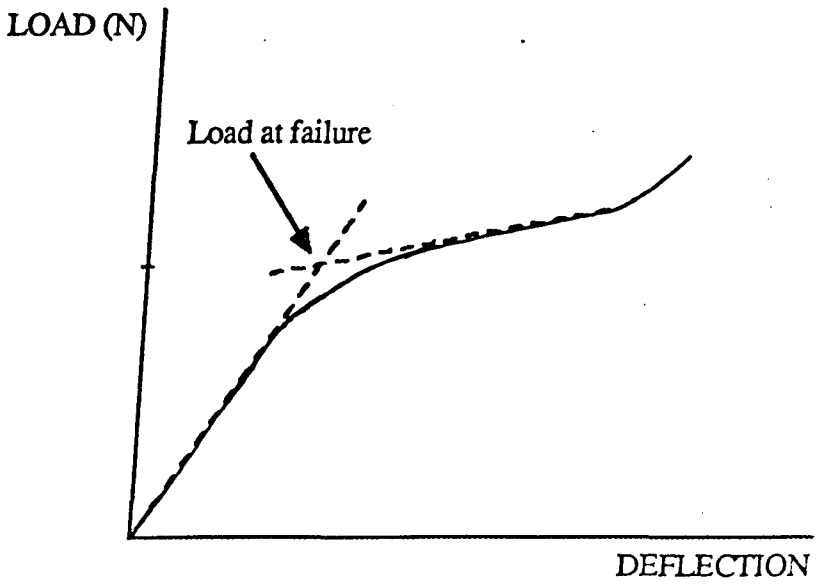

Figure 5.1.8. Determination of load at failure in short beam shear tests in which there was no peak load. The second region of the curve corresponded to the beginning of compressive damage.

Where S is the apparent interlaminar shear strength (MPa), F is the force at fracture (N), b is the specimen width (mm) and d is the specimen thickness (mm).

The two main polymer matrices studied were nylon 12 and polypropylene. Polypropylene is a crystalline thermoplastic which has a T_g of -10°C. It is thus tough and ductile at room temperature and will exhibit necking and drawing behaviour. Because it is above its T_g at normal testing temperatures, it is not possible to carry out short beam shear tests on polypropylene composites. Nylon has a T_g of 60°C and is thus much less ductile than polypropylene at room temperature. No problems therefore arise during short beam shear testing at room temperature.

In addition to the short beam shear tests performed, conventional three point bending tests were carried out, using a span length of 45mm, to determine the flexural strength at maximum load according to BS 2782 : Pt 3: Method 335A . Flexural test samples were cut from positions adjacent to the corresponding short beam shear test samples so as to provide as close a correlation as possible. The standard specimen dimensions for each test are outlined below:

Short Beam Shear	18 mm x 10 mm x 3mm (Nominal)
Flexural (three point bend)	80 mm x 15 mm x 3 mm (Nominal)

The flexural strength of the pultruded strip was calculated using equation 5.1.3.

$$\sigma_f = \frac{3FL}{2bh^2} \qquad 5.1.3$$

where F is the maximum failure load in Newtons, L is the span, h is the specimen thickness and b is the specimen width, all in metres.

Five specimens were tested to provide an average flexural strength for each set of process conditions examined. The flexural modulus was calculated using the expression:

5.1.4

In which L is the span length, b is the width, h is the thickness, F is the load at a chosen point on the linear region of the load-deflection curve and Y is the deflection corresponding to load F. The standard deviation of the flexural strength test results was calculated and a 95% confidence limit will result in flexural strengths of between ±4 to 6%. The coefficient of variation was calculated to lie between 0.1 and 0.03 for the flexural strength results.

5.1.9 Microscopy

Optical light microscopy was carried out in order to investigate the size and distribution of voids and un-wetted fibres, and to examine the fibre distribution in the pultruded products.

The pultruded strip was sectioned perpendicular to the reinforcement direction using a low speed diamond saw, with water as a lubricant. It was found that oil-based lubricants tended to stain the specimen surface and obscure microstructural detail, especially if voids or areas of poor impregnation and fibre wet-out were present. After cutting, the sections were ground using successively finer silicon carbide metallographic wheels, up to 750 μm grit, and then polished using diamond pastes of 6μm and 1μm. In order to increase the contrast between the reinforcing fibres and the matrix polymer, some samples were etched in 40% hydroflouric acid for time periods of between 1 and 5 minutes. The polished and etched surfaces were viewed under reflected polarised light.

A major problem which was encountered with the interpretation of the composite microstructure was the difficulty in distinguishing processing induced defects from comparably sized areas of damage which may have appeared at some stage during sample preparation. In order to identify both processing defects and areas of poor wet out and impregnation before any grinding or polishing took place, sections were cut using a low speed diamond saw so as to have two clean cross-sectional faces. The samples were then coated with a red die penetrant, Ardrock 996P, and allowed to soak for 30 minutes. After this period the sample surfaces were wiped clean and treated with Ardrock 9PR551, penetrant remover. The surfaces were cleaned until there was no red colouration remaining after wiping on a cloth. After this treatment, the sections were polished following the same procedure as detailed previously. It was then possible to distinguish "new" features by their lack of colouration.

5.1.10 Product tolerances

Measurements made during mechanical testing were used to determine product tolerances, however there were some inevitable variations in sectional dimensions due to variations in the polymer volume fraction of the precursor materials and due to unintentional wipe off occurring at the oven guides and exit. However, it was possible to pultrude sections having acceptable dimensional tolerances.

5.1.11 Compression moulding of comparative "pultruded" sections

Using the same precursor materials as used in the pultrusion process, it was necessary to produce a composite strip by an established process to provide comparative property measurements. From these the efficiency of the heating, forming and consolidation stage of the pultrusion process could be determined. A rectangular flat strip section was pressed using a heated compression die, mounted under a hydraulic jack. With the heated die, it was possible to use considerably longer heating, consolidation and cooling times, coupled with greatly increased forming pressures than those experienced during pultrusion. The properties of this pressed section were taken to indicate the optimum which could be achieved by the pultrusion process for the specific precursor materials.

5.1.12 Temperature measurements

It was necessary to record the temperature distributions within the precursor materials as they were pulled through the oven, forming, consolidation and cooling stages of the process. This data was essential to the development and verification of a heat transfer model for the process. This proved to be very difficult at high line speeds and at high forming pressures. However, it was possible to measure temperature distributions at low line speeds and at the minimum forming pressures.

Temperatures were measured continuously during processing using PTFE covered "k" type (Ni Cr/Ni Al) thermocouple wires with a tip diameter of 0.8mm. A 4m length of thermocouple wire was sewn into the centre of an individual precursor tow before the oven entrance, with its tip placed as close as possible to the surface of the tow as shown in Figure 5.1.9. This thermocouple was connected, via a compensating cold junction, to a chart recorder. When the oven temperature had

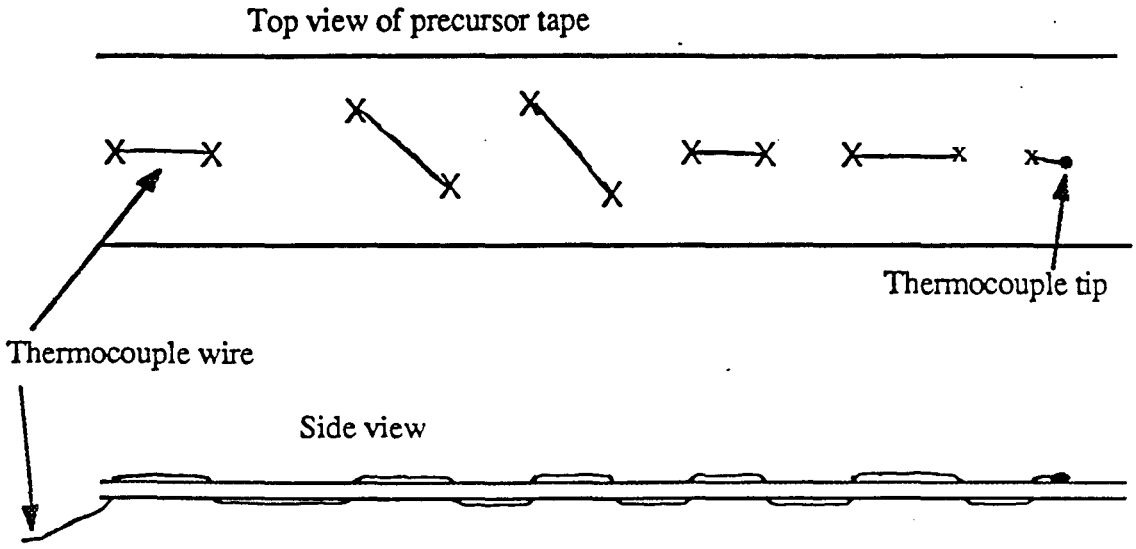

Figure 5.1.9. Method of pulling thermocouples, "sown" into individual tapes, through the process to measure temperature distributions in the section during heating, forming and cooling.

stabilised, the puller was started and the pultrusion line was run as normal. As the thermocouple entered the oven it was important that it was supported with minimum tension to prevent it slipping backwards through the molten uni-directional precursor tow. As the precursor tows were collimated the thermocouple became embedded in the tow bundle and was subsequently formed into the pultruded strip. This embedded thermocouple gave a continuous recording of the temperature within the cooling strip as it passed through the rolls. It was very difficult to pre-determine the position at which the thermocouple tip would measure the temperature, and after cooling the area of product containing the tip was labelled and sectioned using a low speed diamond saw until the tip position could be accurately ascertained.

Although it was possible to pass a maximum of five thermocouple wires through the process in a single run, the identification of the final position of each was difficult and it was more satisfactory to use thermocouples singly, sown into different starting tows, and to superimpose the individual temperature distributions obtained. Although there will be some degree of temperature lag during the temperature recording due to the size of the thermocouple tip, this was not specifically catered for and was ignored.

5.1.13 Differential scanning calorimetry

The technique of differential scanning calorimetry (DSC) was used to determine the thermal heat capacity and melting point as a function of temperature for the nylon 12/glass and polypropylene precursors. This technique continuously monitors the progressive heat release from a sample which was sealed in an aluminium pan. From this it was possible to use the microprocessor system to determine the heat capacity for each sample. Three heating rates were examined: 20°C/min; 50°C/min and 100°C/min. A Du Pont 2000 microprocessor DSC system was used. Typical sample sizes were between 5-10 mg. When using glass reinforced precursors, it was difficult to maintain a volume fraction in the small sample equivalent to the volume fraction in the precursor material. It was also impractible to determine the actual volume fraction of glass which was in the DSC sample.

5.1.14 Determination of void contents

The void contents of sections pultruded under different process conditions were determined according to the following procedure. Samples were cut from pultruded lengths using a low speed diamond saw so as to have smooth edges which minimised air entrapment. The composite density was measured using a displacement method according to the procedure detailed in ASTM D792-86. After determining the density of each sample, burn off tests were carried out to determine the volume fraction ratio of glass and resin in the composite. After combustion in air, the samples were placed in a furnace at 500°C for 4-5 hours before being re-weighed. Using these volume fractions, and assuming the density of glass to be 2540 Kg/m^3, the density of nylon 12 to be 1140 Kg/m^3 and the density of polypropylene to be 900 Kg/m^3, a theoretical composite density was calculated using equation 3.6. The void fraction in the composite was then calculated using:

$$V\% = \frac{\text{Theoretical density - Measured density}}{\text{Theoretical density}} \times 100 \qquad 5.1.5$$

Because the distribution of voids in the pultruded section was not known, the void content for each particular section was determined using samples which were at least 40mm in length. It was also impractible to determine the void content of each sample tested and a representative void content was determined for each set of process conditions.

5.1.15 Measurement of dynamic shear properties

It was not possible to carry out short beam shear tests on pultruded sections having a polypropylene matrix because polypropylene has a glass transition temperature below room temperature. Therefore, the torsion pendulum test was investigated as to its suitability as a characterisation test for polypropylene matrix composites produced under different processing conditions.

The torsional pendulum can be used for the determination of the dynamic shear modulus and the damping characteristics of composites and has been described in detail in Section 2.3.1.2. The basic instrument used is illustrated in Figure 5.1.10 and consists of two vertical columns, coupled with a torsion system consisting of a cross bar on which weights can be placed. The minimum specimen length was 190mm and the distance between the clamps was 160mm. The cross bar was given

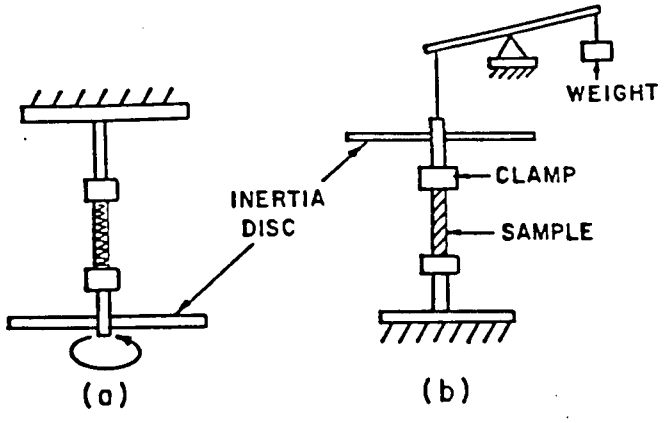

Simple diagram of torsion pendulum.

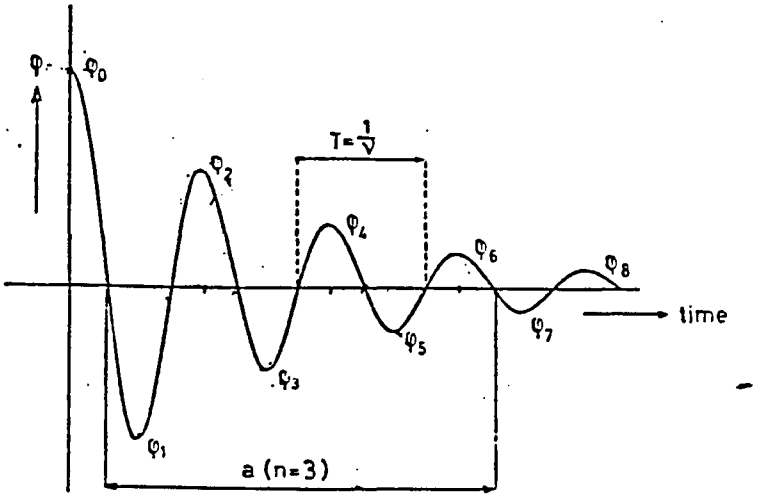

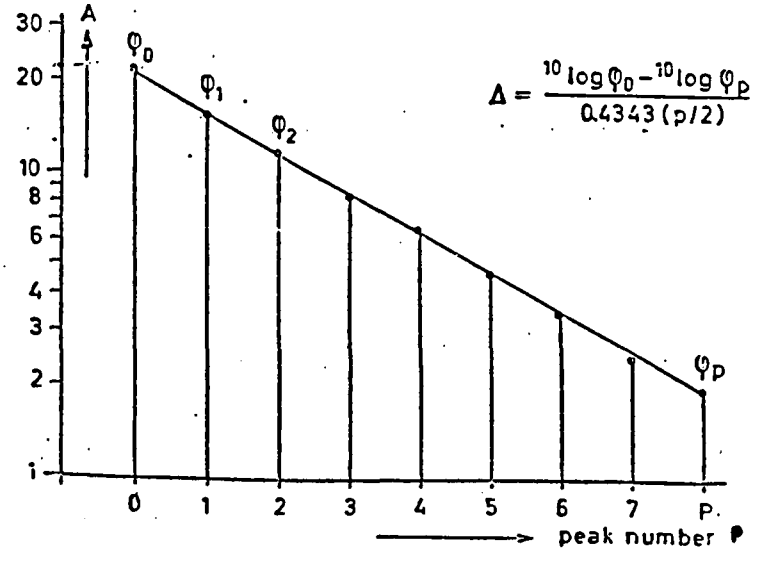

Figure 5.1.10a. Schematic illustration of two variations of the torsion pendulum test. A test similar to test b was used.

Figure 5.1.10b. Typical output trace showing decay in the sample oscillation and a semi-log plot of the peak height against the peak number, p.

a small rotational displacement by hand and the damped vibrations were recorded. The oscillation of the sample was recorded on graphitised paper which was placed on a drum, revolving at a constant speed, coupled to a high voltage generator. A high voltage spark-over from the end of a needle point at the end of the cross bar caused the graphitised paper to darken and the oscillations were recorded as shown in Figure 5.1.10b.

With reference to Figure 5.1.10b, the frequency of oscillation was calculated according to equation 5.1.6:

$$\nu = \frac{n.w}{a} \text{ Hz} \qquad 5.1.6$$

where the drum velocity, w=5.233m/sec, n is the number of cycles and a is the distance measured between 2n+1 intersections with the time axis. The logarithmic decrement, Δ, was calculated according to equation 5.1.7:

$$\Delta = \ln \frac{Q_0}{Q_p} \qquad 5.1.7$$

where Q_0 and Q_p are the extreme values taken from a semi-log plot of the peak height against the peak number,p, as shown in Figure 5.1.10b. The loss factor, tan δ was then calculated:

$$\Delta = \tan \delta \qquad 5.1.8$$

The storage modulus, G', could then be calculated using equation 2.3.4 for a rectangular section of width b and thickness d, setting $I=0.12 Kgm^2$, l=160mm and calculating g according to equation 5.1.9:

$$g = Cbd^2 \qquad 5.1.9$$

The constant c was obtained from tables depending on the ratio d/b.

The loss modulus, G", was calculated using equation 2.3.7.

5.2 Investigating the melt impregnation process

5.2.1 Materials used in impregnation experiments

The material system studied comprised of two E-glass tows of 2400 Tex nylon compatible glass, which were impregnated with a nylon 6,6 (Maranyl A100) melt at 285°C. A graph of the apparent shear viscosity of Maranyl A100 as a function of shear rate over the temperature range 275-295°C is shown in Figure 5.2.1.

5.2.2 Experimental impregnation and force measuring apparatus

The experimental apparatus consisted of a basic creel stand, modified from a pultrusion creel on which tension could be adjusted by increasing the friction on the moving bearings. The glass tows were supplied on two 160mm diameter cores which were mounted vertically onto the creel stand and externally unwound. In order to minimise the tensions generated during unwinding, both tows were adjusted so as to be as free moving as possible. This, however, made it necessary to employ some form of pre- tension between the creel stand and the extrusion bath. To this end, the tows passed around three 10mm diameter bars fixed at different heights, and these were found to be adequate in preventing the tows becoming slack and jerking while being pulled. They also helped to prevent tow twisting prior to the impregnation bath entry. Although it was possible to increase the friction on the creel stand to vary the input tension of the fibre tows, it was very difficult to maintain this tension at a constant level. It was found that the action of unwinding the tows resulted in periodic peaks in the value of the input tension and in order to minimise this effect the tows were unwound with the lowest creel friction possible. At a low creel friction these unwinding peaks were measured and found to be insignificant. No preheating of the glass tows took place before the impregnation bath.

The impregnation bath consisted of a heated cavity with one detachable, heated side. Four heated zones were employed in order to maintain a constant nylon melt temperature throughout the bath. The bath and the tow paths are illustrated in Figure 5.2. . The bath contained three stationary 20mm diameter bars, with fixed centre distances and thus fixed wrap lengths, over which the tows passed before

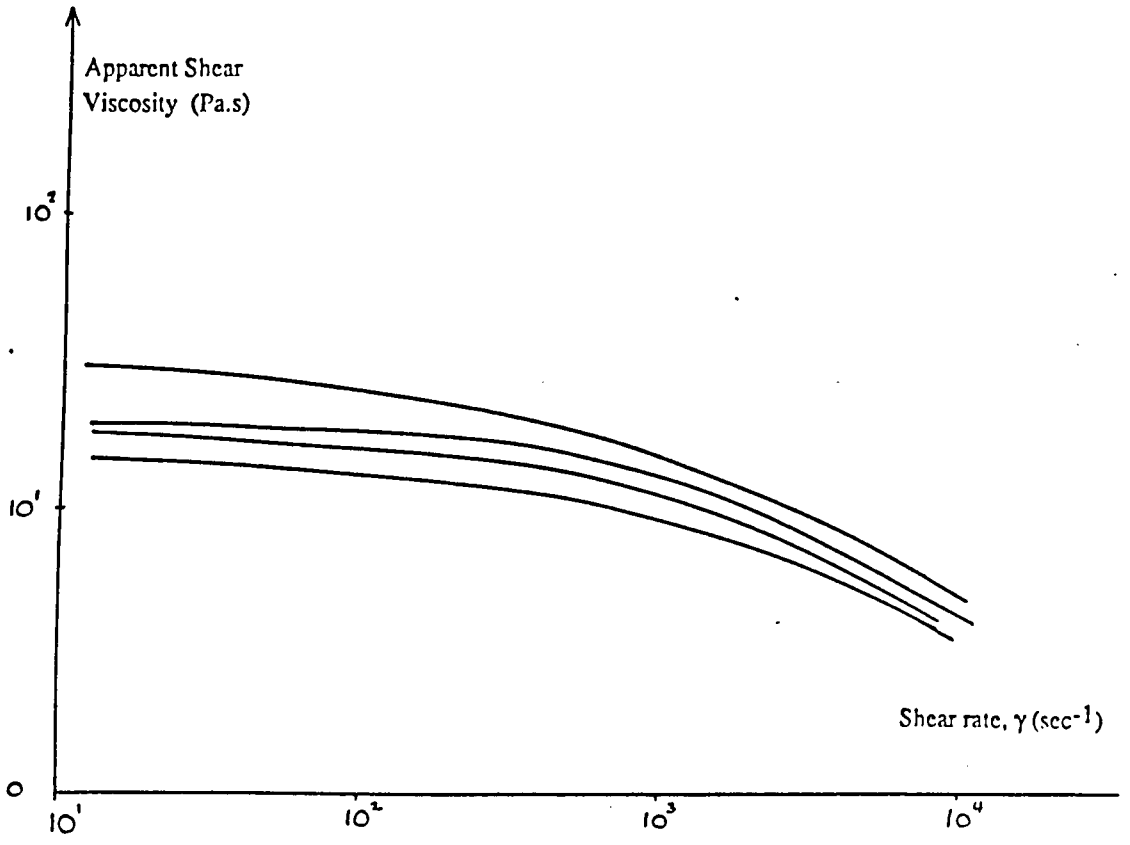

Figure 5.2.1. Apparent Shear viscosity of nylon 6,6 (Maranyl A100)

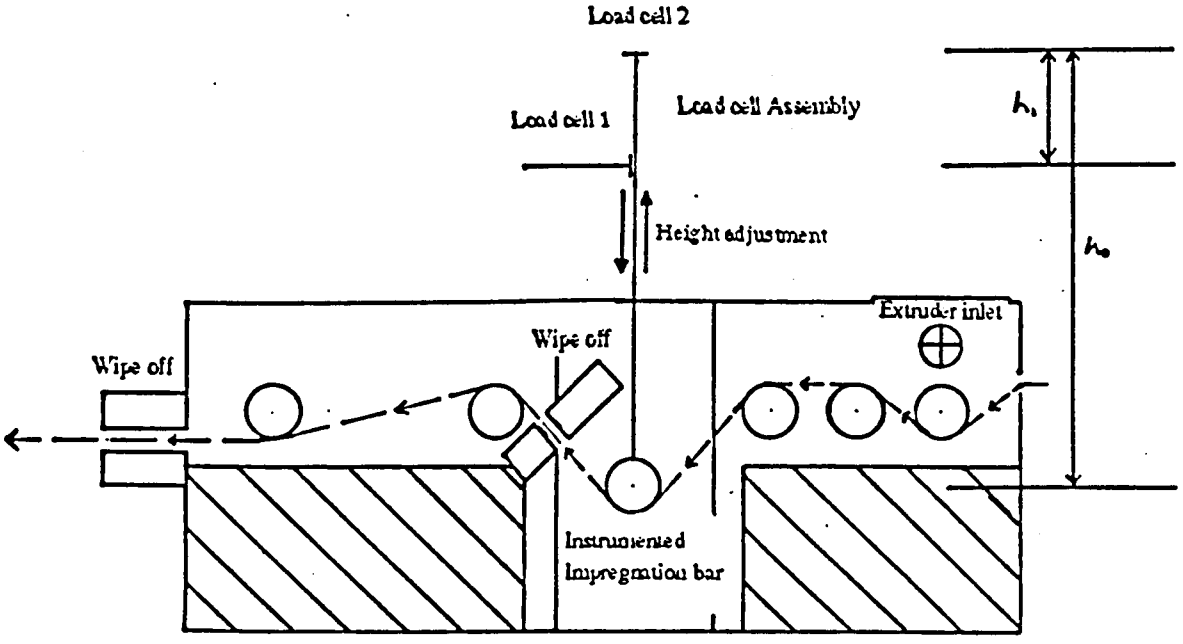

Figure 5.2.2. Schematic diagram of melt impregnation bath, showing fibre tow paths through the bath and around the instrumented impregnation bar. The load cells could be moved vertically up or down to alter the wrap angle of the incoming tows.

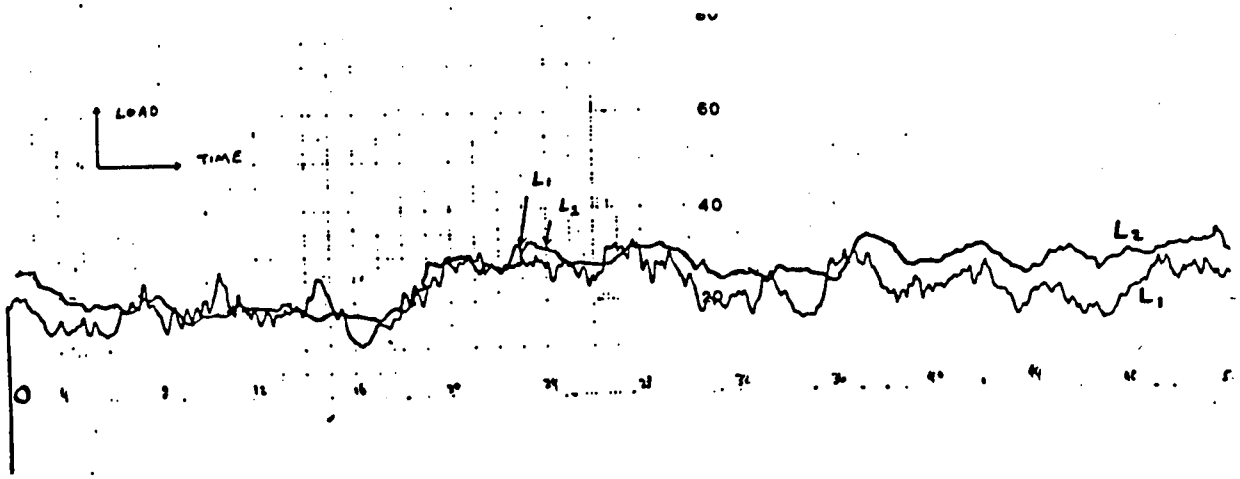

Figure 5.2.3. Typical output from the load cell assembly, in this case for impregnation experiments carried out on a 10mm bar, 60° degree wrap angle, at 5m/min.

passing around the instrumented bar. Two more bars were placed downstream of the instrumented bar, the first of which maintained a symmetrical wrap angle. The bars were made from EN31, silver steel, and all were 30mm wide. To maintain a constant level of nylon melt in the bath, the bath was mounted onto a Reifenhauser single screw extruder which was run continuously to keep all the bars immersed. The extruder output was 10 Kg/hour.

In order to measure the tension generation as the fibre tows passed around the impregnation bar, the bar was mounted directly onto a load cell, with another load cell contacting the support rod as shown in Figure 5.2.2. The maximum operating temperature of the load cells was between 50-80°C and the sliding load cell assembly was water cooled to reduce the operating temperature of the load cells, which were prone to heating from the hot bath. The load cells were also insulated. The two 5 kN tension/compression load cells were connected via an adjustable 10 mV power source to a two channel chart recorder. Calibration using standard weights allowed the recorded millivolt output to be converted into a force measurement. For the vertical load cell this was straightforward and a load was simply hung from the end of the support. In the case of the horizontal load cell, calibration was carried out by applying the load at the end of the support and calibrating according to the moment registering at the load cell.

It was possible to alter the wrap angle, and hence the wrap length, between 15° and 120° by changing the vertical distance between the centre of the measuring bar and the centre line of the fixed bars on either side. To accomplish this the entire load cell assembly was free to slide vertically up and down against a graduated scale on the bath wall. This ensured that the distances h_0 and h_1 remained constant at each wrap angle studied. In cases where the distance (h_0-h_1) in Figure 5.2.2 was altered, the support rod was not the same for each of the bars studied, the load cell was recalibrated. Force measurements were made on one instrumented impregnation bar only. It was also possible to change the diameter of the measuring bar to study the effect of bar radius.

Bars of radii 5, 7.5, 10 and 15mm were examined. These bars were not equipped with any form of side guides to prevent tow spreading and to prevent sideways leakage of polymer. The tows could spread up to the maximum bar width of 30mm. To gain an indication of the effect of tow spreading on the forces generated, an additional set of results were obtained using a bar of 10mm radius

which was equipped with sideguides to limit tow spreading to 20mm and to prevent sideways polymer flow.

The impregnated tows were cooled in air and were pulled through the impregnation bath at a constant line speed by a combined chopper/haul off unit. The maximum achievable line speed was 15m/min.

It was necessary to fit baffles inside the bath during impregnation to try to maintain a constant melt level. These baffles prevented polymer which had accumulated around the fibre tows from being dragged rapidly through to the downstream end of the bath. A 3mm diameter heated wipe off die was used to remove excess polymer from the impregnated tow which flowed back into the bath.

5.2.3 Experimental procedure for melt impregnation

Two glass tows were threaded side by side through the bath, around the fixed bars and into the haul-off. The bath was closed and allowed to heat until the temperature of the cavity was 280-290°C. The bath was then filled with nylon melt using the extruder until all the impregnation bars were submerged. The melt temperature was maintained constant at 285±5°C. The glass was then pulled through at a slow speed until a solid nylon/glass material tow entered the haul off and this prevented large force oscillations occurring due to the action of the haul off on the dry glass. The line was then stopped and the bath was allowed to refill. The load cell support was positioned at a pre-determined height to give the required wrap angle between the instrumented bar and the fixed bars on either side. With the bath level well above the impregnation bars, the experimental run was started. The melt temperature was constantly monitored by a thermocouple placed in the melt directly below the measuring bar.

The tows tended to drag material quite quickly through to one side of the bath and the melt level fell quite rapidly, especially at line speeds of 15m/min. However, the addition of baffles within the bath reduced this problem by causing a recirculating flow of melt around the measuring bar. This effectively kept the instrumented bar submerged and thus allowed runs of sufficient duration to be carried out for each speed/angle/radius combination. Even so, the line was stopped and the bath allowed to refill before each individual experimental run and the duration of each run was determined by the rate at which the level of melt in the bath fell. At the

higher line speeds it was necessary to perform a number of short runs to produce an average result for the each experimental combination. All the nylon used was dried at 75°C for 10 hours prior to use to remove moisture.

The experimental runs carried out are detailed in Table 5.2.1.

Table 5.2.1. Experimental runs carried out using Nylon melt at 285°C.

Pin radius mm	Line speed m/min	Wrap angle °
5mm	5, 10, 15	15, 30,45, 60,120
7.5mm	5, 10,15	15, 30, 45, 60, 120
10mm	5, 10, 15	15, 30, 45, 60, 120
10 with sideguides	5, 10, 15	15, 30, 45, 60, 120
15mm	5, 10, 15	15, 30, 45, 60,

5.2.5 Calculation of tension generation during impregnation

The basic data obtained from the impregnation experiments was in the form of load cell output (millivolts) versus time traces, one for each load cell (LC1=horizontal load cell and LC2=vertical load cell). By using the calibration curves obtained using weights of known value it was possible to convert these into force versus time traces. It was very difficult to obtain a constant force reading, especially using the nylon melt, and all experimental traces were subject to a fluctuation about a mean value. The reasons for these fluctuations were unclear and will be discussed in a later section. In order to calculate the average force experienced by each load cell, a force value was read from the trace at 1 second intervals and an average calculated from these. A typical trace is shown in Figure 5.2.3. It was possible to calculate an average value of the force at each load cell, L1=horizontal load and L2=vertical load. It was then possible to calculate the values of input tow tension,T_o, and the output tension, T_1. With reference to Figure 5.2.4, the total tension in the impregnated tow can be written:

$$T_1 + T_0 = \frac{L_2}{\sin \theta/2} \qquad 5.2.1$$

Where θ is the wrap angle. Assuming a frictionless bearing at A, and taking moments results in the expression:

$$T_1 - T_0 = \frac{L_1 h_1}{h_0 \cos \theta/2} \qquad 5.2.2$$

From equations 5.2.1 and 5.2.2 the input and output tensions can be expressed:

$$T_1 = \frac{L_1 h_1}{2h_0 \cos \theta/2} + \frac{L_2}{\sin \theta/2} \qquad 5.2.3$$

$$T_0 = -\frac{L_2}{2\sin \theta/2} + \frac{L_1 h_1}{h_0 \cos \theta/2} \qquad 5.2.4$$

The build up in tension, T_1-T_0, was then calculated and plotted against wrap length for each bar radius and line speed studied.

Chapter 6. Results and Discussion

6.1 The pultrusion of thermoplastic composites

6.1.1 Review of materials used

Details of the three main precursors used in the pultrusion experiments are given in Table 6.1.1. Precursors A, B, C were available in sufficient quantity to allow the effects of changing process parameters on the mechanical properties of the pultruded sections to be studied. Limited quantities of the other precursors were also available and were used for development work on the basic process. This will be discussed briefly in the following section.

6.1.2 Pultrusion process development

At the start of the project, a limited quantity of a commercial nylon 12/glass precursor, Atochem 'FIT' material was available. The production of this material has been discussed in Section 2.1.3.1. Using the basic experimental set up shown in Figure 5.1.3, a number of sections were produced at speeds between 0.1 and 1m/min. The heating was provided by a hot air oven, 1m long and the forming stage consisted of a heated die, 30mm long, maintained under pressure by compression springs, followed by water cooled forming rolls. A nitrogen atmosphere was used in the hot air oven to reduce degradation. Insufficient material was available to produce a range of sections on which mechanical testing could be carried out, although micrographs of the pultruded sections were taken.

This precursor had some advantages and disadvantages which became apparent during processing. The major problems were associated with the high volume fraction of polymer in the fiber tow, ~65%, and with the resin rich sheath material surrounding it. It was inevitable that some wipe-off occurred at the entry to the heated die and this generally caused birds nest formation and die clogging, which eventually caused fiber breakage and a disruption of the process. Even after passing through the heated wipe off die, the sheath material was difficult to redistribute throughout the cross section of the pultruded strip and is clearly visible

Table 6.1.1. Summary of thermoplastic preimpregnated precursors available for pultrusion experiments

Matrix	Reinforcement	V_f	Melting Temp. °C	Form	Size	Handling	Colour	Trade name
Nylon 6,6	Glass	.35	264	U-D rod	3mm diameter	Very stiff	White	Verton
Nylon 12	Glass	.4	176	U-D tow	3mm diameter	Flexible	White	FIT
(A) Nylon 12	Glass	.5	176	U-D Tape	10x1.5mm	Stiff/springy	White	-----
(B) Polypropylene	Glass	.33	176	U-D Tape	10x.5mm	Stiff/springy	White	Plytron
Polypropylene	Glass	.5	179	U-D Tape	10x1.5mm	Stiff/springy	White	-----
(C) PEEK	Carbon	.61	343	U-D Tape	12.5x0.25mm	Boardy	Black	APC2
Nylon 6,6	Glass	.5	264	U-D Tape	3x1mm	Springy	Brown	Ircha
PPS	Glass	.5	285	Co-mingled	1mm diameter	Yarn	Yellow	-----

in Figure 6.1.1 as resin rich areas surrounding discrete bundles of fibres. Figure 6.1.2 shows that it was possible to increase the level of consolidation and improve the fibre distribution through the cross-section by increasing the oven temperature so that the material entering the roll gap was at a higher temperature.

Figure 6.1.3 shows the 'FIT' precursor and some of the sections produced. As can be seen, it was possible to twist and tie the precursor tow and this gives a good illustration of its ease of handling. The polymer powder remained unfused during the impregnation process and this resulted in a flexible tow, unlike all the other preheated precursors which were very stiff and springy. It was also relatively easy to heat the tows to the required processing temperature, even using a very basic hot air oven.

A quantity of another commercial nylon 6,6/glass precursor was also available. This was produced by Ircha using a proprietary process and was in the form of a very thin, 0.5mm, and narrow, 2mm brown tape. This material can be seen passing through the oven and rolls in Figure 5.1.3. All attempts to pultrude acceptable sections using this material failed. Up to 40 individual tapes were required to produce a 3mm thick section and it was difficult to heat these sufficiently using only a hot air oven before the die entry. The die length was also too short to allow adequate flow and consolidation to occur. This precursor was regarded as highly unsuitable for pultrusion type processes because die lengths would have to be excessively long to achieve consolidation. This precursor was also difficult to handle on account of its springiness and the large number of tapes which were required to produce a section only 3mm thick.

A co-mingled PPS/aramid fibre tow was also evaluated. In this case a 1m long, medium wavelength infra-red oven was used to overcome similar heating problems to those experienced with the Ircha materials and to achieve a sufficiently high temperature to melt the PPS matrix. Again, a large number of individual tows were required to fill the die and again, little consolidation was achieved during processing. It was therefore decided that co-mingled type fibre tows were also unsuitable for pultrusion type processes where success depends to a large extent on achieving short heating, forming and consolidation cycles.

Another precursor which was available, this time in a greater quantity than the others, was a continuous form of ICI's nylon 6,6/glass 'Verton' long fibre injection moulding material. This material was in the form of a 3mm diameter rod and was

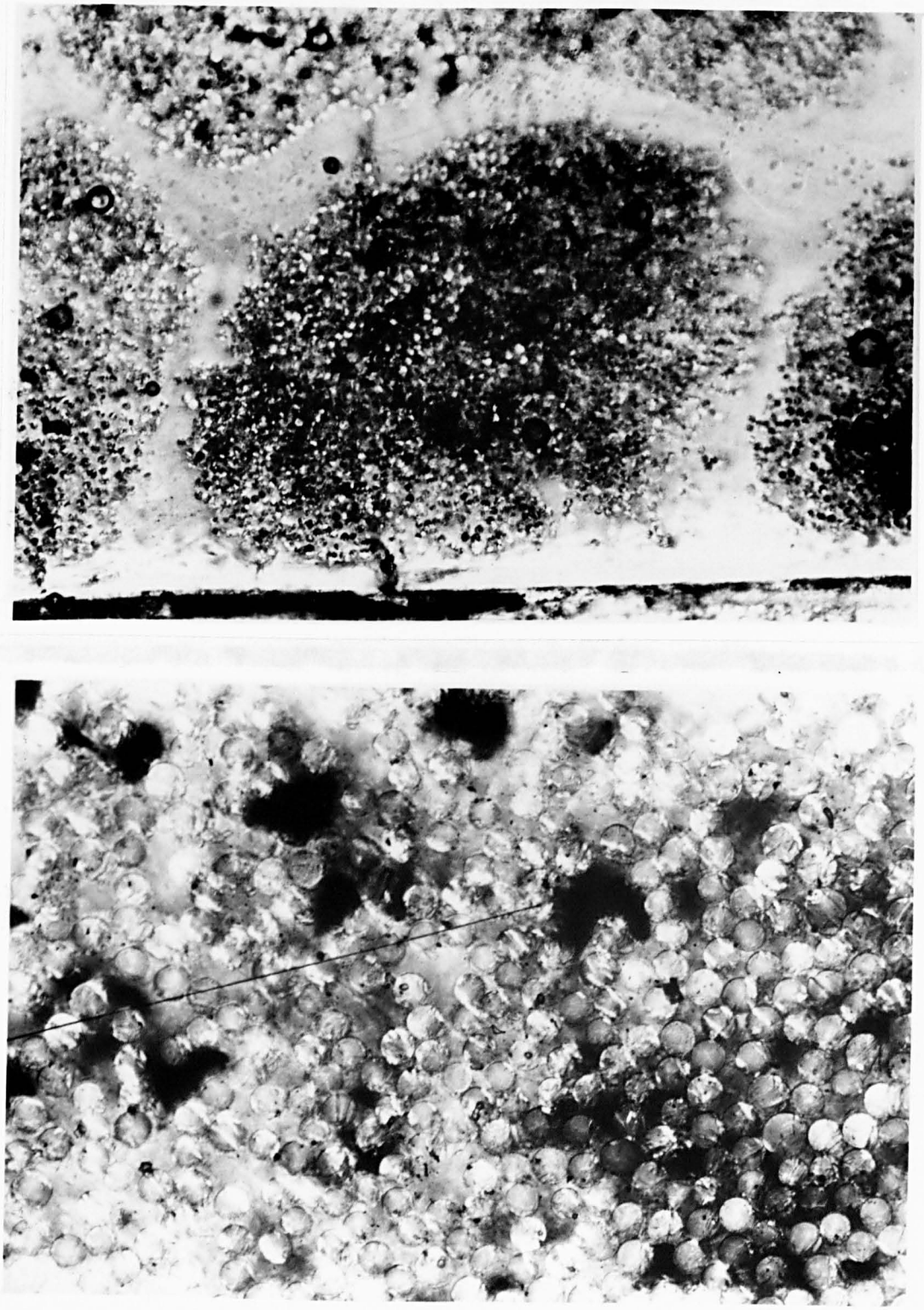

Figure 6.1.1. Micrographs of sections produced using the Ato 'FIT' material. These show the resin rich area surrounding fibre bundles which were caused by the difficulty in re-distributing the precursor sheath material during pultrusion. Some voids can also be seen at higher magnifications. The processing conditions were: line speed 1m/min; oven temperature 250°C; wipe-off die temperature 150°C.

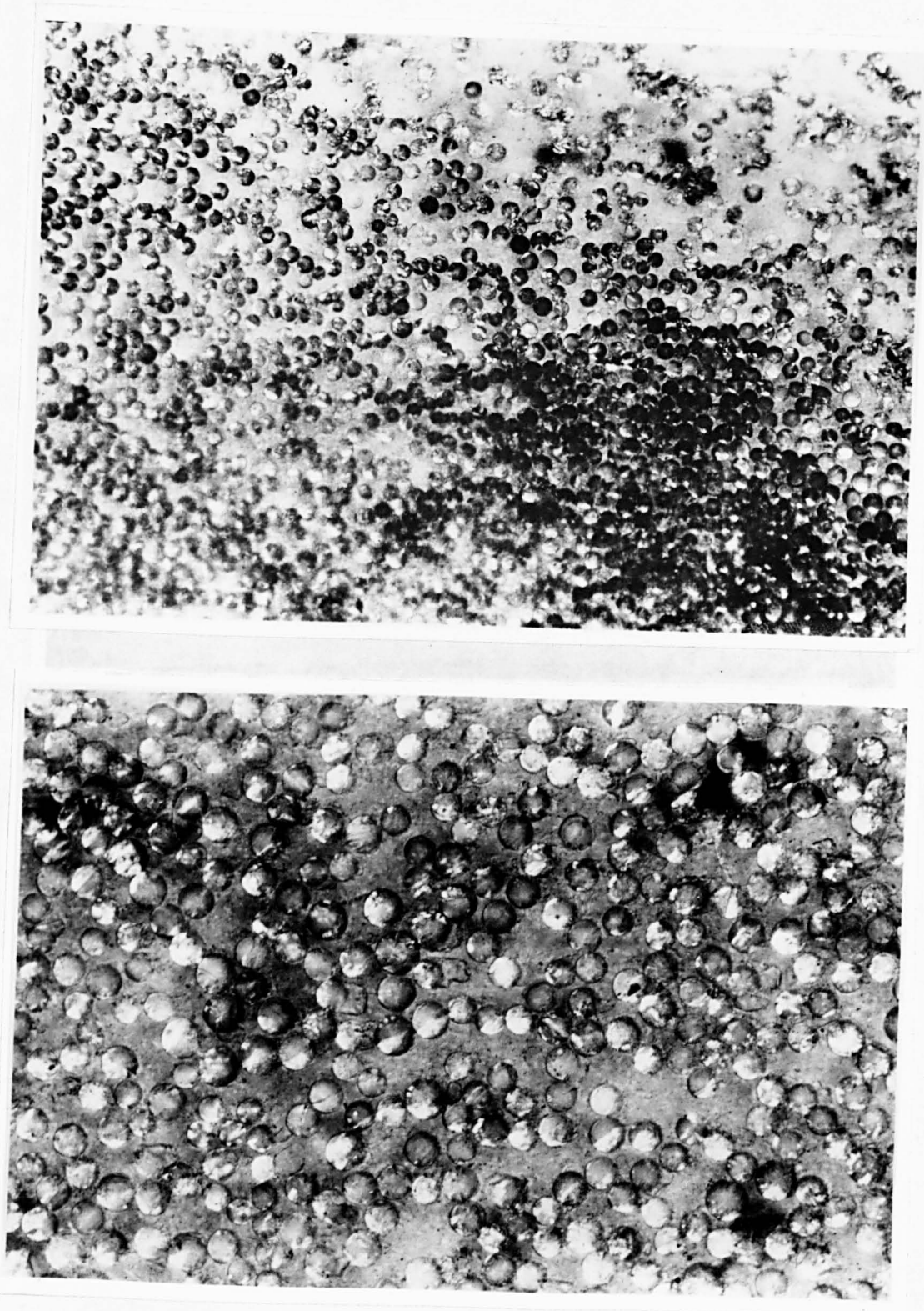

Figure 6.1.2. Micrograph of Ato 'FIT' pultruded section showing the effect of increasing the oven temperature to 300°C. It is impossible to distinguish individual precursor tows and the void content appears to be lower. The processing conditions were: line speed 1m/min; oven temperature 300°C; wipe-off die temperature 200°C.

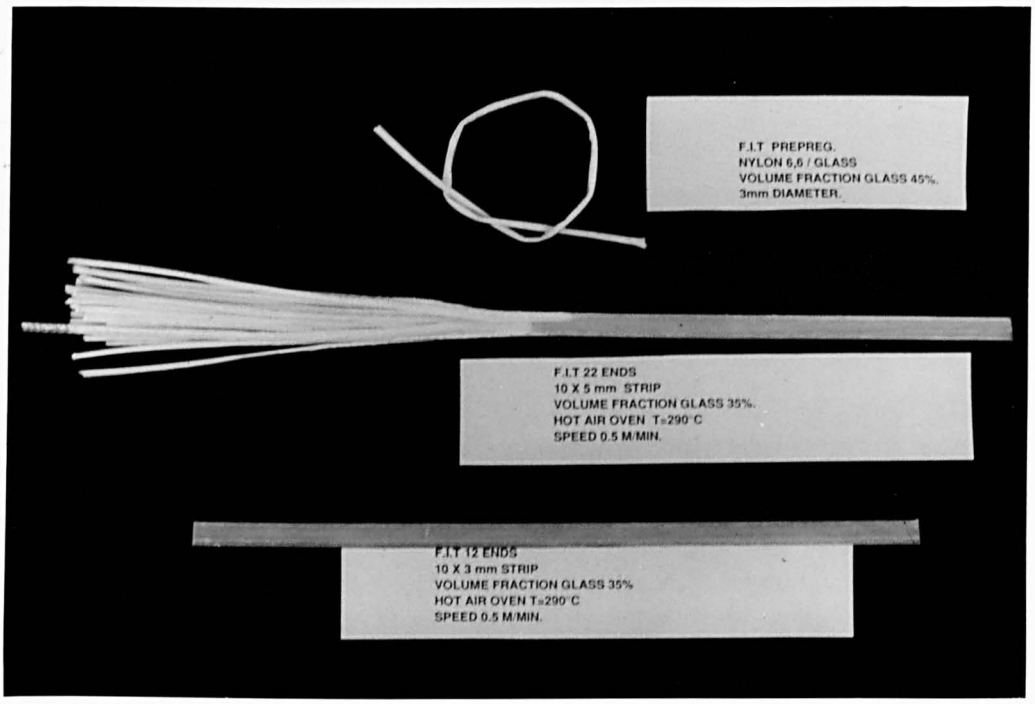

Figure 6.1.3. Pultruded section produced using the 'FIT' precursor.

thus extremely stiff and springy. It was, in fact, too springy to coil up and individual lengths for pultrusion were required to lie loose on the floor. This material was processed using a 1m long infra-red oven and using the forming roll system shown in Figure 5.1.5.

Initially, this precursor was pultruded in its original round form and the effect of increasing the forming pressure on the interlaminar shear strength at a speed of 0.45m/min is shown in Figure 6.1.4. The melting temperature of the nylon 6,6 matrix was 264°C and the processing temperature was 320°C. The variation of interlaminar shear strength with line speed for sections produced at two oven temperatures and at a forming pressure of 90N/mm is shown in Figure 6.1.5.

Increasing the roll pressure appeared to have little effect on the interlaminar shear strength of the composite section. However, increasing the line speed caused a decrease in the interlaminar shear strength for both oven temperatures examined, and pultruding at the higher oven temperature resulted in slightly better properties. It was difficult to heat the relatively thick, round precursor and distinct fibre clumping remained in the final product cross section. This is illustrated in Figure 6.1.6a which clearly shows the formation of voids at the boundaries between individual precursor tows.

In order to achieve better consolidation, some of the round precursor was flattened by pulling individual tows through the oven and the rolls to produce a flat tape, 15mm wide. Eight tapes were then pultruded at a line speed of 0.8m/min. An interlaminar shear strength of 52MPa was achieved at this speed, which was equal to the strength of sections produced using the round precursor at speeds as low as 0.3m/min. This improvement was the result of a combination of improved heat transfer due to the increased surface area perpendicular to the incident radiant heat and a greater degree of consolidation and fibre distribution in the final product. In Figure 6.1.6b it is impossible to distinguish distinct individual tows in the final product microstructure.

A pressed plaque was produced using the round precursor which had an interlaminar shear strength of 61 MPa and a flexural strength of 813 MPa.

As a result of these trials using different precursors, it was found that the pre-impregnated precursor must fulfill several requirements for each of the processing stages to operate effectively, from the initial handling through to the production of a

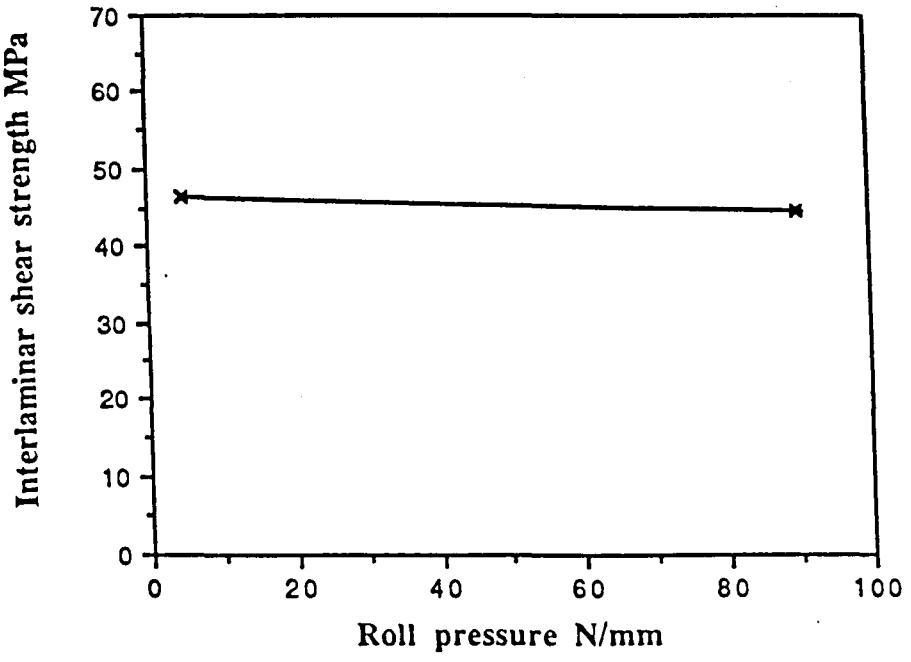

Figure 6.1.4. The effect of increasing the roll pressure on the ILSS of nylon 6,6/glass (Verton) pultruded sections. The sections were produced using an oven temperature of 320°C and at a line speed of 0.45m/min.

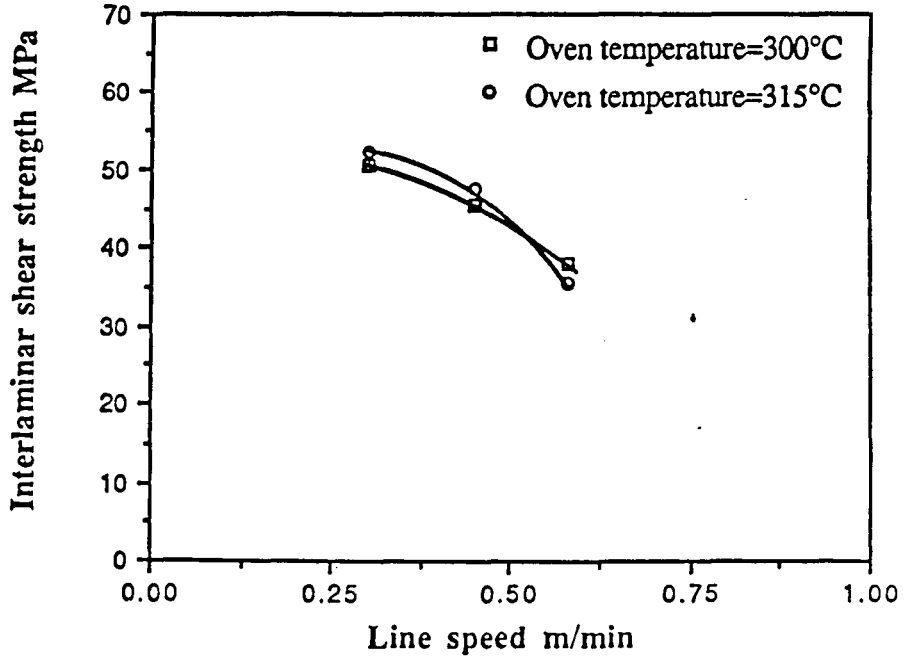

Figure 6.1.5. The effect of increasing line speed and oven temperature on the ILSS of roll formed nylon 6,6/glass pultruded sections. The roll pressure was 90N/mm.

Figure 6.1.6a. Micrograph of pultruded nylon 6,6/glass (Verton) section produced using round precursor material. This illustrates the poor fibre distribution achieved, especially in the areas between individual precursor tows. Voids can also be seen in the regions where the precursor tows have joined together.

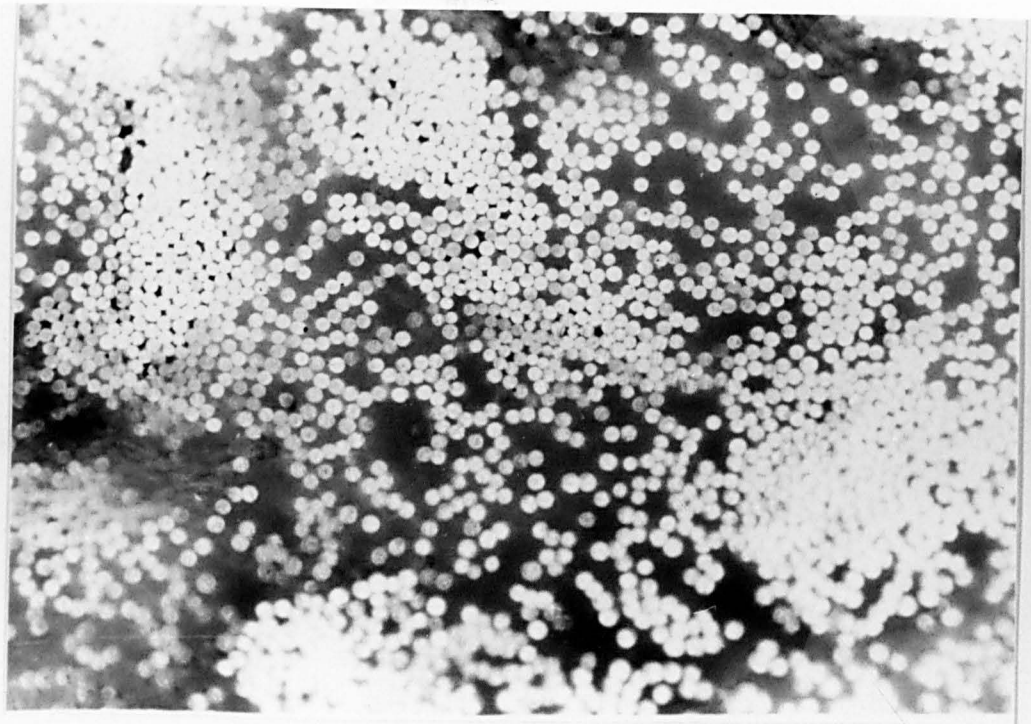

Figure 6.1.6b. Micrograph showing pultruded nylon 6,6/glass section, produced from precursor tows which had been flattened to improve the initial fibre distribution and allow the precursor to be heated more easily. No individual precursor tows can be distinguished in the product cross section. This resulted in an improvement in the ILSS.

finished section. In order to gauge the processability of the various precursors available, it was useful to describe what would constitute an "ideal" precursor for the thermoplastic pultrusion process.

The precursor must firstly be supplied in an easily handled form, ideally stored on a roll or drum with a maximum diameter of 12 inches and in lengths greater than 200m. The precursor should be as flexible and drapeable as possible and have low stiffness and springiness. The individual glass tows used in making the precursor should have as high a Tex (g/Km) as possible in order to reduce the total number required to produce the specified volume fraction of reinforcement in each tape. The precursor should have a uniform fibre distribution through its thickness with no fibre bunching and complete wet out of all fibres. The impregnated precursor should be thin, ideally < 0.25mm thick, with a large surface area and a small cross-sectional area. It should have a constant volume fraction of reinforcement and have a constant thickness and width along its length. For most effective heating using radiative sources it would have been desirable to have had the precursors pigmented black.

Three precursors were eventually made available to carry out a detailed examination of the effect of process conditions on the optimum properties of the pultruded sections. These are detailed in Table 6.1.1 and the details of the processing conditions can be found in Table 5.1.2. A small quantity of APC2 (carbon/PEEK) was also available for some limited processing experiments. All the following experiments were carried out on the pultrusion line described in Section 5.1.5, and shown in Figure 5.1.2 unless otherwise stated.

6.1.2 Roll forming of nylon 12/glass pultruded sections

The first oven temperature examined for the nylon 12/glass precursor was 180°C, just above the melting temperature of the nylon 12 matrix which was 176°C. A rectangular section was pultruded at line speeds between 0.3 m/min and 3.0 m/min. Above this line speed, the residence time in the oven became too short to allow sufficient melting through the thickness of each precursor tow. This resulted in melting only at the tow surfaces which prevented full consolidation of the tows. Sections produced at line speeds in excess of 3m/min were only tacked together and could be easily split apart. The pultruded sections were formed and consolidated by

pulling the heated precursor tows through three consecutive roll stands. Examples of the nylon 12/glass and APC2 pultruded sections are shown in Figure 6.1.7. The effect of four different roll forming pressures, 5, 90, 170 and 260N/mm were examined. The sections were air cooled between the roll stands. The interlaminar shear strength and the flexural strength of the pultruded sections were measured to characterise the effects of changing both the line speed and the applied forming pressure.

Figure 6.1.8 shows the effect of line speed on the interlaminar shear strength of pultrusions produced under four different roll-forming pressures, at an oven temperature of 180°C.

At the lowest applied roll pressure of 5N/mm, the interlaminar shear strength decreased sharply from a maximum of 34 MPa at the lowest pultrusion speed, to a value of between 20-25 MPa at 1m/min. At speeds above 1m/min, the interlaminar shear strength decreased gradually to a minimum value of 15 MPa at the highest line speed, 3m/min. Above this speed the product was not sufficiently consolidated to allow samples to be prepared for testing.

The effect of increasing the applied roll-forming pressure on the interlaminar shear strength can also be seen in Figure 6.1.8 and is surprising. For sections pultruded at each of the higher roll pressures, the interlaminar shear strength at line speeds less than 1m/min was considerably reduced. Above 1m/min, the interlaminar shear strengths corresponded more closely to the values obtained at the minimum forming pressure. The observed decrease in the interlaminar shear strength also appeared to be independent of the size of the forming pressure, and a similar reduction was measured for each of the three higher pressures examined.

The effect of roll pressure is shown more clearly in Figure 6.1.9, as a plot of interlaminar shear strength against roll pressure for four different line speeds. At the lowest line speed of 0.3m/min, the interlaminar shear strength for sections pultruded at 90N/mm showed a marked decrease compared to those sections produced under a pressure of 5 N/mm. At roll pressures above 90N/mm, the interlaminar shear strength remained at a fairly constant value. At the higher line speed of 0.7m/min, the decrease in the interlaminar shear strength for sections pultruded at a pressure of 5N/mm and those pultruded at 90N/mm was much less pronounced and again, the interlaminar shear strength remained fairly constant above 90N/mm. At the two highest line speeds, the interlaminar shear strength

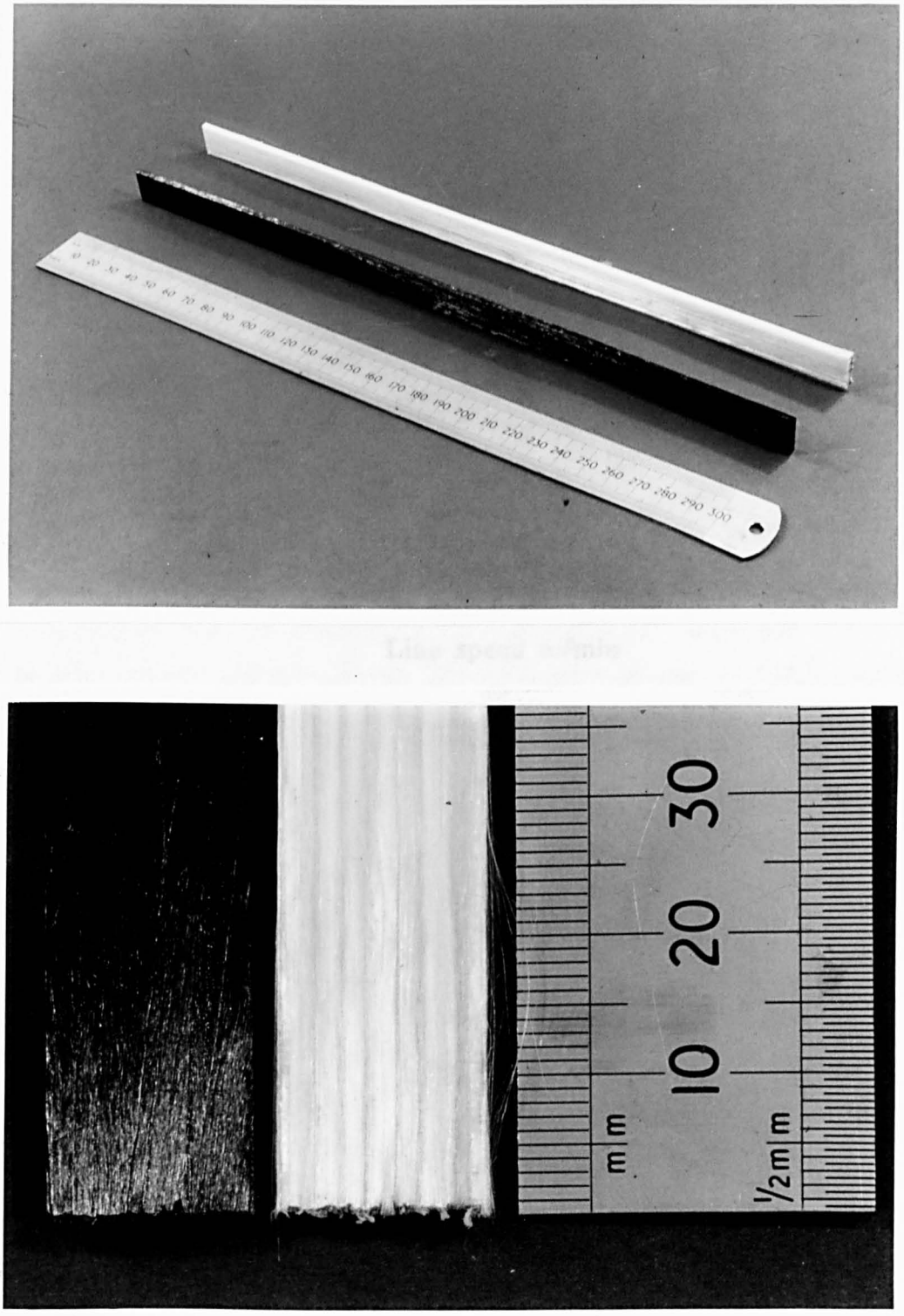

Figure 6.1.7. Examples of pultruded strips produced using nylon 12/glass and APC2 precursors.

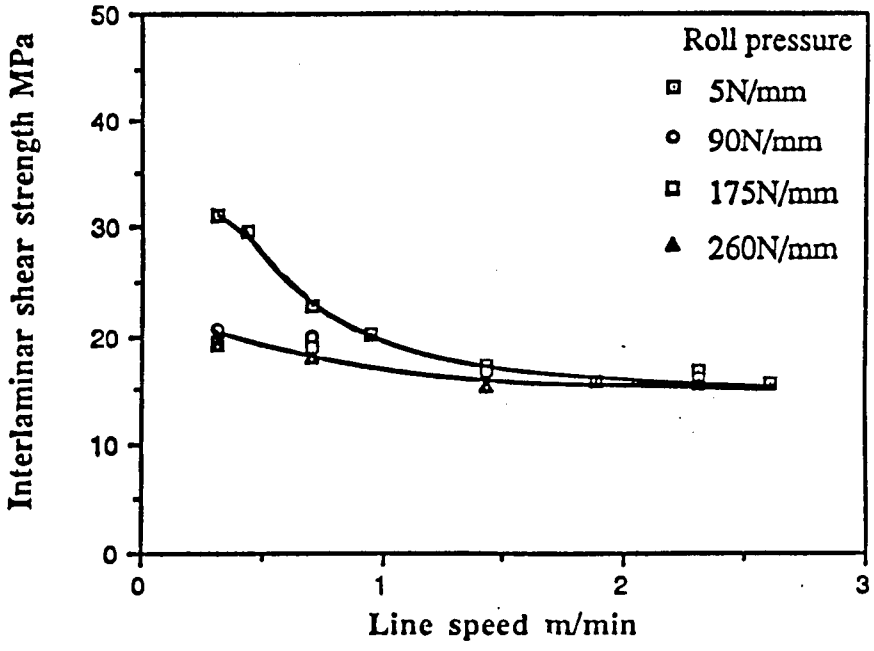

Figure 6.1.8. Effect of increasing line speed and roll pressure on the ILSS of nylon 12/glass sections pultruded at an oven temperature of 180°C.

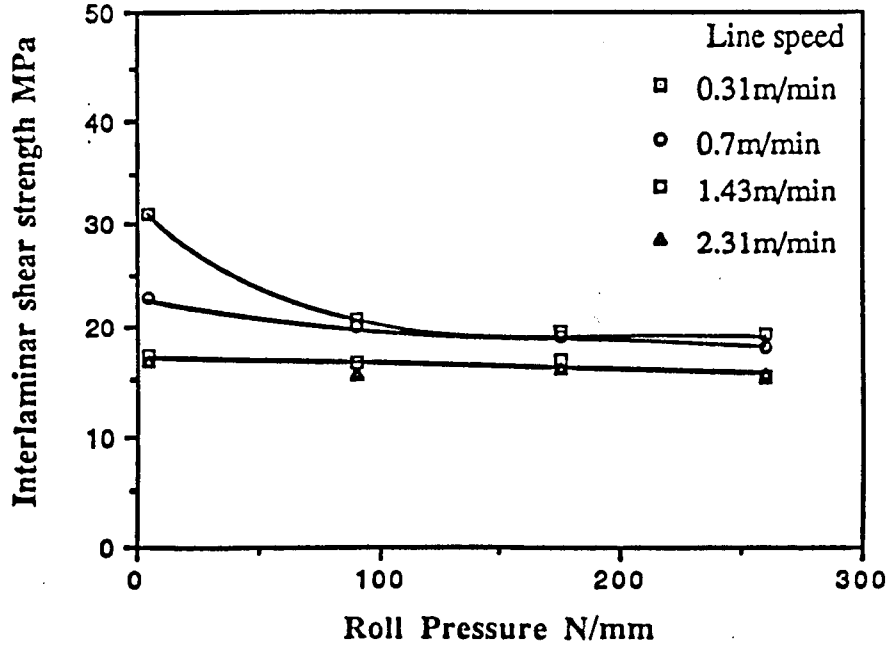

Figure 6.1.9. Effect of increasing roll pressure on the ILSS of nylon 12/glass sections pultruded at different line speeds and at an oven temperature of 180°C.

remained constant throughout the range of roll pressures examined.

The decrease in interlaminar shear strength with increasing line speed was attributed to two main factors. These were the reduced efficiency of the forming and consolidation stage and the reduced efficiency of the heating stage of the process as the line speed was increased. Unfortunately, the oven air temperature was maintained constant and was not controlled directly by measuring the temperature of the precursor leaving the oven. It was thus inevitable that the temperature of the precursor would be reduced at higher line speeds and shorter dwell times.

The residence time in both the oven and in a single set of forming rollers can be represented as a function of line speed as shown in Figure 6.1.10a,b,c. The contact length in the rolls was difficult to measure exactly and has been assumed to be in the order of, and at maximum, 10mm. This was estimated by both measuring the thickness reduction as the material passed through the rolls and by measuring, from experimentally measured temperature distributions, the distance over which quenching took place during forming. The total oven length was 2.8m. As can be seen from Figure 6.1.10b, the residence time can be divided into three regions. Region 1 in which the residence time falls rapidly with only small increases in the line speed, region 2 in which the decrease in the residence time becomes more gradual and region 3 where the residence time decreases very slowly with the increased line speed.

As the line speed increased, the residence time in the oven decreased from 9 minutes at the lowest pultrusion line speed, to 42 seconds at the maximum line speed for which visually acceptable product was produced. On the experimental pultrusion line it was not possible to control the oven temperature directly by measuring the temperature of the precursor material leaving the oven. It was thus inevitable that the efficiency of the pre-heating stage of the process would decrease somewhat as the line speed was increased. However, the decreased dwell time in the oven did not begin to adversely affect the temperature of the precursor tows until running at line speeds in excess of 1m/min. At 1m/min, dwell times still were greater than 3 minutes.

Because the contact length in the rolls is only of the order of 10mm, increases in line speed had a much more pronounced effect on the time period during which the section underwent forming and consolidation. As can be seen in Figure 6.1.10a, even at the slowest possible line speed the residence time in each of the roll stands

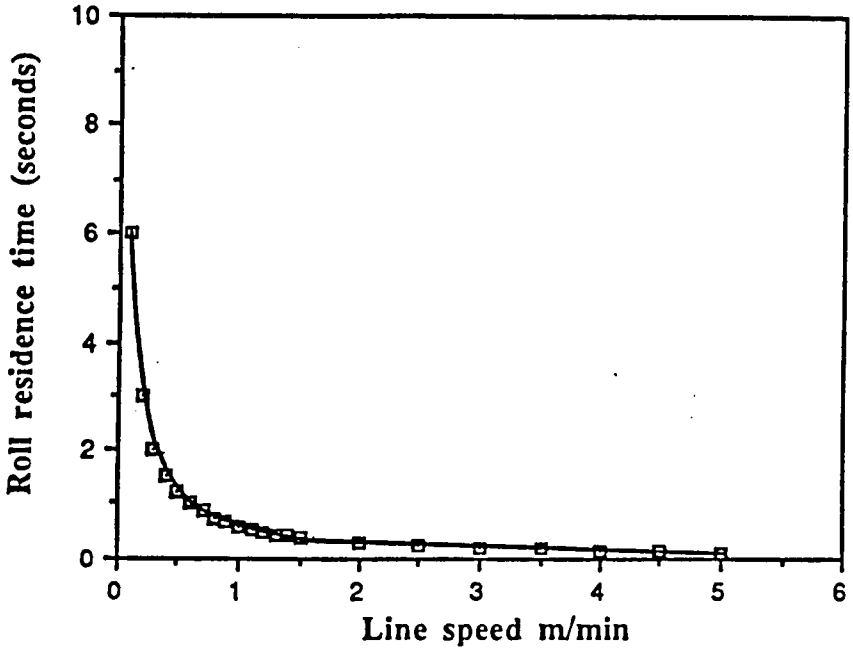

Figure 6.1.10a. Decrease in roll residence time with increased line speed.

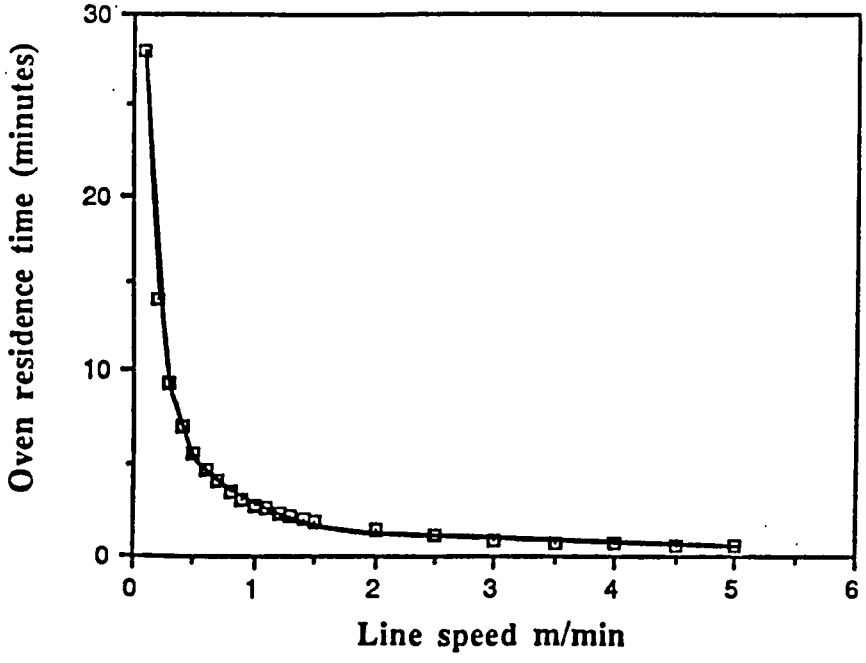

Figure 6.1.10b. Decrease in oven residence time with increased line speed.

was only of the order of 6 seconds.

The decrease in interlaminar shear strength that resulted from increasing the line speed can be correlated directly to the decreased residence time in each of the roll stands. At the lowest line speed examined, the combined forming and consolidation time was only 2 seconds in each roll stand, although this proved to be sufficiently long to produce a pultruded section with acceptable properties. At higher speeds the residence time decreased as shown in Figure 6.1.10a. On comparison to Figure 6.1.8, the decrease in the interlaminar shear strength can be seen to follow a similar trend, in which there is a rapid decrease, followed by a levelling out and then a more gradual decrease.

At line speeds in excess of 1.5m/min the dwell time in the rolls was very short and this, coupled with increasingly poorer heating through the thickness of the precursor tows, combined to produce a pultruded section with interlaminar shear strength values typically only 50% of the maximum achieved. The gradual decrease in properties at higher line speeds was mirrored by the gradual decrease in the roll and oven dwell times in region 3 of Figure 6.1.10.

The effect of increasing the roll pressure was to reduce the measured interlaminar shear strength to values below those achieved with the minimum roll pressure, for the same oven temperature and line speed. This was most apparent at line speeds less than 1m/min.

The most probable reason for the decreased interlaminar shear strength with increased roll pressure at low speeds involved the cooling effect of the contact with the rolls. Increasing the roll pressure will increase both the efficiency of heat transfer from the composite section to the cold, stainless steel rolls and the area available for heat transfer through an increased area of contact. This effect will be most apparent when the contact time in the rolls is relatively long, ie. at speeds less than 1m/min. At higher line speeds, the effect of increasing the roll pressure was less pronounced although a decrease in the interlaminar shear strength was still observed, as shown in Figure 6.1.9. This was attributed to the fact that residence times were sufficiently short to prevent significantly greater heat transfer to that which occurred at the minimum pressure. Although the effect of increasing the roll pressure was unexpected, a similar result has been reported in the literature, Madenjian (1985)[40], whereby the tensile modulus of thermoplastic pultruded sections, produced using a heated die, were observed to decrease with increasing

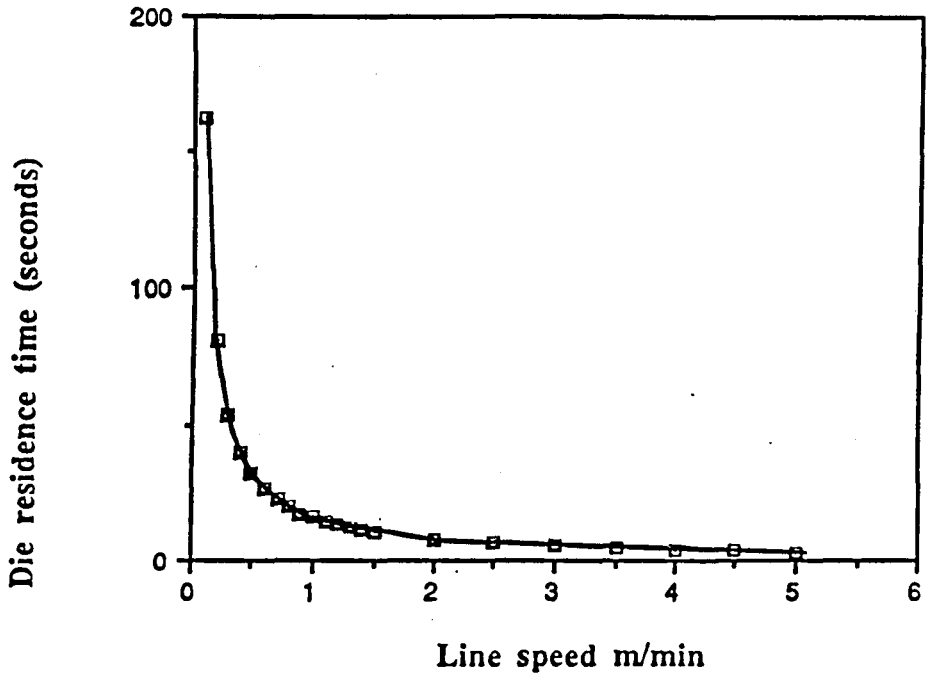

Figure 6.1.10c. Decrease in die residence time with increased line speed.

pultrusion die pressure. This was attributed to fibre misalignment and fibre damage at increased die pressures.

An additional effect of increasing the roll pressure was also observed. Increasing the roll pressure caused the pultruded section exiting the rolls to bow elastically away from the rolling axis in the vertical direction, as shown in Figure 6.1.11. On subsequently cutting up samples pultruded under higher pressures, the outside plies adopted a curved shape suggesting that elastic deformation caused by the high roll forces was frozen into the consolidated section during the rapid surface cooling. The severity of the bowing was dependent on the roll pressure and increased with increasing pressure.

The effect of line speed and roll pressure on the flexural strength of the pultruded sections was also measured. Figure 6.1.12 shows the variation in flexural strength with line speed for sections produced at 180°C using the same four pressures discussed previously. The flexural strengths were measured using a standard three point bend test and although this test was not as sensitive as the short beam shear test to process induced defects, it provided a useful comparative property measurement.

As was found for the interlaminar shear strength, the flexural strength of the pultruded sections decreased as the line speed increased. However, this decrease was less pronounced which reflected the greater sensitivity of the short beam shear test in characterising the effects of changing process conditions. As was found for the interlaminar shear strengths, increasing the roll pressure had a deleterious effect on the flexural strengths achieved. The flexural strength is plotted against the applied roll pressure for three line speeds in Figure 6.1.13. Here, the flexural strength decrease at the higher line speeds was approximately linear. The flexural strength of samples pultruded at a speed of 0.31 m/min and at high pressures can be seen to fall below the strengths measured for the same pressures at the higher line speeds although the reason for this was unclear.

All the results discussed above have been obtained from sections produced at an oven temperature of 180°C.

To determine the effects of increasing the oven temperature on the thermoplastic pultrusion process, a further set of experiments was carried out at an oven

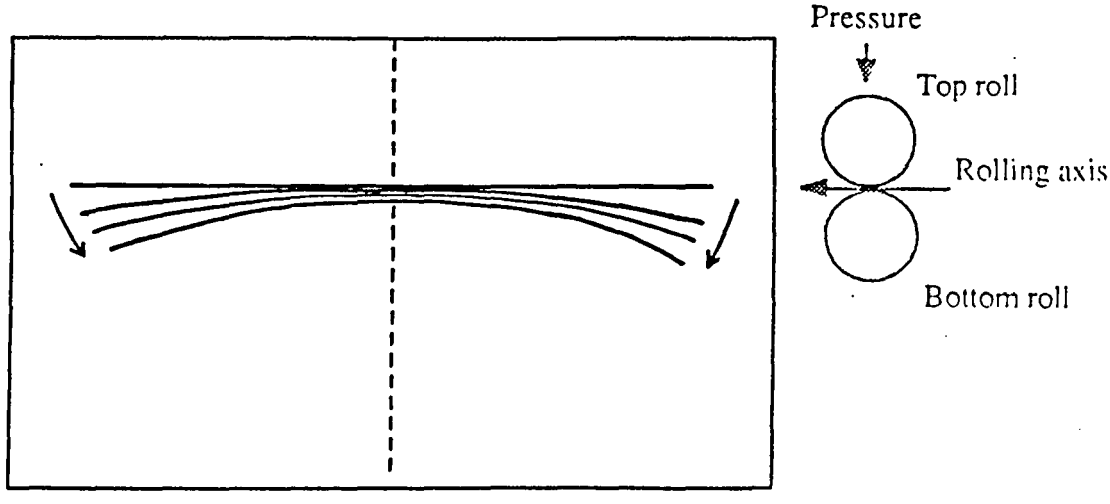

Figure 6.1.11. Schematic illustration of the effect of increased roll pressure on the 'straightness' of pultruded sections.

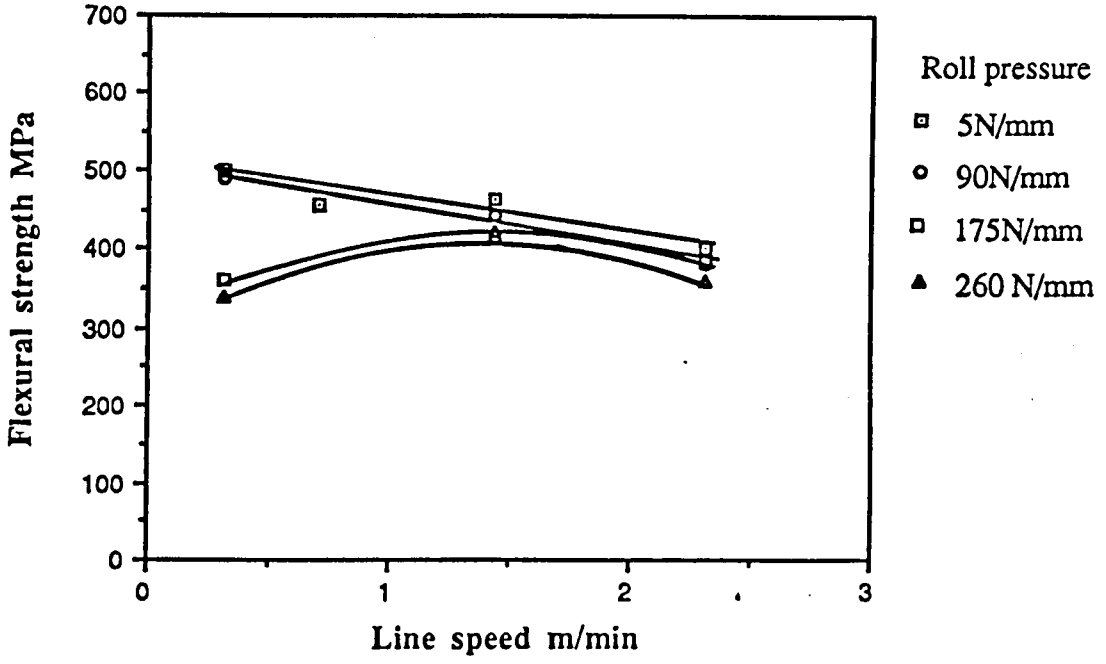

Figure 6.1.12. Effect of increasing line speed and roll pressure on the flexural strength of nylon 12/glass sections pultruded at an oven temperature of 180°C.

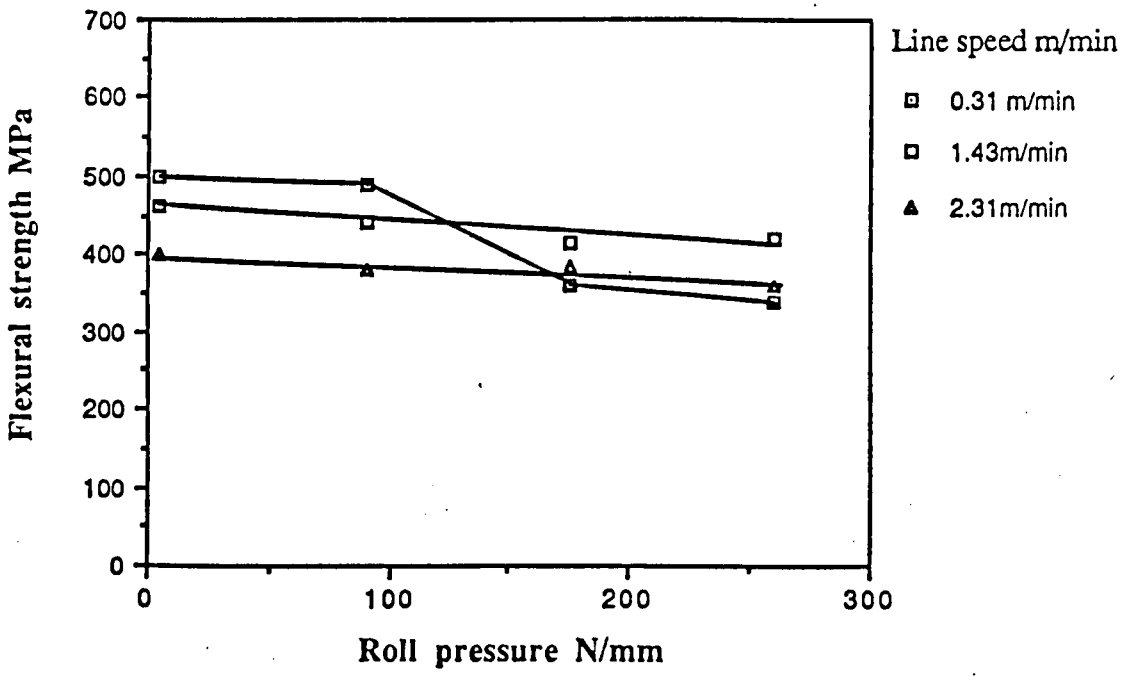

Figure 6.1.13. Effect of increasing roll pressure on the flexural strength of nylon 12/glass sections pultruded at different line speeds and at an oven temperature of 180°C.

temperature of 190°C. The same roll pressures as used at 180°C were examined. Measurements of the exit temperature of the tow bundle indicated that the increased oven temperature increased the efficiency of the oven and thus increased the temperature of the precursor materials exiting the oven.

The interlaminar shear strength is plotted against line speed for an oven temperature of 190°C in Figure 6.1.14.

The effects of increasing line speed were similar to those observed at 180°C, and the maximum pultrusion speed for visually acceptable product was again 3m/min. However, there was an overall increase in the measured interlaminar shear strength throughout the speed range. There was also a small speed range, 0.3 to 0.5m/min, in which the interlaminar shear strength remained constant. In the small constant region, the effect of decreased contact time was overcome because the lower matrix viscosity of the hotter material allowed it to be more readily consolidated. The interlaminar shear strength then decreased in a similar way to that described for the lower oven temperature. Again, this decrease in the interlaminar shear strength was caused by the reduction of the residence time in the rollers as the line speed increased.

At line speeds above 1m/min, a reduction in heat transfer to the precursor due to the reduced dwell time in the oven also added to the decrease in the interlaminar shear strength. The minimum interlaminar shear strength was found to be the same as found at the lower oven temperature. Although the oven temperature was not substantially increased, the higher temperature of the precursor leaving the oven at low speeds had a positive effect on the efficiency of the forming stage of the process. Because the material bundle entering the rolls was at a higher temperature, a greater degree of consolidation was achieved in the rolls and this increased the measured interlaminar shear strength.

The effect of increased roll pressure on the interlaminar shear strength is shown in Figure 6.1.15.

As before, the interlaminar shear strength decreased at increased roll pressures. Comparing Figures 6.1.9 with 6.1.15, shows that the variation in the interlaminar shear strength for all speeds above 0.31m/min at 190°C was almost the same as was measured at 180°C. This reinforces the conclusion that increasing the roll pressure resulted in increased heat transfer between the pultruded section and the roll

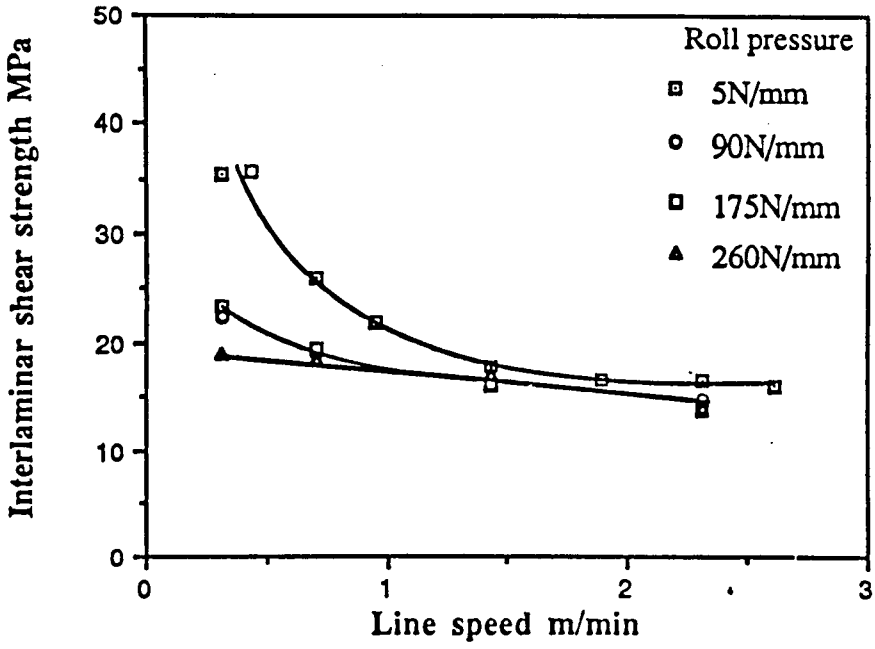

Figure 6.1.14. Effect of increasing line speed and roll pressure on the ILSS of nylon 12/glass sections pultruded at an oven temperature of 190°C.

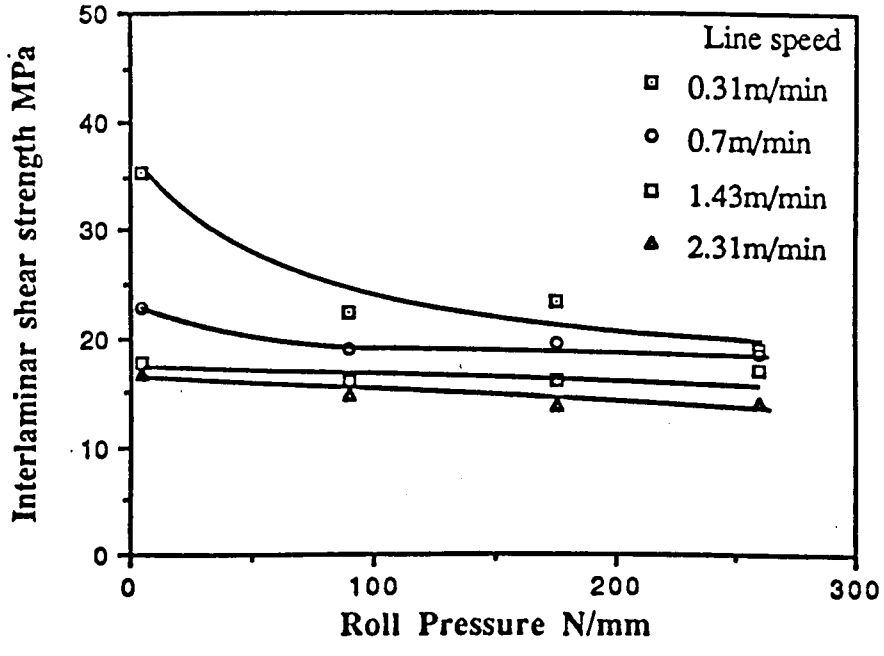

Figure 6.1.15. Effect of increasing roll pressure on the ILSS of nylon 12/glass sections pultruded at different line speeds and at an oven temperature of 190°C.

surface. This heat transfer was the dominant factor in controlling the interlaminar shear stress at high roll pressures. Therefore, this was likely to outweigh any advantages of applying a high forming pressure using unheated rolls.

Figure 6.1.16 shows the effect of line speed on the flexural strength of the pultruded sections. As before, the flexural strength was reduced at higher line speeds although the results were much more inconclusive than the interlaminar shear results. The flexural strengths achieved using the minimum roll pressure and pultruding at the higher oven temperature were also higher than were obtained at 180°C. This was consistent with the measured results for interlaminar shear strength.

The effect of roll pressure on the flexural strength is shown in Figure 6.1.17. These results were also inconclusive and seemed to indicate that increased forming pressures at the higher line speeds produced a product with a higher flexural strength. This did not agree with the interlaminar shear strength measurements on similar sections under the same processing conditions and was not thought to be significant.

Overall, increasing the oven temperature was found to produce a better product, with both an improved interlaminar shear strength and flexural strength compared to sections produced at a lower temperature, 180°C, under the same speed and minimum pressure conditions. The effect of increasing both the line speed and roll pressure were very similar to the effects observed at 180°C. This seemed to indicate that forming and consolidation at the minimum roll pressure was influenced by the temperature of the precursor materials, and that the efficiency of forming and consolidation at increased roll pressures was controlled by increased heat transfer between the section and the rolls. Micrographs of two sections produced at an oven temperature of 190°C are shown in Figure 6.1.18a and b. In Figure 6.1.18a it is possible to see linear, resin rich areas which distinguish individual precursor tapes. This section was pultruded at a line speed of 2m/min. Figure 6.1.18a was pultruded at only 0.8m/min and the fibre distribution can be seen to be much better. This was a result of the material having a higher temperature entering the roll gap and also experiencing a relatively long forming time in the rolls at the lower speed.

In order to investigate the effect of heating the precursors to well above the melting temperature of the nylon 12 matrix, a set of experiments was carried out at an oven temperature of 240°C. Unfortunately, it was not possible to examine the full range

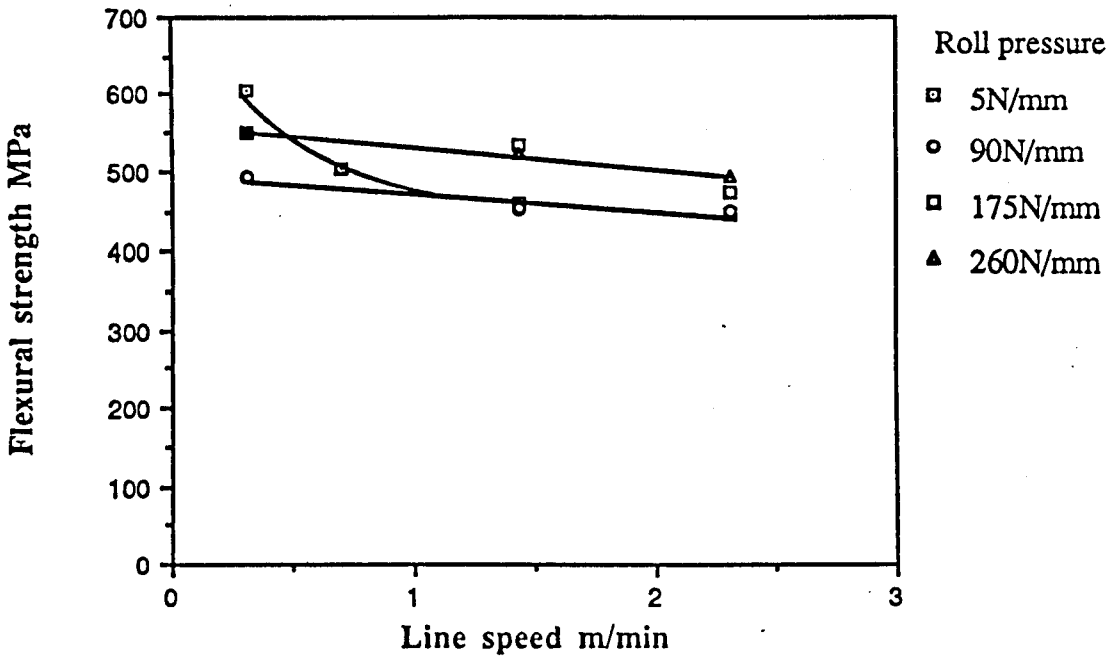

Figure 6.1.16. Effect of increasing line speed and roll pressure on the flexural strength of nylon 12/glass sections pultruded at an oven temperature of 190°C.

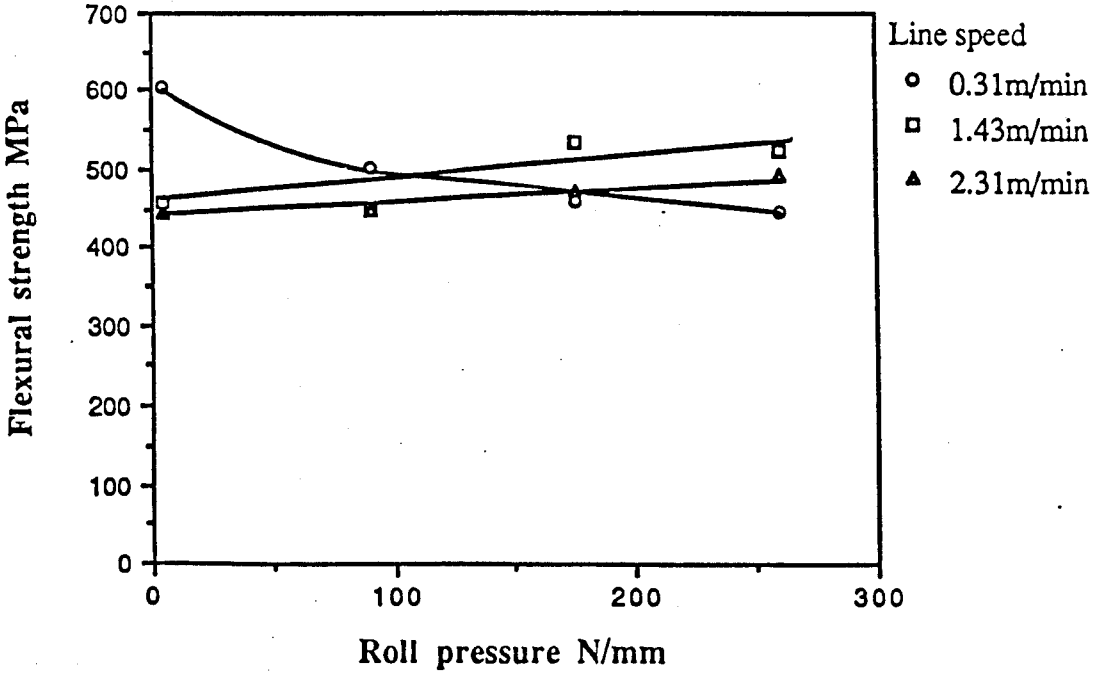

Figure 6.1.17. Effect of increasing roll pressure on the flexural strength of nylon 12/glass sections pultruded at different line speeds and at an oven temperature of 190°C.

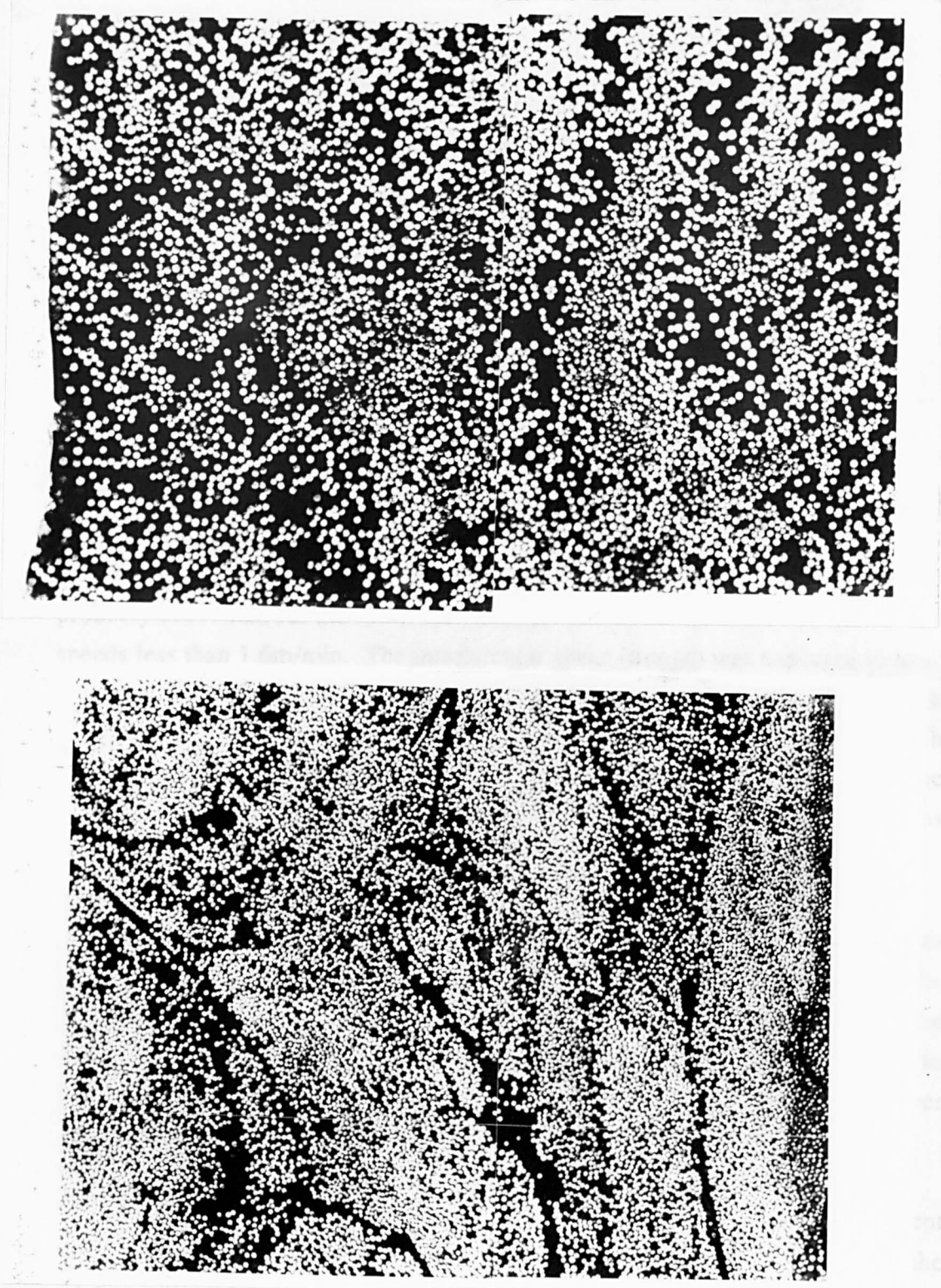

Figure 6.1.18. Micrographs showing fibre distributions in sections pultruded at 0.8 and 2m/min and at an oven temperature of 190°C. It can be seen at the higher speed that individual precursor tows can be distinguished as a result of incomplete heating through the tape thickness and reduced consolidation.

of roll pressures because of a shortage of the nylon 12/glass precursor.

Figure 6.1.19 shows the variation of interlaminar shear strength with line speed for sections produced at 5N/mm, the minimum roll pressure, and for all three oven temperatures studied; 180, 190 and 240°C.

It can be seen that the speed range at which acceptable product could be produced was increased to 4.5m/min at the highest oven temperature of 240°C. It was not possible to run at line speeds less than 0.8m/min because of excessive degradation. A constant interlaminar shear stress was achieved up to line speeds of about 1.6m/min. However, running at low line speeds resulted in noticeable discolouration, due presumably to resin degradation, not only on the tow surfaces but through the tow thickness prior to forming and consolidation. This degradation probably accounted for the lower than expected interlaminar shear strength at line speeds less than 1.6m/min. The interlaminar shear strength was expected to have been higher considering the trends observed at the lower temperatures. Above 1.6m/min, the degradation problem diminished and the interlaminar shear strength decreased in a similar way to that seen for the lower oven temperatures. The interlaminar shear strength achieved at the maximum line speed of 4.5m/min was about 20MPa.

The flexural strength variation with line speed is shown in Figure 6.1.20 for all three oven temperatures examined. Increasing the oven temperature increased the flexural strengths achieved throughout the temperature range. As was seen for the interlaminar shear strength, the flexural strength remained fairly constant up to 1.6m/min and then decreased in much the same way as measured for the lower processing temperatures.

Figure 6.1.21 shows the interlaminar shear strength and the measured void content plotted against line speed for a number of samples pultruded at 180°C, under the minimum pressure of 5N/mm. It was not practical to determine the void content in the actual samples tested and a void content was measured on an untested sample, taken from a position adjacent to the test samples. It is unlikely that there will be a uniform distribution of voids in any particular length of pultrusion and so the measurements were expected to exhibit some degree of scatter. Nevertheless, an increase in the void content at low line speeds correlated with the measured decrease in interlaminar shear strength up to a line speed of 1.5m/min. At speeds in excess

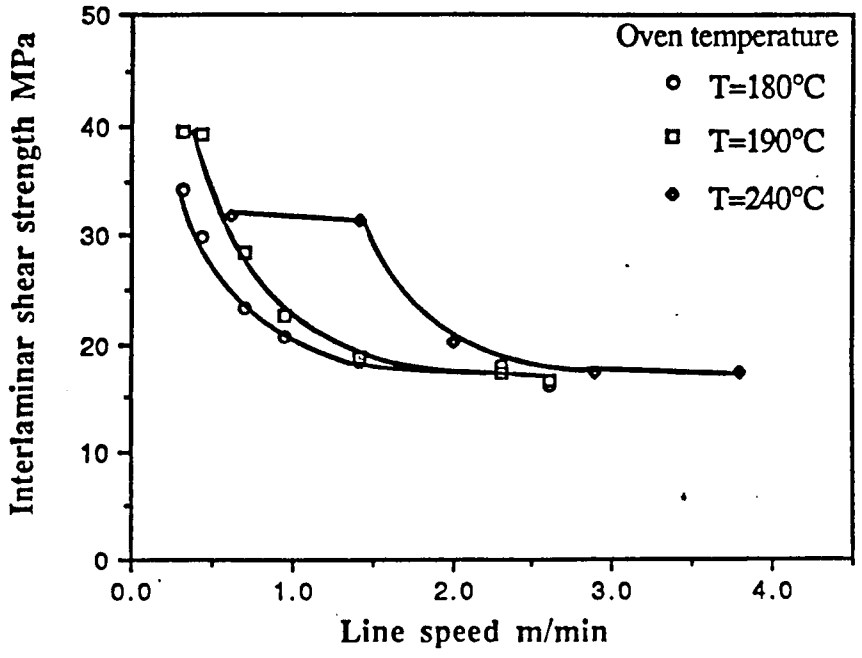

Figure 6.1.19. Effect of increased oven temperature on the ILSS of nylon 12/glass pultruded sections. All sections were produced using a roll pressure of 5N/mm.

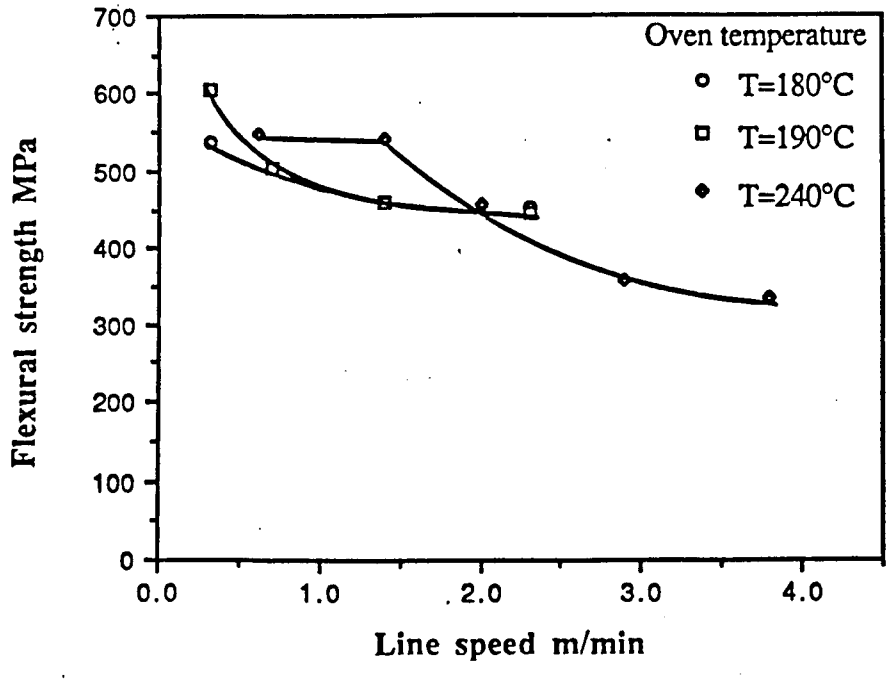

Figure 6.1.20. Effect of increased oven temperature on the flexural strength of nylon 12/glass pultruded sections. All sections were produced using a roll pressure of 5N/mm.

of this, both the interlaminar shear strength and the void content remained at a constant value. The actual void contents in the samples tested ranged from 6.5 to 10.9% which are high when compared to typical void contents of between 1 and 5% achieved with other composite manufacturing processes. In Figure 6.1.21, an approximate 11% decrease in interlaminar shear strength occurred with each 1% rise in the void content.

The effect of increasing the oven temperature to 190°C is illustrated in Figure 6.1.22. As was observed for the lower oven temperature, the decrease in interlaminar shear strength was mirrored by the increase in the void content. At the lowest line speed the void content was considerably less than for the equivalent speed at 180°C. At higher line speeds, the maximum void content was also lower than at 180°C and this was reflected in the higher interlaminar shear strengths measured for equivalent speeds. A 7% decrease in interlaminar shear strength has been measured to occur for each 1% increase in void content during processing at this oven temperature.

The interlaminar shear strength and void content are also plotted against line speed for an oven temperature of 240°C and forming pressure of 5N/mm in Figure 6.1.23. Again, the void content increased with increasing line speed and this was again accompanied by a decrease in the interlaminar shear strength. The void content was lower than that measured for either of the lower temperatures throughout the range of line speeds, as shown in Figure 6.1.24. As can also be seen, the increase in void content with increasing line speed appeared to be much more gradual than measured previously.

Figure 6.1.25 shows the effect of increasing the forming pressure on the measured void content. This can be compared to Figure 6.1.22, which shows the void content measured for the same oven temperature at the lowest roll pressure. The purpose of increasing the forming pressure was to provide better consolidation. However, as can be inferred from the values of both the interlaminar shear strength and the void content of sections produced at the maximum pressure of 260N/mm, the consolidation efficiency appears to decrease.

Figure 6.1.26 shows the relationship between interlaminar shear strength and void content for all the samples tested, irrespective of the line speed, roll pressure or oven temperature processing conditions. Although there is a degree of scatter, the interlaminar shear strength decreased linearly with void content. Approximately,

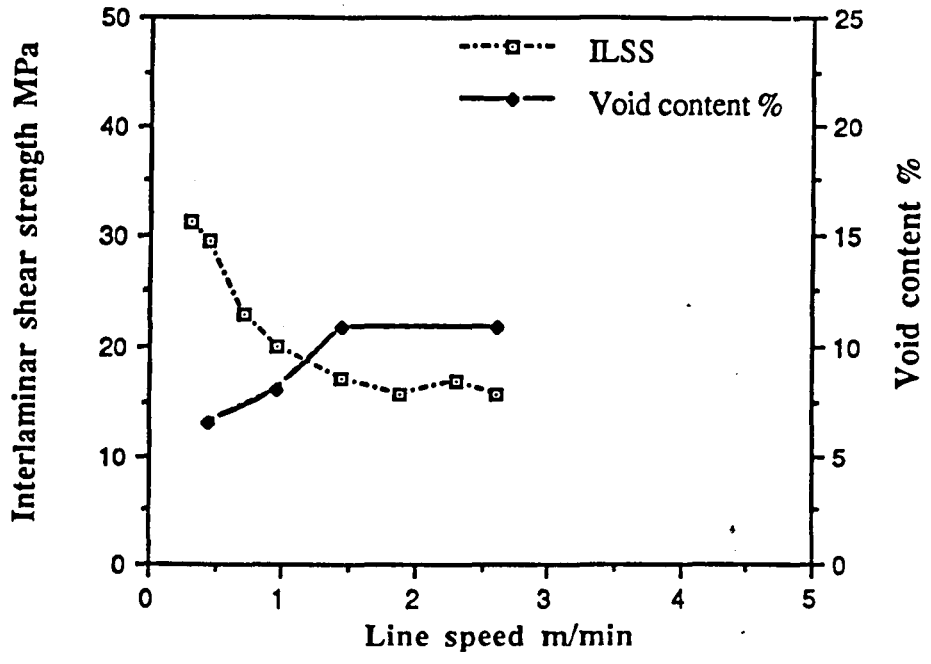

Figure 6.1.21. Variation of ILSS and void content with line speed for a nylon 12/glass pultruded section. The processing conditions were: line speed 1m/min; oven temperature 180°C; roll pressure 5N/mm.

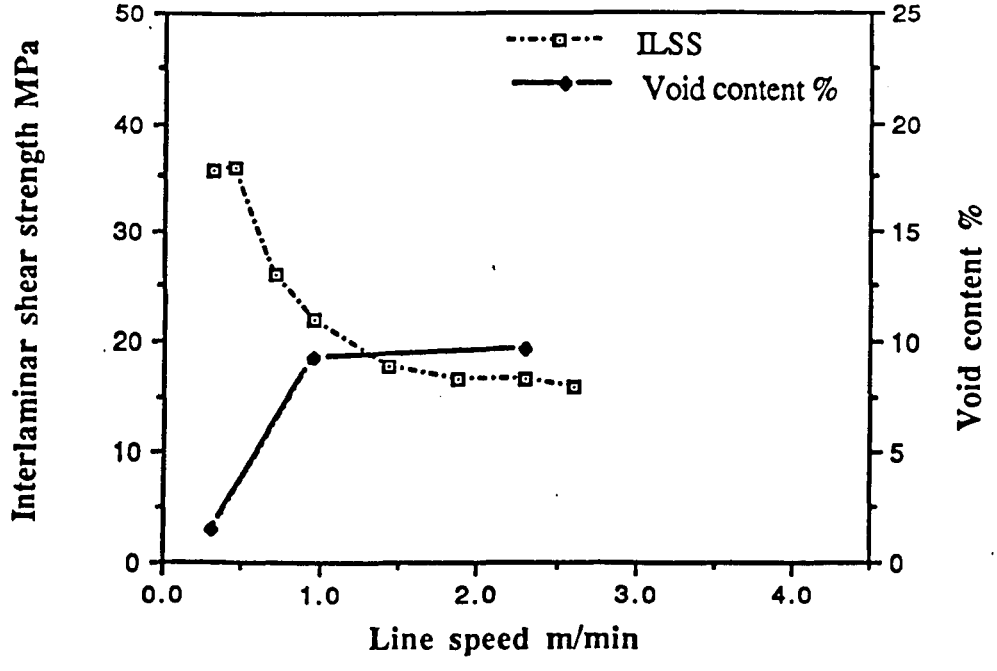

Figure 6.1.22. Variation of ILSS and void content with line speed for a nylon 12/glass pultruded section. The processing conditions were: line speed 1m/min; oven temperature 190°C; roll pressure 5N/mm.

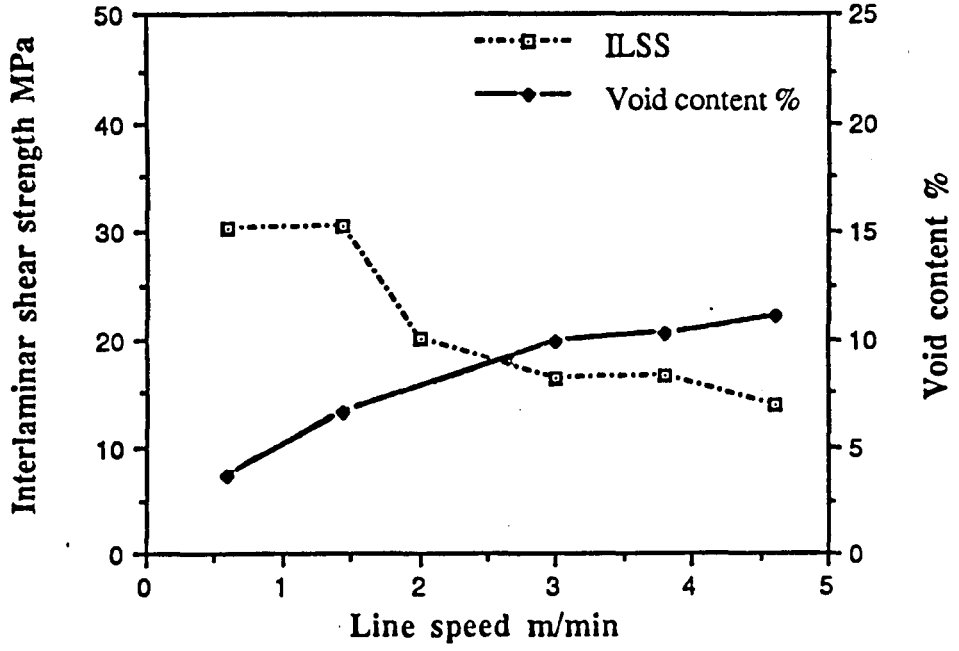

Figure 6.1.23. Variation of ILSS and void content with line speed for a nylon 12/glass pultruded section. The processing conditions were: line speed 1m/min; oven temperature 240°C; roll pressure 5N/mm.

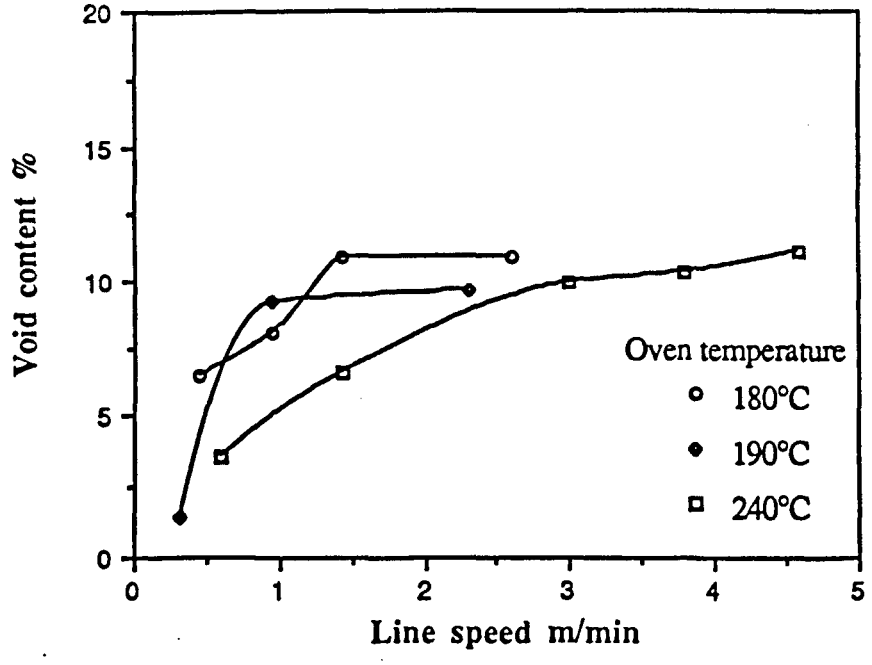

Figure 6.1.24. Effect of line speed and oven temperature on the void content of nylon 12/glass pultruded sections, produced using a roll pressure of 5N/mm.

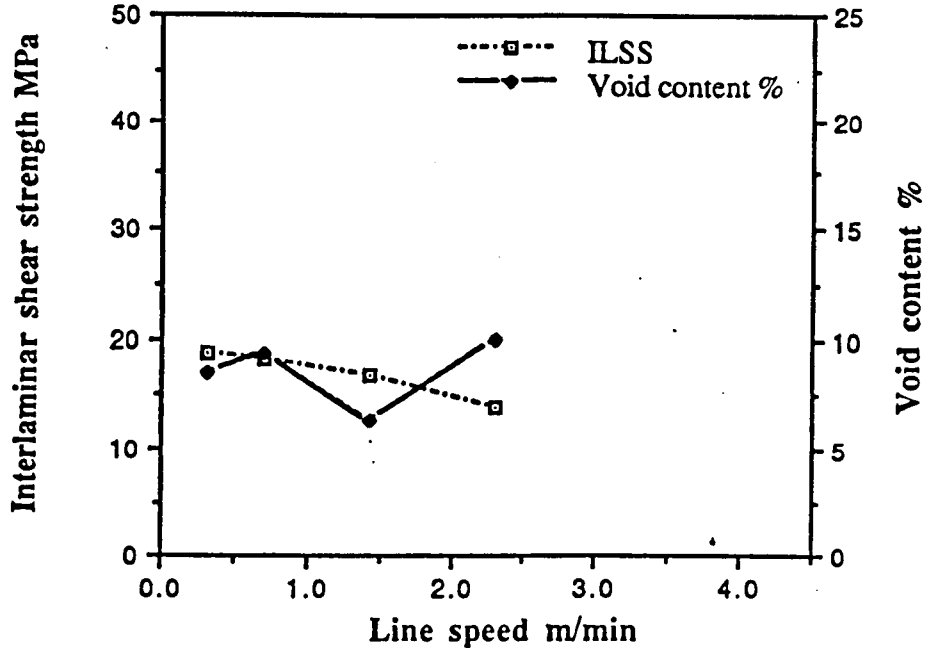

Figure 6.1.25. Effect of increased forming pressure, 260N/mm, on the variation of ILSS and void content with line speed for a nylon 12/glass section pultruded at an oven temperature of 190°C.

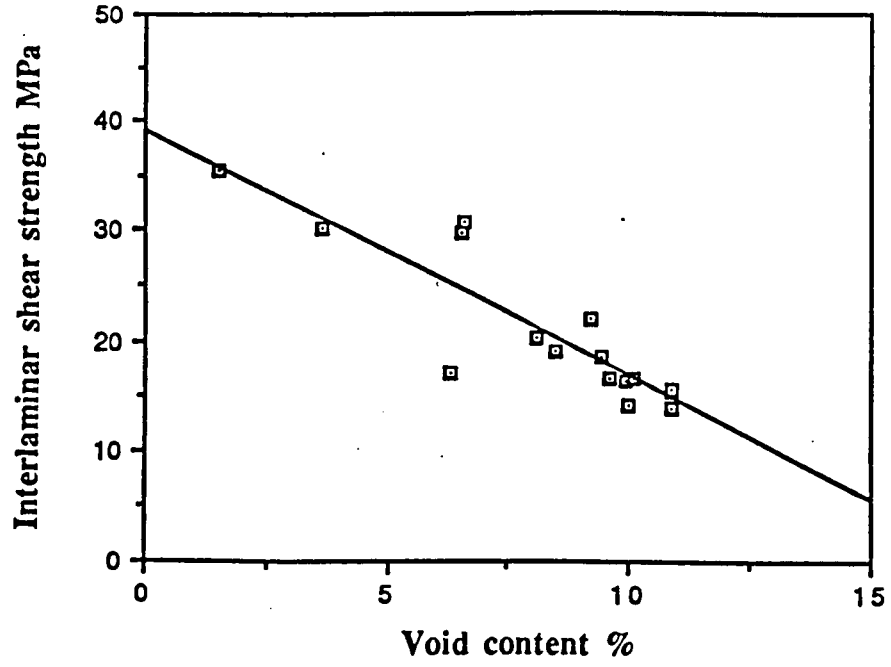

Figure 6.1.26. Relationship between ILSS and void content of pultruded sections. The data has been taken from a number of sections, produced under a range different processing conditions.

for each 1% increase in the void content, a 6% decrease in the interlaminar shear strength occurred.

In summary, it was found that the interlaminar shear strength decreased with increasing line speed as a result of a combination of two factors. At line speeds less than 1m/min, the decrease has been attributed to the rapid decrease in the forming and consolidation time in the rollers. The increasingly inefficient forming and consolidation was highlighted by the significant increase in the void content of samples produced at line speeds below 1 to 1.5m/min, especially at the oven temperatures of 180 and 190°C.

For the two lowest oven temperatures and at line speeds between 1 and 2m/min, the reduced preheating time in the oven resulted in the precursor bundle becoming increasingly colder on entering the rolls, resulting in a higher matrix viscosity and surface skinning. Considering both this and the very short forming and consolidation times, the forming and consolidation stage was unlikely to fully eliminate trapped air and reduce the void content in the pultruded section. Therefore, the efficiency of the forming and consolidation gradually decreased and this contributed to the reduction in the interlaminar shear strength.

At higher line speeds, > 2m/min, both the void content and the interlaminar shear strength remained at a relatively constant level. This indicated that the forming and consolidation stage, in addition to performing at its lowest efficiency due to short roll dwell times, also appeared to be influenced by the temperature of the precursor bundle entering the rolls. Below some cut off temperature, the dominant influence on the interlaminar shear strength became temperature and the viscosity limitations to consolidation, regardless of the applied pressure. Eventually, the temperature became too low to allow any consolidation to occur and either the line speed had to be reduced or the oven temperature increased to allow further pultrusion.

It was not possible to match the oven temperature to the line speed during experimental runs but this should contribute to improving the overall properties at higher line speeds.

The flexural strength of the pultruded sections was also found to decrease as the line speed increased, although the interaction effects of speed, forming pressure and temperature were less obvious than those highlighted by short beam shear testing of equivalent samples. The correlation of flexural strength with void content was also

less conclusive and this may have been due to variations in the distribution of voids in the samples tested.

It was found that increasing the oven temperature caused an increase in both the interlaminar shear strength and flexural strength of the pultruded sections, especially at line speeds less than 1m/min. This was a direct result of improved consolidation of the pultruded section when the precursor matrix material was at a higher temperature and thus at a lower viscosity. This increase was also apparent from the decrease in the void content with oven temperature for equivalent line speeds, as seen in Figure 6.1.24. Increasing the oven temperature also increased the range of line speeds at which acceptable product could be made. This was due to improved heat transfer in the oven, especially in the infra-red section. However, at high oven temperatures problems occurred during start-up due to matrix degradation and in extreme cases the precursors were found to catch fire if the line speed was too low.

Increasing the roll pressure was expected to improve the consolidation and produce an improvement in the product properties. However, the opposite was found to occur and increased roll pressures had a deleterious effect on both the interlaminar shear and flexural strengths. This was the result of increased heat transfer between the composite section and the unheated rolls which caused the material to cool more rapidly to below a sufficiently high forming temperature. Even though acceptable product was produced at the lowest roll pressure, the quenching effect of the cold rolls probably still had an undetected detrimental effect. It is interesting to note that increasing the oven temperature from 180-190°C had no effect on sections produced at the three highest roll pressures, whereas it increased the interlaminar and flexural strengths at the lowest roll pressure. This further indicates that increased heat transfer dominated the forming and consolidation efficiency at high roll pressures. The void content was also unaffected by increasing the roll pressure as would be expected if further consolidation was still taking place.

As the roll pressure was increased the pultruded sections became less straight, although this only became apparent after cutting the sections into separate lengths for testing, according to process conditions. Depending on the applied roll pressure, the sections adopted various degrees of bowing vertical to the rolling axis, as illustrated schematically in Figure 6.1.9. The rolls were of equal diameter, therefore the contact area was the same on both surfaces and both were subjected to similar cooling rates. This bowing thus indicated that both elastic deformation

caused by the high roll forces along with stresses in the precursor tows, must have been frozen into the consolidated section. The increased bow observed in section lengths as the applied pressure was increased indicated that the severity of the quench experienced by the top and bottom surfaces increased with higher roll pressures, due to better thermal contact and increased physical contact.

6.1.3 Compression moulding of nylon 12/glass sections

In order to obtain the maximum interlaminar shear and flexural strengths for sections produced using the nylon 12/glass precursor, a rectangular strip section was compression moulded in a heated matched mould. The process cycle is shown in Figure 6.1.27 and the optimum properties for the flat strip produced are given in Table 6.1.2.

6.1.4 Temperature distributions and heat transfer modelling of pultrusion roll forming

In any thermoplastic processing operation it is important that the temperature distribution during the various process stages, heating, forming and cooling are known. This becomes even more important when considering a continuous process such as thermoplastic pultrusion. Although it would have been possible to experimentally determine the temperature distributions for a wide range of process conditions, it was useful to model the temperature distributions for different conditions as an aid in optimising and understanding the process.

6.1.4.1 Measured temperature distributions

Heating

The heating stage of the process consisted of a combined infra-red and hot air oven. The individual precursor tapes were heated flat and side by side in the infra-red section and then collimated into a rectangular bundle from about 1m inside the oven. The total heated length was 2.8m. A typical example of a temperature profile measured during the heating can be seen in Figure 6.1.28. This particular profile

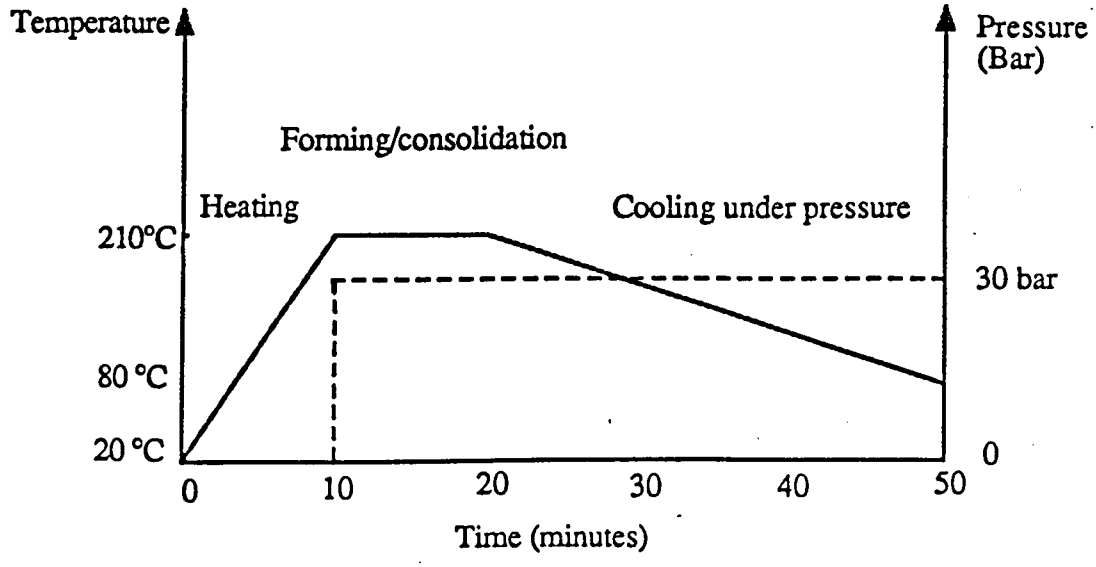

Figure 6.1.27a. Process cycle for compression moulding a reference 'pultruded' flat strip section.

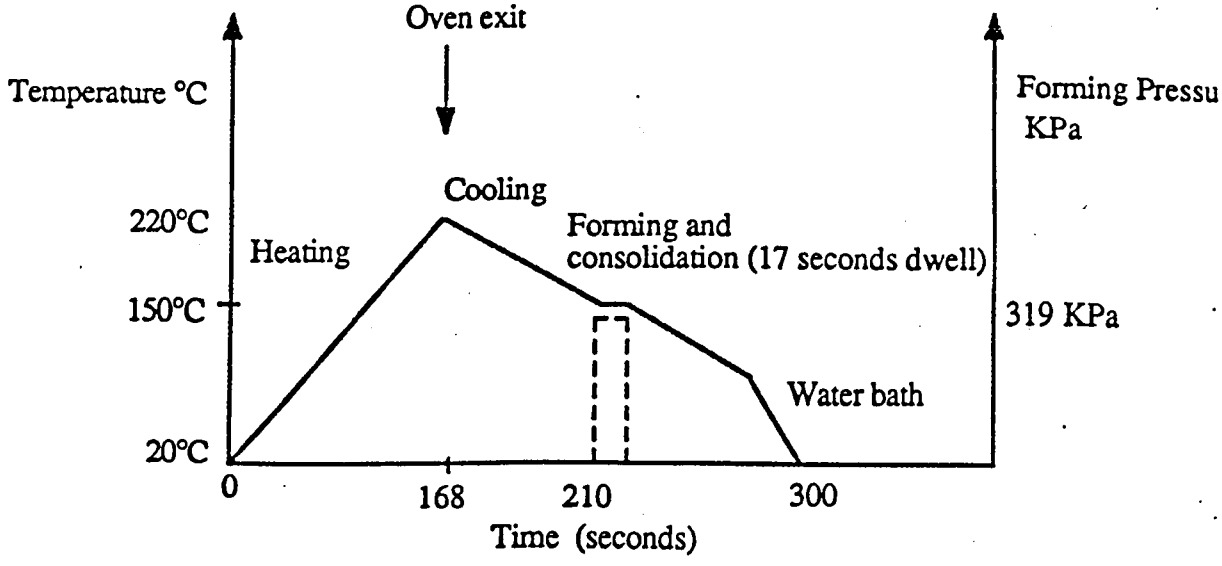

Figure 6.1.27b. Typical process cycle for thermoplastic pultrusion using a forming die system. In this instance at a line speed of 1m/min and under a forming pressure of 319KPa.

Table 6.1.2. Properties of a press moulded nylon 12/glass strip.

Precursor	Volume fraction glass	Interlaminar Shear Strength MPa	Flexural strength MPa	Void content %
Nylon 12/glass	0.45	61.2	720	3.6

was for a nylon 12/glass precursor tape, pulled through the oven at 1m/min at an air temperature of 180°C.

The infra-red heating section caused a rapid temperature increase in the first two thirds of the infra-red heated length, followed by a temperature soak in which the entire material bundle gradually reached the oven set temperature. For this line speed/oven temperature combination, it can be seen that the precursor bundle leaving the oven was above the melting temperature of the nylon matrix as required. It was only possible to measure temperatures using a thermocouple which was positioned on the tape surface, and because the absorbtion characteristics of the thermocouple tip were likely to be different to the white precursor surface, this distribution probably represents the air temperature, measured adjacent to the precursor tape surface.

Cooling

The temperature distribution in an unconsolidated composite section which has been allowed to cool in air, without the influence of any forming or consolidation stages, typically takes a form as shown in Figure 6.1.29. This particular distribution shows the results of measurements taken during two separate experimental runs in which individual thermocouples were placed in a polypropylene/glass tow bundle, heated to 190°C before being pulled through air at a line speed of 2.1m/min. When cooled in air, the tow bundle can be seen to remain above 140°C for a distance of about 1.5 metres from the oven exit.

Forming, consolidation and cooling

A typical cooling temperature distribution through the thickness of a section, produced using three roll stages is shown in Figure 6.1.30. The temperatures were determined experimentally by forming thermocouples into the consolidated section and the relative positions of these, for this instance, are shown. This particular distribution was measured on a nylon 12/glass flat strip, pultruded at a line speed of 1m/min and at an oven temperature of 200°C. The roll forming pressure was 5N/mm and the section was allowed to cool in air between the roll stands.

The most obvious feature of this distribution when compared to Figure 6.1.29 is the quenching effect of the rollers, especially for thermocouple positions nearest the tow surfaces. The thermocouple closest to the surface registered an almost

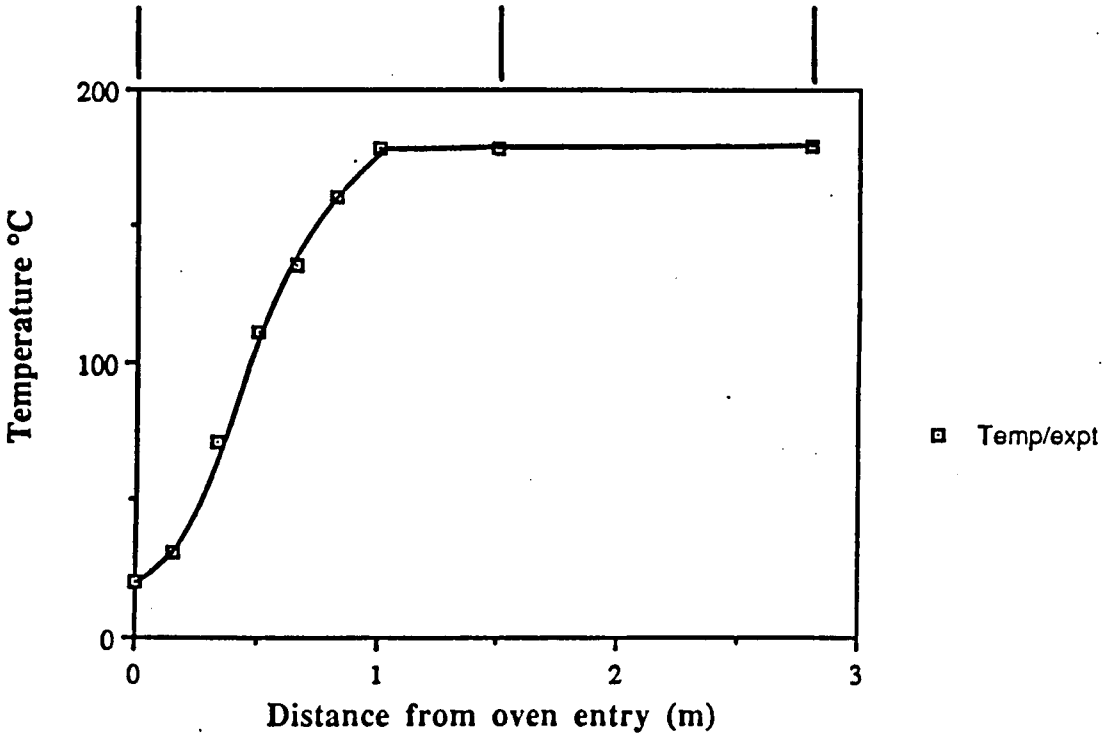

Figure 6.1.28. Experimentally measured heating profile for a nylon 12/glass precursor, pulled at a line speed of 1m/min through a combined infra-red and hot air oven at 180°C.

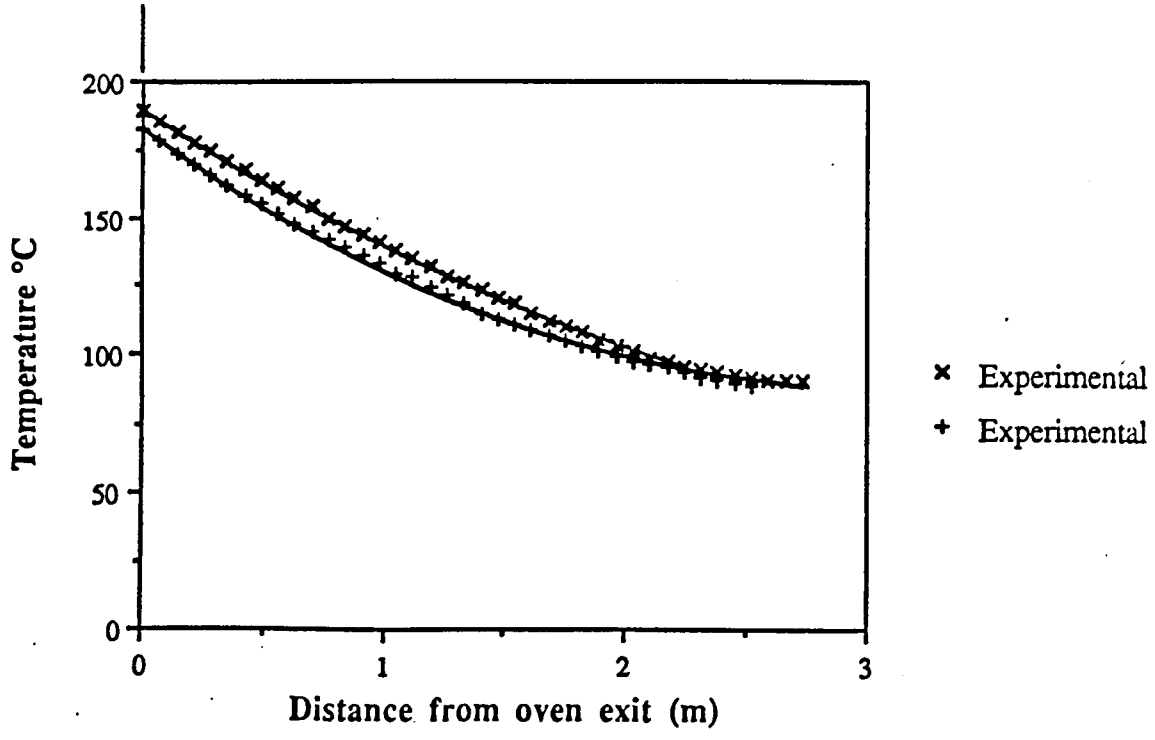

Figure 6.1.29. Experimentally measured cooling profile for a polypropylene/glass precursor bundle, pulled at a line speed of 2.1m/min through air with no forming or consolidation stage.

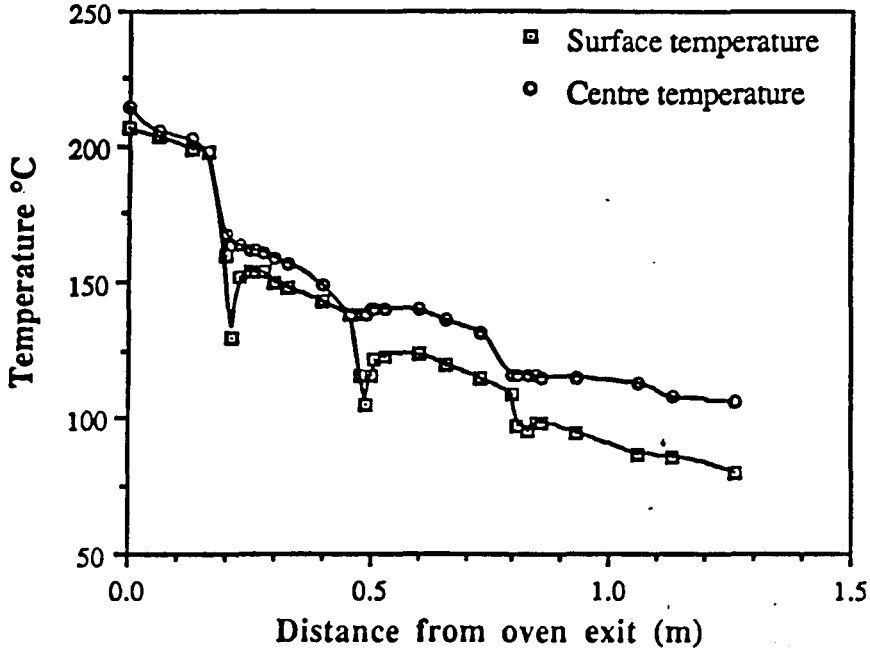

Figure 6.1.30. Experimentally measured cooling temperature distribution for a nylon 12/glass section, pulled at 1m/min through three roll forming stages.

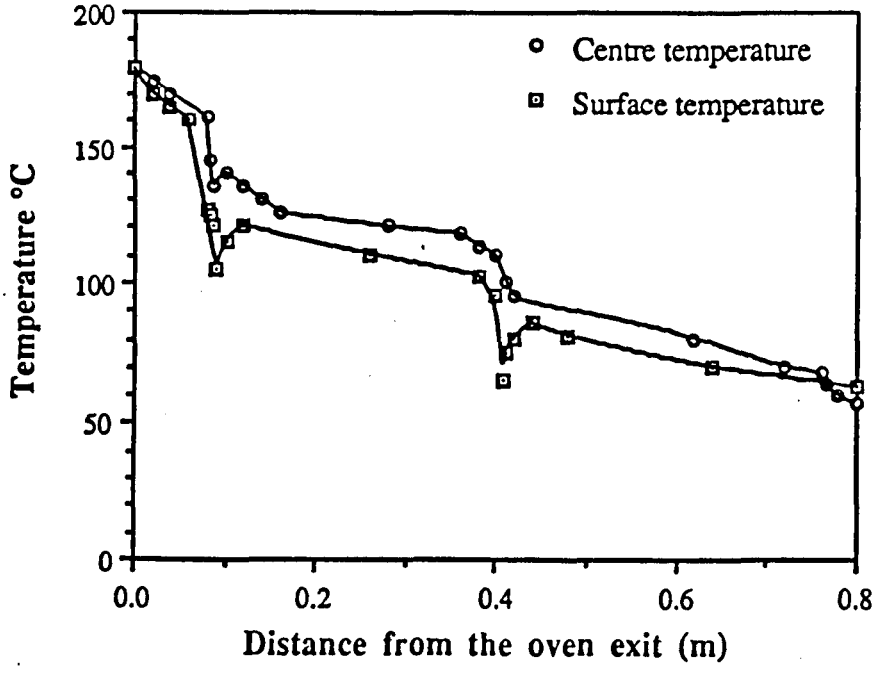

Figure 6.1.31. Experimentally measured cooling temperature distribution for a nylon 12/glass section, pulled at 0.5m/min through two roll forming stages.

instantaneous temperature decrease of 70°C, from approximately 200°C to 130°C. In comparison, the internal temperature decreased by only approximately 30°C, to a temperature of about 180°C, over the same contact distance. The contact distance could be estimated from this distribution by taking the exit of the roll gap to coincide with the point of lowest temperature, for this case the contact distance was only about 8mm. As the section leaves the roll gap and moves further down the pultrusion line, the surface temperature can be seen to rise once more to 150°C as heat flows back from the centre of the consolidated composite section. Both the surface and centre then continued to cool by a combination of surface convection and internal conduction until the entry to roll 2.

Roll 2 also causes a rapid temperature decrease to occur near the tow surface, although in this case the temperature decrease is only approximately 40°C. As can be seen, the temperature of the layers near the surface fall to as low as 100°C at the exit of roll 2. The central temperature was also lowered on contact with roll 2 but still remains at about 140°C. The surface again re-heats due to conduction from the interior as the section leaves roll stand 2.

Roll 3 exerts a similar influence on the temperature of the section as rolls 1 and 2. Although the temperature decrease in the interior was about the same as measured during contact with roll 2, the temperature decrease near the surface was smaller. On leaving roll 3, the composite strip was at a temperature too low for any further consolidation to occur.

A similar cooling temperature distribution can be seen in Figure 6.1.31. This was measured for a nylon 12/glass section pultruded using two roll stands, at a line speed of 0.5m/min and using a lower oven temperature, 180°C. The forming pressure was 5N/mm. Again, the first roll caused a temperature decrease of approximately 70°C near the surface tows upon entering the roll gap. Roll 2 also had a similar effect on the temperature decrease of the composite section.

Some features which directly influenced the overall pultrusion process were apparent from these experimentally determined temperature distributions.

Roll 1 was expected to provide the major consolidation while the precursor was still above its melting temperature, however, consolidation was coupled with a temperature decrease to below the solidification temperature of the nylon matrix, especially in the layers near to the surface. Although the surface layers did re-heat

to some extent, they did not re-melt and this will have reduced the degree of consolidation which could have been achieved in the interior of the section. It will also have caused any air remaining in the centre of the tow bundle to become trapped within two solidified skins where it may have formed voids.

It was also interesting that in Figure 6.1.31, it appears that pultruding with an oven temperature of 180°C was insufficient to enable the precursor bundle entering roll 1 to remain above the melting temperature of the nylon matrix. Therefore, in the distance between the oven exit and the roll gap, a thin solidified skin would have already formed before the rolls at a line speed of 0.5m/min. Even without the quenching effect of the rolls, this would have resulted in incomplete consolidation and air entrapment. It was found earlier that increasing the oven temperature from 180 to 190°C caused an increase in the interlaminar shear strengths for equivalent line speeds and this was a direct result of the precursor entering roll 1 at a higher temperature, especially at the surface. From Figure 6.1.30, at an oven temperature of 200°C, the temperature of the material leaving the oven was measured to be 210°C and it entered roll 1 above 200°C, ie. without skinning. This was reflected in an improved interlaminar shear strength. Providing that no degradation occurred, processing at a higher oven temperature resulted in higher strengths by improving the consolidation, by reducing surface skinning of the unconsolidated tow bundle, by allowing trapped air to escape and by reducing the matrix viscosity to allow a greater degree of flow and fibre re-arrangement to occur.

It was not possible to measure temperature distributions at higher roll pressures due to the difficulty of preventing the thermocouples from becoming damaged during forming. However, increasing the pressure would be expected to cause a larger temperature decrease through the thickness and into the interior of the section. This, coupled with a better thermal contact would then increase the thickness of the surface solidified layer and prevent complete consolidation.

6.1.4.2 Heat transfer modelling of pultrusion roll forming

The development of the heat transfer model has been described in Chapter 3. It was possible to use this model to calculate the temperature distributions in the composite section during thermoplastic pultrusion, using in this case a roll forming mechanism.

Heating

The combined infra-red and hot air oven was modelled by assuming a combined radiative and convective surface heat transfer coefficient, h_r, for the oven. The value of this heat transfer coefficient was estimated by fitting curves calculated for different values of h_r to experimentally determined heat up curves. It was found that a good approximation was achieved for h_r=50 W/m^{2}k. A comparison between the measured and modelled temperatures can be seen in Figure 6.1.32. This was measured and modelled for a nylon 12/glass precursor, pulled at a line speed of 1m/min through an oven at 180°C. A satisfactory degree of fit was achieved. The actual temperature increase was steeper than predicted because of two possible reasons. The method of measurement required the thermocouple tip to sit on the surface being heated. It was possible that both the absorption characteristics and the response time of the thermocouple to temperature changes would have been greater than that of the precursor surface. Also, the precursor tapes begin collimation at about 1m inside the oven. This is where the measured temperature distribution flattened out. At this stage the thermocouple became embedded loosely into the precursor bundle. The main objective in modelling the heating stage was to determine optimum line speed/oven temperature conditions to ensure efficient heating, and as such the model was regarded as adequate.

The effect of increasing the oven temperature on the interlaminar shear strength has been discussed previously. In order to highlight the effect of the heating stage on the overall process, the effect of different line speed/oven temperature combinations has been modelled.

Figure 6.1.33 shows the effect of increasing line speed ie. decreasing dwell time on the temperature of the precursor leaving the oven for a constant oven temperature of 180°C, just above the melting temperature of the nylon matrix. It can be seen that for all speeds up to 1m/min the precursor will fully melt before the oven exit. However, increasing the speed to 2m/min will cause the precursor to reach the oven exit at a lower temperature. Although forming was still possible at this speed, the combination of a lower temperature material and a reduced residence time in the rolls resulted in a poor interlaminar shear strength. For a line speed of 3m/min, the precursor tapes were found to only tack together during forming. This was a result of the precursor tows being at too low a temperature for polymer flow and fibre re-

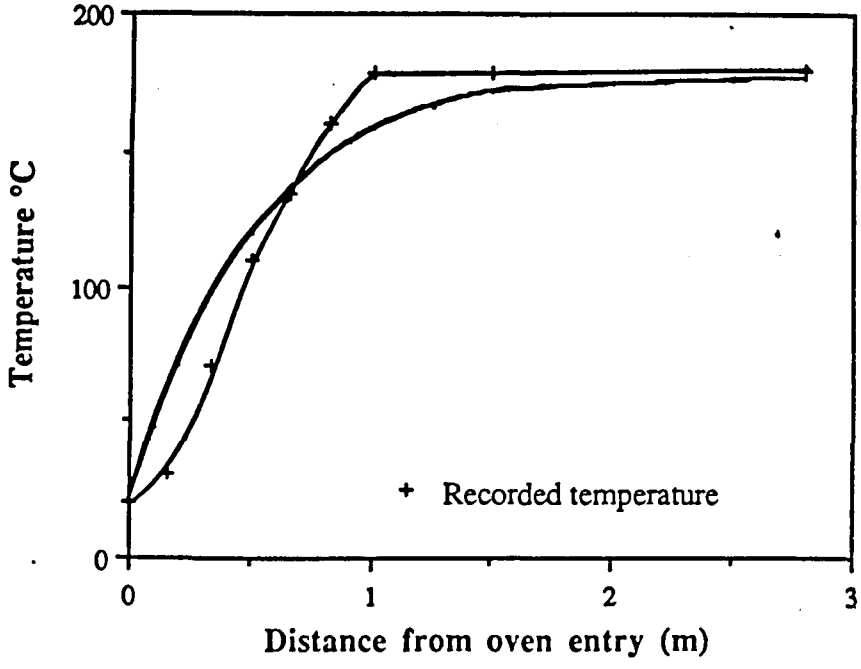

Figure 6.1.32. Modelled heating distribution for a nylon 12/glass precursor pulled at 1m/min through through an oven at 180°C. The measured temperatures are shown superimposed on the modelled solution.

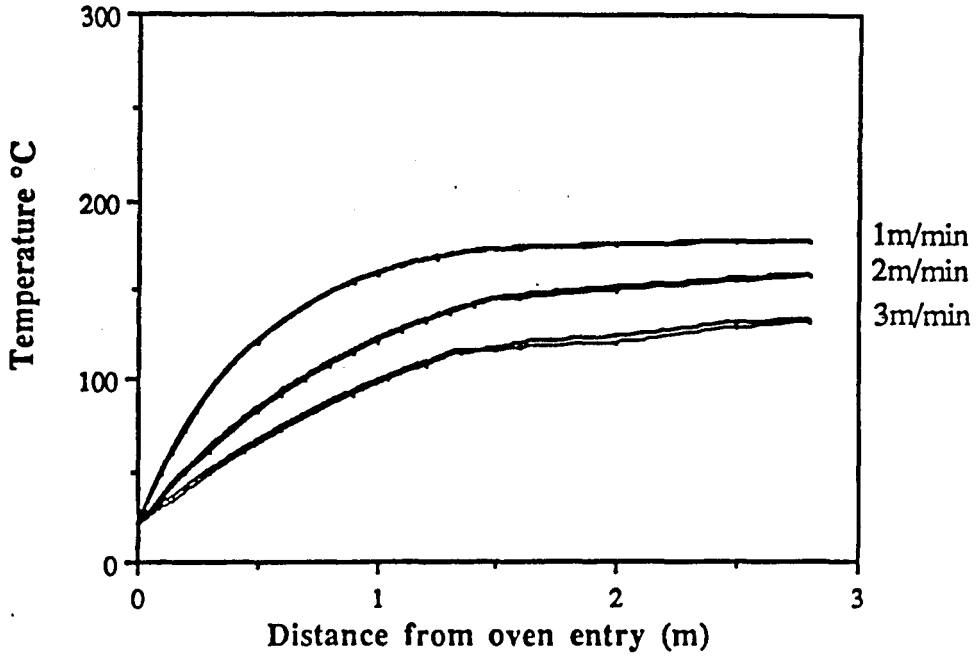

Figure 6.1.33. Modelled heating curves for a nylon 12/glass precursor pulled through the infra-red and hot air oven at 180°C and at three different line speeds.

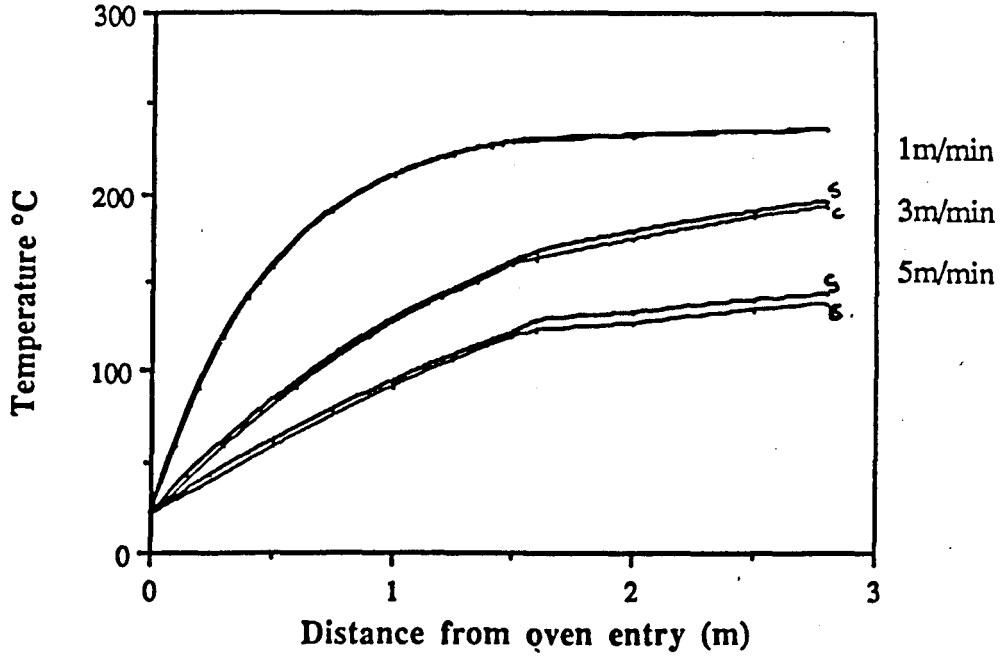

Figure 6.1.34. Modelled heating curves for a nylon 12/glass precursor pulled through the infra-red and hot air oven at 240°C and at three different line speeds.

organisation to occur and this was reflected in the poor interlaminar shear strength achieved.

The effect of pultruding at a high oven temperature, 240°C, can be seen in Figure 6.1.34. It was observed that severe degradation occurred while running at low speeds at this temperature. As can be seen, even at a line speed of 1m/min the precursor leaving the oven will have overheated by as much as 60°C. Only on increasing the line speed to 3m/min did the precursor temperature at the oven exit approach the melting temperature of nylon 12. It can be seen that at 5m/min the residence time in the oven was insufficient to allow the precursor to heat fully, even at an elevated temperature.

It can be seen from Figure 6.1.34 that increasing the processing temperature did increase the line speed range for which pultruded sections could be produced. It has also been found that this was accompanied by an increase in the interlaminar shear strength for any particular line speed. However, the interlaminar shear strength decreased with line speed regardless of oven temperature. The rate of decrease in the interlaminar shear strength also appeared to be independent of the oven temperature and any of the curves could conceivably have been shifted onto the other. This indicated that the dominant factor in causing the decrease in properties was the reduction of residence time in the roll gap rather than incomplete heating.

Cooling

The cooling temperature distribution illustrated by Figure 6.1.29 was measured at a line speed of 2.1m/min, after heating a polypropylene/glass precursor bundle to 190°C and allowing it to cool in air. The modelled temperature distribution corresponding to these conditions is shown in Figure 6.1.35. For a convective, surface heat transfer coefficient of 30 W/m^2k there is quite good agreement between the modelled and the measured results. It was therefore possible to model the cooling of the precursor bundle in air prior to forming and consolidation.

Forming, consolidation and cooling

Modelled temperature distributions, incorporating forming and consolidation by two roll stands and calculated for the same processing conditions as the measured distributions in Figure 6.1.30, can be seen in Figure 6.1.36. The model can be

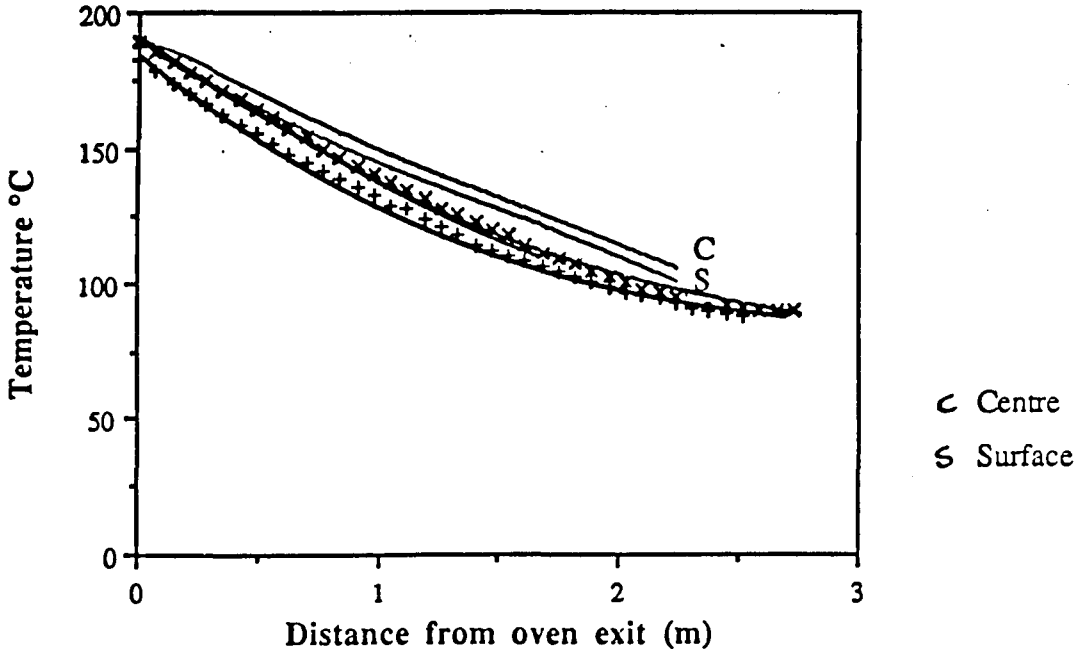

Figure 6.1.35. A comparison between the measured and modelled air cooling temperature distribution, for a polypropylene/glass unconsolidated section pulled with a line speed of 2.1m/min.

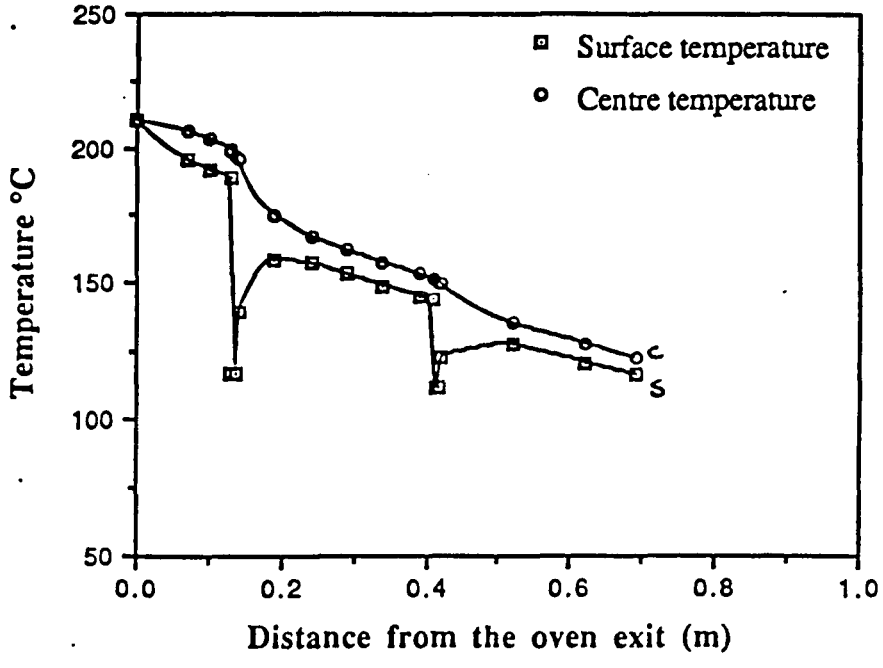

Figure 6.1.36. Modelled cooling temperature distribution, at the surface and centre of a nylon 12/glass section, pulled with a line speed of 1m/min through two roll forming stages.

seen to incorporate the cooling effect of the forming and consolidation rolls, especially at the surface of the pultruded section. A direct comparison to the experimental results can be made in Figure 6.1.37. The solid lines represent the modelled temperatures at the surface and at the centre of the composite strip section. Good agreement between the modelled and measured temperatures can be seen, although there is some discrepancy. There are a number of features which may influence the fit of the model. The thermal conductivity has been calculated assuming that there is no trapped air in the composite. However, in some instances, void contents of up to 11% have been measured and this will cause a reduction in the thermal conductivity. The effect of this will be to reduce the flow of heat from the centre of the section, preventing the outer layers from re-heating.

In addition, thermal lag effects due to the response time of the thermocouples has not been considered and may introduce an error into the experimental results. The presence of the thermocouple in the tow bundle will also introduce a void immediately in the vicinity of the measurement tip. Also, the thermocouples were not positioned either on the surface or in the centre of the section and it was difficult to pre-determine where they actually measured the temperature. They also moved within the section during experimental runs so that their final position was not necessarily where they measured the temperature. If a tension was applied to try and prevent this movement, the thermocouples tended to slip backwards through the molten unidirectional precursor tows.

Although the model requires further refinement, it was capable of modelling the effect of the forming rollers during pultrusion. Figure 6.1.38 shows the results of the model for two line speeds: 1m/min and 3.5m/min. These results are for a 45% glass/polypropylene section pultruded into air. The same heat transfer coefficient, $30W/m^2K$, was used at each line speed. Even though the quenching effect of the rolls was still present, the reduced residence time in the rolls has reduced this and the formed section has remained above 150°C for a distance greater than 0.8m from the oven exit.

It was possible to model the thermal history of the precursor material during heating and the consolidated section during forming and consolidation by the use of a relatively simple, one-dimensional heat transfer model. The model has been verified under a number of different processing conditions and shows good agreement with measured temperature distributions.

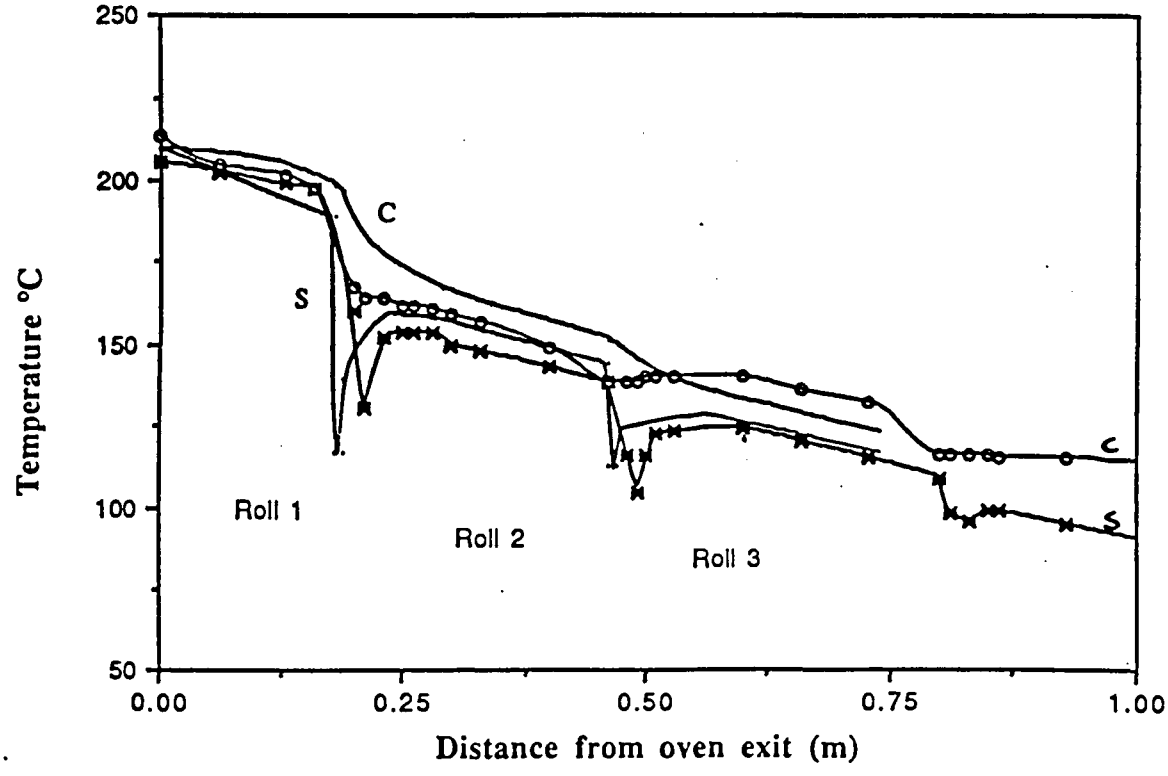

Figure 6.1.37. A comparison between the measured and modelled cooling temperature distributions for a roll formed nylon 12/glass pultruded section.

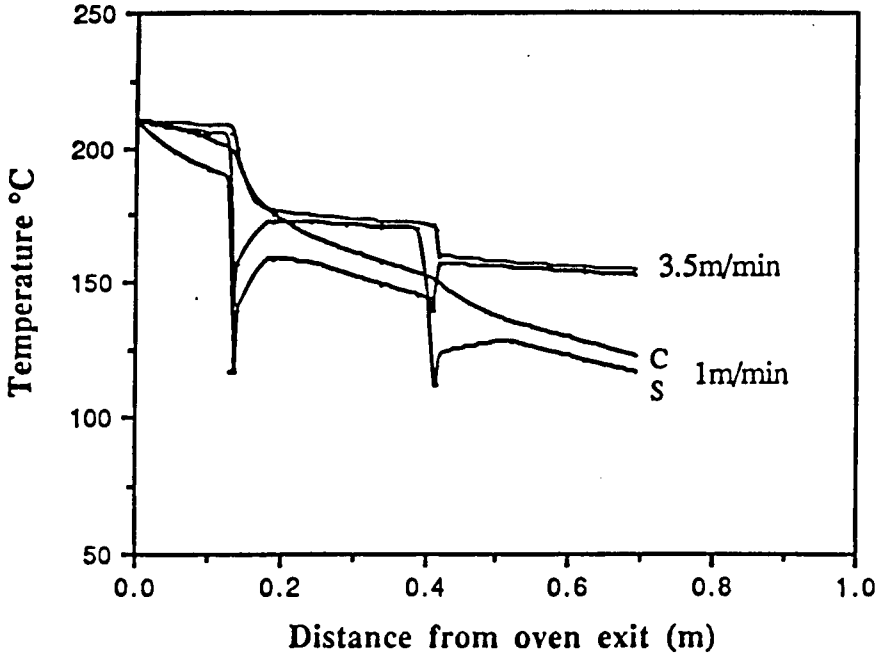

Figure 6.1.38. Modelled cooling distributions for roll forming a nylon 12/glass section at two different line speeds, 1m/min and 3.5 m/min.

6.1.5 Roll forming of APC2 precursors

A quantity of APC2 (carbon/PEEK) precursor was supplied in order to investigate the feasibility of thermoplastic pultrusion with this material. Of all the materials supplied this was the most commercially developed and has found a large number of applications, especially in the aerospace industry. Even in its precursor form, this material was fully wetted-out and the requirement of the pultrusion process was to re-heat the polymer and form and consolidate a section from a number of precursor tows. With all the other precursor materials examined, it was necessary for additional impregnation to occur during processing due to incomplete impregnation in the starting materials. The material was supplied as a single roll and the discontinuous pultrusion technique which was developed to produce sections using this material has been detailed in Section 5.1.7.

Table 6.1.3 shows the interlaminar shear strength, the flexural strength and modulus of pultruded APC2 sections. An example of an APC2 pultruded section has been shown previously in Figure 6.1.7.

Table 6.1.3. Properties of a press moulded APC2 strip.

Precursor	V_f reinforcement	Line speed	Oven temperature ℃	Roll pressure N/mm	ILSS MPa	Flexural strength MPa	Flexural modulus Gpa
APC2	0.61	1	380	5	97.1	1420	92.8
		1	380	90	92.7	1323	84.7
		1	380	175	92.3	1247	77.7
		1	380	260	90.6	1329	73.2

The average interlaminar shear strengths obtained ranged from 85% to 92% of the optimum value of 105MPa quoted in the product data sheet. Only one line speed, 1m/min was studied. The effect of roll pressure on the interlaminar shear strength

of the APC2 section can be seen in Figure 6.1.39. As the pressure was increased a decrease in the interlaminar shear strength was measured. This was consistent with the previous observations made for the nylon 12/glass pultrusion experiments which indicated that increased heat transfer at high roll pressures reduced the consolidation efficiency. Flexural strengths achieved were between 75 and 66% of the optimum quoted value of 1880MPa. A decrease in the flexural strength and modulus with increasing roll pressure can also be seen in Figure 6.1.40, again for a line speed of 1m/min. A micrograph of a polished section of a pultruded APC2 strip can be seen in Figure 6.1.41 and shows a good fibre distribution although the individual precursor tapes can still be distinguished.

An ultrasonic C-scan of a pultruded APC2 section can be seen in Figure 6.1.42. This test was carried out by ICI Advanced Materials, Wilton. The pink colour indicates areas of excellent consolidation and poorer consolidation is denoted by blue, yellow, purple, green and orange respectively. As can be seen, excellent consolidation has occurred in the central areas of the section. However, fibre damage resulting from the cut edges of the tapes and the tendency for the tapes to fold and wrinkle at the edges of the section as they entered the roll gap reduced the consolidation near to the edges. Nevertheless, over 60% of the section was pink or blue. A good contrast can be made with Figure 6.1.43 which shows a C-scan representation of an APC2 section in which thermocouples were embedded into the precursor, passed through the oven and formed into the section. The large white areas correspond to the voids caused by the presence of the thermocouple wire. However, some areas of good consolidation can also be seen around the smaller void on the left hand side.

Although only a small amount of material was available, the feasibility of pultruding good quality APC2 sections at a line speed of 1m/min was demonstrated.

6.1.6 Compression moulding of polypropylene/glass 'pultrusions'

Unfortunately, after the experiments described previously had been carried out, an insufficient quantity of the nylon 12/glass precursor remained to investigate thermoplastic pultrusion using temperature controlled dies instead of cold rollers. However, a commercially available polypropylene/glass precursor, "Plytron", was made available. This precursor had a glass volume fraction of 33% and was supplied as a 10mm wide tape, 0.5mm thick. As a standard against which the

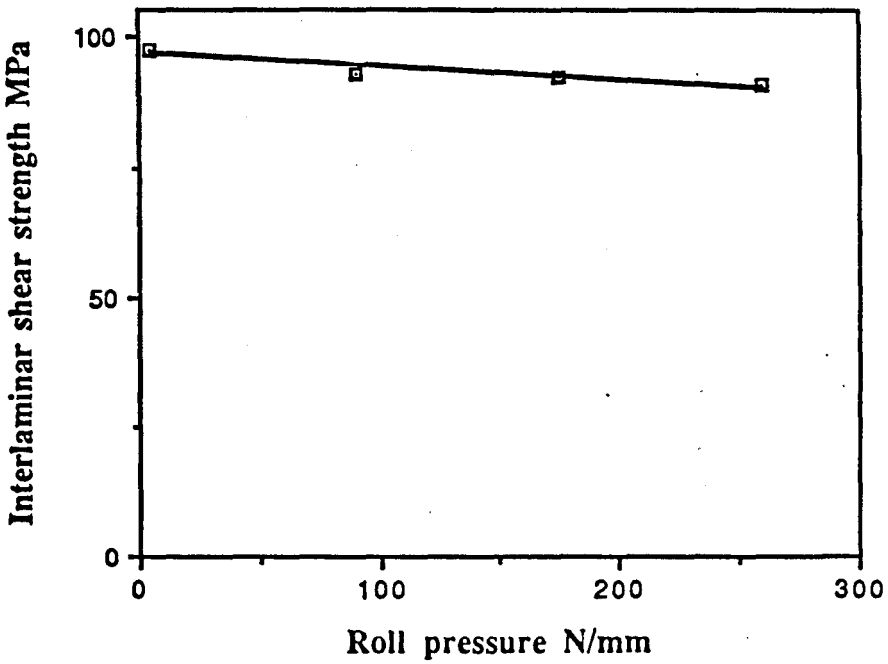

Figure 6.1.39. Effect of increased roll pressure on ILSS of an APC2 section, pultruded at a line speed of 1m/min and at an oven temperature of 380°C.

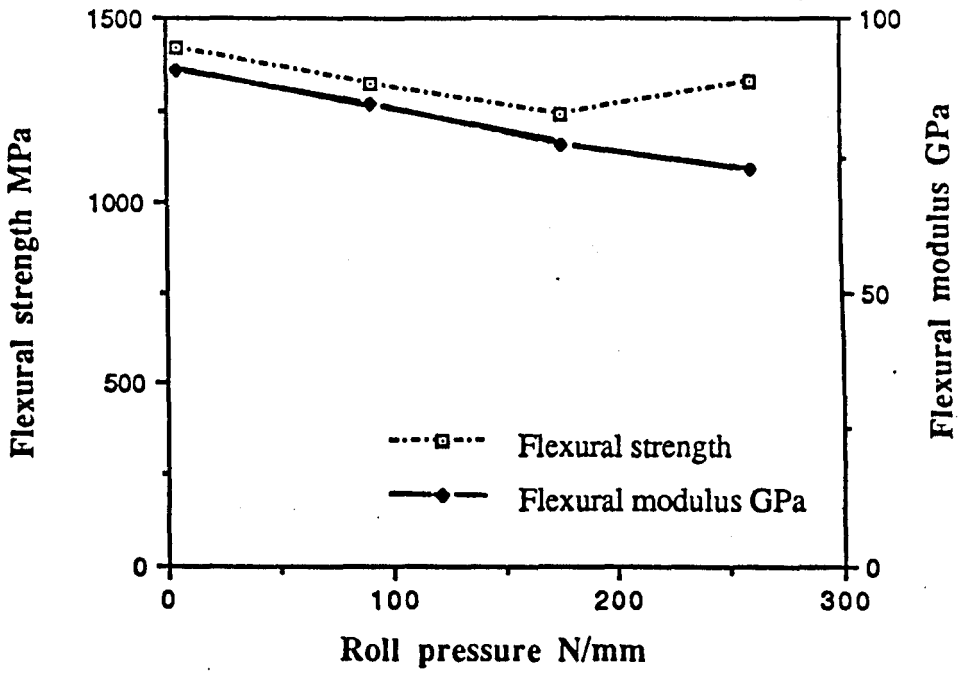

Figure 6.1.40. Effect of increased roll pressure on the flexural strength and modulus of an APC2 section, pultruded at 1m/min.

Figure 6.1.41. Micrograph showing section of pultruded APC2 strip.

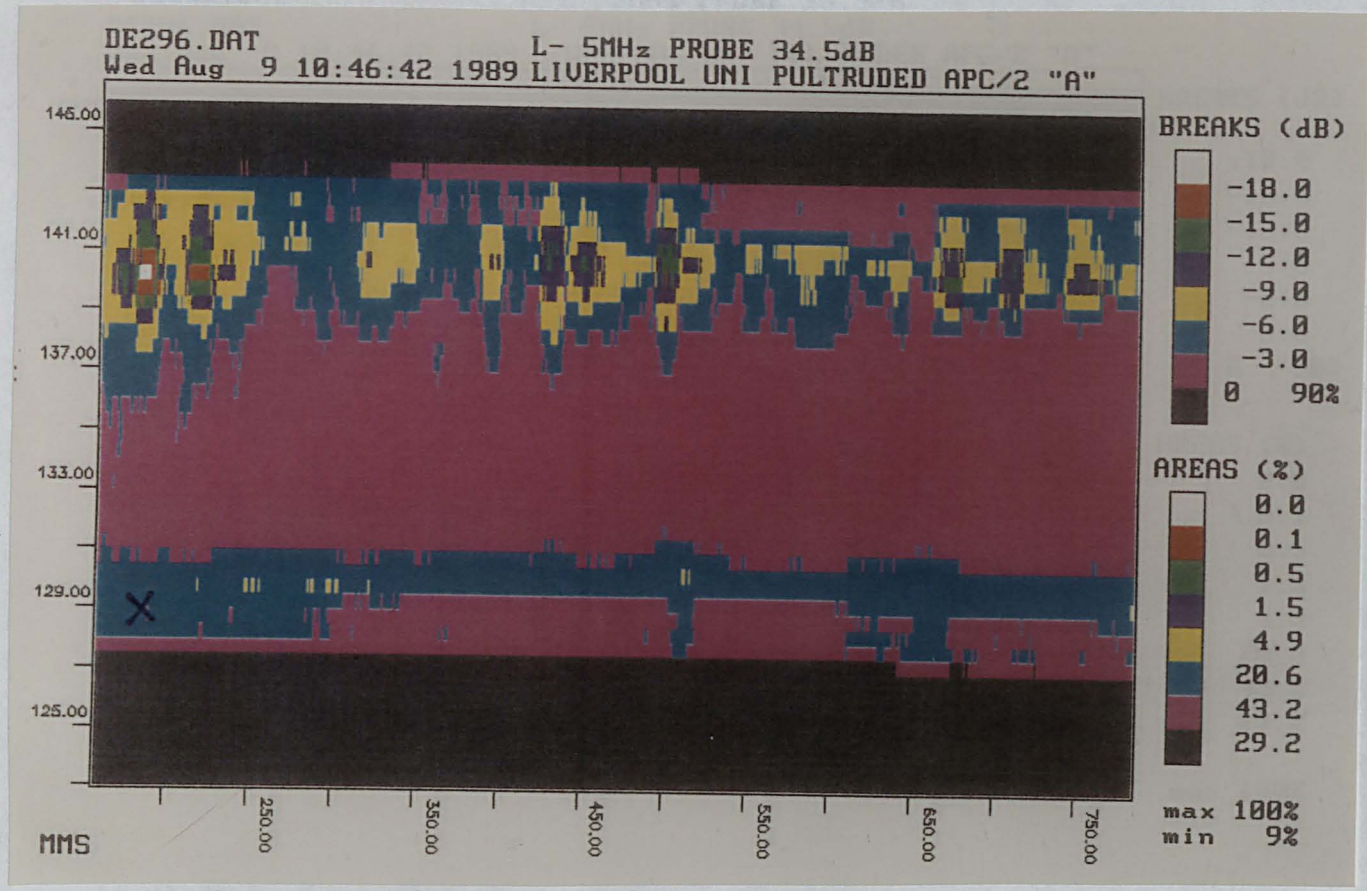

Figure 6.1.42. Ultrasonic C-scan of pultruded APC2 strip in which the pink areas denote good consolidation and void free areas. Processing conditions: Line speed 1m/min; Oven temperature 380°C; Roll pressure 90N/mm.

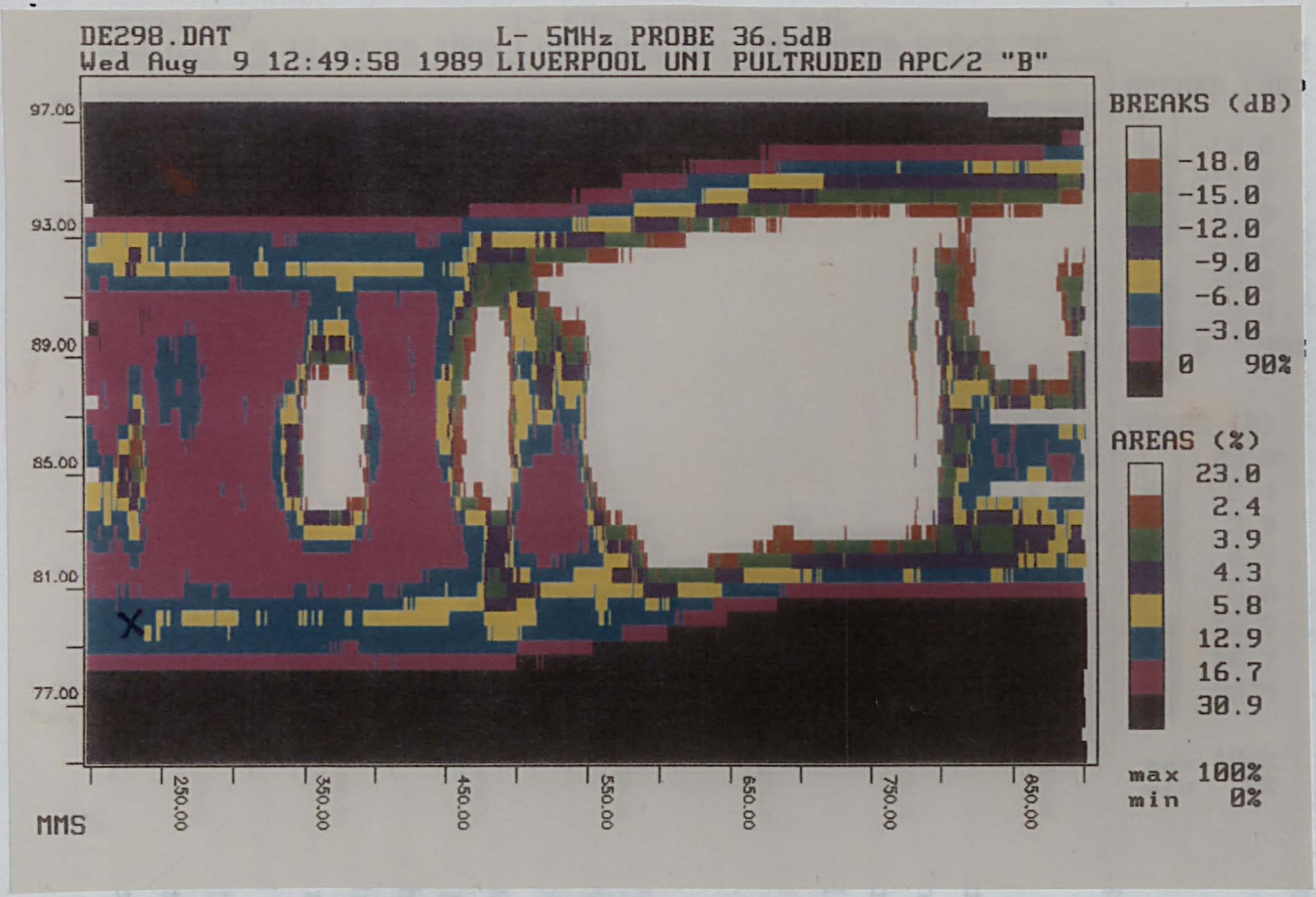

Figure 6.1.43. Ultrasonic C-scan of pultruded APC2 strip showing areas in which a thermocouple was formed into the section, forming large voids. Processing conditions: Line speed 1m/min; Oven temperature 380°C; Roll pressure 90N/mm.

pultrusion process could be evaluated, a rectangular strip section was pressed from this precursor using the heated matched mould. The mould temperature was 215°C, and the section was pressed under a cylinder pressure of 30 bar. It was then allowed to cool under pressure to below 80°C. The process cycle is illustrated in Figure 6.1.44. The flexural strength and moduli and the void content obtained for this section are given in Table 6.1.4.

6.1.7 Die forming of 'Plytron', polypropylene/glass, pultruded sections

Although the cooling effect of the forming rolls appeared to be far too severe to allow the forming conditions to be optimised, it was possible to pultrude reasonably good sections at a range of line speeds using the forming roll system. However, it appeared that it would be better to apply the initial forming and consolidation without cooling the tow bundle and then gradually cooling the section under pressure, therefore improving the overall properties.

The pultrusion die set-up has been shown schematically in Figure 5.1.6. Three identical dies, each 270mm long were used to produce a 15mm wide rectangular section at different line speeds and under a range of forming pressures. The thickness of the pultruded section varied depending on the processing conditions and was in the range 2.95 to 3.7mm. Polypropylene is above its glass transition temperature at room temperature, so it is not possible to carry out short beam shear tests on polypropylene matrix composites because the dominant failure mode is not true shear because the material is too ductile. This would result in artificially high interlaminar shear strengths. The properties of the pultruded sections were determined by measuring the flexural strength and modulus as a function of line speed and forming pressure. The oven temperature was maintained at 220°C throughout the experimental runs. In addition, measurements of the torsional shear modulus, by use of the torsional pendulum test, was investigated as to its suitability as a characterisation test.

The first die was positioned 160mm from the oven exit. This die was heated and maintained at a constant temperature of 180°C. A small forming pressure was applied to this die using springs under compression. It was found that too large a force on die 1 caused wipe-off to occur in the die entry. This wipe-off was generally undesirable and caused a build-up of resin at the die entry and a poor

Table 6.1.4. Properties of a press moulded polypropylen /glass (Plytron) strip.

Precursor	V_f glass	Flexural strength MPa	Flexural modulus GPa	Void content %
Plytron PP/glass	0.35	442	22.1	3.5

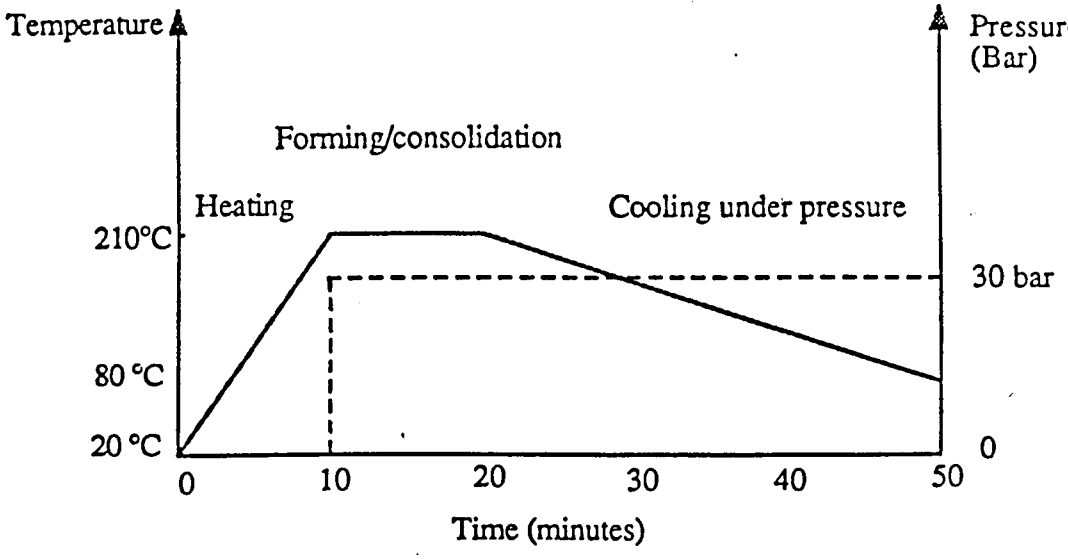

Figure 6.1.44. Process cycle for compression moulded "Plytron" section.

surface finish, with fibre damage in the surface layers of the partly consolidated material bundle. The use of this die ensured that the temperature of the precursor bundle leaving the die was independent of line speed. Also, some pre-consolidation of the formed section occurred without reducing the material temperature to below the melting temperature of the matrix. The material was allowed to air cool before entering die 2.

Initial experiments were carried out with dies 2 and 3 which had no temperature control. This proved unsuccessful because the uncontrolled dies gradually warmed up as the pultrusion line was operated. It took up to 30 minutes continuous operation before the dies could be considered to be operating under steady state temperature conditions. The temperature of dies 2 and 3 were measured continuously during a trial pultrusion run and were found to reach a steady state at temperatures of 100°C and 90°C respectively. In the experimental pultrusion runs, die 1 was therefore maintained at 100°C and die 2 at 90°C. A water bath placed after the exit of die 3 cooled the pultruded section to room temperature before it entered the haul off and thus prevented damage caused by the haul-off belts.

The relative positions of dies 2 and 3 with respect to die 1 were chosen initially using a process of trial and error during a series of trial runs carried out at a line speed of 1m/min. The temperature of the material entering die 2 was measured for various die positions and it was found that the surface temperature of the precursor was required to be at a temperature of between 145 and 150°C in order to produce a section with a visually acceptable surface finish. At temperatures between this and the melting temperature, friction between the moving material and the die wall resulted in sticking and wipe off of polymer within the die. This resulted in a poor and uneven surface finish and a visually unacceptable product. Although this was itself insufficient to stop the process, it did eventually lead to clogging of the die. This in turn caused progressively greater wipe-off, which eventually caused the material to stop in the die as the force required to pull it through increased.

At too low a precursor surface temperature, incomplete consolidation occurred and the material did not completely fill the die profile. The distance between the exit of die 2 and the entrance of die 3 was maintained constant at 330mm. Using a surface temperature of 145°C as a processing guideline, a heat transfer model was used to determine the position of die 2 relative to die 1 for different line speeds. This model will be discussed separately.

The die positions used experimentally are detailed in Table 5.1.3. It was not possible to increase the distance between die 1 and die 2 in excess of 2m. At this distance from die 1, the precursor material sagged and it was difficult to prevent it trying to rotate and twist. There was also a limitation placed on the distance by the length of the pultrusion bed on which the dies were fixed.

The line speeds examined were limited to a maximum of 3.5m/min. Above this speed it was not possible to reduce the surface temperature of the tow bundle to the required 145-150°C by altering the die positions coupled with air cooling. The use of additional cooling mechanisms such as water sprays were investigated but were found to quench the surface to well below temperatures at which forming could occur.

The effect of four forming pressures on the properties of the pultruded sections were investigated and these were 5, 162, 319 and 475 KPa. The lowest forming pressure of 5 KPa corresponds to the weight of the upper half of the die only. At pressures above the maximum, the generation of friction in the dies caused the pull force to increase to such an extent that it became difficult to maintain a constant line speed. The magnitude of the pull force was not measured directly. Although it was not possible to express the forming pressure in the same units as used for the rolls, in which the contact length was not known exactly, a comparison can be made by assuming a reasonable 10mm contact length. In this were the case, the equivalent roll forming pressures would be 0.13, 4.5, 9 and 18 MPa for the same applied thrusts and are considerably higher than the die pressures used.

The effect of forming pressure on the flexural strength and modulus of a section pultruded at a line speed of 1m/min is shown in Figure 6.1.45. The minimum forming pressure resulted in strength and modulus values which were only 50% of the maximum achieved for a compression moulded plaque. Applying an increased forming pressure caused both the strength and modulus to increase, unlike the effect seen with the forming rollers. As can be seen from Figure 6.1.45, the flexural strength increased to a maximum at a forming pressure of 319KPa and then showed a slight decrease at the highest die pressure. The maximum flexural strength for the section pultruded at 1m/min was 80% of that obtained for the pressed section. Although the application of additional die pressure increased the flexural modulus, the magnitude of this pressure seems to have had little effect on the moduli of the pultruded sections, which remained constant at about 70% of the

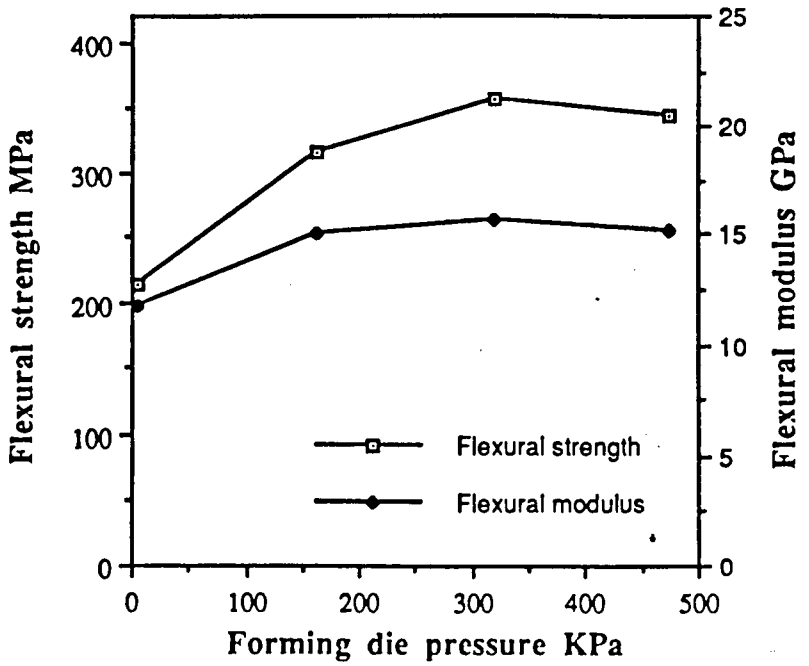

Figure 6.1.45. The effect of forming pressure on the flexural strength and modulus of a section pultruded at a line speed of 1m/min.

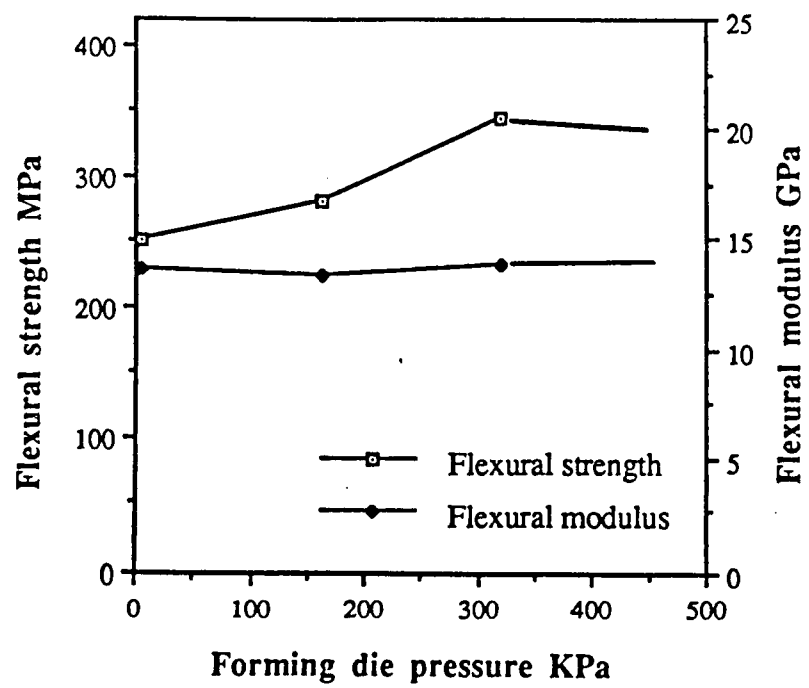

Figure 6.1.46. The effect of forming pressure on the flexural strength and modulus of a section pultruded at a line speed of 1.5m/min.

value obtained for a pressed section. At the highest die pressure, friction build-up between the moving composite and the stationary die was observed both through a deterioration in the surface finish and also through the haul-off having to exert a higher pull force to maintain a constant line speed.

It was possible to produce sections at a line speed of 1.5m/min using the same die positions as for 1m/min. Figure 6.1.46 shows the variation in flexural strength and modulus with increasing die pressure at this speed. As was observed at the lower speed, the flexural strength increased with increasing die pressure to a maximum value and then decreased. The optimum die pressure again appeared to be 319KPa. The maximum value of the flexural strength was slightly lower at this speed than at 1m/min. The flexural modulus was also lower than obtained at 1m/min and remained at a constant value for all forming pressures.

In order to produce acceptable product at 2m/min it was necessary to increase the distance between dies 1 and 2 so that the surface of the precursor bundle cooled to the required temperature. Figure 6.1.47 shows the effect of pressure on the strength and modulus at this speed. As before, the strength increased with pressure and the maximum value was again obtained at a die pressure of 319 KPa. Above this the flexural strength was reduced. The modulus also increased with die pressure from an initially low value to a constant level. Both the strength and modulus achieved were lower than the values obtained for sections produced at lower line speeds.

The effect of pultruding at a line speed of 3m/min is shown in Figure 6.1.48. The increase in flexural strength with applied die pressure was not as great as was measured at lower line speeds. Although the optimum die pressure was again 319KPa, the flexural strength at 3m/min was only 56% of the strength of the pressed section. The modulus also showed a small increase with die pressure and values were similar to those achieved at 2m/min.

At the highest line speed examined, 3.5m/min, only a very small increase in the strength and modulus was measured as a result of increasing the die pressure. This is illustrated in Figure 6.1.49. The maximum flexural strength was again produced using a die pressure of 319 KPa, although the flexural strength was only 50% of the value obtained for the pressed section.

Unlike the effect of applying higher pressures to the forming roll system, it was

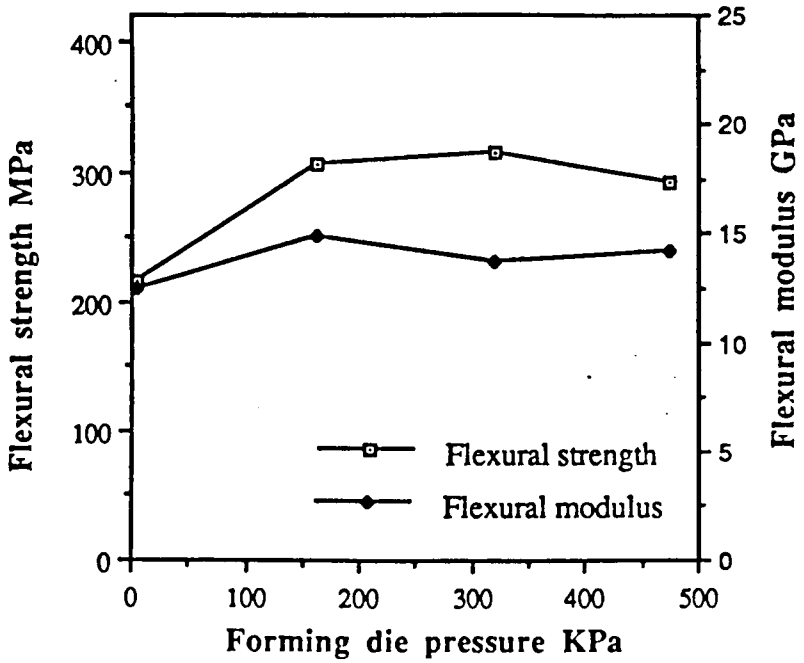

Figure 6.1.47. The effect of forming pressure on the flexural strength and modulus of a section pultruded at a line speed of 2m/min.

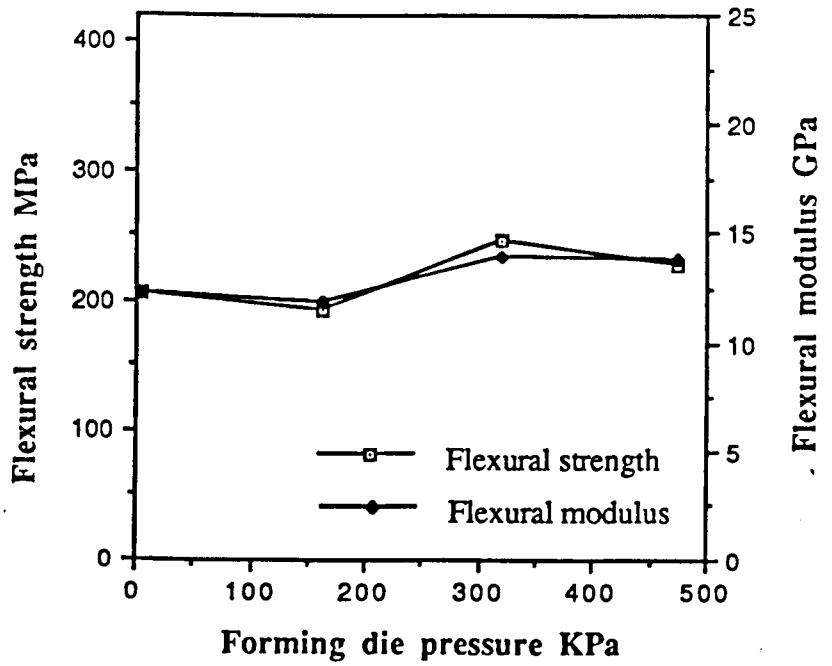

Figure 6.1.48. The effect of forming pressure on the flexural strength and modulus of a section pultruded at a line speed of 3m/min.

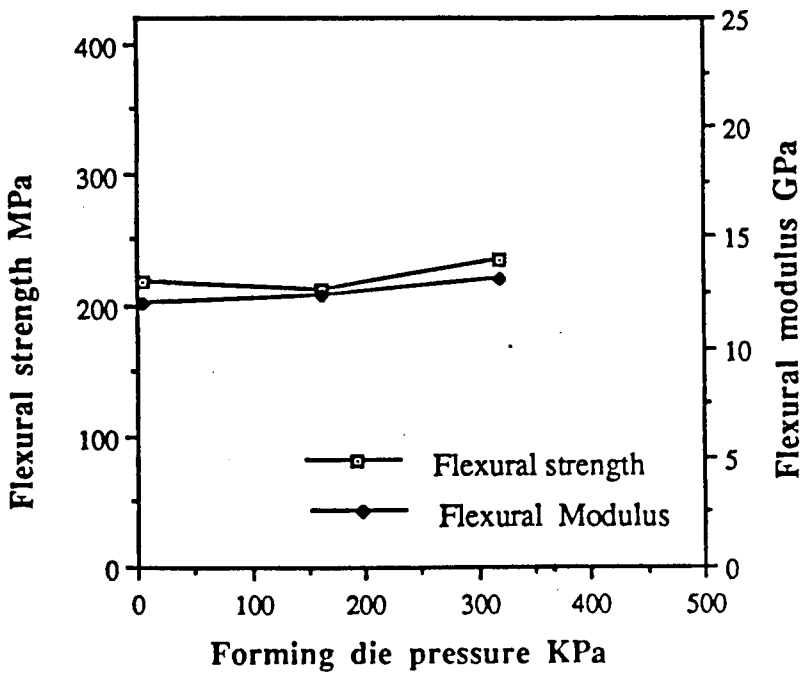

Figure 6.1.49. The effect of forming pressure on the flexural strength and modulus of a section pultruded at a line speed of 3.5m/min.

possible to increase the strength and moduli of the pultruded sections by increasing the die pressure. The optimum die pressure appeared to be 319 KPa. The optimum pressure also appeared to be independent of the line speed. At die pressures in excess of 319 KPa, the flexural strength of the pultruded sections decreased slightly. The values for the modulus appeared to be sensitive to an increased pressure above the minimum, but increasing the magnitude of this pressure appeared to have little effect on the modulus, which remained fairly constant at all three higher die pressures.

The increase in flexural strength with die pressure can be directly attributed to improved consolidation at higher die pressures. During roll forming in which the rolls were cold, increasing the pressure was found to cause the pultruded section to cool too rapidly to allow full consolidation at high roll pressures. Because the dies were heated, this did not happen on increasing the die pressure and the consolidation efficiency was able to increase with die pressure.

The increased consolidation was also evident from measuring the thickness of the pultruded sections. At the minimum applied pressure, the sections were generally between 0.4 to 0.7mm thicker than sections produced at the next highest pressure, without additional wipe off occurring. A further small thickness reduction, 0.1 to 0.4mm was also measured for sections pultruded at the next highest die pressure. The thickness then remained constant even after further increasing the pressure. No additional wipe-off was observed to occur at the higher die pressures.

The drop off in flexural strength at the highest die pressure was accompanied by a visible increase in the friction between the composite and the die wall. This friction increase was apparent because the surface of the pultrusion became rougher, showed visible signs of fibre damage and acquired a black colouration as it rubbed against the brass dies. Although the pull force was not measured directly, it was observed to increase by noting that the haul-off began to labour audibly as it maintained a constant line speed. In some cases the pull force was sufficiently high to cause the product to slip in the belts of the haul-off and so stop the pultrusion line. In this case, it was necessary to apply a substantially higher gripping pressure through the belts in order to pull the product through the dies. However, this was not ideal as the gripping pressures required were sufficient to damage the pultruded section. It is thought that fibre damage, especially at the surface, resulted in the reduction in the flexural strengths obtained at the highest die pressure.

It was also interesting that, in contrast to the rolling experiments, no bowing of the pultrusions occurred as the pressure was increased and all sections produced were equally straight.

The effect of line speed on the flexural strength is illustrated in Figure 6.1.50 for each of the four die pressures examined. The effect of line speed on the flexural modulus is shown in Figure 6.1.51. The values of flexural strength and modulus for the pressed section were included on these graphs to represent an 'ideal' pultrusion, produced under stationary conditions.

The flexural strength decreased considerably with line speed for all the higher forming pressures studied. However, at the minimum die pressure, both the flexural strength and modulus showed only a relatively small decrease as the line speed increased. When this was compared to the decrease observed at the higher pressures, the strength and modulus could be considered to remain constant throughout the range of line speeds examined. Although the residence time in the die was continually decreasing, this appears to have had little effect on the flexural properties achieved under the lowest pressure. The reduction in flexural strength was therefore predominantly the result of incomplete consolidation due to an insufficiently large forming pressure, rather than being due to the reduction in dwell time in the dies.

A similar situation existed at the highest line speed studied, where only a relatively small variation in the flexural strength between the highest and lowest forming pressures was measured. This was a direct result of the reduction in die residence time at the highest line speeds, which resulted in increasingly poorer consolidation even when running using increased die pressures.

The variation in residence time with line speed for each of the 270mm long forming dies is shown in Figure 6.1.10c. Although this takes the same form as seen in Figure 6.1.10b for the forming rollers, the residence times are 27 times longer. For instance at a line speed of 2m/min, the residence time in a single die is 81 seconds compared to 3 seconds for a single set of rolls.

The observed decrease in the flexural strength and modulus when using dies was much more gradual than the decrease in interlaminar shear strength with line speed for roll-formed pultrusions. Nevertheless, in the case of the rolls it was possible to

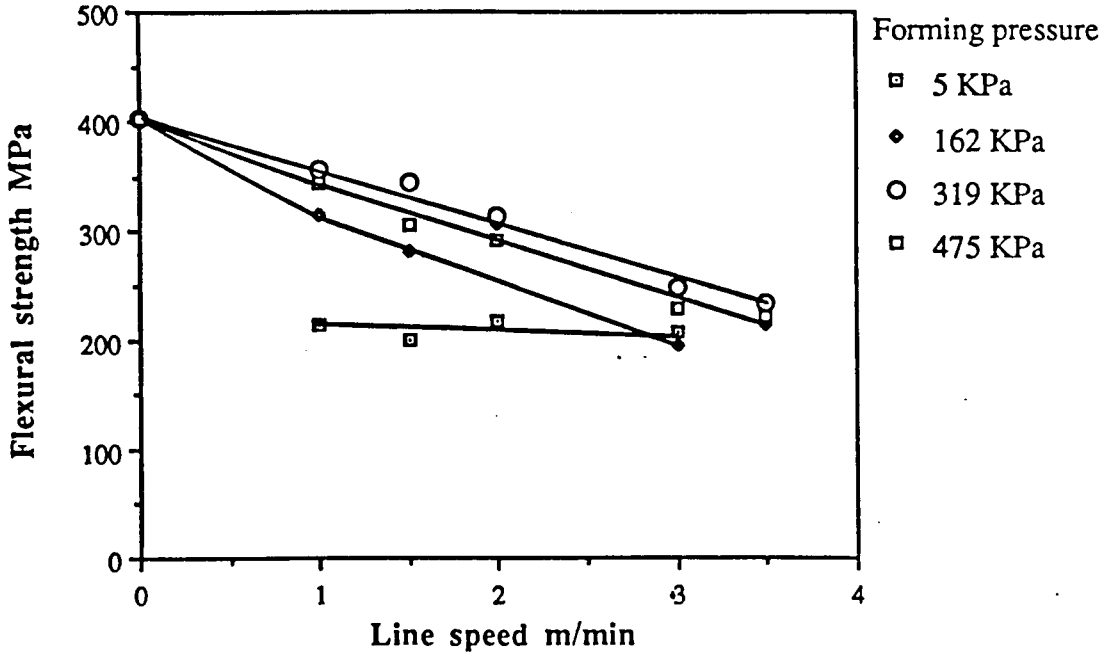

Figure 6.1.50. The effect of line speed on the flexural strength of sections pultruded at each of the four die pressures studied.

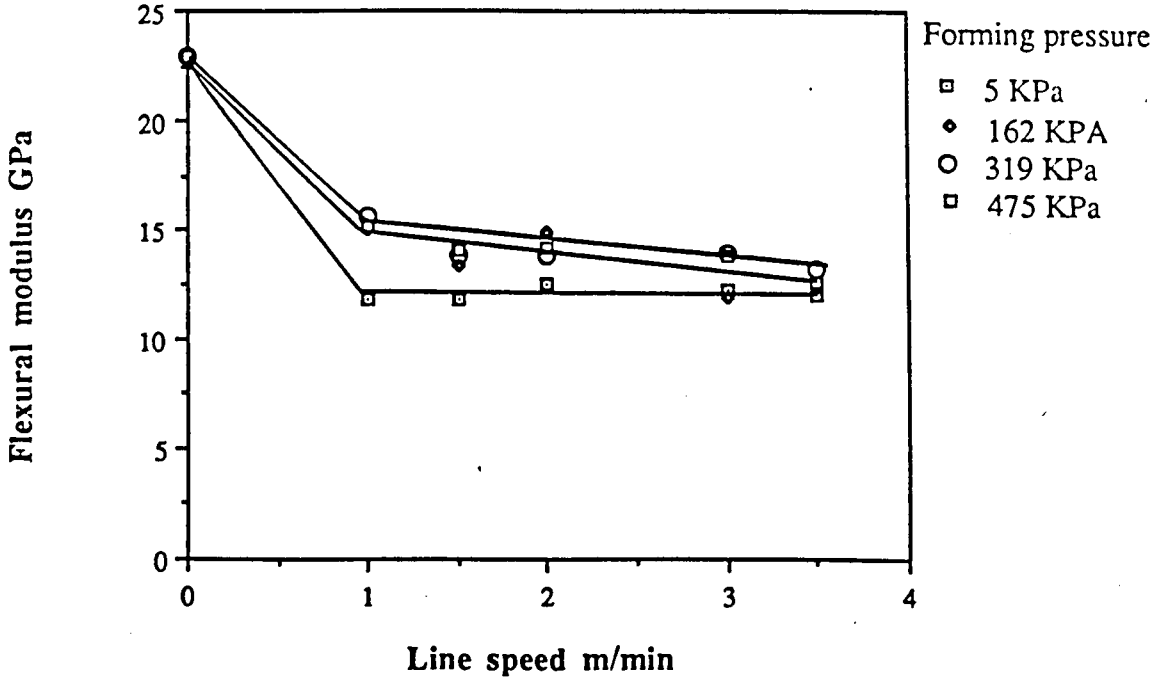

Figure 6.1.51. The effect of line speed on the flexural modulus of sections pultruded at each of the four die pressures studied.

produce acceptable pultrusions even when contact times were as low as 2 seconds. This corresponded to very slow line speeds and a rapid decrease in interlaminar shear strength was measured as the speed was increased up to 1m/min at which the forming times were less than 1 second.

Considering the forming pressures have been applied for much longer forming times at equivalent line speeds, it was not surprising therefore that the reduction in strength and modulus with line speed was less severe for this pultrusion die system. In addition to this, the presence of the heated die immediately after the oven exit ensured that the material bundle leaving die 1 was at a constant temperature, regardless of line speed. This reduced the effect that residence time in the oven had on the overall drop-off in section properties.

The void contents of sections produced using dies were also measured and can be seen, along with the corresponding flexural strength and moduli, plotted against line speed in Figures 6.1.52 and 6.1.53. Although a large degree of scatter was present, the void content of a section produced at 3.5m/min using dies was only 4.5%, compared to 10% for the same line speed using rollers.

The torsion pendulum test was also investigated as a characterisation test for polypropylene based composites produced using the thermoplastic pultrusion process. The torsion pendulum can be used to measure the complex modulus and thus the storage shear modulus, G', the loss shear modulus, G", and the mechanical loss factor, tan δ, and has been described in Section 2.3.

Figure 6.1.54 shows how the flexural strength and the loss modulus, G", were found to vary with line speed for a range of polypropylene/glass pultruded sections. The decrease in the flexural strength was accompanied by an increase in the loss modulus and the samples produced at higher speeds exhibited higher damping characteristics. Changes in G" are typically the result of poor interfacial bonding which causes large viscous dissipation at the fiber-matrix interface. In this case, however, the interface should not have been significantly altered by processing at a higher line speed and the increase in G" was likely to have been the result of incomplete consolidation, coupled with a higher void content as the line speed increased. The flexural modulus was found to remain almost constant throughout the speed range, although the loss modulus increased as shown in Figure 6.1.55.

The variation of flexural strength and tan δ with line speed is shown in Figure

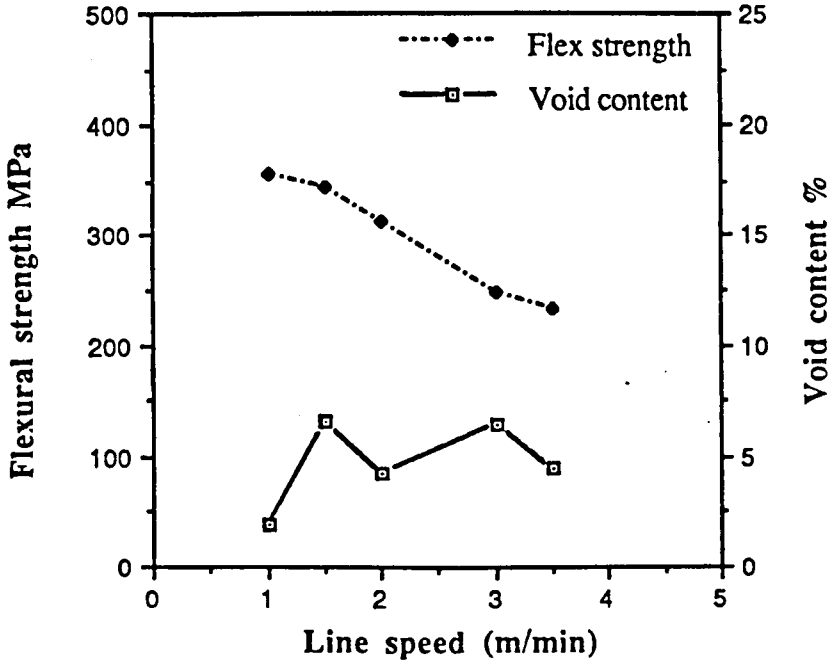

Figure 6.1.52. Correlation between flexural strength and void content with line speed for a "Plytron" pultrusion, produced using a forming pressure of 319KPa.

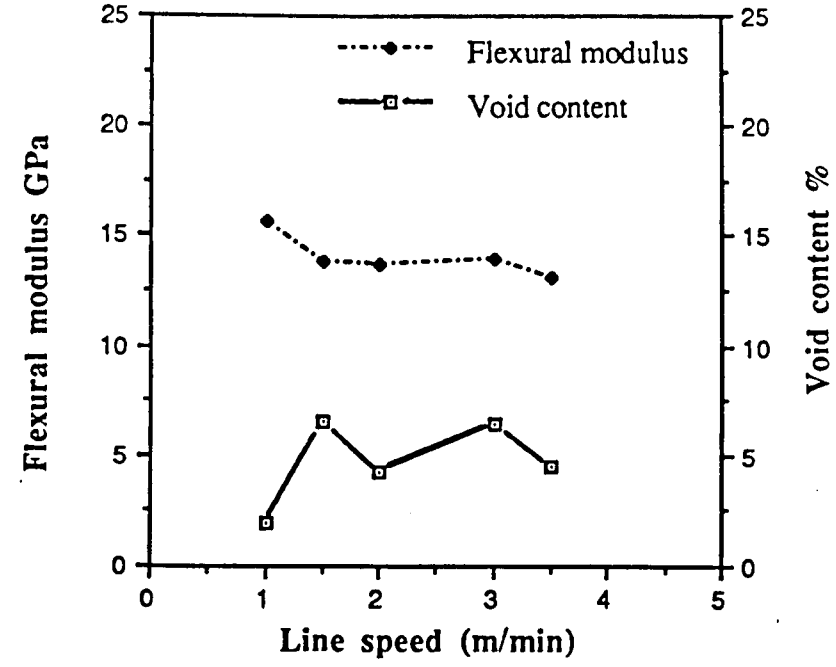

Figure 6.1.53. Correlation between flexural modulus and void content with line speed for a "Plytron" pultrusion, produced using a forming pressure of 319KPa.

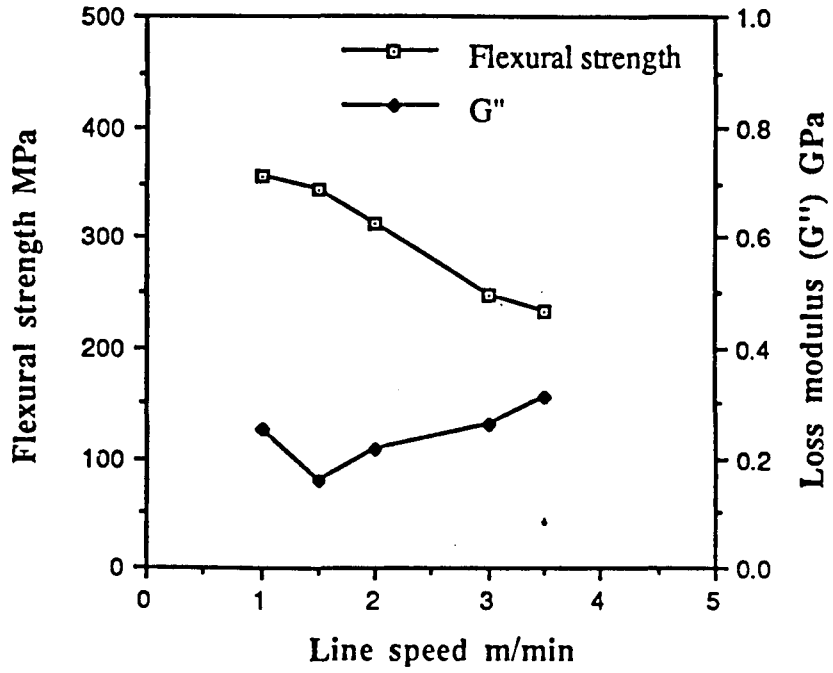

Figure 6.1.54. The variation of flexural strength and loss modulus, G", with line speed for "Plytron" sections pultruded using a die pressure of 319KPa.

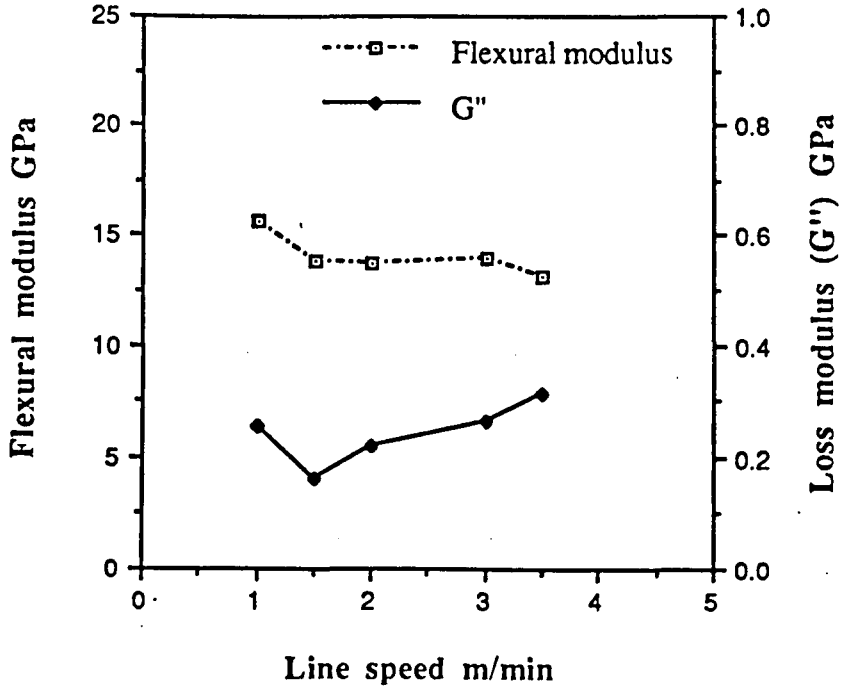

Figure 6.1.55. The variation of flexural modulus and loss modulus, G", with line speed for "Plytron" sections pultruded using a die pressure of 319KPa.

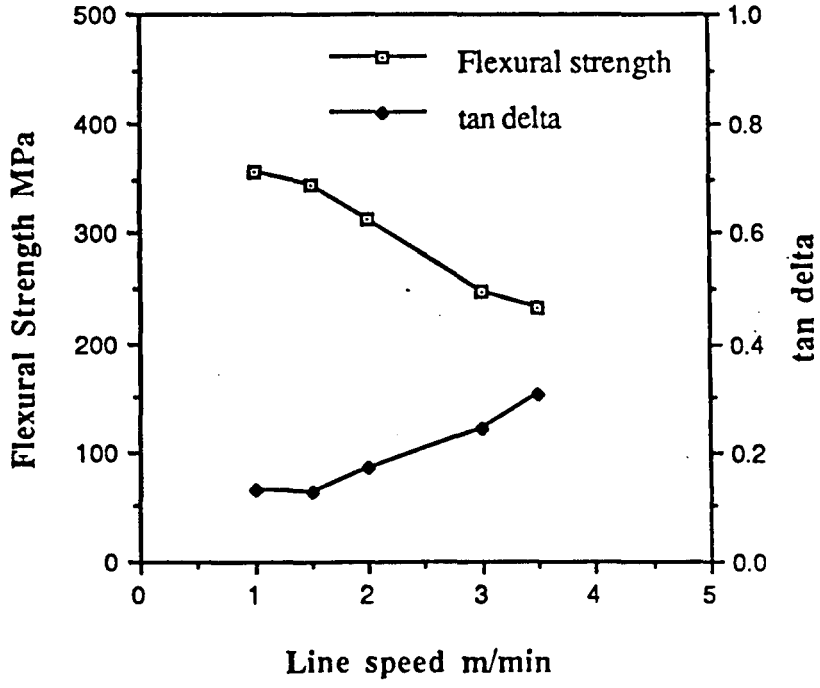

Figure 6.1.56. The variation of flexural strength and tan δ with line speed for "Plytron" sections pultruded using a die pressure of 319KPa.

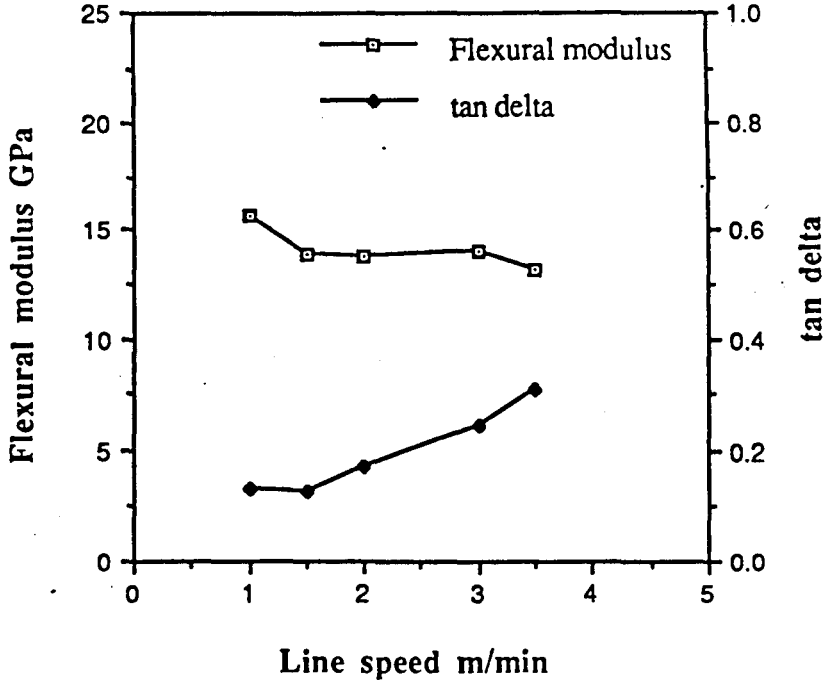

Figure 6.1.57. The variation of flexural modulus and tan δ with line speed for "Plytron" sections pultruded using a die pressure of 319KPa.

6.1.56. Again, the decrease in flexural strength is accompanied by an increase in tan δ, which has been interpreted to indicate poorer consolidation and a higher void content at higher line speeds. As was seen for G", tan δ also increased while the flexural modulus remained constant, as shown in Figure 6.1.57.

The torsion pendulum test was found to be insufficiently sensitive to processing induced changes in the behaviour of the pultruded sections to provide useful comparisons. However, when it was necessary to evaluate the interface formation and to compare different precursors, the test did produce some interesting results. Tests were carried out on two polypropylene/glass precursors, known to have good and poor interfacial bonding. The angular displacement-time curves from each can be seen in Figure 6.1.58 and the calculated values for the loss shear modulus, G", and loss factor, tan δ, are given in Table 6.1.5.

Table 6.1.5. Variations in the loss modulus, G", and tan δ for two different polypropylene/glass precursors, with a known good or bad interface.

Precursor	V_f glass	G'' GPa	Tan δ	Known interface
PP/glass TPD 049	0.5	0.2	0.16	Bad
PP/glass TPD 053	0.5	0.23	0.09	Good

Noticeable differences can be seen between the material responses to torsional deformation. The lower loss factor and higher shear modulus of the TPD 053 material is in keeping with a good interfacial bond, which promotes continuity of strain within the sample and gives a low level of internal friction. The higher loss factor and lower shear modulus of the TPD 049 material suggests a lack of bonding, resulting in a lower modulus and increased losses due to friction at the fibre-matrix interface.

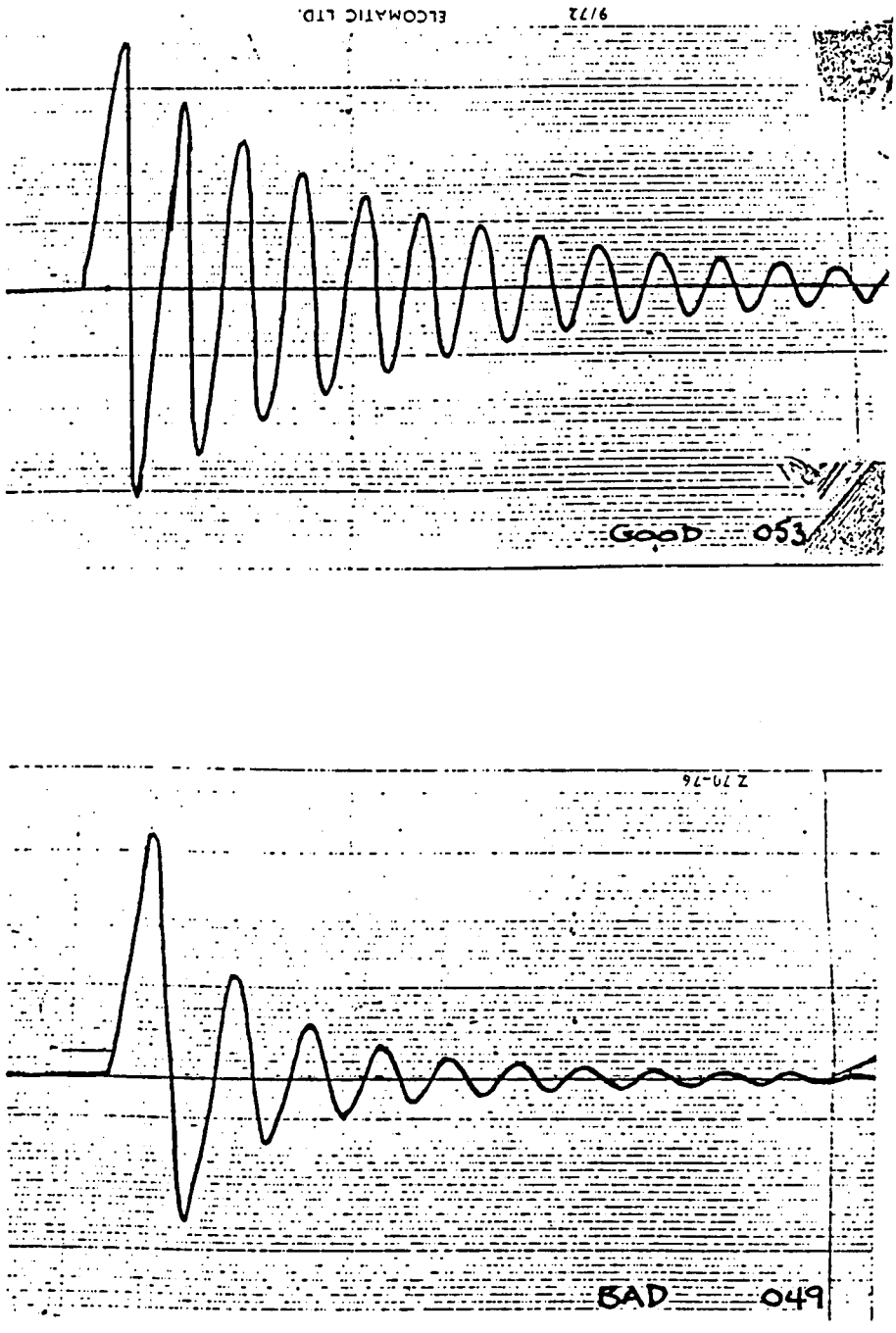

Figure 6.1.58. Angular displacement-time curves for two different polypropylene precursors, which have different interfacial bonding.

6.1.8 Heat transfer in pultrusion die forming

The heat transfer model used to determine the optimum positions for the dies and the temperature distributions during processing has been described in Chapter 3. The model used for cooling in air before the die entry was very similar to the model used to calculate the cooling temperature distribution in air without forming or consolidation stages, as demonstrated in Section 6.1.4.2. Temperature measurements during preliminary pultrusion runs indicated that the optimum surface temperature to produce an acceptable surface finish with minimum sticking at the die walls appeared to be between 145 and 150°C. It was possible to run the heat transfer model to determine the distance from the exit of die 1 at which the surface temperature was optimised for different line speeds. Figure 6.1.59 illustrates the effect of increasing the line speed from 1 to 2m/min, for a die positioned at 0.69m from die 1. For the lower line speed, the surface temperature was at the required 145°C. Pultruding at this line speed/die distance combination was successful and a product with a good surface finish was produced. However, at a line speed of 2m/min the surface temperature remained too high and wipe-off and sticking in the die appeared likely to occur. Pultruding at this die distance and at 2m/min did in fact cause an unacceptably poor section to be produced. Figure 6.1.60 shows the surface and centre temperatures for a line speed of 1m/min and a die distance of 0.69m. It also shows the temperatures through the section for a line speed of 2m/min at a die distance of 1.29m from die 1. It can be seen that the temperature of the precursor material entering the die is about the same for each line speed. As indicated by the model, it was possible to produce a much improved pultruded strip at 2m/min when the die was moved further away from die 1.

The cooling profile in the heated die can be compared to the cooling profile caused by roll-forming a similar pultruded section. It can be seen that the quenching effect of the rolls was not present at the die entry and it was possible to apply a forming and consolidation pressure without solidifying the material instantly on contact with the die walls. This was reflected in the increase in the flexural properties as the forming pressure was increased. The improvement in properties was also influenced by the longer contact length in the dies, 0.27m compared to 10mm maximum in the rolls.

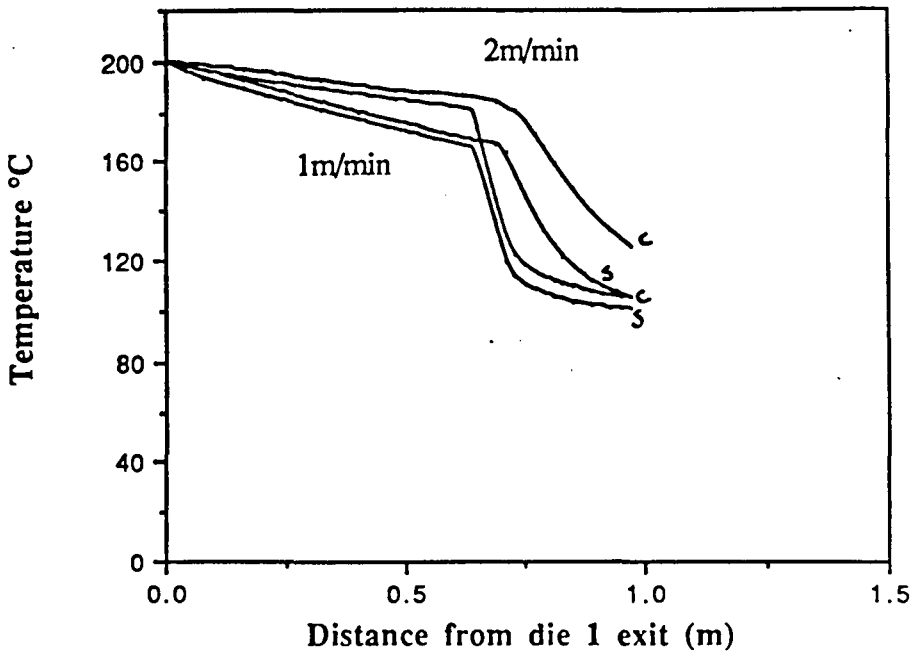

Figure 6.1.59. Modelled temperature distributions showing the effect of increasing line speed on the temperature of the precursor bundle entering die 2, placed 0.69m from die 1. The two lines represent the surface and the centre temperatures of the pultruded section.

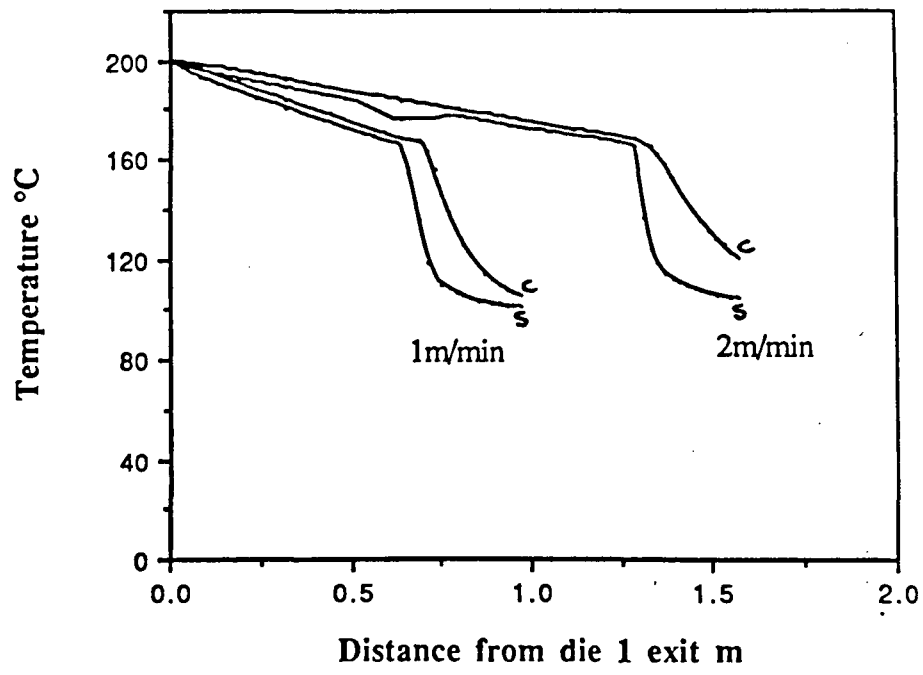

Figure 6.1.60. Modelled temperature distributions for die pultrusion showing the effect of moving die 2 relative to die 1 for an increase in line speed from 1 to 2m/min. This illustrates the use of the model to determine the position of die 2 for sucessfull processing.

6.2 Thermoplastic melt impregnation

6.2.1 Introduction

The main body of work carried out was on the pultrusion of thermoplastic composites using preimpregnated precursors. No on-line impregnation facility was developed. However, the impregnation stage is very important to the success of the overall process and a number of difficulties arise in attempting to integrate impregnation on-line with the pultrusion process. A major difficulty lies in matching the optimum impregnation line speed with the optimum pultrusion speed and in impregnating sufficient numbers of tows for large sections. For instance, each nylon 12/glass precursor tape used in the previously described pultrusion experiments contained four 2400Tex glass tows. For a section only 3mm thick, four tapes, 16 ends, were required.

The majority of commercial impregnation processes use melt impregnation. An integral feature of the melt bath is cylindrical bars which aid the impregnation of the fibre tows. The problem of tension build-up during melt impregnation was brought to attention as a possible limiting factor to the maximum line speeds achievable. A pilot study into the causes of this tension generation and into the mechanisms of melt impregnation was carried out in addition to the work carried out on the pultrusion process itself and some interesting results were obtained which have been included in the following section.

6.2.2 Review of material studied

The material system investigated comprised of two E-glass tows of 2400 Tex nylon compatible glass, which were impregnated with a nylon 6,6 (Maranyl A100) melt at 285°C. A graph of the apparent shear viscosity of Maranyl A100 as a function of shear rate over the temperature range 275-295°C is shown in Figure 5.2.1.

6.2.3 Impregnation of glass fibres with a nylon 6,6 melt

Experiments were carried out on a number of instrumented impregnation bars, with

or without sideguides to prevent lateral flow of resin from underneath the fibre tows during passage around the bar. Details of the experiments and the experimental conditions have been given in Table 5.2.1.

6.2.3.1 Characterisation of force traces

The force measuring apparatus has been described in Section 5.2.2. Although it proved possible to measure the tension generation in the fibre tows, the force traces generated were not constant and were subject to a degree of scatter. Typical output traces showing the output of the two load cells are shown in Figure 6.2.1. As can be seen, the output consisted of a fairly uniform tension variation with time which was accompanied by non periodic peaks. Numerous attempts were made to reduce the occurrence of the peaks but this proved very difficult. There may be a number of reasons for the tension peaks observed and while these were undesirable from a measurement point of view, their presence was important. If they were a usual occurrence during processing they may cause fibre damage or even fibre failure in extreme cases. A number of steps were taken to minimise the occurrence of the peaks, the most successful being the application of the lowest possible tension to the unwinding fibres. The causes of the peaks were not investigated in detail, however there were a number of possible reasons. The tension in the fibres pulled from the creel stand was very low and this allowed the fibre tows to twist at the entry of the impregnation bath. Because the fibres did not necessarily contact the first impregnation bar horizontally, this twist may have remained throughout the impregnation bath. It was also possible that the sizing distribution on the fibres was non-uniform and concentrated along short lengths along the fibres. The fibres were not pre-heated before the impregnation bath and it was possible that the peaks were influenced by lengths of fibre on which the size had not fully melted. This would also have restricted the spreading of the fibres as they passed around the impregnation bars.

The size of the peak tension measured was also dependent on the line speed and the level of polymer melt in the bath, covering the impregnation bars. This is illustrated schematically in Figure 6.2.2 for a line speed of 15m/min. At this speed it was difficult to maintain a constant level of polymer melt in the bath due to the low extruder output. It was also difficult to control the input tension T_0 while at the same time keeping the tension on the fibre tows as low as possible to minimise the peak values. In order to calculate an average force reading from each load cell, the

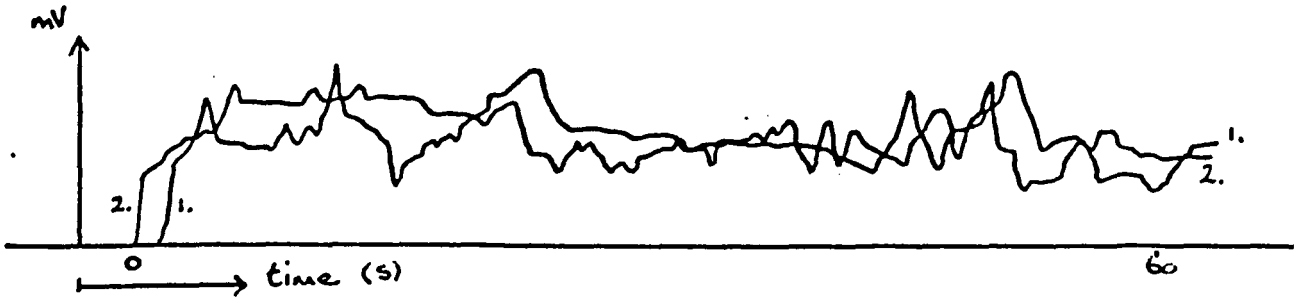

Figure 6.2.1. Typical output trace obtained from the measuring load cells during melt impregnation. This trace was for a 10mm bar and recorded at an impregnation line speed of 5m/min.

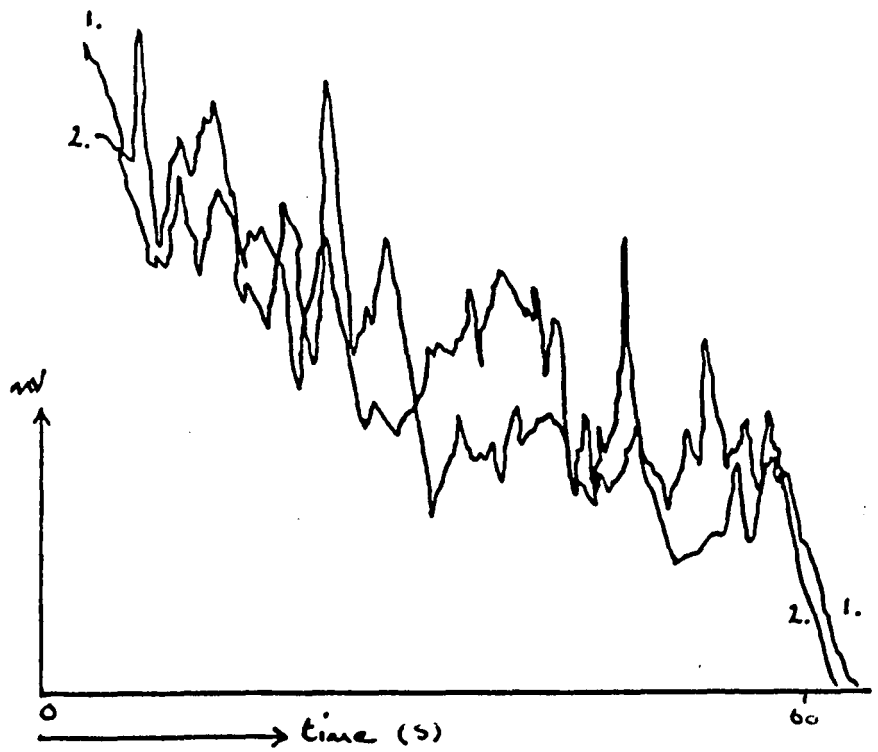

Figure 6.22. Output trace obtained during melt impregnation at a line speed of 15m/min, showing the reduction in the forces measured as the level of melt in the bath falls.

peak values were disregarded and an average force was calculated by taking readings at 1 second intervals. These values were then used to calculate the tension build-up in the fibre tows during their passage over the instrumented impregnation bar.

6.2.4 Results

The input and output tensions, T_0 and T_3, were calculated from the recorded load cell output as detailed in section 5.2.5. The tension build-up, T_3-T_0, was then plotted against the wrap length, $R\theta$, for each line speed and bar radius studied.

The relationship between the tension build-up and wrap length for an impregnation bar of radius 5mm, at impregnation line speeds of 5, 10 and 15m/min is shown in Figure 6.2.3. The most noticeable feature was that the tension build-up with increasing wrap length was non-linear and a higher tension build-up occurred for increased line speeds. Extrapolating each of the curves to a zero wrap length gave rise to non-zero tension, which also increased with line speed. The different points plotted for each wrap length in Figure 6.2.3 illustrate the range of values calculated for T_3-T_0 and a greater scatter was present for runs carried out at 15m/min. This was mainly due to difficulties in maintaining a constant melt level in the impregnation bath. As the level fell, the measured forces decreased rapidly and a number of short impregnation experiments were required at high line speeds. This applied equally to all the different bar radii studied.

The form of the curve fitted to the experimental points was somewhat open to interpretation. However, it was possible to distinguish three stages of tension build-up. The tension appeared to build up from an initially low value and then rise more steeply in the intermediate wrap lengths examined. At higher wrap lengths the tension build-up appeared to increase linearly with wrap length.

The effect of increasing the radius of the impregnation bar can be seen in Figure 6.2.4, which shows the tension build-up with wrap length and line speed for a 7.5mm radius impregnation bar. The biggest effect of increasing the bar radius was that the tension generation was lower for equivalent wrap lengths. It was interesting that the form of the increase was similar to that seen in Figure 6.2.3 and again three stages of tension generation were identified. Extrapolating to a zero wrap length gave rise to a non-zero tension, which was similar in magnitude to that

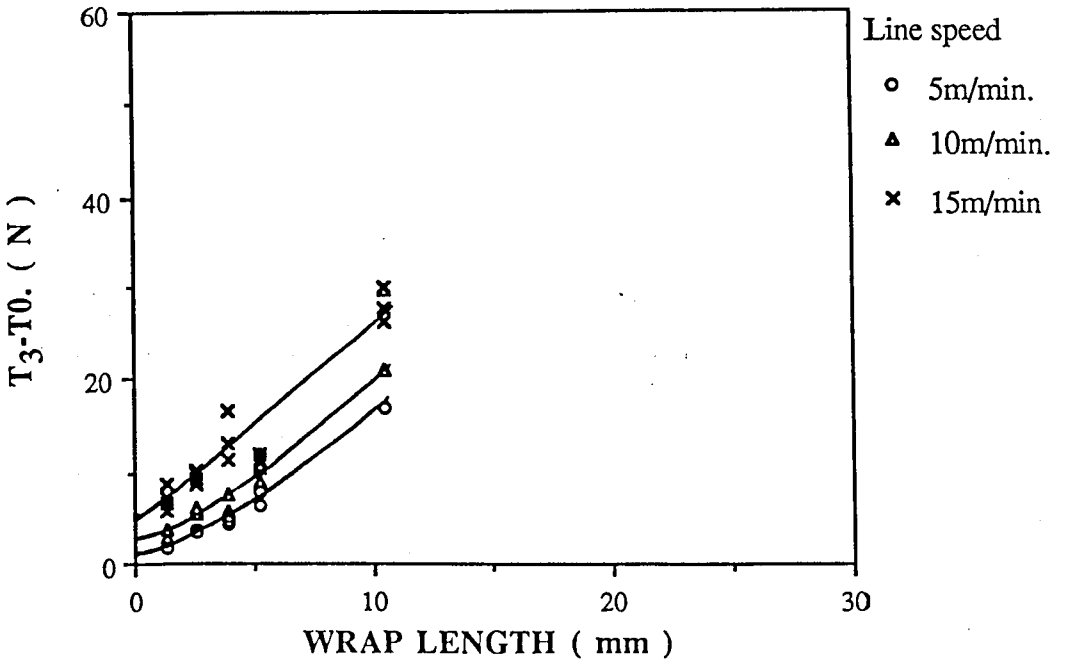

Figure 6.2.3. Relationship between tension build-up and wrap length for an impregnation bar radius 5mm, at line speeds of 5,10 and 15m/min.

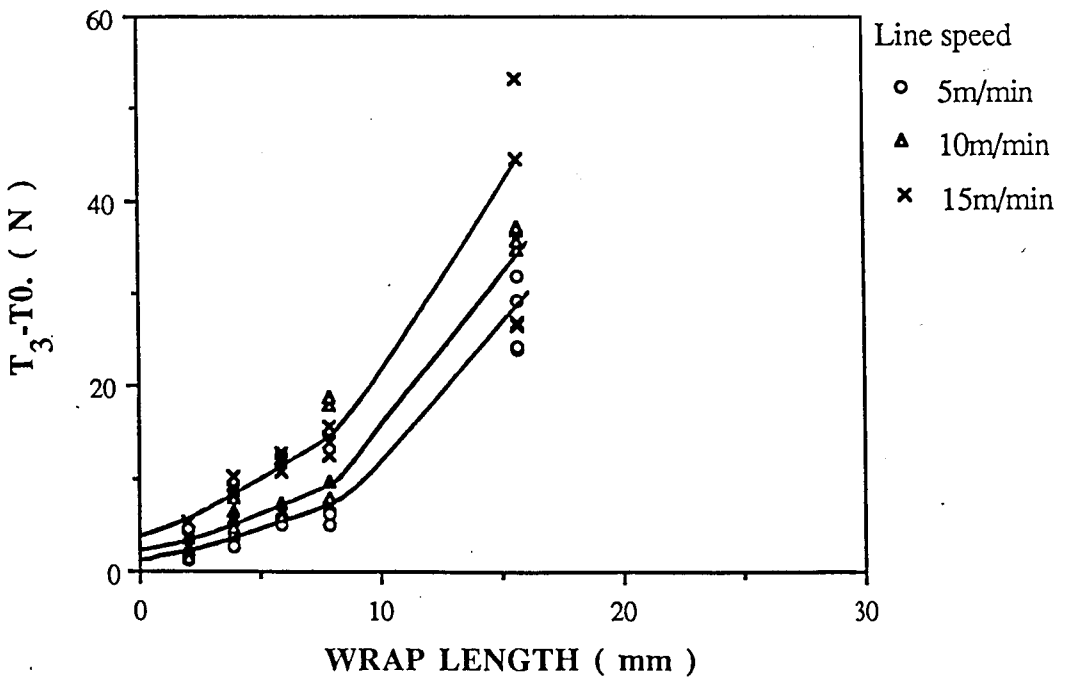

Figure 6.2.4. Relationship between tension build-up and wrap length for an impregnation bar radius 7.5mm, at line speeds of 5,10 and 15m/min.

observed for the 5mm radius bar.

Neither the 5mm or 7.5mm bars were equipped with sideguides to limit the lateral flow of resin from beneath the fibre tows, sideways in the direction of lowest resistance to flow. In order to examine the effect of restricting such flow, which was likely to increase the thickness of the polymer film between the tow and the bar, experiments were carried out on a 10mm radius impregnation bar without and with sideguides. These restricted the maximum tow-spreading to 20mm and prevented lateral polymer flow.

Figure 6.2.5 shows the tension build-up as the tows passed under the 10mm bar without sideguides. The form of the increase was similar to that seen for the 5 and 7.5mm bars and once again the tension build-up was higher for increasing line speeds. The tension build-up was also lower than measured on either the 5 or 7.5mm bar. For instance the tension build-up at 5m/min, for a wrap length of 10mm, on the 5, 7.5 and 10mm bars was recorded as 16N, 9N and 7N respectively. Extrapolating to a zero wrap length resulted in a non zero tension, as was found for all the impregnation bars.

Although it was not possible to measure the tow spreading when the bath was full of molten nylon, visual observation of the tows passing around the bars indicated that the fibres usually spread to the full 30mm width of the bar. Because the measuring bar was suspended in the nylon melt without touching the sides of the bath, in some cases the tows spread over the edges of the bar. This made it necessary to stop the experimental run while the tows were replaced beneath the bar. The addition of the side guides prevented the tows from spreading further than 20mm.

The tension build-up in the fibre tows passing around the 10mm bar with sideguides is shown in Figure 6.2.6. As expected, the form of the increase in tension build-up was similar to that observed for all the previous bar sizes and extrapolating to zero wrap length resulted in a non-zero tension. It was however, interesting that the overall tension increase was significantly reduced by the addition of sideguides, while all the other processing parameters; bar radius, line speed, wrap angle and melt viscosity remained constant. This result indicated that the spreading of the fibre tows and the thickness of the resin film between the fibres and the impregnation bar was very important in determining the tension build-up.

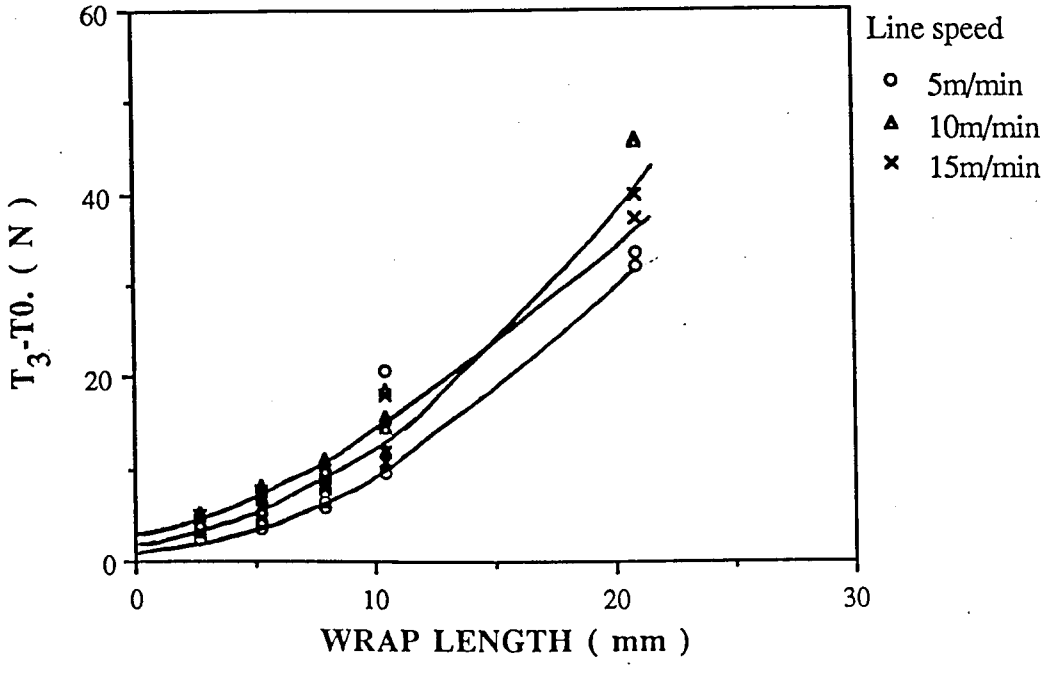

Figure 6.2.5. Relationship between tension build up and wrap length for an impregnation bar radius 10mm, at line speeds of 5,10 and 15m/min.

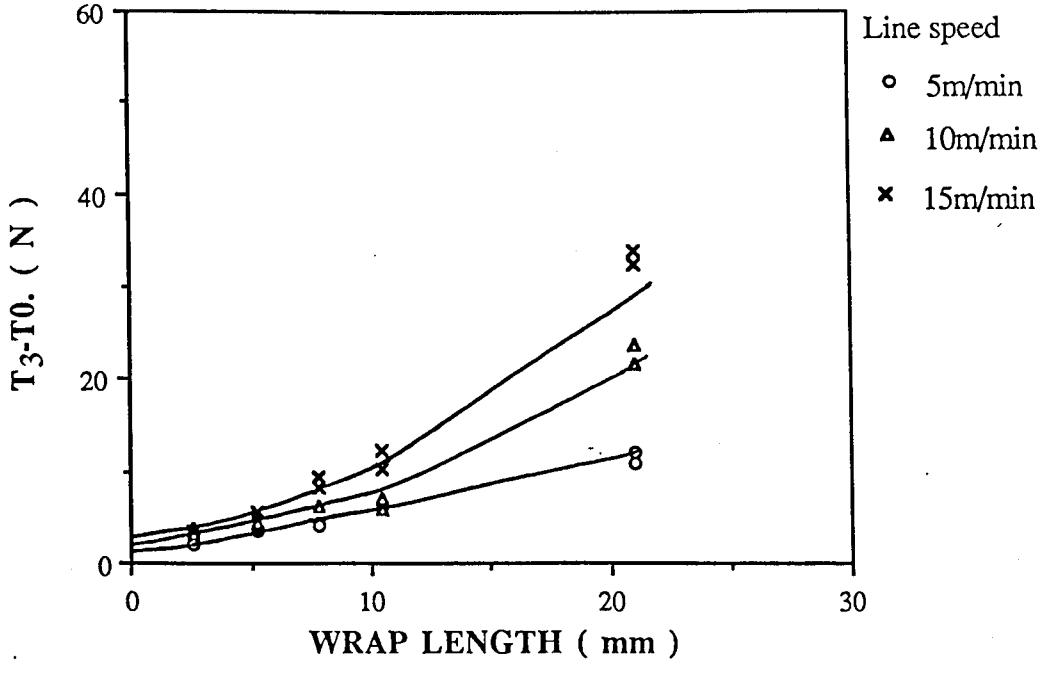

Figure 6.2.6. Relationship between tension build-up and wrap length for an impregnation bar radius 10mm, equipped with sideguides, at line speeds 5, 10 and 15m/min.

The increase in tension build-up at higher wrap lengths also appeared to be much more gradual when sideways flow was restricted.

The largest bar radius examined was 15mm, and the tension build-up with wrap length is shown in Figure 6.2.7. Only two line speeds, 5 and 10m/min were studied for this bar radius. The tension build-up for equivalent wrap lengths at this radius was lower than at any of the smaller bar radii. The increase in tension build-up, although smaller, followed similar trends to those observed for all the bars examined previously. At 5m/min and at a wrap length of 10mm, the tension build-up was only approximately 4N.

A number of features of the tension build-up during the impregnation of two glass fibre tows with a nylon 6,6 melt were apparent from Figures 6.2.3 to 6.2.7.

It was found that the forces T_3-T_0, increased non-linearly with increasing wrap length and that the form of the increase appeared to be independent of the radius of the impregnation bar and the impregnation line speed. For each bar radius examined, the forces increased with impregnation line speed. Extrapolating to zero wrap length gave rise to a non-zero tension value. This initial tension appeared to be independent of bar radius but was dependent on line speed. The value of the initial tension build-up was estimated as approximately 1N at 5m/min, 2N at 10m/min and 4N at 15m/min. As the radius of the impregnation bars were increased, the tension build-up decreased for equivalent wrap lengths. It was also found that the tension build-up could be significantly reduced by using side guides to restrict tow spreading and to prevent the lateral flow of nylon melt from beneath the fibre tows.

It was possible to interpret the increase in T_3-T_0 as taking place in three stages. The first of these was a low tension increase at small wrap lengths. As the fibres approached the bar they dragged a certain thickness of resin into the gap between the fibres and the bar. However, at low wrap lengths the pressure build-up in this resin film was unlikely to become sufficiently high to pump resin through and out from under the tows, so causing impregnation and reducing the film thickness sufficiently to initiate contact between the fibres and the bar. Therefore, because the film thickness remained relatively high at low wrap lengths, impregnation flow, contact resistance and drag forces did not contribute greatly to the overall tension increase.

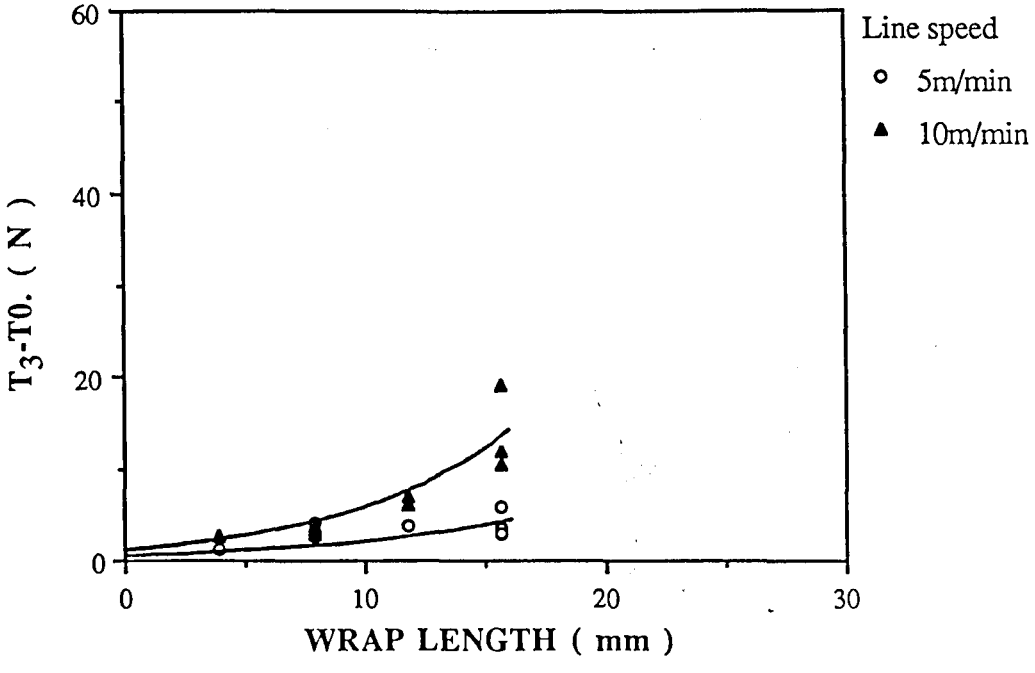

Figure 6.2.7. Relationship between tension build-up and wrap length for an impregnation bar radius 15mm, at line speeds 5 and 10m/min.

The second region of tension build-up occurred at intermediate wrap lengths and marked a transition between the low tension build-up at short wrap lengths and the rapidly increasing build-up observed at higher wrap lengths. In this region the pressure build-up in the resin film had increased sufficiently to cause flow of resin through and out from beneath the fibre tow. This caused impregnation of the fibre tows accompanied by a gradual reduction in the film thickness between the fibres and the bar. This in turn was accompanied by increased viscous drag and contact forces acting on the fibre tows which increased the total tension build-up.

The third region of tension build-up occurred at high wrap lengths and indicated a high rate of tension build-up. As the film thickness was reduced during impregnation, the fibre tows came more closely into contact with the impregnation bar and drag and friction forces became more important to the overall tension increase. Only a certain maximum level of impregnation was likely to occur as the permeability of the fibre tow became reduced as it filled with resin. Therefore, at some stage no more resin was removed from beneath the fibres and the film thickness remained constant until the fibres left the bar. Then the dominant forces acting on the fibre tows were drag forces in the thin resin film coupled with coulomb friction where the fibres contacted the bar. It was possible that both these mechanisms were operating simultaneously across the width of the bar, with some fibres contacting the bar while others were lubricated.

Lubrication theory has been applied to explain the behaviour of lubricated foil bearings and has been detailed in Section 2.2.2. To recap, in the case of a foil bearing, three regions of different behaviour were identified; an exponential entry region in which the pressure increased as the film thickness decreased, a central region in which the film thickness and pressure remained constant and an exit region. The form of the film thickness and pressure variation with wrap length are illustrated in Figure 6.2.8. It is possible that similar regions exist according to the variation of resin film thickness in the case of a tow of fibres pulled over a stationary impregnation bar immersed in a polymer melt.

In the melt impregnation process, an entry zone was formed in which the gap between the fibre tow and the bar decreased as the fibres approached the bar. A pressure was generated in the resin film which eventually reached a value sufficient to pump resin through the porous fibre tow and, if allowed, laterally out from beneath the fibre tows. This was the second region of behaviour and was probably the region in which the majority of impregnation took place. The third region of

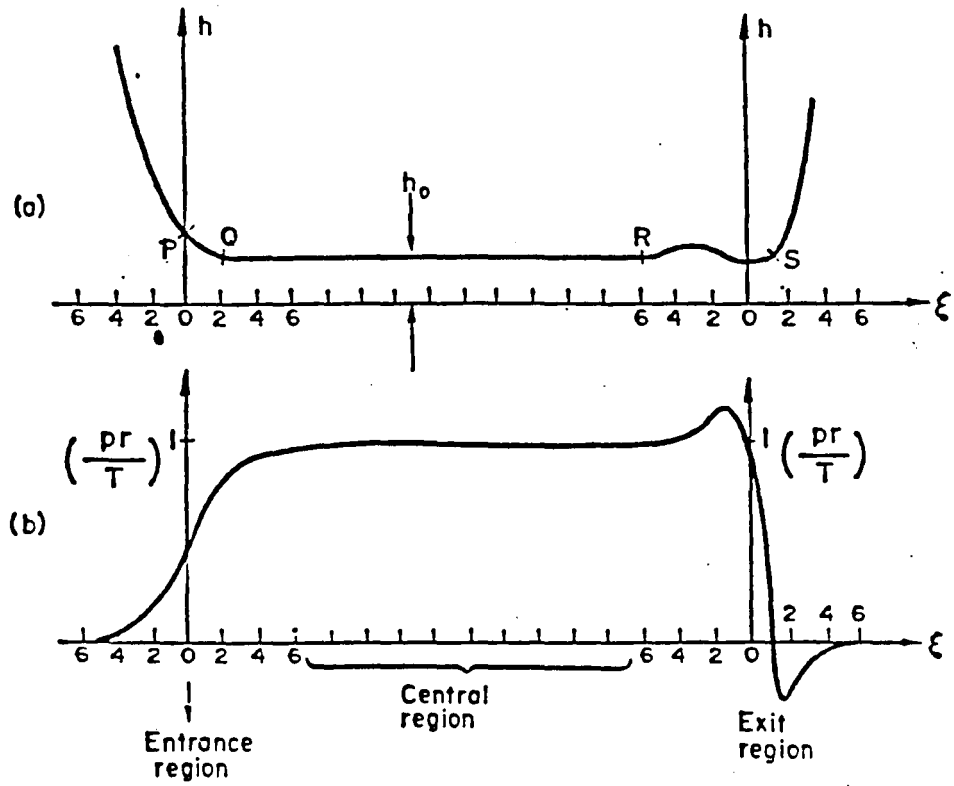

Gap and pressure in perfectly flexible foil bearing.

Figure 6.2.8a. Film thickness variation and pressure profile plotted against wrap length around a perfectly flexible foil bearing, after Moore (1975).

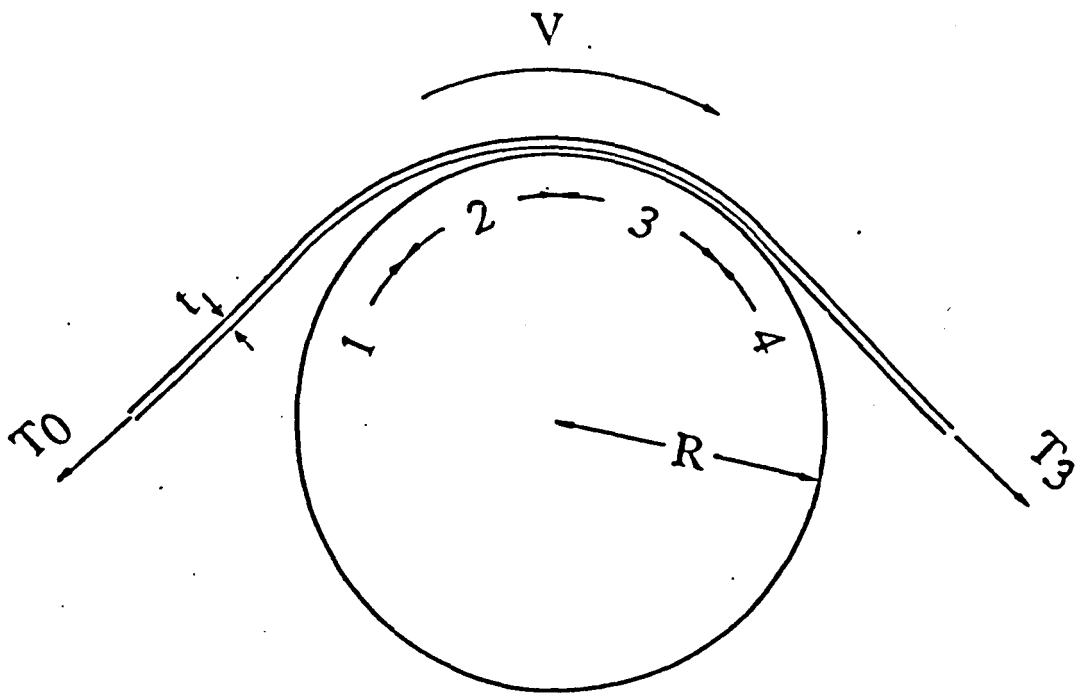

Regions of behaviour in pin impregnation: 1 entry; 2 impregnation; 3 contact; 4 exit.

Figure 6.2.8b. Possible impregnation zones when a fibre tow is pulled around a cylindrical bar, after Chandler et. al. (1992).

behaviour was one which began when sufficient resin had been pumped through and out from under the fibre tow to cause contact with the surface of the impregnation bar. The final region was the exit region where the impregnated fibre tow left the bar.

The effect of increasing the line speed was to generate a higher tension build-up throughout the range of wrap lengths. Nylon is non-Newtonian and its viscosity is dependent on the applied shear rate as illustrated in Figure 5.2.1. Therefore, at higher line speeds the melt viscosity would have been lower because of the increased shear rate. This resulted in an increased polymer flow through and from beneath the fibre tows which in turn generated higher tensions in the fibre tows.

The addition of side-guides to the 10mm bar resulted in a significant reduction in the overall tension build-up. In this case, the reduction in the film thickness occurred only by resin flow through the fibre tows, without any accompanying lateral flow. Assuming that the pressure build-up and the initial film thickness were the same, regardless of the presence of the sideguides, then the film thickness would have reduced over a much shorter wrap length in the case of the "open" bar, mainly due to the additional lateral flow. Therefore contact and drag forces would have started to build-up at relatively short wrap lengths. In the case of the bar with sideguides, a certain film thickness would have remained beneath the tows over a longer contact length, trapped between the polymer-filled tow and the side guides. This would have resulted in the reduction in the tension build-up at higher wrap lengths for the bar with sideguides.

The effect of side-guides on the velocity dependence of tension build-up can be seen by comparing Figures 6.2.5 and 6.2.6. Because of the side restraint, no polymer flow could occur sideways, regardless of the line speed or the melt viscosity. The flow of polymer melt through the fibre tows would have therefore increased due to the decreased melt viscosity. As the speed increased the fibre tows created a thicker film in the entry gap, shown by the increase in the initial tension at zero wrap length. This increase in the initial film thickness, coupled with the restriction on sideways flow resulted in the length of the impregnation zone increasing with line speed. This was important because in order to optimise impregnation it is necessary to make the impregnation region as long as possible.

The effect of increasing the radius of the impregnation bar was to reduce the overall

tension generation throughout the range of wrap lengths. The tension build-up on the 5mm bar was substantially higher than measured on the 15mm bar for equivalent wrap lengths. As the radius of the bars was increased, it should be noted that smaller wrap angles were required to give equivalent wrap lengths. This will have resulted in a smaller pressure build-up in the resin film for higher bar radii. The wrap length over which the intermediate tension build-up occurred, ie. region 2, also appeared to increase with bar radius. Because of the reduction in the pressure build-up in the film, a longer wrap length would be required to cause a reduction in the film thickness to a level where contact and drag forces began to significantly effect the tension build-up. Thus the impregnation region would be extended. Eventually the resin film would reduce sufficiently to create drag and contact resistance between the fibres and the bar and the tension would begin to rise. Although the overall tension build-up was lower at higher radii, the form of the tension build-up was independent of bar radius. Therefore it can be assumed that similar mechanisms were contributing to the tension build-up regardless of the radius of the bar.

6.2.5 Modelling the melt impregnation process

A simple impregnation model has been used to describe the tension build-up per unit width in a permeable tow of fibres, as they are pulled around a cylindrical bar immersed in a viscous liquid, Chandler et al. (1992). The model has been described fully in Chapter 4 and was developed using basic lubrication theory. The model applies, in this instance, only to the case in which no lateral polymer flow takes place, ie. bars equipped with sideguides. In the experimental program only one bar was equipped with sideguides and the results from these experiments have been used to verify the modelled tension build-up. The bar radius was 10mm and the tow width was restricted to 20mm. Because of the difficulty in controlling the value of the initial tension T_0, an average of 30N was calculated from the experimental results and this value was used in the modelled solutions. The model also assumed a Newtonian viscosity, whereas the nylon melt obeys a power law relationship in the form: $n=A.\dot{\gamma}^{n-1}$.

The constants A and n were calculated from Figure 5.2.1 as A=62.1 (for shear rates in /s and viscosity values in Pa.s) and n=0.81. The effective shear rate in regions 1 and 2 was taken to be V/h_0 and this was used to calculate the viscosity. The

viscosities for line speeds 5, 10 and 15m/min in regions 1 and 2 were calculated as 18.5 Pa.s, 17.6 Pa.s and 17.1 Pa.s respectively. In region 3 the shear rate was assumed to be V/h_1.

In modelling the observed tension build-up three parameters could be varied: the permeability/tow thickness ratio, Φ/t ; the effective film thickness in region 3 after the tow has been impregnated, h_1; and the friction coefficient, μ. The first two could in principle, be calculated, but both required an in-depth consideration of polymer flow through fibre beds. This was beyond the scope of the initial modelling described in this case. The modelling of polymer flow through porous media has been reviewed in detail by Astrom et al. (1991)[49]. All three parameters were varied and their effect on the predicted values of tension build-up examined. It was found that very low values of the friction coefficient were required for the present results, so this parameter was set to zero.

Good degrees of fit were achieved for a range of values of h_1 and Φ/t, using equations 4.13, 4.14, 4.19 and 4.21, as described in Chapter 4. A physically reasonable value of 50 microns was chosen for h_1 and Φ/t was varied to optimise the fit to the experimental results.

The computed results for h_1=50 microns and $\Phi/t=1.5.10^{-7}$m and μ=0 were compared to the experimental data in Figures 6.2.9 to 6.2.11. It can be seen that, within the range of experimental scatter, there was good agreement between the model and the experimental results over the range of line speeds and wrap lengths studied. For each speed there was an initial region of low tension build-up, corresponding to the entry and impregnation region, followed by a zone of linear tension build-up, associated presumably with the contact region. Each of the curves approached a constant value at zero wrap length. This initial tension build-up also increased with line speed as was found for the experimental results shown in Figure 6.2.6. The predicted values of initial film thickness, h_0, were 143, 220 and 282 microns respectively for the three increasing velocities. The length of the impregnation region increased with line speed, as seen by comparing Figures 6.2.9 to 6.2.11.

In conclusion, this model was capable of describing the experimental tension build-up in glass tows passing over a cylindrical bar immersed in a nylon melt. The key features of the experimental tension build-up measured on impregnation bars with side-guides were reproduced.

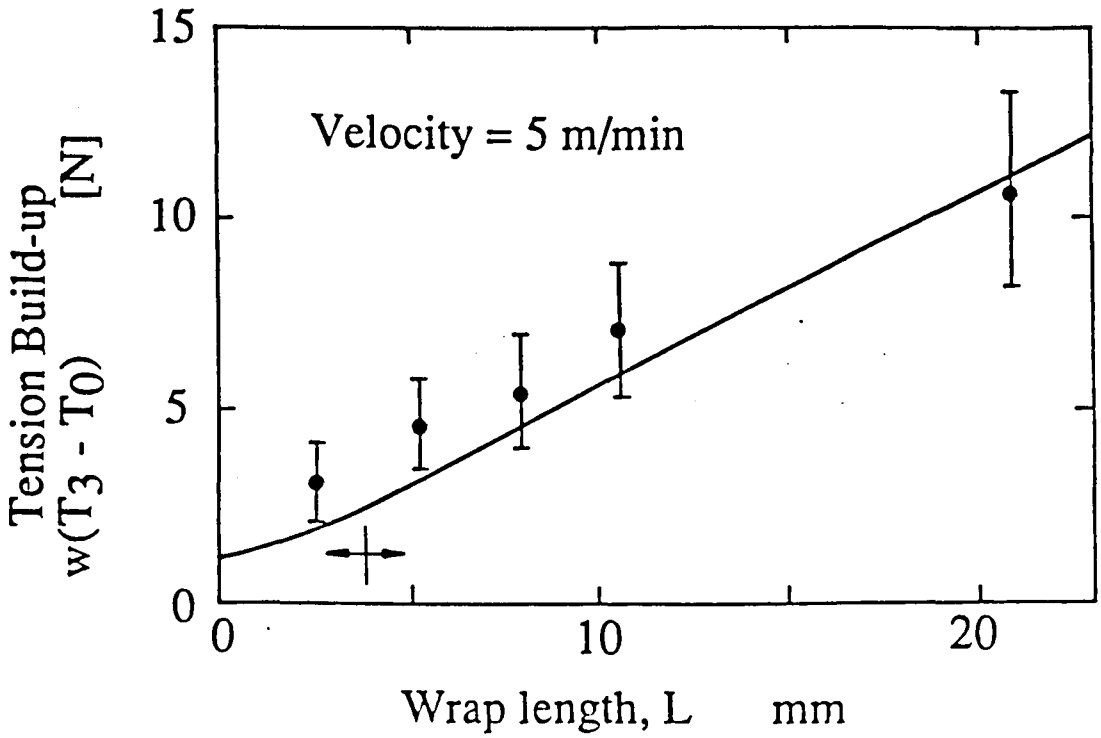

Figure 6.2.9. Relationship between tow tension build up, $w(T_3-T_0)$, and wrap length for impregnation of two 2400 Tex E-glass tows in nylon 6,6 resin at 285°C. R=10mm; w=20mm. Initial tension=30N. Velocity=5m/min.

o Experimental points. Continuous line is the model prediction for h_1=50μm, $\phi/t=1.5.10^{-7}$m and μ=0. Arrow indicates transition from impregnation region to contact region. Error bars: 95% confidence interval.

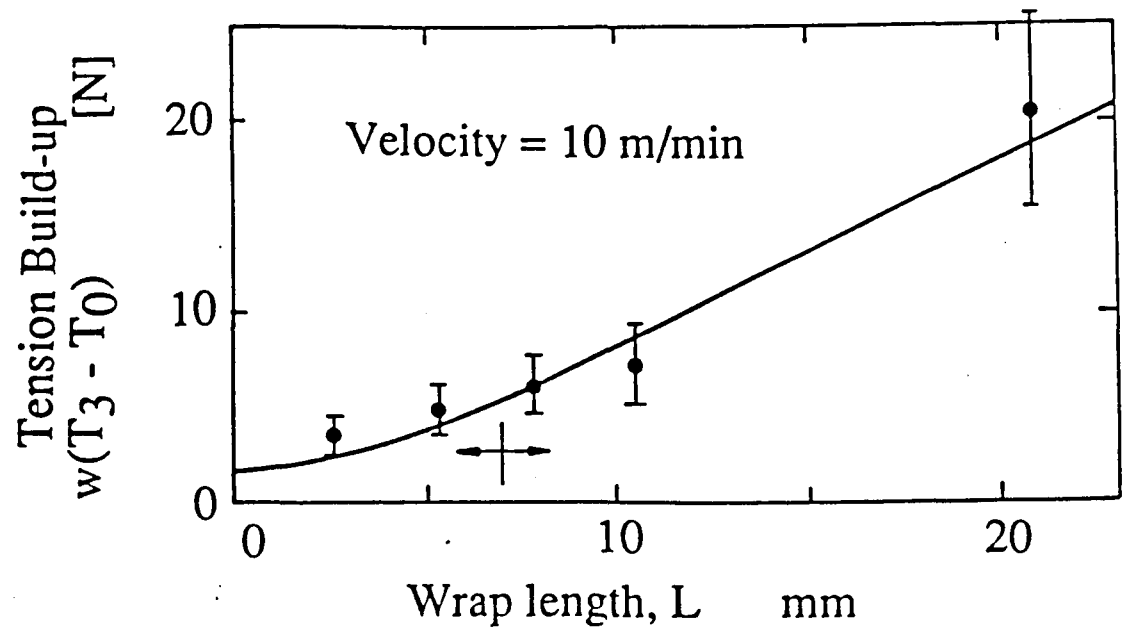

Figure 6.2.10. Tow tension build-up vs. wrap length for velocity 10m/min. Key as for Figure 6.2.9.

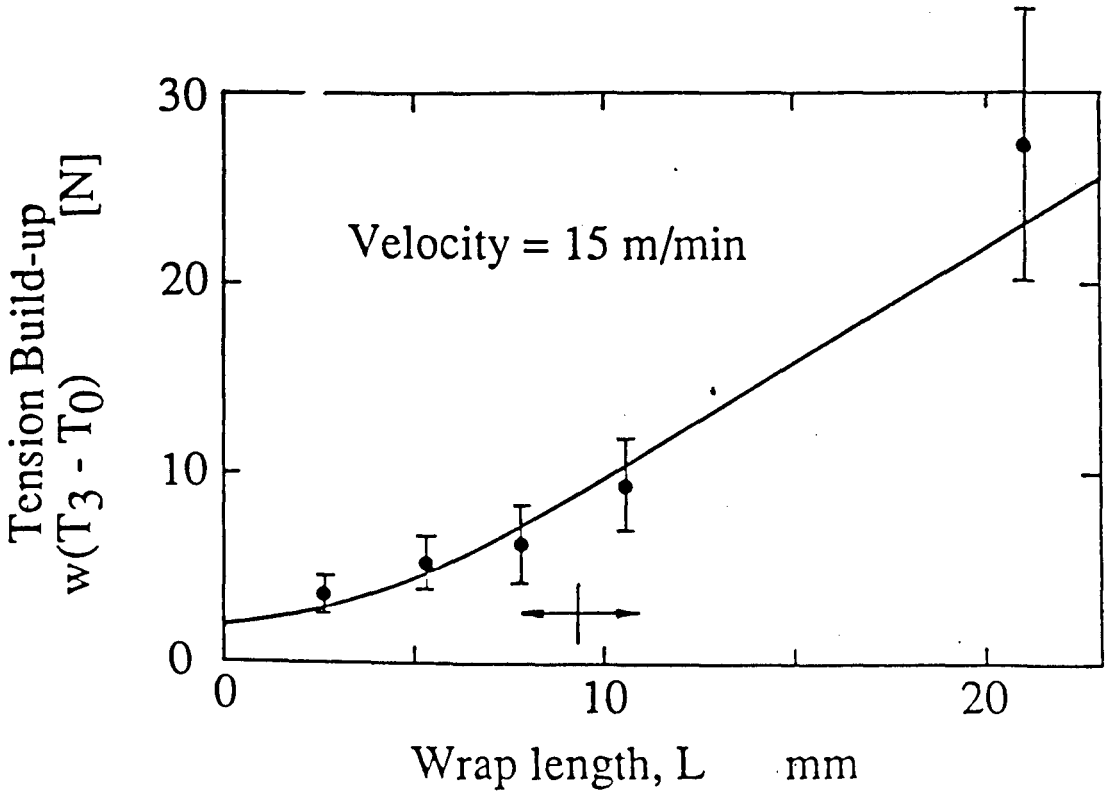

Figure 6.2.11. Tow tension build-up vs. wrap length for velocity 15m/min. Key as for Figure 6.2.9.

Chapter 7. Conclusions

7.1 The pultrusion of thermoplastic matrix composites

An experimental pultrusion line was developed which consisted of a combined infra-red/hot air heating stage followed by either cold, temperature un-controlled forming rolls or temperature controlled dies. It was possible to produce a rectangular flat strip section using various pre-impregnated, unidirectional reinforced precursors and line speeds up to 8.5m/min were achievable. The effect of changing process parameters on the mechanical properties of sections produced using nylon 12/glass, polypropylene/glass and PEEK/carbon were investigated. It was necessary to limit line speeds to a maximum of 5m/min in the experimental work reported because of the limited availability of precursor materials.

7.1.1. Roll forming

It was found that the interlaminar shear strength and flexural strength of roll formed sections pultruded using nylon 12/glass precursors were dependent on the line speed, oven temperature and roll forming pressure.

The dominant factor controlling the quality of the roll formed pultruded sections at speeds below 1.5m/min was found to be the contact length in the forming stage of the process and the time for which the forming pressure was applied. As the line speed increased, there was a rapid decrease in the forming and consolidation time which corresponded to a decrease in the interlaminar shear strength, a reduction in the flexural strength and an increase in the void content. The void content for roll formed sections ranged between 1.5 to 11%, depending on the line speed and processing temperature. It was found that a rapid temperature decrease occurred in the surface layers of the unconsolidated prepreg bundle immediately on contact with the cold roll surfaces. This caused air to become trapped in the consolidated section, forming voids and reducing the interlaminar shear and flexural strength of the pultruded sections.

At higher line speeds, >2m/min, the dominant effects on the properties of the sections produced were the very short forming times combined with the reduction

in the temperature of the precursor material entering the roll gap. As the line speed increased there was a reduction in the dwell time in the oven which, because the oven was not directly controlled by sensing the temperature of the material leaving the oven, resulted in a gradual reduction of the precursor temperature at higher line speeds.

It was possible to improve the properties and reduce the void content of the pultruded sections by increasing the oven temperature. Increasing the oven temperature also increased the range of line speeds for which acceptable pultrusions could be produced. The maximum oven temperature was limited by degradation of the precursor tows, although it was possible to produce acceptable sections at up to 60°C above the melting point of the nylon matrix material.

It was found that increasing roll pressure was deleterious to the overall properties of the sections produced. This was due to improved heat transfer between the composite section and the cold roll surfaces. No reduction in void content was found in sections produced at higher roll pressures and this gave a further indication that no additional consolidation was occurring. Increasing the roll pressure was also found to cause sections to bow due to stresses being frozen into the rapidly cooled and consolidated sections. This bowing increased with roll pressure.

It was possible to pultrude sections at speeds up to 0.7m/min which achieved up to 65% of the interlaminar shear strength and 80% of the flexural strength of comparable compression moulded sections. For roll formed PEEK/carbon sections, interlaminar strengths of 92% and flexural strengths of 72% of the optimum quoted for compression moulded sections were achieved at a line speed of 1m/min.

7.1.2. Die forming

It was also possible to pultrude polypropylene/glass sections using constant pressure, heated forming dies. In this instance the contact length was 270mm compared to a maximum of 10mm in the rollers. Using the die system, it was possible to increase the degree of consolidation and thus increase the strength and modulus of pultruded sections by increasing the forming pressure. The optimum die pressure was found to be 319KPa. The decrease in flexural strength and modulus with increasing line speed was more gradual than that observed for the

interlaminar shear strength of roll formed sections. This was attributed to the increased contact length in the dies and the application of the forming pressure without solidifying the surface layers of the precursor bundle. No bowing occurred in sections produced at high pressures using the dies. The void content of die formed sections were also lower than found for sections produced at the same line speeds using rollers. The pulling force necessary for die pultrusion appeared to be higher than in the case of the rollers and some wipe-off occurred in the die entry region. The position of the dies and the temperature of the material entering the dies was found to be very important in producing a section with a good surface finish.

7.1.3 Heat transfer modelling

It was possible to model heat transfer during the heating, forming, cooling and consolidation stages of the pultrusion process using a one dimensional, finite difference model. The model could be applied to either roll or die forming and was used as a process aid to determine the optimum positions of the forming dies for different line speeds.

7.1.4. Summary of conclusions

It was possible to pultrude thermoplastic composites using forming and consolidation rollers. However, the contact length was very short and increasing line speed caused a sharp decrease in the contact time in the rolls. This was reflected in a decrease in the mechanical properties of the pultruded sections. The cold, stainless steel rolls resulted in quenching which caused a solidified skin to form at the surfaces of the partially consolidated section. This in turn caused air entrapment and the formation of voids. As the forming pressure was increased the thermal contact was improved and this resulted in additional cooling which prevented further consolidation. High roll pressures also caused sections to bow as a result of frozen in deformation. Overall, the main drawback to roll forming was the short contact length and the quenching effect of the cold rolls.

It was also possible to use heated dies to pultrude thermoplastic composites. The heated dies allowed forming and consolidation to occur without uncontrolled quenching of the partially consolidated section. Increasing the die pressure was

found to improve the overall product properties. The optimum die pressure was found to be 319KPa, above which friction and pull forces in the die increased. This caused a reduction in the flexural strength and modulus and in the quality of the surface finish. Void contents were generally lower than found for roll formed sections. The main advantage in using heated dies was more efficient forming and consolidation. However pull forces appeared to be higher than in roll forming and it was difficult to prevent additional wipe-off.

In summary, it was possible to pultrude sections using either rolls or dies and the contact length was a very important factor. It was important to control the initial cooling during forming and consolidation. Although the mechanical properties decreased with line speed it was possible to alter this by either: increasing the contact length; increasing the temperature of the material entering the forming stage; or increasing the temperature of the forming/consolidation stage. It was possible to model the temperature distributions during the different process stages for different line speeds, oven temperatures and die temperatures.

7.2. Thermoplastic melt impregnation

The tension build-up during thermoplastic melt impregnation was investigated. The tension build-up was found to increase non-linearly with increasing wrap length and was found to increase with line speed. The form of the increase appeared to be independent of the bar radius and line speed. The tension build-up for equivalent wrap lengths decreased as the bar radius was increased. The effect of tow spreading was significant and restricting tow spreading caused a reduction in the tension build-up. It was possible that three stages of tension build-up occurred. These corresponded to an entry region as the fibres approached the bar, an impregnation region as resin flowed through the fibre bed and a region in which drag and friction forces predominated as the fibres came into contact with the impregnation bar.

Lubrication theory was applied to model the tension build-up during the impregnation process and good degrees of fit were obtained in the case of a 10mm radius impregnation bar fitted with side-guides to restrict tow spreading.

7.3 Future work

Although it is possible to pultrude thermoplastic composites in simple sections, further work is required to make the process commercially viable.

Possible future work includes a determination of the optimum forming length and forming pressures for pultrusion at increased line speeds and preventing a decrease in properties with line speed. An investigation of heated rollers would be useful and it may be the case that the process could use a combination of dies and rollers as the forming/consolidation stage. Work remains to be carried out on producing a range of sectional shapes, including round rod and channel sections. Also the feasibility of producing thick, wide sections and the possibility of incorporating non-unidirectional reinforcement needs to be examined. The magnitudes and origin of pull forces generated during pultrusion need to be measured and modelled for different process conditions as a further step in optimising the process. Also, the design of the die entry region in order to minimise force generation and wipe-off remains to be optimised.

The basic heat transfer model requires further development to model the effect of increased roll pressure on the temperature distributions during forming and to model the effect of heating the forming rolls. It also requires to be adapted for other sectional shapes, most importantly circular and channel or top-hat sections.

Further work is also required on the basic mechanisms operating during thermoplastic melt impregnation in order to optimise the impregnation processing step. This work may include a study of the optimum bar radius, bar cross-sectional shape, tow paths in the impregnation bath and a possible re-design of the wipe-off die to reduce tension generation and aid impregnation. A more reliable method than visual examination for determining the impregnation efficiency also needs to be developed.

List of publications.

1. B.J. Devlin and A.G. Gibson.
Pultrusion of Unidirectional Composites with Thermoplastic Matrices.
In press, Composites Manufacturing, April 1992.

2. Chandler, H., Devlin, B.J., Gibson, A.G.
The Mechanics of Impregnation of Unidirectional Fibre Tows.
In press, Plastics and Rubber Processing and Applications, March 1992.

References.

1. Yarsley, V.E., Couzens, E.G.
Plastics, Penguin Books, 1941.

2. Gordon, J.E. The New Science of Strong Materials., Penguin, 1968.

3. Cox, H.L. The elasticity and strength of paper and other fibrous materials. British Journal of Applied Physics, Vol 3 (1952), pp 72.

4. Kelly, A., Tyson, W.R.
Tensile properties of fiber reinforced metals: Copper-Tungsten and Copper-Molybdenum. Journal of Mechanics and Physics of Solids, Vol 13, 1965, pp329.

5. Crawford, R.J. Plastics Engineering, Pergammon Press 1987, pp 95.

6. Leach, D.C. Advanced Composites, Ed. I. K. Partridge, Elsevier Applied Science, 1989, pp 43.

7. Cattanach, J.B., Cuff,G., Cogswell, F.N.
The processing science of thermoplastics containing long and continuous reinforcing fibres. J. Polymer Eng. 6, 1986, pp 345-363

8. Bader, M.G., Bowyer, W.H.
An improved method for production of high strength fibre reinforced thermoplastics. Composites, July 1973, pp 150.

9. Von Turkovich et al.
Fiber fracture in reinforced thermoplastic processing. Polymer Engineering and Science, 23, 1983, pp743.

10. Franzen, B., Klason,C.,Kubat,J.,Kitano,T.
Fibre degradation during processing of short fibre reinforced thermoplastics. Composites 20, No 1. January 1989 pp 65-75.

11. Lunt, J.M., Shortall J,B.
The effect of extrusion compounding on fibre degradation and strength properties in short glass-fiber-reinforced nylon 6,6. Plastics and Rubber Processing, June 1980, 37.

12. Price, R.V. Patent Appln., 127 302, June 25 ,1973.

13 Chabrier, G U.S. Patent No. 4,626,306, Dec 2 1986.

14 Hartness T. Thermoplastic powder technology for advanced composite systems Proc. 33rd International SAMPE Symposium, March 7-10 1988 pp 1458-72.

15 Friedrich K. Thermoplastic impregnated fibre bundles: Manufacturing of laminates and fracture mechanics characterization. Composites Science and Technology, 33, 1988, pp 97-120.

16. Carlsson, L, A., Pipes, R. B
Experimental Characterization of of Advanced Composite Materials, Prentice Hall, Englewood Cliffs, NJ, 1987.

17. Titow W,J., Lanham B,J.
Reinforced Thermoplastics, Chapter 1, Applied Science Publishers Ltd. 1975.

18. Bader, M.G., Bowyer, W.H.
An improved method for production of high strength fibre-reinforced thermoplastics. Composites July 1973, pp 150.

19. McMahon, P.E.
Developments in Reinforced Plastics 4. Applied Science Publ. 1984, Ch.1. pp1.

20. Folkes, M.J., Kells, D.
Fundamental considerations in the injection processing of fibre reinforced thermoplastics. Plastics and Rubber Processing and Applications 5, 1985, pp124-131.

21. Moyer, R.L. U.S. Patent No. 3,993,726. Nov. 23, 1976.

22. Chandler, H., Devlin, B.J., Gibson, A.G.
Mechanics of the impregnation of unidirectional fibre tows. Plastics and Rubber Processing and Applications. In press, March 1992.

23. Cowen, G., Measuria, U., Turner, R.M.
Section pultrusions of continuous fibre reinforced thermoplastics. Proc. Fibre Reinforced Composites 1986, C22, pp105.

24. Bijsterbosch, H., Gaymans, R.J.
Pultrusion with a nylon 6 melt. Proceedings Fibre Reinforced Composites 1990.

25. Mc Mahon, P.E., Maximovich M.
Development and evaluation of thermoplastic/carbon fiber prepregs and composites. ICCM-III Proc., Vol II. pp1663. 1980.

26. Custer , M.F. Pultrusion impregnated thermoplastic tape. 20th International SAMPE technical conference, Sept 1988, pp366.

27. Goodman, K.E., Loos, A.C. Thermoplastic prepreg manufacture. Journal of Thermoplastic composite materials, Vol 3, January 1990, pp34.

28. Van Loo, K. Cost effective processing with continuous fibre reinforced Thermoplastics. Proc. Fibre Reinforced Composites 1988, Paper 10.

29. Courtaulds 'Heltra' product data sheet, 1988.

30. Schappe product data sheet, 1988.

31. Van Damme, P.A.
Economic composites for mass production in the automotive industry. Proc. Fibre Reinforced Composites 1988, Paper 1.

32. Cuff, G. Paper 19, Proceeding of the British Plastics Federation 14th Reinforced Plastics Congress, Brighton, November 1984.

33. Henshaw J.M., Wilkins D.J.
Comparison of long and short fiber injection moulded electrical connector housings. Composites Manufacturing, Vol. 1 No.1, March 1990 pp26.

34. Cogswell, F.N.
The processing science of thermoplastic structural composites. Int. Polym. Proc. 1 (4) 1987 pp157-65.

35. Friedrich K. Stamp forming of continuous carbon fibre/polypropylene composites. Composites Manufacturing Vol 2. No.1. March 1991, pp3.

36. O'Bradaigh C., Mallon, P.J.
Development of a pilot autoclave for polymeric diaphragm forming of continuous fibre-reinforced thermoplastics. Composites, 19, 1, 1988 pp 37-47.

37. Monaghan, M., Mallon, P.J.
Development of a computer controlled autoclave for forming thermoplastic composites. Composites Manufacturing, Vol. 1 No.1, March 1990 pp8.

38. Whiting J.A.S.
Thermoplastic filament winding using controlled infra-red heating. Proceedings ICAC 91,15-17 October 1991, paper 27.

39. Anderson ,T.L.
Room temperature filament winding of thermoplastic fibre composites. Proceedings ICAC 91,15-17 October 1991, paper 26.

40. Cattanach, J.B., Harvey R.C.
ICI, Application note, Roll forming. 1984.

41. Martin J. Pultrusion, Chapter 3, pp37

42. Ed. J.R O'Connell.
Committee for Electroheat. Electric infra-red heating for industrial processes.

43. Grove, S. Heat transfer in thermoplastic composites short course (1988), course notes

44. Astrom B.T., Pipes R.B.
A modelling approach to Thermoplastic pultrusion. 1. Formulation of Models. In press Polymer Composites, 1991.

45. Madenjian, A.R.
Effect of Significant Process Variables on Thermoplastic Matrix Pultruded Composites. 40th Annual Conference, Reinforced Plastics/Composites Institute, The Society of the Plastics Industry, Jan. 28-Feb. 1 1985. Paper 11-F, pp1.

46. Larock, J.A. et al.
Pultrusion processes for Thermoplastic Composites. 44th Annual Conference, SPI, Feb. 6-9, 1989. Session 8A.

47. Wilson M.L. et al.
Pultrusion process development of a graphite reinforced polyetherimide thermoplastic composite. 44th Annual Conference, SPI, Feb. 6-9, 1989. Session 8C.

48. Ma et al.
Processing and properties of pultruded thermoplastic composites (I). Composites Manufacturing, Vol. 1 No.3, September 1990 pp191.

49. Astrom B.T., Pipes R.B.
A modelling approach to Thermoplastic pultrusion. 1. Formulation of Models. In press Polymer Composites, 1991.

50.Astrom B.T., Pipes R.B.
Development of a facility for the pultrusion of Thermoplastic matrix composites. Composites Manufacturing, Vol.2 No.2 1991.

51. Skartsis, L. et al.
Resin Permeation of fiber beds during manufacturing of composite materials. Proceedings Comp.'90. University of Patras,Greece, 20-24 Aug. 1990.

52. Lee, W.I., Springer, G.S.
A model of the Manufacturing Process of Thermoplastic Matrix Composites. Journal of Composite Materials, Vol. 21-November 1987, pp1017.

53. Bascom W.D.
Some surface chemical aspects of glass-resin composites. Part 1. Wetting Behaviour of Epoxy Resins on Glass Filaments. 1965.

54. Elmendorp J.J.
Dynamic wetting in composite preparation: a model study. 2nd International symposium on Phase interaction in composite materials, Patras, Greece, 22-27 August 1988.

55. Cameron, A. Basic Lubrication Theory. Ellis Horwood series in Engineering Science, 1981.

56. Moore. Principles and Applications of Tribology.. Pergammon Press, 1975.

57. Eshel, A. The theory of the infinitely wide, perfectly flexible, self acting foil bearing. Journal of Basic Engineering, December 1965, pp831.

58. Ma, J.T.S. An investigation of self acting foil bearings. Journal of Basic

Engineering, December 1965, pp837.

59. Hull, D. An introduction to composite materials. Cambridge University Press, 1981.

60. Chiao, C.C, Moore, R.L and Chiao, T.T.
Measurement of the shear properties of fibre composites. Part 1. Evaluation of test methods. Composites, July 1977, pp 161-169

61. BS 2782: Part 3: Method 341A.

62. ASTM D-2344-72.

63. Chiao, C.C and Moore, R.L.
Evaluation Of Interlaminar Shear Test For Fiber Composites. Lawrence Livermore Lab., Report UCRL-51766, 5 March 1975.

64. Harris, B. Engineering Composite Materials. The Institute of Metals, 1986. pp 50

65. Sattar, S.A and Kellogg, D.H.
The Effect of Geometry on the Mode of Failure of Composites in Short-Beam Shear Test. Composite Materials: Testing and Design, ASTM STP-460, 1969, pp 62-71.

66. Whitney, J.M. and Short, S.R.
A Modified Short Beam Shear Test. Proceedings of the American Society for Composites, 2nd Technical Conference (Interlaminar Fracture) September 1987.

67. Banerjee, A., Edie, D.D., Ogale, A.A.
Interfacial Characteristics of Carbon-Epoxy Composites, Fiber-Matrix Interface Studies, pp259-266, 1988.

68. Yoshida, H. Statistical Approach to the Relationship between ILSS and Void Content of CFRP. Composites Science and Technology, 25,1986, pp 3-18.

69. Beaumont, P.W.R and Harris, B.
J. Mater. Sci. 7, 1972, pp 1265-1279.

70. Palley, I. A Fracture Mechanics Approach to Interlaminar Failure of Unidirectionally Reinforced Composites. Proceedings of the American Society for Composites, 2nd Technical Conference (Interlaminar Fracture II) September 1987.

71. Murayama Dynamic Mechanical Testing of Polymers, 1978.

72. Rogers, G.F.C., and Mayhew, Y.R.
Engineering Thermodynamics, Work and Heat Transfer, Longmans, Green and Co., 1967.

73. Ott, H.J. Thermal conductivity of composite materials. Plastics and Rubber Processing and Applications 1, 1981, pp 9-24.

74. Springer, G.S. and Tsai, S.W.
Thermal Conductivities of Unidirectional Materials. J. Comp. Mater, Vol. 1, 1967, pp 166-173.

75. Halpin, J.C and Tsai, S.W
Environmental factors in composite materials design. Air Force Materials Laboratory Technical Report, AFML-TR-67-423, 1967.

76. Richardson, M.J.
Quantitative Differential Scanning Calorimetry. Developments in Polymer Characterisation-1. Ch.7. Ed. Dawkins, J.V. Appl. Science Publishing Ltd. 1978, pp 205-244.

77. Blundell, D.J and Willmouth, F.M.
Crystalline morphology of the matrix of Peek-Carbon Fiber Aromatic Polymer Composites, SAMPE Quarterly, Vol. 17, No. 2, 1986, pp 50-57.

78. Velisaris, C.N. and Seferis J.C.
Heat transfer effects on the Processing-Structure relationships of PEEK based Composites. Polymer Engineering and Science, Mid-May, Vol. 28, No. 9, 1988, pp 583-591.

79. Croft, D.R and Stone J.A.R.
Heat transfer calculations using Finite Difference Equations. Applied Science Publishers Ltd, 1977.

80. Ogorkiewicz, R.M. Ed.
Engineering properties of Thermoplastics. Wiley.

81. Roff and Scott, Ed.
Fibres, Films, Plastics and Rubbers.

82. ICI 'Plytron' Product data sheet, 1988.

83. Young, A.
Advanced Composite Thermoplastics: A new structural material. Proceedings of 40th Annual Conference, SPI January 28- Feb 1 1985. Session 4-D, Pp 4-6.